

Near Infrared Spectroscopy and Electroencephalography  
For an Assessment of Brain Function in patients with  
Disorders of Consciousness

By

Agnieszka Maria Kempny

---

*A THESIS SUBMITTED FOR THE DEGREE OF DOCTOR OF PHILOSOPHY*

*Department of Brain Repair and Rehabilitation*

*Institute of Neurology*

*UNIVERSITY COLLEGE LONDON*

*15<sup>th</sup> of January 2018*

## Declaration

I, Agnieszka Maria Kempny confirm that the work presented in this thesis is my own. Where information has been derived from other sources, I confirm that this has been indicated in the thesis.

Signature:

Dr Agnieszka Maria Kempny, MD

“..From the brain, and the brain alone, arise our pleasures, joys, laughter and joke, as well our sorrows, pains, griefs and tears...”

Attributed to Hippocrates, 5<sup>th</sup> Century BCE, quoted by Kandel, *et al.* 1991

## **ACKNOWLEDGMENTS**

The completion of the thesis would not be possible without support of my supervisors: Professor Diane Playford-Principal Supervisor Primary Supervisor, Professor Alexander Leff- Subsidiary Supervisor and Dr Simon Farmer-Tertiary Supervisor, my colleagues, friends and family.

First, I would like to thank Professor Diane Playford for giving me the opportunity to participate in this PhD programme and supporting me through all those years that I have spent on this project. I would like to thank her as well as Dr Sophie Duport for their help on logistics related to the EEG and NIRS laboratory, which was established at Royal Hospital for Neuro-disability in Putney. I would like to sincerely thank Dr Leon James for his help on technical aspects of this work such as collection of NIRS and EEG signals, delivery of the paradigms and for the baseline neurophysiological measurements performed on pDOC patients.

I would also take the opportunity to thank my supervisors Professor Alexander Leff and Dr Simon Farmer, for their patience and commitment, including multiple meetings on data signal analysis, for teaching me how to interpret the findings of this research and their hard work on reviewing posters, presentations and publications, which resulted from this work. I am very grateful for the time Professor Leff spent with me to teach me how to interpret EEG data and how to analyse it using the Statistical Parametric Mapping software.

I would like to thank also my family and friends, whose continuing support was vitally essential for me. I cordially thank also the staff and the inpatients from the Royal Hospital for Neuro-disability, who took part in this study. Without their trust and willingness to participate in this project, surely I would not be able to finish this study.

Finally, I would like to thank my family, my parents, my daughters Barbara and Agatha and my beloved husband Aleksander Kempny, since without their help, love and support I would not be able to work six years on this study.

## **ABSTRACT**

There is growing evidence that some of the patients presenting with the Vegetative State (VS), also known as Unresponsive Wakefulness State, can respond to environmental stimuli. This response can be detected by using functional brain imaging, including electroencephalography (EEG) or Near Infrared Spectroscopy (NIRS). By definition, the VS patients are awake but not aware, unlike the patients in the Minimally Conscious State (MCS), who have some fluctuating awareness. Since consciousness is impaired in both conditions, these states are also referred as Disorders of Consciousness (DOC) or prolonged Disorders of Consciousness (pDOC)

This thesis aims to develop a bedside applicable tool using the EEG and NIRS for brain function assessment in VS and MCS patients. In this study, two experimental protocols have been developed and validated on healthy subjects. The results showed that using the motor imagery and own subject name stimuli, some of the VS patients were able to wilfully modulate their brain activity in response to those stimuli. The results presented in this thesis can be implemented as a part of a protocol for brain function assessment in pDOC patients and can be used for the further studies for better understanding of the brain function in these patients.

## **ABBREVIATIONS**

*BAEP*            *Brainstem Auditory Evoked Potential*

*BCI*              *Brain Computer Interface*

*CBF*             *Cerebral Blood Flow*

*CCP*             *Cerebral Perfusion Pressure*

*CRS-R*          *Coma Recovery Scale-Revised*

*CW*              *Continuous Wave*

*DAI*             *Diffuse Axonal Injury*

*DeoxyHb*       *Deoxyhemoglobin*

*DMN*           *Default Mode Network*

*DOC*           *Disorders of Consciousness*

*DPF*           *Differential Pathlength Factor*

*EEG*           *Electroencephalography*

*ERD*           *Event Related Desynchronization*

<i>ERS</i>	<i>Event Related Synchronization</i>
<i>FDR</i>	<i>False Discovery Rate</i>
<i>FEW</i>	<i>Family Wise Error Corrections</i>
<i>fMRI</i>	<i>Functional Magnetic Resonance Imaging</i>
<i>GCS</i>	<i>Glasgow Coma Scale</i>
<i>GLM</i>	<i>General Linear Model</i>
<i>ICP</i>	<i>Increased Intracranial Pressure</i>
<i>MCS</i>	<i>Minimally Conscious State</i>
<i>NCC</i>	<i>Neural Correlates Of Consciousness</i>
<i>NIRS</i>	<i>Near Infrared Spectroscopy</i>
<i>OxyHb</i>	<i>Oxyhemoglobin</i>
<i>PCC</i>	<i>Posterior Cingulate Cortex</i>
<i>pDOC</i>	<i>Prolonged Disorder Of Consciousness</i>
<i>PET</i>	<i>Positron Emission Tomography</i>
<i>RAS</i>	<i>Reticular Activating System</i>

<i>RCP</i>	<i>Royal College of Physicians</i>
<i>SD</i>	<i>Standard Deviation</i>
<i>SMART</i>	<i>Sensory Modality Assessment and Rehabilitation Technique</i>
<i>SPM</i>	<i>Statistical Parametric Mapping</i>
<i>HbT</i>	<i>Total Haemoglobin</i>
<i>TOI</i>	<i>Tissue Oxygen Index</i>
<i>VS</i>	<i>Vegetative State</i>
<i>WHIM</i>	<i>Wessex Head Injury Matrix</i>

## **PUBLICATIONS AND PRESENTATIONS RESULTING FROM THIS WORK**

### **Publications**

1. *Kempny, A. M., James, L., Yelden, K., Duport, S., Farmer, S., Playford, E. D., & Leff, A. P. (2017). "Some Patients with a Disorder of Consciousness show classical EEG responses to their own name compared with others' names- under review, submitted to Clinical NeuroImage*
2. *Yelden, K., Duport, S., Kempny A. M, L., Farmer, S., Leff, A. P & Playford, E. D., (2017). "Late Recovery of Awareness in Prolonged Disorders of Consciousness A cross-sectional cohort study, Disability and Rehabilitation, Disabil Rehabil. 2017 Jun 21:1*
3. *Kempny, A. M., James, L., Yelden, K., Duport, S., Farmer, S., Playford, E. D., & Leff, A. P. (2016). "Functional near infrared spectroscopy as a probe of brain function in people with prolonged disorders of consciousness." Neuroimage Clin 12: 312-319*
4. *Tak, S, Kempny, A.M, Friston, K.J., Leff, A.P., Penny, W.D., (2015) Neuroimage 111, 338-349. "Dynamic causal modelling for functional near-infrared spectroscopy." Neuroimage 111: 338-349*
5. *Yelden, K., Duport, S., Kempny, A., Playford, E.D., "A rehabilitation unit at night: environmental characteristics of patient rooms." Disabil Rehabil 37(1): 91-96*

## **Posters and presentations**

1. *Philadelphia, May 2016 WNRC Annual Meeting, poster “Near Infrared Spectroscopy as a tool for bedside assessment of consciousness in patients with prolonged Disorders of Consciousness”*
2. *Bristol, October 2014 BSRM Annual Meeting, poster, “Did you call me? How Patients with Prolonged Disorders of Consciousness respond to their own name – an EEG validation study”*
3. *London, February 2014-UCL Faculty of Brain Sciences, poster “Characterising Brain Function in Vegetative and Minimally Conscious State Patients with EEG and NIRS signals”*
4. *London, December 2013, BSRM Annual Meeting, poster “Simultaneous Recording of EEG and NIRS Signals during Motor Imagery in DOC Patients”*
5. *London, June 2013, UCL Neuroscience Symposium 2013 “Simultaneous Recording of EEG and NIRS Signals during Motor Imagery in Healthy Adult Control Subjects” (10 controls)*
6. *London, April 2013, BNA Festival of Neuroscience, poster “Simultaneous Recording of EEG and NIRS Signals during Motor Imagery in Healthy Adult Control Subjects” (five controls)*
7. *Belfast, November 2012, British Society of Rehabilitation Medicine- Autumn Meeting, “Survival and Predictors of Mortality in Patients with Disorders of Consciousness”-oral presentation*

8. *Prague, June 2012; European Neurological Society Meeting, poster “Motor function as an indicator of consciousness in bedside assessment, the Sensory Modality Assessment and Rehabilitation Technique (SMART) scale analysis”*
9. *Edinburgh, March 2012; World Brain Injury Congress, poster “What Component of the Sensory Modality Assessment and Rehabilitation Technique (SMART) is the best the Predictor of Diagnosis of Disorders of Consciousness?”*

## **TABLE OF CONTENTS**

<b>ACKNOWLEDGMENTS</b> .....	<b>2</b>
<b>ABSTRACT</b> .....	<b>4</b>
<b>ABBREVIATIONS</b> .....	<b>5</b>
<b>PUBLICATIONS AND PRESENTATIONS RESULTING FROM THIS WORK</b> .	<b>8</b>
Publications .....	8
Posters and presentations .....	9
<b>TABLE OF CONTENTS</b> .....	<b>11</b>
<b>LIST OF FIGURES</b> .....	<b>15</b>
<b>LIST OF TABLES</b> .....	<b>18</b>
<b>LIST OF EQUATIONS</b> .....	<b>20</b>
<b>OUTLINE AND AIM OF THE THESIS</b> .....	<b>21</b>
<b>CHAPTER 1 GENERAL INTRODUCTION TO THE PATIENT POPULATION</b>	<b>25</b>
1.1 Definition of Vegetative State and Minimally Conscious State .....	26
1.2 Prognostic factors for recovery after severe brain injury.....	33
1.3 Pathophysiology of prolonged Disorders of Consciousness.....	37
1.4 The role of functional imaging in assessment of brain function.....	44

<b>CHAPTER 2 GENERAL METHODOLOGY – NEAR INFRARED SPECTROSCOPY AND ELECTROENCEPHALOGRAPHY .....</b>	<b>50</b>
2.1 Near Infrared Spectroscopy for assessment of brain function .....	51
2.2 Electroencephalography for assessment of Brain Function.....	68
2.2.1 <i>Standard Electroencephalography</i> .....	68
<b>CHAPTER 3 GENERAL METHODS.....</b>	<b>74</b>
3.1 Behavioural scales used for detection of awareness in pDOC .....	74
3.2 Near Infrared Spectroscopy .....	81
3.3 Electroencephalography .....	85
<b>CHAPTER 4 PATIENT CHARACTERISTICS .....</b>	<b>93</b>
4.1 Demographic characteristic .....	93
4.2 Assessment of the awareness using bedside tools .....	96
4.3 Brainstem Auditory Evoked Potentials.....	98
4.4 Qualitative analysis of Electroencephalography.....	100
4.5 Quantitative analysis of encephalography .....	102
<b>CHAPTER 5 NEAR INFRARED SPECTROSCOPY FOR BRAIN FUNCTION ASSESSMENT IN PDOC PATIENTS .....</b>	<b>108</b>
5.1 Introduction .....	108
5.2 Aims.....	109
5.3 Methods .....	110
5.4 Results .....	120
5.5 Discussion.....	137

5.6 Conclusion.....	141
<b>CHAPTER 6 EVENT RELATED EEG SYNCHRONIZATIONS AND DESYNCHRONIZATIONS DURING MOTOR IMAGERY IN PDOC PATIENTS</b>	<b>143</b>
6.1 Introduction .....	143
6.2 Aims.....	145
6.3 Methods .....	145
6.4 Results .....	150
6.5 Discussion.....	155
6.6 Conclusion.....	159
<b>CHAPTER 7 HAEMODYNAMIC AND ELECTRICAL BRAIN RESPONSES IN PDOC PATIENTS.....</b>	<b>161</b>
7.1 Introduction .....	161
7.2 Aims.....	162
7.3 Methods .....	162
7.4 Results .....	165
7.5 Discussion.....	169
7.6 Conclusion.....	172
<b>CHAPTER 8 ABILITY TO DISCRIMINATE BETWEEN OWN NAME AND OTHER NAMES IN PDOC PATIENTS.....</b>	<b>174</b>
8.1 Introduction .....	174
8.2 Aims.....	177
8.3 Methods .....	178
8.4 Results .....	181

8.5 Discussion.....	187
8.6 Conclusion.....	192
<b>CHAPTER 9 GENERAL DISCUSSION.....</b>	<b>194</b>
9.1 Summary of the experiments results performed for this thesis.....	194
9.2 Further work and future prospects .....	197
<b>APPENDIX 1.....</b>	<b>198</b>
<b>APPENDIX 2.....</b>	<b>199</b>
<b>APPENDIX 3.....</b>	<b>206</b>
<b>COPY OF PUBLICATIONS ARISING DIRECTLY FROM THIS WORK .....</b>	<b>208</b>
<b>REFERENCES .....</b>	<b>229</b>

## LIST OF FIGURES

Figure 2.1 Commercially available NIRS devices.....	52
Figure 2.2 Absorption spectra for oxy and deoxy haemoglobin.....	57
Figure 2.3 Typical pattern of haemodynamic response to a motor task .....	63
Figure 2.4 Near Infrared Spectroscopy - basic principles .....	66
Figure 2.5 Near Infrared Spectroscopy and Blood Oxygen Level Dependent response to a motor task .....	67
Figure 3.1 Near Infrared Spectroscopy laboratory .....	82
Figure 3.2 Motor task experiments .....	84
Figure 3.3 The 64 electrode EEG cap.....	87
Figure 3.4 EEG layouts used in the PhD study.....	88
Figure 4.1 EEG spectral analyses in a healthy subject .....	103
Figure 4.2 Spectral analyses of EEG signals in positions C3 and C4 in patients with prolonged disorder of consciousness included to the study.....	104
Figure 5.1 Overview on the motor task experiment .....	111
Figure 5.2 Waveguard cap and fibre arrangement.....	114

Figure 5.3 Changes in oxygenated haemoglobin in a control subject during the motor imagery task.....	125
Figure 5.4 Changes in deoxygenated haemoglobin in a control subject during the motor imagery task.....	126
Figure 5.5 Combined changes in oxy and deoxyHb during the motor imagery task in healthy subject.....	127
Figure 5.6 Changes in oxygenated haemoglobin in a vegetative state patient during the motor imagery task .....	132
Figure 5.7 Changes in deoxygenated haemoglobin in a vegetative state patient during the motor imagery task .....	133
Figure 5.8 Distribution of concentration changes in total, oxy and deoxyHb across all three study groups.....	136
Figure 6.1 Motor imagery task used to evoke EEG oscillatory changes .....	147
Figure 6.2 Example of EEG response to the motor imagery task.....	152
Figure 7.1 NIRS and EEG integrated head cap for data collection .....	164
Figure 8.1 Auditory paradigm used for event related potential responses to subject's own name paradigm.....	179
Figure 8.2 Control subjects response to own name at latency of 250-350 ms and at 600-800 ms.....	182

Figure 8.3 Patients' responses to own name at latency of 250-350 ms and at 600-800 ms

.....185

## LIST OF TABLES

Table 1.1 Diagnostic criteria for Vegetative State.....	28
Table 1.2 Annual incidence of Vegetative State.....	31
Table 1.3 Marshall Computer Tomography Classifications .....	36
Table 1.4 Rotterdam brain injury score .....	36
Table 1.5 Summary of different functional imaging methods.....	47
Table 2.1 Classification of haemodynamic components of near infrared spectroscopy.	64
Table 2.2 Prognostic significance of standard EEG .....	69
Table 3.1 Summary of the behaviours observed on SMART, WHIM and CRS-R .....	80
Table 3.2 Wavelengths, the differential pathlength factor and epsilon of NIRS system	83
Table 4.1 Study group characteristics.....	95
Table 4.2 Patients 'responses to the environmental stimuli measured with WHIM, CRS- R and SMART .....	97
Table 4.3 Brainstem Auditory Evoked Potentials in pDOC patients.....	99
Table 4.4 Resting state EEG to obtain the background electrical activity in the study population .....	101

Table 5.1 Global relative changes in Oxy and DeoxyHb in controls .....	121
Table 5.2 Oxy and deoxyHb concentration changes in controls in relation to the hemisphere.....	122
Table 5.3 Concentration changes in oxy and deoxyHb during a motor imagery task in pDOC patients over the left and right hemisphere .....	130
Table 5.4 Identifiable types of fNIRS responses based on the polarity.....	134
Table 6.1 EEG event related desynchronizations and synchronizations. ....	151
Table 6.2 EEG event related desynchronization and synchronisations for the alpha band. ....	154
Table 7.1 ERD and NIRS responses to a motor task in control subjects.....	166
Table 7.2 ERD and NIRS response to a motor task in pDOC patients.....	168
Table 8.1 Early and late EEG responses to subject own name paradigm in in control subjects .....	183
Table 8.2 Responses from four pDOC patients showing the ERP different response to subject own name paradigm .....	186

## LIST OF EQUATIONS

Equation 2.1 Beer-Lambert Law equation.....	54
Equation 2.2 Modified Beer-Lambert Law equation.....	55
Equation 2.3 Formula for derivation of Blood Oxygen Level Dependent signal. ....	62
Equation 2.4 Formula for assessment event related desynchronization. ....	71

## **OUTLINE AND AIM OF THE THESIS**

The aim of this thesis was to assess the feasibility of the use of Near Infrared Spectroscopy (NIRS) for the assessment of brain function in patients with Vegetative state (VS), known also as Unresponsive Wakefulness Syndrome and Minimally Conscious State (MCS). NIRS is a novel technique and has not been used on patients with prolonged Disorders of Consciousness (pDOC) yet. Therefore, this thesis has a preliminary and exploratory character. Additionally, brain function in pDOC patients was assessed using electroencephalography (EEG), which is a technique with well-established value for brain function assessment. However, a novel approach was taken in regard to the data analysis.

In this thesis, brain function was assessed using not only two techniques (EEG and NIRS) but also two conceptually different approaches namely: the passive and active paradigms. In the active paradigm the controls and the subjects were asked, “imagine you are squeezing your right hand” for assessment of activation of motor cortex. In the passive paradigm the controls and the subjects listened to the own name and a presence of cognitive evoked potentials was assessed. This approach was first validated on healthy controls and then a large cohort of pDOC patients was included to the study.

The detailed assessment of brain function of pDOC patients is important because, it can help clinicians to get a better picture of patients’ ability to respond to external stimuli and hence, stratify patients into two groups: VS or MCS.

The VS characterises patients, who are awake but not aware of themselves or their surroundings, while MCS describes a state of wakefulness and partial awareness. The diagnosis of VS or MCS is usually made using behavioural assessment tools, which have an intrinsic level of subjectivity leading to a high rate of misdiagnosis. Studies

using fMRI and EEG techniques have shown recently that some of the pDOC patients retain potential for communication and have preserved brain function. Although fMRI has great potential, it has limitations including cost, availability, and the fact that it cannot be used at the bedside. Hence, other complementary methods should be used for the detection of brain function in DOC that would be available at the patients' bedside. EEG and NIRS techniques seem to fulfil the criteria of cost and availability.

The thesis consists of a systematic literature review, experimental and developmental chapters organised as follows:

Chapter 1 – this chapter focuses on literature review on pDOC with the comprehensive review of the aetiology, epidemiology, pathophysiology and management.

Chapter 2 – this chapter provides a detailed literature review on the use of NIRS technique for cerebral blood flow (CBF) detection in particular on neurovascular coupling and on the use of the EEG Event Related Potentials and Event Related Desynchronizations for detection of the cognitive functions.

Chapter 3 – this chapter focuses on general methods used in this study and consists of literature review. The chapter is divided into three parts: the first focuses on behavioural scales used for assessment of responsiveness and awareness with the critical review of their validity and reliability. The second part of this chapter focuses on literature review of the use of NIRS for brain function assessment using a motor task. The third part of the chapter consists of a review of the use of EEG and specifically the use of own subject name and motor task in patients with pDOC.

Chapter 4 – this chapter shows results and describes in detail the pDOC patients included to this study. This chapter aims to give a detail picture of the patients; this

includes demographic data, results of behavioural assessment using the Sensory Modality Assessment and Rehabilitation Technique scale (SMART), and results of auditory brainstem evoked potentials, results of qualitative and quantitative EEG results from all included patients to this study.

Chapters 5, 6 and 7 – these chapters present the results of the use of NIRS and EEG for brain function assessment in pDOC patients using a motor task.

Chapter 8 – this chapter shows the results of EEG responses to subject's own name and its use for assessment of brain function.

Chapter 9 – this chapter consists of a general discussion and the future use of the results from this thesis.

## Chapter One

## **CHAPTER 1 GENERAL INTRODUCTION TO THE PATIENT POPULATION**

Vegetative and Minimally Conscious State are severe disorders of consciousness observed in patients emerging from coma and are called disorders of consciousness (DOC). The patients are awake with lack or only intermittent awareness. However, it remains unclear whether DOC patients are aware about their condition, whether they can feel pain or have emotion and memory. For this reason, effort has been made to understand brain function in patients in VS or MCS. This field has been very dynamic and new concepts have been introduced over time. However, the preliminary results show that at least some of the DOC patients have preserved a good brain function, indicating awareness.

This opened a vital question if this cortical activity is enough for a patient to be aware, hence, conscious. Christof Koch and Giulio Tononi (Tononi and Koch 2008) investigated how brain activity changes during the functional activation and why some of stimuli reach conscious perception and others not. They developed a concept of neural correlates of consciousness (NCC) and defined it as the “minimal neuronal mechanism jointly sufficient for any one specific conscious percept“.

The NCC refers to the content of consciousness, namely to a particular experience we are having at a given time, for instance auditory, tactile, visual or somatosensory, while all other variables are constant all the time. The content of consciousness is distinguishable from the level of consciousness, which is for example decreased during sleep or diminished in coma.

During brain activation but not during resting state, there are marked neuronal and hemodynamic changes in brain activity. For instance, visual stimulation can elicit measurable changes in both EEG and fMRI signal. Haemodynamic changes that occur in response to stimuli are measured by using fMRI and Blood oxygen level dependent (BOLD) signal, which increases with decreasing concentration of deoxyHb in the brain tissue (Ogawa and Lee 1990).

This chapter gives background information on the patients' characteristic, introduces the anatomical brain models that can explain some of cognitive dysfunctions and provides overview on functional neuroimaging for assessment of the brain function in pDOC patients.

## **1.1 Definition of Vegetative State and Minimally Conscious State**

The term “*Vegetative State*” was coined, later, by Fred Plum and Bryan Jennett when they described patients after severe brain damage emerging from a coma to a state of wakefulness without detectable awareness (Jennett and Plum 1972).

The Royal College of Physicians (RCP) in their guidance from 2013 defined the VS as:

*“a clinical condition of unawareness of self and environment in which the patient breaths spontaneously, has a stable circulation, and shows a cycle of eye closure and opening which may simulate sleep and waking”* (Royal College of Physicians 2013).

Additionally, patients in the VS can be characterised by the presence of the following features:

1. Periods of wakefulness (eye opening) and eye closure giving the appearance of at least partially preserved sleep-wake cycles (Laureys and Boly 2008)
2. Lack of awareness of self and the environment
3. Presence of hypothalamic and brainstem autonomic functions (The Multi-Society Task Force on PVS 1994)

The RCP guidance (Royal College of Physicians 2013) considers the VS as persistent when it lasts longer than one month and permanent when it lasts longer than six months or one year for anoxic and traumatic brain injury aetiologies respectively.

Although the VS patients are considered to be unaware of themselves or their environment, they can exhibit various behaviours (Table 1.1) (Bernat 2006).

Table 1.1 Diagnostic criteria for Vegetative State

Criteria for VS diagnosis	Behavioural repertoire of VS patients
<ul style="list-style-type: none"> <li>· Unaware of self and environment</li> <li>· No interaction with others</li> <li>· No sustained, reproducible or purposeful voluntary behavioural response to visual, auditory, tactile or noxious stimuli</li> <li>· No evidence of speech understanding or speech production</li> <li>· No blink to visual threat</li> <li>· Preserved cranial nerve reflexes, such as corneal and gag reflexes</li> <li>· Bowel and bladder incontinence</li> </ul>	<ul style="list-style-type: none"> <li>· Sleep wake cycle with eyes closed and opened</li> <li>· Spontaneous breathing</li> <li>· Spontaneous blinking and roving eye movement</li> <li>· Nystagmus</li> <li>· Vocalisation of sounds but no words</li> <li>· Brief unstained visual pursuit</li> <li>· Yawning, chewing jaw movements</li> <li>· Swallowing of saliva, but not able to eat</li> <li>· Non-purposeful limb movements</li> <li>· Flexion withdrawal from noxious stimuli</li> <li>· Brief movement of head or eyes towards sound or movement without apparent localization or fixation</li> <li>· Auditory startle</li> <li>· Startle myoclonus</li> </ul>

*This table presents a diagnostic criteria and behavioural repertoire for the Vegetative State patient modified from (Bernat 2006).*

Some alternative names have been proposed to replace the use of “vegetative state”, because of the negative associations with being called “vegetative”. For example, Bernat (Bernat 2010) named VS as a “disconnection syndrome” due to damage to white matter tracts connecting thalamus and cortex. Other authors working for the European Task Force on DOC proposed to replace the term VS with “Unresponsive Wakefulness Syndrome” (Laureys, Celesia et al. 2010), where the term “Unresponsive” indicates lack of voluntary responses, while “Wakefulness” refers to the ability to open eyes spontaneously or after stimulation.

In the United Kingdom the term “*prolonged Disorders of Consciousness*” has been used, as an umbrella term for both VS and MCS.

The term MCS was developed later than the term VS, and as a result of series meetings called the “Aspen Workgroup”, which were held between March 1995 and October 2000 (Giacino, Ashwal et al. 2002). The Aspen Group proposed following MCS definition:

*”The minimally conscious state is a condition of severely altered consciousness in which minimal but definite behavioural evidence of self or environmental awareness is demonstrated”*

Additionally at least one of the following criteria must be met in order to make a diagnosis of MCS (Giacino, Ashwal et al. 2002):

- Following simple commands
- Gestural or verbal yes/no responses
- Intelligible verbalisation
- Purposeful behaviour, including movements or affective behaviours that occur in contingent relation to relevant environmental stimuli and are not due to reflexive behaviour include:
  - Appropriate smiling or crying in response to the linguistic or visual content of emotional but not neutral topics or stimuli
  - Vocalisation or gestures that occur in direct response to the linguistic content of questions
  - Reaching for objects that demonstrates a clear relationship between object location and direction of reach
  - Touching or holding objects
  - Pursuit eye movement or sustained fixation that occurs in direct response to moving or salient stimuli

Emergence from the MCS is described by a reliable and consistent demonstration of functional communication (accurate yes/no responses to six basic situational orientation questions) or functional use of two different objects on two consecutive assessments (for example appropriate use of a pen or a comb).

The current WHO International Classification of Disease (2011 ICD-9-CM) contains codes for disorder of consciousness and locked-in syndrome, with diagnosis code 780.03 describing persistent VS and MCS with a code of 780.04

*"MCS defined as non –communicative wakeful patients with inconsistent but clearly discernible behavioural evidence of consciousness to be distinguished from comatose, vegetative or unresponsive patients by the presence of non - reflex movements or following commands"* (Gosseries, Bruno et al. 2011).

VS is a relatively rare condition and develops in approximately 1 to 14 % of patients following prolonged, longer than four weeks, coma after the traumatic brain injury and in 12 % of patients who are comatose due to hypoxic brain injury (Multi-Society Task Force on PVS 1994).

Estimation of the VS/MCS prevalence and incidence is challenging. The definitions of DOC have evolved over time and have been differently interpreted (Strauss, Shavelle et al. 1999). Additionally, the patients are placed in various institutions including hospitals, nursing facilities, rehabilitation centres, geriatric units, psychiatric hospitals as well as private homes. The incidence (new cases per year) of patients being in the VS for longer than 6 months was estimated for United Kingdom approximately around 2.5/100,000 population/year (Beaumont and Kenealy 2005). This is lower than the incidence of new cases of VS secondary to traumatic brain injury identified in studies performed in USA, France or UK (Table 1.2) (Jennett 2002).

Table 1.2 Annual incidence of Vegetative State

Country	Incidence of VS / 100 000 population / year	
	1 month post ictus	6 months post ictus
UK	1.4	0.5
USA	4.6	1.7
France	6.7	2.5

This table presents the annual incidence of Vegetative State per 100'000 population in the UK, USA and France at 1 and 6 months post injury, modified from (Jennett 2002).

The estimation of prevalence (existing cases per year) is, for the same reasons, incomplete and may be inaccurate. Overall, the prevalence of patients in VS and MCS varies across countries. Among residents in long term facilities in Austria it was reported to be as high as 3.36 for VS and 1.5 for MCS per 100,000 population (Donis and Kraftner 2011).

In contrast, a lower prevalence of VS patients was found in nursing homes in Denmark and in the Netherlands (0.13/100,000 and 0.2/100,000 respectively) (Engberg and Teasdale 2004; Lavrijsen, van den Bosch et al. 2005).

Unfortunately, for the reasons listed above, the data on prevalence of the patients in the MCS is also sparse. Giacino *et al.* estimated the prevalence of MCS in the United State of America to be as high as 4.8-9.6/100,000 (Giacino, Ashwal et al. 2002). Furthermore, the combined prevalence of VS and MCS patients was estimated to be in the US being as high as 8.8-26.4/100,000. This is different from Japanese and French studies, which indicated a prevalence of 2-10/100,000 for PVS and MCS (Beaumont and Kenealy 2005).

Nevertheless, because of the improvements in emergency medicine and intensive care management it is very likely that the incidence of VS and MCS patients will increase in

the future (Beljaars, Valckx et al. 2015). Another factor contributing to the increased prevalence of pDOC patients may be increased survival rates. Recent studies have suggested that advances in intensive care have improved survival among patients with severe brain injury (Marshall 2000; Hinchey, Myers et al. 2010; Di Saverio, Gambale et al. 2014), (Tresch, Sims et al. 1991). Early reports suggested that the life expectancy for patients in VS was approximately 3 years. A 1999 study revealed that the mortality rate decreases with increasing follow-up with it being the highest during the first three years after brain injury (Strauss, Shavelle et al. 1999). For instance, the mortality rate was 46% up to three-year post ictus and 12%/year for patients in VS for longer than 9 years. A study reported in 2013 using data from the National Institute on Disability and Rehabilitation Research framework for inpatient rehabilitation of traumatic brain injury patients showed that survival rates for pDOC at 1, 2, and 5 years were 95.3%, 92.2%, and 89.0%, respectively (Whyte and Nakase-Richardson 2013).

The reason for the discrepancy between the reported mortality rates by these two studies may be multifactorial; both studies differ significantly in methodology and the patient's characteristic. Hence, still, little is known about the temporal dynamic of mortality rate in pDOC population with mixed aetiology. For instance, a recent study from Germany showed an average survival post discharge from rehabilitation centre in VS patients as short as 2.7 years and longer survival in MCS patients on average 4.5 years (Steppacher, Kaps et al. 2014). However, the cause of death in pDOC patients has remained the same for many years, recurrent infections of either pulmonary or urinary tract were identified both thirty years ago and more recently (Multi-Society Task Force on PVS 1994; Luaute, Maucourt-Boulch et al. 2010).

## **1.2 Prognostic factors for recovery after severe brain injury**

Neurological bedside examination can predict poor outcomes defined as: coma, VS or MCS after a brain injury as early as on the third day after brain injury (Young 2009). For instance, lack of pupillary light reaction on the third day after anoxic and traumatic brain injury predicts poor prognosis (Berek, Lechleitner et al. 1995; Balestreri, Czosnyka et al. 2004). Also lack of motor response to noxious stimuli or only extensor posturing (i.e., decerebrate response or no response) at 72 hours post injury were also associated with no false positives for a poor outcome (Levy, Caronna et al. 1985). Seizures and sporadic focal myoclonus do not predict poor outcome, however, myoclonus status epilepticus occurring on day 1 after Cardio-Pulmonary-Resuscitation predicts poor outcome (Zandbergen, Hijdra et al. 2006).

Neuro-physiological assessments also assist in the prediction of the poor outcome after a brain injury. The most accurate electrophysiological predictor of a poor outcome is the measurement of N20 response from the primary somatosensory cortex on somatosensory evoked potentials (SSEPs). Lack of response on the third day after cardiac arrest predicts poor outcome with high sensitivity (Gendo, Kramer et al. 2001). Many studies also showed that an assessment of SSEP was useful in predicting outcome after traumatic brain injury. Lew and colleagues (Lew, Dikmen et al. 2003) reported that bilateral absence of N20 in SSEPs within eight days after a severe trauma was a strong predictor of death or persistent VS. Meta-analysis has also shown that bilaterally negative SSEPs are a strong predictor of unfavourable outcome (Carter and Butt 2001). It remains unclear whether EEG findings have clinical efficacy in predicting poor outcome. However, patients who have a reactive EEG, have a better prognosis compared to those who do not have such EEG responses (Young 2000). Poor prognostic EEG includes the presence of: triphasic waves, burst suppression, no

reactive alpha/theta/spindle coma and generalized suppression (Young and Doig 2005),(Young, Kreeft et al. 1999) (for more detail on malignant EEG please see the Chapter 2” EEG for assessment of Brain Function”).

Another predictor of poor outcome after a hypoxic brain injury is related to changes in serum concentration of several biomarkers including: serum neuron-specific enolase, serum S100 protein and creatine kinase brain enzyme (Clemmensen, Strandgaard et al. 1987; Pfeifer, Borner et al. 2005; Zandbergen, Hijdra et al. 2006) (Wijdicks, Hijdra et al. 2006). However, recent studies confirmed that only the neuron-specific enolase has predictive value of poor outcome with a cut-off for serum level of >33 µg/L at days 1 to 3 post CPR (Wijdicks, Hijdra et al. 2006).

After brain injury, intracranial pressure may be increased due to masses, haematoma focal swelling of brain tissue or hydrocephalus. Furthermore, increased intracranial pressure (ICP) can lead to decrease in cerebral blood flow and subsequent additional brain tissue ischemia (Hutchinson, Koliass et al. 2016). Unfortunately, the ICP cannot be established by clinical assessment of a patient and should be measured by using either interventricular catheters or microtransducer systems (Smith 2008). It was found that the best clinical outcome can be achieved when cerebral perfusion pressure (CCP) after brain injury is maintained between 50 and 70 mmHg (Smith 2015).

Brain imaging can be informative for the prediction of outcome. Computed tomography of a brain may not show any abnormalities immediately after a cardiac arrest, but by the third day it usually shows brain swelling and inversion of the grey–white densities in patients with a poor clinical outcome (Zingler, Krumm et al. 2003). An inverted grey /white matter ratio in Hounsfield Units less than 1.22 is predictive for death or VS (Choi, Park et al. 2008). Another factor is an obliteration of the basal cistern and the presence of subarachnoid haemorrhage (Bratton, Chestnut et al. 2007). For clinical purposes the severity of the brain injury has been assessed using two classifications:

Marshall's and the Rotterdam Brain Injury, with a scoring based on assessment of the mass lesions and an increased intracranial pressure (compression of basal cisterns and midline shift) (Table 1.3 and 1.4) (Maas, Hukkelhoven et al. 2005). Recently a study showed, that on both scales: the Marshall CT Classification and the Rotterdam brain injury the scores above three were significant predictors for death within first two weeks after injury (Deepika 2015). Follow-up scans have the same important predictive values as an initial CT scan. A survey among patients with moderate to severe TBI showed that substantial proportion of patients with diffuse injury (no mass lesion) on their first CT scan had progressive intracranial damage on subsequent CT examinations (Servadei, Murray et al. 2000). Therefore, "the worst scan" should be used for outcome prediction.

*Table 1.3 Marshall Computer Tomography Classifications*

<b>Definition</b>	<b>Description</b>
Diffuse Injury I	No visible intracranial pathology
Diffuse Injury II	Cisterns are presented with midline shift of 0-5mm and /or no high or mixed density lesions >25cm <sup>3</sup> , may include bone fragments and foreign bodies
Diffuse Injury III (swelling)	Cisterns compressed or absent with midline shift of 0-5mm, no high mixed density lesion >25cm <sup>3</sup>
Diffuse Injury IV (shift)	Midline shift>5mm, no high mixed density lesion >25cm <sup>3</sup>

*This table presents the Marshall Computer Tomography Classification used for assessment of the severity of traumatic brain injury, modified from (Maas, Hukkelhoven et al. 2005).*

*Table 1.4 Rotterdam brain injury score*

<b>Basal cistern</b>	
normal	0
compressed	1
absent	2
<b>Midline shift</b>	
No shift or <5 mm	0
Shift>5 mm	1
<b>Epidural mass lesion</b>	
present	1
absent	0
<b>Intra-ventricular blood or traumatic SAH</b>	
absent	0
present	1

*This table presents the Rotterdam brain injury score for the assessment of severity of brain injury using Computer Tomography, where depending on changes in basal cistern and presence of midline shift, epidural mass lesions and bleeding with maximum severity scored as “5” and minimum as “0” modified from (Maas, Hukkelhoven et al. 2005)*

## **1.3 Pathophysiology of prolonged Disorders of Consciousness**

### ***1.3.1 Mechanisms of brain injury***

Although the pathophysiology differs in traumatic and anoxic brain injuries, there is a common denominator for all injuries leading to pDOC. Usually, there is a diffuse damage of cortical neurons, thalami, or the white matter tracts, that connect the thalamus with the cortex, with relative sparing of the brainstem and hypothalamus (Kinney and Samuels 1994).

Trauma to the brain may result in a range of injury mechanisms and pathologies. These mechanisms can be divided into two main categories: focal brain injury and diffuse axonal injury (DAI). Depending on the mechanism of injury they may occur in isolation or together (Smith, Meaney et al. 2003). The focal brain injury is usually associated with blows to a head that result in cerebral contusions and haematomas causing “mass effect” and leading to herniation and brainstem compression (Gennarelli 1993). Inertial forces leading to white matter in the brain damage usually cause the DAI. This type of injury is commonly seen in motor vehicle crashes, falls and assaults (Adams, Doyle et al. 1984), (Blumbergs, Jones et al. 1989).

Adams *et al.* (Adams, Doyle et al. 1989), described the DAI mechanism and graded this into a three level scale depending on the extent of anatomical changes.

In the first grade, there is an axonal injury in the white matter of the cerebral hemispheres, in the second grade a focal lesion in the corpus callosum and in the third

grade; the lesions extend into the dorsolateral quadrant or quadrants of the rostral brainstem.

Severe traumatic brain injury with the white matter tissue tearing may lead to an immediate disruption of axons (primary axotomy). Also, following a brain injury a secondary axotomy can occur (Pierce, Smith et al. 1998). Axonal stretch leads to cytoskeletal damages (Smith, Wolf et al. 1999), in particular, to a damage of sodium channels, which causes an massive influx of sodium and calcium into the cells and results in neuronal swelling (Wolf, Stys et al. 2001). Axonal swelling also impairs the transport along the axons causing further proteins accumulation ( $\beta$ - amyloid precursor protein) (Gentleman, Nash et al. 1993). This may lead to progressive disorganisation of the axonal cytoskeleton, disconnections of axons and dysfunction of a neural network. Unfortunately, only minority of DAI patients can achieve functional recovery due to local plasticity in the grey matter and healing of damaged axons in the white matter (Smith, Meaney et al. 2003).

Prolonged Disorders of Consciousness due to anoxia or ischaemia also results in a diffuse injury producing widespread damage to cortical and thalamic neurons, which are more susceptible for lack of oxygen than brainstem neurons (Dougherty, Rawlinson et al. 1981). Depending on aetiology, different patterns are observed after hypoxic – ischemic brain injury, for instance, in a post-mortem examination in patients after cardiac arrest there is a layered cortical neuronal damage called laminar necrosis, whereas diffuse boundary-zone infarcts occur after severe hypotension (Kinney and Samuels 1994).

### ***1.3.2 The role of reticular activating system in consciousness***

Even minor lesions to the reticular activating system (RAS), hence, to the brainstem can produce coma. However, a well-functioning brainstem alone is insufficient to generate consciousness. If there is a lesion compromising a thalamo-cortical tract, then a patient remains awake but not aware, therefore, in the VS.

*“ it is unclear, whether the cortico-thalamic system alone can generate consciousness when the RAS has been completely damaged, however, evidences from deep cortical stimulation to the median thalamus, suggested that the RAS has a role of an on-off switch rather than a generator of consciousness”*(Laureys and Tononi 2009).

Almost a hundred years ago, a Viennese pathologist Constantin Von Economo suggested, that the upper brainstem and posterior hypothalamus are arousal generators. Another scientist, Bremer in 1929, noticed that a dysfunction in arousal might be caused by an impairment of the ascending sensory pathways. Later his student – Giuseppe Moruzzi developed a concept of the ascending RAS (Zeman 2001). Jonathan Schwartz and Thomas Roth (Schwartz and Roth 2008) in their review on “Neurophysiology of Sleep and Wakefulness: Basic Science and Clinical Implications” listed the “key cell population of the ascending pathway, which include: cholinergic, noradrenergic, serotonergic, dopaminergic and histaminergic neurons located in the pedunculopontine and laterodorsal tegmental nucleus, locus coeruleus, dorsal and median raphe nucleus and tuberomamillary nucleus. Projections of the above mentioned structures to promote arousal. Additionally these structures are inhibited during sleep by neurons of the ventrolateral preoptic nucleus.

### ***1.3.3 The role of thalamus in consciousness***

There is evidence from both pathological studies and neuro-imaging studies demonstrating that loss of consciousness in VS patients is usually related to widespread lesions of cortical grey or white matter with involvement of cortico-thalamic system with a central role of the intralaminar nuclei of thalamus (Laureys and Tononi 2009).

Our understanding of the role of thalamus has changed over time. Initially, the thalamus was considered as a simple relay-like-machine, however, currently it is known that it modulates and actively alters the sensory information reaching the cortex (Sherman and Guillery 2002). Indeed the thalamus can be considered as both: the first order relay, which transmits the signal without changing it and as a second order relay. The second order relay, the pulvinar region of the thalamus provides afferents to the visual and auditory cortex and efferent projections from a tegmentum. Animal models provide more information on the complexity of the connections between thalamus, cortex and tegmentum. For example, the lateral geniculate nucleus and the pulvinar region have a complex distribution of afferents and modulators from cortical areas 17,18 and 19, layer 6, where afferent nerve fibres divers afferents carry the information, while modulators, alter and modulate the information (Sherman and Guillery 1998). That is why thalamus has been called “seventh layer of the cortex”, to illustrate the close connection between thalamus and neocortex, and lack of connections with hippocampal and olfactory cortex (Sherman and Guillery 2001).

The regulation of the cortico-thalamic connection is complex and modulated by other brain regions as well, for instance, striatum. Opstal *et al.* (Van Opstal, Van Laeken et al. 2014) in their study discussed the striatal modulation of the cortico-thalamic connection. They measured the PET activation in striatal dopamine and its influence on visual consciousness and suggested that the visual awareness is related to striatal dopamine.

Structural studies, using MRI tractography, for assessment of the fiber tracts connectivity, showed that the subcortico (striatum, globous pallidus, thalamus) – cortical connections were significantly damaged in VS patients and the severity of damage correlated with the impairment of consciousness, measured using the Coma Recovery Scale-Revised (CRS-R) (Lant, Gonzalez-Lara et al. 2016). There were dense connections between thalamus and motor cortex in healthy subjects (Fernandez-Espejo, Rossit et al. 2015). Additionally, not only connections and fiber tracts were disturbed in pDOC patients, but also the subcortical structures, including thalamus, were found to exhibit significant atrophic changes (Lutkenhoff, Chiang et al. 2015).

Even small, but direct injury to the central thalamus can produce significant disturbance in consciousness. Bilateral lesions result in coma. Unilateral lesion to thalamus can result in range of symptoms such as: hemispatial unawareness or altered states of consciousness such as mania or delirium. Recovery from thalamic injury is slow and uncertain (Schiff 2008). As shown by Nicolas Schiff in his manuscript the parallel contribution of several brain structures is vital for the maintenance of arousal (Schiff 2008). Furthermore, Schiff says:

*“The connections of the central thalamus support its role in arousal regulation mechanism that adjusts activity levels over the large-scale networks during behaviours. The central thalamus has strong reciprocal connections with several sub-regions of the frontal cortex engaged in planning and execution of movement, and more posterior cortical association areas that support poly-sensory integration. Also bottom-ups connection to the central thalamus includes projections from the brainstem arousal system”.* (Schiff 2008)

#### ***1.3.4 The role of hypothalamus in consciousness***

The hypothalamus consists of number of small nuclei occupying the ventral part of the diencephalon. The hypothalamus controls many metabolic processes and it secretes neuro-hormones that further control the function of the pituitary hormones. The hypothalamus was also included into a theoretical framework of brain structures supporting consciousness (Parvizi and Damasio 2001). An injury to hypothalamus can cause somnolence (Laureys and Tononi 2009). In particular one of the hypothalamic nuclei, the tuberomamillary nucleus was found to have a significant role in the control of learning and memory (Huston, Wagner et al. 1997). Others also found that the tuberomamillary nucleus is critical for maintenance of wakefulness and modulates function of the other basal nuclei (Benarroch, Schmeichel et al. 2015).

### ***1.3.5 The role of cerebellum in consciousness***

The cerebellum has a multiple connections with the cerebral cortex, a complex neuro-anatomy, a high density of neurones, and receives sensory input and produces motor output, however, even widespread lesions do not lead to disturbances in consciousness (Laureys and Tononi 2009). However, cerebellar lesions can cause attention and short-term-memory deficits (Glickstein 2007).

### ***1.3.5 The role of neuronal networks in pDOC***

The more recent studies also shed light on neuronal networks as an important potential contributor to consciousness, which may be dis-functioning in pDOC.

For instance, the default mode network (DMN), which consists of anterior and posterior midline regions and is involved in conscious and self –related cognitive processes. So far, many studies have confirmed that the activity of the DMN is significantly decreased in VS and MCS patients when compared with healthy subjects (Boly, Tshibanda et al. 2009; Vanhaudenhuyse, Noirhomme et al. 2010). Within the DMN, the posterior cingulate cortex (PCC) appears to play an important and significant role. Crone *et al.* (Crone, Schurz et al. 2015) demonstrated that in healthy controls PCC receives a strong positive input from frontal and parietal cortex, while this influence is weak but still existing in the MCS . Unfortunately, the PCC does not act any longer as a hub in VS patients.

## **1.4 The role of functional imaging in assessment of brain function**

The first studies on brain function in pDOC patients were performed in nineties last century using two techniques: the EEG and positron emission tomography (PET). The H<sub>2</sub><sup>15</sup>O PET studies showed, that the brain metabolism-level in VS patients can be reduced up to 40-50% of normal values (Laureys, Goldman et al. 1999). However, this global depression of cerebral metabolism is not specific for VS or coma patients, but for instance, can be seen in healthy controls during physiological sleep (slow wave sleep stage III and stage IV) when, the brain metabolism decreases to 60% of normal values (Maquet, Degueldre et al. 1997). Nevertheless, the H<sub>2</sub><sup>15</sup>O PET studies were important, because they shed new light on the VS problem, and proved that, the VS patients are not brain dead.

The early EEG studies described the clinical characteristics of the EEG in patients with VS, such as lack of diurnal/nocturnal changes, lack of sleep pattern, slow not higher than 6 Hz main background rhythm, lack of EEG reactivity to noxious stimuli (Kobylarz and Schiff 2005).

EEG has an established role for assessment of brain function in pDOC patients. In this chapter I discuss research on resting state connectivity, while the use of the standard EEG is discussed in Chapter 2.2 and the use of functional EEG for assessment of motor cortex and ability to detect own name is discussed in Chapter 3.3.

Resting state connectivity is defined as quantitative, spectral, analysis of high density EEG. A recent study assessing state connectivity in 104 pDOC patients suggests that it may be useful for establishing VS or MCS diagnosis, for assessment of brain

metabolism and for prediction of the likelihood of emergence from pDOC within 1 year (Chennu, Annen et al. 2017).

So far the functional Magnetic Resonance Imaging (fMRI) studies, not only showed that it would be feasible to detect a subject's conscious experience using fMRI technique, but also remains the golden standard for brain function assessment in pDOC patients.

Boly *et al.* (Boly, Coleman et al. 2007) validated several tasks for assessment of volitional brain activity, based on sensory information input, but without any motor output. For instance, a visuo-spatial imagery task was initially validated on 12 healthy controls, when the controls were instructed to mentally inspect the rooms in their houses, to imagine going from the entrance door, visiting all rooms in their house and to be attentive to detail as they looked around, rather than concentrating on walking. This task activated the bilateral precunues/parieto-occipital junction and retrosplenial cortex in all volunteers and parahippocampal cortex in 11 out of 12 healthy subjects.

Another task for assessment of volitional brain activity was an imagery of singing of a song "Jingle Bells". During this task, Boly *et al.* (Boly, Coleman et al. 2007) noticed a weak activation in 3 out of 12 controls in left superior temporal gyrus; therefore, this type of activation was considered not sensitive enough to be introduced to the pDOC patients.

Boly *et al.* (Boly, Coleman et al. 2007) also assessed the brain responses to a visual imagery of the faces. The volunteers were asked to imagine the familiar faces of their relatives. This task elicited right fusiform gyrus activation in 11 healthy volunteers (n=12), however, with lower spatial extent and greater inter-subject variability. Also, elsewhere this paradigm has been used on the pDOC patients confirming its feasibility in awareness detection (Sharon, Pasternak et al. 2013).

Finally, Boly *et al.* (Boly, Coleman et al. 2007) validated the use of the motor imagery for awareness assessment. The healthy controls were asked to imagine playing tennis. This task elicited a robust activation in bilateral supplementary motor area in all volunteers and in inferior parietal lobule in 11 out of 12. Based on the controls' responses the conclusion was that the motor and spatial imagery tasks, in particular, the instructions "imagine playing tennis" and "imagine walking from room to room in your home", can elicit reliable, robust and statistically distinguishable patterns of activation in specific regions of the brain (Owen, Coleman et al. 2007). Hence, these imaginary tasks were used by Monti *et al.* (Monti, Vanhaudenhuyse et al. 2010) in their elegant study. They included 54 patients with pDOC, who performed these two mental imagery tasks while the CBF was assessed using fMRI. Five patients (9%, 5 out of 54) showed a voluntary brain activity modulation as a response to the motor imagery tasks. However, the careful bedside assessment of these five patients showed that three of them had some evidences of awareness using a behavioural assessment, but two of them met criteria of VS diagnosis. Moreover, one patient (one out of five) used the wilful modulation of the brain activity for functional communication purposes, for instance, the patient was asked a question "Is your father's name Alexander?" If the answer was "yes" a patient was instructed, "imagine that you are waking around your house" if the answer was "no" "imagine you are playing tennis". The authors were able to identify the response based only on fMRI signal change.

Overall, for functional assessment of the brain function in pDOC patients, several techniques can be used for instance: fMRI, EEG, transcranial magnetic stimulation (TMS), near infrared spectroscopy (discussed in Chapter 2), with significant differences between modalities (Tab 1.5).

*Table 1.5 Summary of different functional imaging methods*

Technique	Pros	Disadvantages
Resting state fMRI	<ul style="list-style-type: none"> <li>• Whole brain image</li> <li>• High spatial resolution</li> <li>• Efficient study of cortical studies</li> </ul>	<ul style="list-style-type: none"> <li>• Low temporal resolution</li> <li>• Prone to noise contamination</li> <li>• Unknown significance</li> </ul>
TMS-EEG	<ul style="list-style-type: none"> <li>• Perturbation-causal effect</li> <li>• High temporal resolution</li> <li>• Direct cortical access</li> <li>• High intra-subject reliability</li> </ul>	<ul style="list-style-type: none"> <li>• Cannot be performed at the bedside</li> <li>• Cannot be directly compared inter subjects</li> <li>• Covers only part of a brain</li> </ul>
Sensory EEG, for instance, ERP or ERD	<ul style="list-style-type: none"> <li>• Perturbation – causal effect</li> <li>• High temporal resolution</li> <li>• Easy to acquire at a bedside</li> </ul>	<ul style="list-style-type: none"> <li>• Covers only part of a brain</li> <li>• Can be contaminated by subcortical processes</li> </ul>
Near infrared spectroscopy	<ul style="list-style-type: none"> <li>• Perturbation –causal effect</li> <li>• Easy to acquire at a bedside</li> </ul>	<ul style="list-style-type: none"> <li>• Poor spatial and temporal resolution</li> <li>• Prone to artefacts</li> <li>• Signal can be contaminated by non-brain haemodynamic signal</li> </ul>

*This table presents different functional imaging techniques, which can be used for brain function assessment in pDOC patients, modified from (Boly, Massimini et al. 2012)*

The major question is the whether pDOC patients have some conscious perception that cannot be inferred from careful clinical observation. If pDOC patients have residual consciousness then they may be aware of their severe physical disability, they may have emotions, memories and can experience pain. The two major components of consciousness are wakefulness and awareness. The wakefulness is defined as an ability to open eyes, while the awareness is defined as ability to respond to external stimuli. All

patients in VS have periods of wakefulness, they are able to keep their eyes opened for several hours per day, and however, per definition these patients are not responsive to external stimuli. MCS patients by definition can be aware, albeit inconsistently. The previous studies using fMRI and PET, showed unequivocally, that approximately 10% of the VS patients have almost normal brain activity, and it was suggested that these patients should have diagnosis of “functionally locked in syndrome” (Bruno, Vanhaudenhuyse et al. 2011).

Nevertheless, the use of the fMRI assessment for the neuronal correlates of speech, vision or motor function remains limited with significant accessibility /costs/ and patients’ eligibility issues. One of the most common limitations that prevent pDOC patients undergoing fMRI study is inability to remain motionless during the investigation. Many pDOC patients exhibit involuntary movements including frequent jaw or neck movements. In addition, pDOC patients have often undergone shunt, pacemaker or venous filter insertion and these materials may not be compatible with the MRI technique.

Hence, there is a need for developing a cost-effective bedside method for assessment of brain function in pDOC patients. Electroencephalography and Near Infrared Spectroscopy may be suitable and feasible techniques for bedside use in the assessment of brain function assessment in pDOC patients.

This thesis addresses this gap through the development and validation of the robust EEG and NIRS paradigms for assessment of brain function in pDOC patients. Preliminary results indicate that both the EEG and NIRS have great potential in the assessment of pDOC patients. Some studies have been recently published. The next chapter focuses on the literature review on use of the EEG and NIRS for brain function assessment in healthy subjects.

## Chapter Two

## **CHAPTER 2 GENERAL METHODOLOGY – NEAR INFRARED SPECTROSCOPY AND ELECTROENCEPHALOGRAPHY**

The aim of this chapter is to provide general information on the use of NIRS for assessment of cerebral oxygenation in clinical settings, for instance, during surgery or for the neurofeedback in rehabilitation. In the first part of the chapter I discuss how the NIRS technique is feasible to estimate the cerebral oxygenation changes.

In the second part of the chapter I discuss the use of cognitive potentials derived from the EEG, such as event related EEG rhythm desynchronizations/synchronizations and event related potentials and their use in assessing brain function. Both approaches, NIRS and EEG are suitable for the bedside use, since the EEG and NIRS recording devices are small, portable and can be built within a mobile unit. The techniques detect different aspects of the brain function, the NIRS detects haemoglobin concentration changes, and hence the haemodynamic changes during the brain activation, while the EEG provides information dynamic electrical activity of the cerebral cortex. A theoretical framework of neurovascular coupling, which links the neuronal and haemodynamical changes during the brain activation, will be also discussed here.

## **2.1 Near Infrared Spectroscopy for assessment of brain function**

### ***2.1.1 Near Infrared Spectroscopy in clinical use***

NIRS is a non-invasive technique that has potential to assess the cerebral tissue oxygenation levels, hence became a functional brain imaging technique. The NIRS technique relies on transmission and absorption of near infrared light (700 to 1000 nm) as it passes through tissue. The NIR light is generated at specific wavelengths, shone onto tissue, travels through the tissue and is being absorbed by chromophores, such as oxygenated and deoxygenated haemoglobin (Smith and Elwell 2009). The NIR light that was not scattered or absorbed during its travel through the tissue, is detected by NIR light detectors.

The NIRS devices are commercially available and used in clinical settings for monitoring of cerebral tissue oxygenation. There are several types of devices for monitoring the brain frontal lobes oxygenation that are mainly used during anaesthesia for cerebral oximetry (Figure 2.1). The NIRS measurement can be combined with bispectral index monitoring, which is derived from the frontal EEG signal (Murkin and Arango 2009). Additionally, it has also been shown that NIRS was feasible to use even in very low-birth-weight infants (Pichler, Cheung et al. 2014). Currently there is an ongoing phase II randomized clinical trial on cerebral NIRS for monitoring and treatment of hypoxia in the preterm neonates (SafeBoosC).

Figure 2.1 Commercially available NIRS devices



This figure presents the examples of the commercially available NIRS devices for monitoring of the cerebral oxygenation, a- CerOx (Ornin), b- Equinox (Nonin), c- Fore-Sight (CASMED), d- INVOS (Covidien).

NIRS is also a promising tool in clinical neurology as it offers continuous recording of brain oxygenation. The NIRS strength is that it can monitor a brain oxygenation continuously and at the bedside.

Another area of potential use of NIRS is for the preoperative function localization in the brain tumours and epileptic disorders. The expressive and receptive language functions in patients with glioma have been evaluated using the NIRS followed by a Wada test, where sodium amobarbital is injected into left and right internal carotids artery to establish which hemisphere is dominant in regard to language. This can be performed prior to the neurosurgical treatment of the refractive epilepsy (Ryvlin and Rheims 2008). These results have shown the feasibility of the use of NIRS for pre-surgical

identification of language lateralisation (dominant left versus right hemisphere) since in all subjects (n=9) the NIRS results corresponded with the lateralization of the Wada test (intra-carotid amobarbital procedure) results (Sato, Uzuka et al. 2012). Others studies have confirmed that NIRS can be used in children for evaluation of treatment efficacy of epilepsy (Monrad, Sannagowdara et al. 2015).

NIRS can be also used for neurofeedback protocols in neuro-rehabilitation. For instance, Obrig, *et al.* (Obrig 2014) showed that by a mental training and mental imagery of the daily, usual activities it was possible to achieve better response to the rehabilitation interventions when the efficacy of this mental training was controlled using NIRS.

Mihara, *et al.* (Mihara, Miyai et al. 2012) assessed the feasibility of the use of NIRS neurofeedback in patients after stroke for mental imagery of a hand movement and found that the NIRS based neurofeedback induced significantly greater activation of the contralateral premotor cortex then compared to those patients, who did not performed mental imagery exercises.

Furthermore, the subsequent studies on the role of NIRS based neurofeedback in functional recovery after stroke showed that the motor imagery could enhance ipsilesional premotor cortex activation and hence, has a positive effect on the future functional recovery, as expressed on the Fugl-Mayer scale (Mihara, Hattori et al. 2013). These finding may also suggest that increased activation of the premotor cortex positively modulate excitability of the primary motor cortex (Sitaram, Veit et al. 2012)

### *2.1.2 Near Infrared Spectroscopy - physical principles*

The use of a NIRS technique in medicine was introduced by Frans Jobsis, who described transparency of biological tissues for a near infrared light and suggested that this could be used for monitoring of a tissue oxygenation (Jobsis 1977). Near-infrared technique uses light of the wavelength ranging from 650 nm to 1000 nm. This wavelength of light is easily absorbed by chromophores, such as water, lipids, melanin, oxy/deoxyhaemoglobin as well cytochrome oxidase C. Furthermore, these variables remain stable during an experiment, and only oxy and deoxyhaemoglobin's concentration will change during a brain activation (Pellicer and Bravo Mdel 2011).

The Beer-Lambert Law describes how the NIR light is absorbed in a non-scattering medium. This law states that the attenuation (A) is proportional to the concentration of the compound in the solution (c) and the optical pathlength (d):

$$A = \log_{10} \left[ \frac{I_0}{I} \right] = adc$$

*Equation 2.1 Beer-Lambert Law equation.*

where  $A$  is the attenuation measured in optical densities,  $I_0$ -input light intensity,  $I$ - light intensity transmitted through the medium,  $a$ - extinction coefficient of the absorbing compound expressed  $\mu\text{M}/\text{cm}$ ,  $c$  - concentration of the absorbing compound in the solution measured in  $\mu\text{M}$ ,  $d$  -distance between the points where the light enters and leaves the medium (Elwell and Hebden).

Since the Beer–Lambert Law is only valid in non-scattering media and cannot be applied to biological tissues, Delpy developed a modified Beer-Lambert law, which is applicable for biological tissues (Delpy, Cope et al. 1988). The modified Beer-Lambert law was described based on NIR light transport in a rat's brain (in vivo) and also took into account detectors and transmitter geometry, head shape, scattering and absorption properties of the tissue.

$$\text{attenuation}(OD) = \log\left(\frac{I}{I_0}\right) = B\mu_a * dp + G$$

*Equation 2.2 Modified Beer-Lambert Law equation.*

*“Where  $I$  is the transmitted intensity,  $I_0$  the input light intensity,  $B$  is a pathlength factor dependent upon the absorption and scattering coefficients  $\mu_a$  and  $\mu_s$  and the scattering phase function,  $G$  is an unknown geometry dependent factor and the  $dp$  is the inter-optode distance” (Delpy, Cope et al. 1988).*

What the modified Beer-Lambert law indeed says, is that if the light attenuation are measured at two or more wavelengths, then it is possible to estimate changes in concentration of chromophores (oxy and deoxyhemoglobin). The modified Beer-Lambert law was also validated on an animal model, when Baker *et al.* (Baker, Parthasarathy et al. 2014), injected a drug dinitrophenol in a pig to induce 200% increases in cerebral flow, which was measured using MRI and NIRS. The modified Beer-Lambert law used in NIRS technique not only correlated with the MRI measurement but also as authors suggested (Baker, Parthasarathy et al. 2014) using modified Beer-Lambert law it was possible to filter out superficial tissue effects and monitor blood flow in cerebral tissue.

There are several methods, discussed more in detail in this chapter that can be implemented in order to minimize probability that the NIRS signal originates from cerebral cortex. These include: filtering, implementation of differential path length factor (DPF), extraction of evoked response, removal of physiological noises, instrumentation, and environmental noises (Kamran, Mannan et al. 2016).

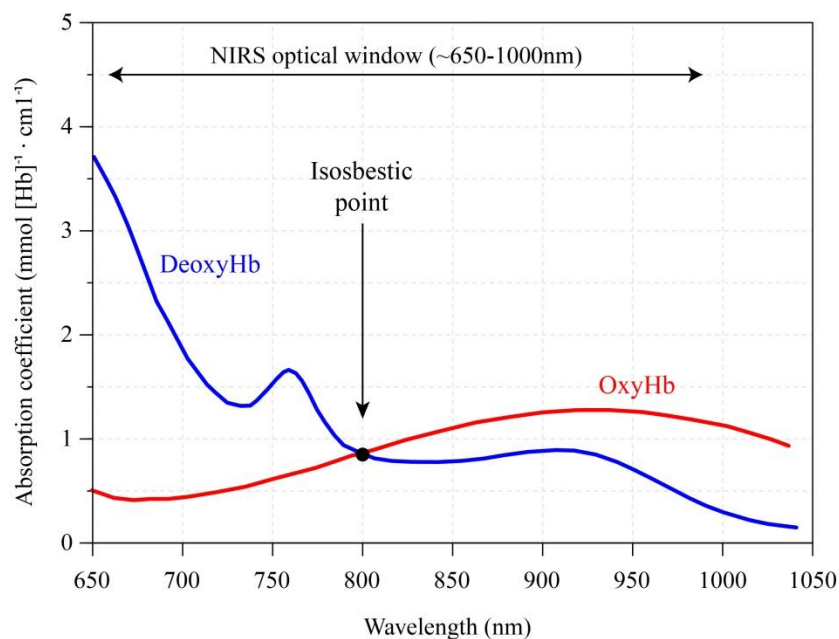
When Jobsis described feasibility of use of NIRS for the detection of the level of tissue oxygenation, he used a CW device. The term CW refers to the fact that the instrument emits the light at a constant intensity and is scattered and absorbed while passing through the tissue and detected again at a constant intensity (Figure 2.2) (Scholkmann, Kleiser et al. 2014).

It is not possible to obtain an absolute value of chromophore concentration using the CW NIRS systems, the CW technology has been widely adopted by neuroscience, because it is possible to estimate the changes in concentration of oxyhemoglobin (oxyHb) and deoxyhemoglobin (deoxyHb) during a brain activation and resting state. Additionally, the CW systems are safe, portable and they use non-ionizing radiation.

As mentioned above the human body consist of chromophores such as deoxyHb, oxyHb, cytochrome C oxidase and water.

Although, these chromophores have generally different absorption spectra in near infrared light, but here is one point, called an isobestic point, where these spectra overlaps themselves. The isobestic point is around wavelength 800 nm, this is important especially for estimation of concentration changes in oxy and deoxyHb (Wray, Cope et al. 1988), (Bakker, Smith et al. 2012)(Figure 2.2).

*Figure 2.2 Absorption spectra for oxy and deoxy haemoglobin*



*This figure presents absorption spectra for oxy and deoxygenated haemoglobin, with the isobestic point at 800 nm at which oxy and deoxyHb have identical absorption coefficients; adapted from (Wray, Cope et al. 1988; Bakker, Smith et al. 2012).*

As shown on the Figure 2.2, the NIR light absorption spectra can be overlapping, and caused a phenomenon of so called “cross talk” between chromophores. To minimize this effect, an appropriate NIR light wavelength should be chosen. Furthermore a differential path length factor (DPF) was introduced by Wray and Cope (Delpy, Cope et al. 1988; Wray, Cope et al. 1988). The DPF accounts for the additional path taken by the scattered light, which is the actual mean distance travelled by NIR light from the source to detector. By knowing the DPF it is possible to calculate the arbitrary chromophore concentration baseline, from which the change in concentration of oxy and deoxyHb can be estimated (Ghosh, Elwell et al. 2012).

Much research was done to estimate which pairs of wavelengths will be the most suitable for oxy and deoxyHb concentration change measurement. For instance, Yamashita, *et al.* (Yamashita, Maki et al. 2001) showed that accurate results can be achieved using the wavelength pair between 664 and 830 nm respectively. Others have shown that paired wavelengths at 690 nm and 830 nm were optimal for reducing of “crosstalk” between oxy and deoxy haemoglobin spectra. Therefore, the NIRS instrumentation should have one emitter with the wavelength below 720 nm and the other emitting the light wavelength above 730 nm (Lloyd-Fox, Blasi et al. 2010).

### 2.1.3 Neurovascular coupling

As discussed above the oxy and deoxyhaemoglobin concentration changes as response to brain activation can be measured using the NIRS technique.

Neurovascular coupling from a morphological point of view, was at least partially explained by Duvernoy, who published in 1981 and 1983 his papers on “Cortical Blood Vessels of the Human Brain” and “The Vascularization of the Human Cerebellar Cortex”, and described in depth the anatomy of the two main vascular systems of the brain: pial and inter-cortical (Duvernoy, Delon et al. 1981; Duvernoy, Delon et al. 1983). The cortical vascularisation consists of three elements: arteries, veins and fine vascular network. The fine vascular network is dense, but also has a layer structure, which mirrors the arrangement of the nerve fibres (Duvernoy, Delon et al. 1981).

The cerebral cortex has been supplied with blood from as described by Dormanns, *et al.* (Dormanns, Brown et al. 2015).

*“The outside inwards, starting at the pia matter into the cortex with penetrating arteries which repeatedly bifurcates from the large root vessel, into the vessels of shorter length and smaller radius. A cerebral vascular tree may comprise up to 20 or more bifurcations. Variation in the resistance of these vascular trees can modify blood flow in a highly localized manner, but also if the resistance of blood vessels in particular region decreases, then blood flow will be diverted through those vessels from other parts of the tree”*

Neurovascular coupling describes the relation between neuronal brain activity and subsequent changes in the regional CBF. The presence of this phenomenon has

been widely accepted by neuro-science community, although, the exact mechanism causing the local changes in brain perfusion following neuronal activation remains unclear. Takano, *et al.* (Takano, Tian et al. 2006) explained the neurovascular coupling from a cell biology point of view and they showed that the astrocytes play an important role in this process due to anatomical and morphological relations of the brain-blood barrier. Apart from astrocytes, also pericytes and interneurons control the CBF (Hillman 2014).

Still, there is lack of consensus, about the exact mechanism leading to cerebral vasodilatation, for instance, Takano *et al.* (Takano, Tian et al. 2006) showed that an increase in the concentration of calcium in astrocytes corresponds with 37% increase in blood flow with the latency of 1-2 seconds post neuronal-activation. Apart from the direct endothelium responses to the increased level of calcium, there are other mechanisms linking neuronal activity and vasodilatation. For instance, because neuronal activity triggers phospholipase A 2 to produce arachidonic acid, the arachidonic acid is then metabolized by the cyclooxygenase COX-1 into a vasodilating prostaglandin (Rossi 2006).

Another model of the neurovascular coupling was proposed by Ostby, *et al.* (Ostby, Oyehaug et al. 2009). It focuses on the importance of potassium influx mediated via astrocytes. This causes shrinkage of the extracellular space following neuronal activity and hence, vasodilatation.

Others proposed that, pericytes can cause vasodilatation as response to bradykinin and histamine, while the interneurons respond to acetylcholine, additionally the interneurons can modulate the astrocytes and pericytes activity (Hillman 2014)

As shown above the neurovascular model is complex and can be explained from functional and morphological point of view. Also several components contribute to this model, namely, neurons, the synaptic cleft, the astrocyte, the perivascular space, the smooth muscle, the endothelial compartments and the arteriolar lumen (Dormanns, Brown et al. 2015)

The neurovascular coupling theory attempts to explain the fMRI technique. The fMRI detects blood flow by detecting changes in concentration of deoxyHb, which is a paramagnetic. Ogawa, *et al.* (Ogawa and Lee 1990) developed a theory of a blood oxygenation level dependent signal (BOLD), which increases with decreasing concentration of deoxyHb.

The BOLD signal may result from or be dependent on several factors such as Cerebral Metabolic Rate of Oxygen, CBF, deoxyHb and oxyHb concentration or concentration of total Haemoglobin. The biophysical model describing these variables is called a “venous balloon”. The venous balloon occurs secondary to changes in CBF, in particular to a change in deoxyHb concentration, which is the main component of the BOLD signal (Steinbrink, Villringer et al. 2006). However, this model is still under evaluation, because according to Steinbrink (Steinbrink, Villringer et al. 2006), this model assumes that only the venous balloon feeds into the changes of the cerebral blood and it mainly relaying deoxyHb concentration. There may be other, however, variables contributing to the cerebral blood flow such as arterial inflow, volume of the cerebral compartment or the venous outflow.

The venous outflow ( $\dot{V}_{out}(t)$ ) is dependent on venous compliance with different values for inflation and deflation. An equation below explains how the venous outflow is related to the volume, defined by Grubb as  $v = \int_{out}^{\infty}$  with  $\alpha = 0.36$  (Steinbrink, Villringer et al. 2006) and its relation between the volume and the viscoelastic time ( $\alpha$ ),

which value differs depending on increased or decreased CBV. This induces a fundamental nonlinearity, which is strong enough to create a detectable BOLD signal, according to Equation 2.3.

$$\int out(t) = v \frac{1}{\alpha} + a \mp dv/dt$$

*Equation 2.3 Formula for derivation of Blood Oxygen Level Dependent signal.*

Furthermore, S-G Kim and S Ogawa (Kim and Ogawa 2012) characterised the BOLD signal by both prolonged positive and a prolonged negative response. A prolonged positive response is “ where stimulus induced signals evokes a higher than baseline signal and in the same way the negative BOLD signal is when the signal is lower than a baseline i.e. an initial dip or post-stimulus undershoots. The observed phenomenon of post-stimuli negative BOLD may be explained by several factors including: decrease in CBF due to neural inhibition or redistribution of regional CBF into nearby active regions, therefore, the negative BOLD signal depends on stimulus type and brain region as well (Kim and Ogawa 2012).

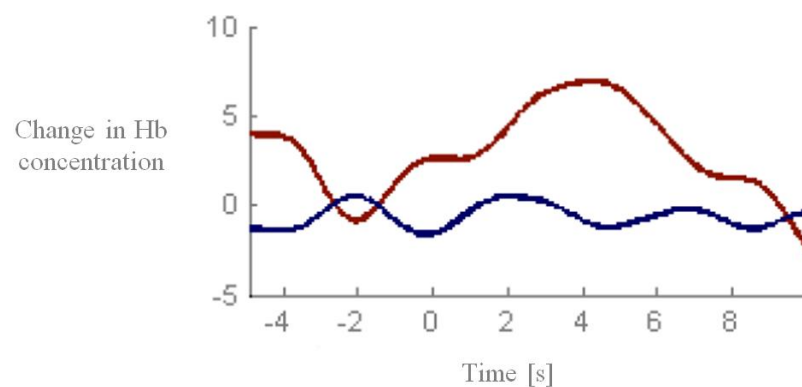
The BOLD signal can be also modulated by arterial pressure of carbon dioxide and oxygen but also other systemic factors such as the intake of certain drugs or post caffeine or alcohol consumption. Additionally the haemodynamic response is sensitive to age and has an identifiable resting-state fluctuations pattern (Kim and Ogawa 2012).

Similar to the BOLD signal the neuronal activation of the brain can be detected using the functional NIRS. The most typical pattern of a haemodynamic response to stimulation is shown on the Figure 2.3 showing an increase in concentration of oxyHb along with decrease in deoxyHb during the brain activation, during a motor task lasting

7 seconds (own data, right hand movement, control subjects,). Changes in concentration of oxyHb are usually several times stronger than changes in concentration of deoxyHb, also the NIRS response characterises a delay from onset to peak, on average 2s (Huppert, Hoge et al. 2006).

Notwithstanding, the use of BOLD signal has been considered as a gold standard for quantifying the NIRS derived functional responses (Dunn, Nathoo et al. 2014).

*Figure 2.3 Typical pattern of haemodynamic response to a motor task*



*This figure presents a typical pattern of haemodynamic response to a motor task (squeezing a ball, self-paced) with an increase in Oxy-hemoglobin (red line) and decrease in deoxyhemoglobin (blue line), y axis denotes the changes in concentration of oxy-deoxyHb in  $\mu\text{Mol/L}$ , x axis denotes time in seconds (own data collected for this study, a male control subject; 38 years old, right handed, NIRS signal collected from left parietal area).*

The exact shape of the haemodynamic response measured by NIRS is still under evaluation. So far, many studies have confirmed that using NIRS, it was possible to detect haemoglobin concentration changes during volitional brain activation.

However, there are potentially some other variables contributing to the detected changes of the NIRS signal, for instance, extra-cerebral or skin arteries and veins that can influence the NIRS results.

Two major components contributing to the NIRS signal can be distinguished: namely cerebral and extra cerebral CBF and with former further division into the evoked response to a stimuli and a background CBF (Scholkmann, Kleiser et al. 2014) (Table 2.1).

*Table 2.1 Classification of haemodynamic components of near infrared spectroscopy.*

Evoked NIRS response		Non-evoked NIRS response		
	Neuronal	Systemic	Neuronal	Systemic
<b>Cerebral</b>	Functional brain activity	changes in blood pressure, CBV	Spontaneous brain activity –resting state functional connectivity	Systemic activity type 3- heart rate, respiration, Mayer waves, very low frequency oscillations
<b>Extra-cerebral</b>	-	changes in blood pressure, skin blood volume	-	Systemic activity – extra-cerebral

*This table presents classification of haemodynamic components of near infrared spectroscopy (NIRS) detected from the human scalp, modified by A. Kempny from Scholkmann et al. (Scholkmann, Kleiser et al. 2014).*

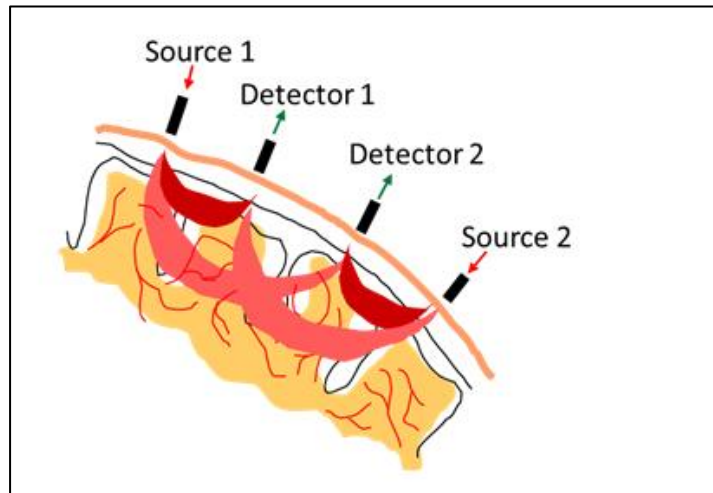
The haemodynamic responses listed in table 2.1 are linked together and it is a challenge to separate the signals originating in the cerebral cortex from the extra cerebral one. Gagnon, *et al.* (Gagnon, Yucel et al. 2012) in their study investigated the effect of the pial veins and their influence on the NIRS signal detected over the motor cortex. They quantified cortical and pial vein contribution to the NIRS response using a Monte Carlo

simulation and showed that the cortical contribution of the oxyHb change was equal 80% of the cortical contribution to the total haemoglobin change and the cortical contribution to the DeoxyHb changes was 20% of the cortical contribution to the total haemoglobin change. Therefore, the authors suggested, that the total haemoglobin change should be used to map the cortical changes using NIRS, because is less sensitive to extra cerebral blood flow from the pial matter (Gagnon, Yucel et al. 2012). However, others showed that deoxyHb is mostly correlated with the BOLD signal from fMRI (Huppert, Hoge et al. 2006).

Also emotional processes can affect peripheral physiology by influencing a heart rate, respiration, blood pressure and skin perspiration and, hence, can affect the NIRS measurements (Minati, Kress et al. 2011).

All of these physiological processes can contribute to NIRS signal attenuation while the NIR light is passing the several tissue layers such as: skin, skull, dura mater, arachnoid mater, pia matter before it finally reaches the cerebral cortex. The NIR light forms a theoretical banana shape between NIR light source and a NIR light detector (Figure 2.4). It was shown that the elliptical photon distribution and its mean depth is proportional to separation of the optodes by a factor  $\sim 1/3$ , so it would minimize the effect of extracebral tissue (Murkin and Arango 2009).

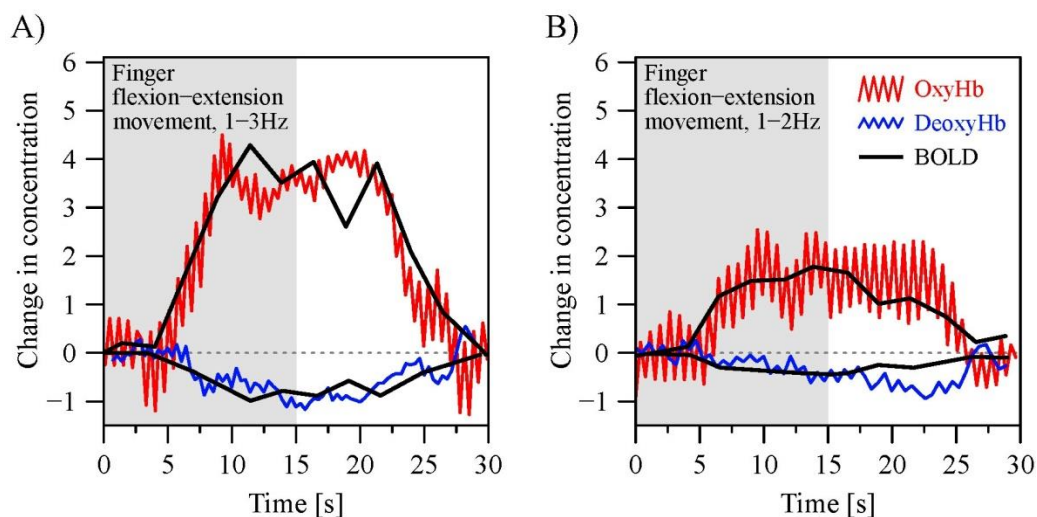
Figure 2.4 Near Infrared Spectroscopy - basic principles



*This figure presents a basic principle of Near Infrared Spectroscopy. NIRS light that is shone into the tissue forms a banana shaped beam and is detected by a NIR light detector. The pink and red shapes indicate that with the increased distance between a source and detector, the deeper light penetration can be achieved. Source: <http://nirx.net/fnirs-and-nirx/>; picture by the NIRS vendor providing equipment used in this study.*

As discussed above, the NIRS and fMRI techniques share some similarities because both techniques can detect changes in concentration of deoxyHb in response to the brain activation, either as in fMRI by detection of the ferromagnetic changes in deoxyHb or as in NIRS by detection of the differences in light absorption. Studies comparing haemodynamic response detected by these two techniques showed high correlation level between these responses, for instance, Strangman *et al.* (Strangman, Culver et al. 2002), showed not only spatial correspondence between NIRS and fMRI responses, but also a similar amplitude of the hemodynamic responses, but with the high inter-subject variability (Figure 2.5)

Figure 2.5 Near Infrared Spectroscopy and Blood Oxygen Level Dependent response to a motor task



This figure represents Near Infrared Spectroscopy for oxyhemoglobin (OxyHb) and deoxyhemoglobin (DeoxyHb) as well as Blood Oxygen Level Dependent (BOLD) response to a motor tasks using different motor task frequency; the task was finger flexion-extension; Figure adapted from Strangman et al. (Strangman, Culver et al. 2002).

Unlike, the fMRI technique, the NIRS measures concentration changes in both oxygenated- and deoxygenated haemoglobin, has better temporal resolution and the NIRS can be easier in management. However, the NIRS is inferior to fMRI in some aspects, for instance, because of lower spatial resolution and decreased signal-to-noise ratio (Cui, Bray et al. 2011)

## **2.2 Electroencephalography for assessment of Brain Function**

### ***2.2.1 Standard Electroencephalography***

EEG assesses the electrical activity of the brain. The dominant EEG rhythm in healthy adults is alpha rhythm. Alpha activity refers to the frequency range of from 8 to 13 Hz, which is seen mainly over the occipital regions. Alpha activity attenuates with attention (opening eyes, mental activity). The usual alpha wave amplitude is in the range 20 to 60 microvolts ( $\mu\text{V}$ ). Other frequencies in human EEG are beta (15-30 Hz), theta (4-7.5 Hz) and delta (1-3 Hz) rhythms. The delta and theta waves are “slow waves” and they occur during physiological sleep and drowsiness, if they occur in excess or in awoken adults, they are abnormal.

The EEG background activity changes after severe brain injury. In 1988 Synek (Synek 1988) reviewed the EEG features that can occur in diffuse anoxic and traumatic encephalopathies in adults and suggested a five grade prognostication scale, where grade 1 indicates higher likelihood of favourable outcomes while the grade 5 almost certainly a poor outcome defined as death or VS (Table 2.2).

Table 2.2 Prognostic significance of standard EEG

Prognostic significance of EEG in anoxic and traumatic brain injury	
<b>Grade 1</b>	Alpha rhythm activity, some scattered activity of theta band, a patient can be roused
<b>Grade 2</b>	Dominant activity in theta band, with some alpha and delta,
<b>Grade 3</b>	Dominant widespread delta activity, reactive to external stimulation,
<b>Grade 4</b>	Frequent isoelectric intervals lasting more than 1 sec, with burst suppression pattern, Or alpha coma- 8-12 Hz activity frontal, not reactive to any external stimulation, or theta pattern coma – usually after severe brain trauma or hypoxia after cardiorespiratory arrest,
<b>Grade 5</b>	Complete absence of EEG activity while using a maximal gain (2 $\mu$ V/mm)

*This table presents prognostic significance of standard EEG in coma after anoxic or traumatic brain injury, modified from Synek (Synek 1988).*

Bagnato, *et al.* (Bagnato, Boccagni *et al.* 2010) used the above-mentioned criteria to determine the prognosis in traumatic and non-traumatic cases of DOC following coma. In their study, 40 patients with pDOC underwent several standard EEG recordings over the period of three months. The EEG findings were correlated with the behavioural responses from the pDOC patients. These behavioural responses were classified according to the Level of functioning scale also known as Rancho Los Amigos scale from level one – no response to external stimuli to level 8 purposeful and appropriate response to external stimuli (Wilcox and Stauffer 1972). Bagnato showed that the standard EEG may be useful in predicting the cognitive outcome in pDOC patients, especially in patients post traumatic brain injury.

Another study of resting state EEG (Fingelkurts, Bagnato *et al.* 2011) assessed the potential prognostic value of resting EEG with regard to the clinical outcome after brain

injury irrespective of ethology and the authors found that a slow EEG background activity, such as delta and theta rhythm has a prognostic value for predicting poor outcome (death) at 6 months' time post injury.

### ***2.2.2 Cognitive Potentials derived from standard Electroencephalography***

Pfurtscheller and Lopes da Silvia (Pfurtscheller and Lopes da Silva 1999) in their publication "Event-related EEG/MEG synchronization and desynchronization: basic principles" described an EEG phenomenon occurring during motor imagery and motor movement. They reported that during motor movement and/or during motor imagery over the sensorimotor cortex (C3 and C4 EEG standard International 10-20 position), the EEG within certain frequency bands (alfa and theta) changes in amplitude. These changes of EEG may be either the desynchronizations, which is a decrease in power or synchronizations, which is an increase in power. Because, these changes occur as a response to an event, they were called an event related desynchronization (ERD) and event related synchronization (ERS).

The ERD and ERS are expressed as a percentage of EEG power change during an event (for instance three seconds of movement imagery) in relation to a pre-stimulus baseline.

The ERD calculation formula is as follows (Pfurtscheller and Lopes da Silva 1999).

$$ERD\% = \frac{A - R}{A} * 100\%$$

*Equation 2.4 Formula for assessment event related desynchronization.*

where 'A' is the baseline EEG power and 'R' is the EEG power during the event (Pfurtscheller and Lopes da Silva 1999).

Applying this formula to the EEG signal the ERD as a percentage value where %ERD <0 corresponds to ERD and a %ERS>0 corresponds to ERS.

Interestingly, during a motor imagery and motor movement, both phenomena occur, but they are spatially separated. The ERD was defined as 'focal phenomenon surrounded by ERS', which was explained as a focal activation (ERD) surrounded by an inhibition (ERS). Further extension to this interpretation would be, that a thalamo-cortical mechanism facilitate a focal cortical activation ("focal ERD") by a simultaneous deactivation or inhibition of surrounding cortical areas (Neuper, Wortz et al. 2006).

Hans Berger, who discovered EEG in 1929, indeed also discovered event related potentials (ERP), however, he thought that these were an artefact (Luck 2005). Later, it become apparent that the ERPs exist and that they represent the brain electrical activity changes in response to sensory stimuli such as auditory, visual or tactile (Sur and Sinha 2009). Not only sensory stimuli can evoke an event related response, but also cognitive stimuli, in particular response to language, (Van Petten and Kutas 1991), furthermore, also a semantic (unexpected word) or physical (male vs female voice) incongruities can evoke an ERP response (McCallum, Farmer et al. 1984).

The general approach to design an ERP paradigm would be to present frequent stimuli (for instance 80% of other first names) and rare stimuli (for instance 20% of own name). Sounds, words, phrases or visual stimuli can be used. The human brain will develop a stronger ERP towards on odd or infrequent stimuli around 300 ms post stimuli (Luck 2005).

The clinical use of these techniques on pDOC patients will be discussed in Chapter 3.

## Chapter Three

## **CHAPTER 3 GENERAL METHODS**

The aim of this chapter is to discuss the research methods used in this study.

The research methods I have used to assess awareness in pDOC patients encompass both the behavioural assessments and physiological approaches for brain function assessment the NIRS and EEG techniques. The traditional established behavioural approach relies on using validated tools such as: Wessex Head Injury Matrix (WHIM), the Coma Recovery Scale-Revised (CRS-R) and the SMART. The psychometrics of these scales will be discussed in this chapter. In addition to the behavioural assessment, both the EEG and NIRS techniques were used. The brain function in pDOC patients was assessed using both active and passive paradigms. In active paradigms, the patients were asked to actively imagine squeezing own right hand, while in passive paradigms, the patients were asked to listen to pre-recorded names. The results obtained from the pDOC patients were compared to the results from the healthy controls. The results of NIRS and EEG are presented and discussed in Chapters 5-8.

### **3.1 Behavioural scales used for detection of awareness in pDOC**

All patients included in the study had an acquired, global and severe brain injury and met the criteria of disorders of consciousness or prolonged disorders of consciousness. The diagnosis of VS or MCS was made based on the results of the bedside, behavioural tests.

The diagnosis of VS or MCS made using behavioural assessments depends on patients' ability to follow commands or ability to respond to environmental stimuli. These commands may be the verbal such as "look at me", "show me how to use a pen", while the ability to respond to stimuli includes the use of the painful stimuli or various sensory stimuli such as light shone into an eye, touch, should tap etc. or by observing the patient's responses to painful stimuli.

Previously, the assessment was less formal and depended on an assessor experience; however, studies showed almost 50 percentage misdiagnosis if the behavioural assessment of pDOC was not structured (Andrews, Murphy et al. 1996; Schnakers, Vanhaudenhuyse et al. 2009). The first study that showed the problem of misdiagnosis was performed by Keith Andrews (Andrews, Murphy et al. 1996) on the patients admitted to the Royal Hospital for Neuro-disability in which it was shown that without a multi-disciplinary team approach and without using the validated tools for assessment of brain function up to 40% patients were not correctly diagnosed with VS and indeed many were reclassified as at least MCS.

Hence, the RCP in their National Clinical Guidelines from 2013 strongly recommend using validated behavioural scales for assessment of pDOC patients, because not only do they help to reduce the diagnostic errors, but they also provide a baseline for monitoring of emergence of consciousness or behavioural changes over time. In particular, the RCP suggest using one or more of the following scales to diagnose and monitor people with pDOC: the WHIM, the CRS-R and the SMART (Royal College of Physicians 2013).

These scales are validated, which means that their psychometric features, including validity, predictive validity, reliability and responsiveness have been determined.

Validity refers to the accuracy of a measure, i.e. whether a scale measures what it is supposed to measure. For example, the scales used for awareness detection should help with stratifying the responses to stimuli into two main categories: reflexive or cortically mediated responses and this should help to make the diagnosis of VS or MCS, with cortically mediated responses occurring in the latter patient group. The predictive validity refers to the degree to which a scale predicts clinical outcome. The convergent validity measures correlation between two measures, for instance, the convergent validity between the two different measures for pDOC assessment. Finally, the discriminant validity, describes how measure can discriminate between two conditions, which can be similar in presentation but only one should be measured, for instance, in pDOC patients a scale should measure responses to external stimuli and based on this, a diagnosis of VS or MCS should be established, however, the responses to external stimuli can be diminished during an acute deterioration in general conditions, due to for example, septicæmias.

The reliability refers to the consistency of a measure i.e. it should give the same or very similar results, regardless of when it is used and who is using it. Reliability has two components, first is called an intra-rater reliability, which occurs when the same assessor assesses the same patient in a stable condition on different occasions and the measure shows the same or a very similar result. The second aspect is inter-rater reliability. This is when two different assessors assess the same patient, and the measure shows the result or very similar result.

The reliability can be measured by using a correlation Kappa. If Kappa equals Zero this means there is a random agreement, or no agreement, hence, that a measure is not reliable. If Kappa equals one then there is a perfect agreement. It has been suggested that the Kappa result be interpreted as follows: values of 0 indicate no agreement and values in the range 0.01–0.20 as showing no to slight agreement, values in the range

0.21–0.40 as fair agreement, values in the range 0.41– 0.60 as moderate agreement, values in the range 0.61–0.80 as substantial agreement, and values in the range 0.81–1.00 as almost perfect agreement (McHugh 2012).

Seel, *et al.* (Seel, Sherer et al. 2010) reviewed the commonly used tools for assessment of awareness. The authors provided an evidence based recommendation on reliability, diagnostic validity and ability to predict functional outcomes. The review examined the 37 publications concerning 13 different scales such: CRS-R, SMART, WHIM also the Western Neuro Sensory Stimulation Profile, Sensory Stimulation Assessment Measure and Coma/Near Coma (CNC) and others.

The first scale introduced for assessment of comatose patients was the Glasgow Coma Scale (GCS) by Teasdale and Jennett in 1974. Initially the GCS was designed for clinical assessment of then post-traumatic unconsciousness only, however, since then has been widely used in acute and sub-acute settings for monitoring of consciousness. Nevertheless, its validity for discrimination between VS from MCS patients and for monitoring of emergence of consciousness was questioned (Schnakers, Giacino et al. 2007).

Based on the GCS and its structural design, another scale has been developed – the CRS-R. In this study the CRS-R scale (Giacino, Kalmar et al. 2004) was used to discriminate patients into two groups – VS and MCS. The structure of the CRS-R is similar to the GCS scale and it includes visual, motor and verbal tasks. Additionally, CRS-R assesses the auditory and communication responses and scores a patient's arousal as well. The scoring is based on presence or absence of specific behavioural responses to sensory stimuli and can range from zero to 23, where the score from zero to ten denotes VS, from 11 to 21 denotes MCS and between 21 to 23 emergence from

MCS. Each modality is scored hierarchically starting from reflexive responses (for example: flaccid/no response to pain) to cortically mediated (for example: functional use of items). The functional use of an object and accurate communication denote emergence from the MCS. The scale identifies a portfolio of patients' behaviours indicating diagnosis of MCS or above, for instance, consistent and reproducible movement to command, object recognition and object reaching, visual pursuit using a mirror and fixation at the bright coloured cards, further on the motor scale localisation to noxious stimulation, an object manipulation. The CRS-R also scores attention and communication.

The CRS-R similarly captures the reflexive behaviours for instance: startle responses, reflexive response to pain and to oral stimulation. A study performed on 80 patients showed a good psychometric integrity of the CRS-R including a very good reliability, with the adequate intra-rater correlation ( $k=.60$ ,  $p=.03$ ), and better correlation for a single rater on two occasions ( $k=.82$ ,  $p<.004$ ). Overall rate of inter-rater agreement of was 87.5%., (Spearman  $\rho=.94$ ) (Giacino, Kalmar et al. 2004).

Another scale used in this study was SMART, which consists of both formal and informal components. The formal component consists of ten sessions of both the behavioural observations and assessment of patients' responses to sensory stimuli. In addition, the patient's family contributes during the assessment by providing a "life style questionnaire", which encompasses questions about the premorbid life, hobbies, favourite food or music, important places and people, so that the therapy team can use this knowledge to tailor the individualised assessment programme. Using the formal part of the SMART scale an assessor evaluates patient's responses within sensory system and scores them according to the five points- scale as follows: level 1 = no response, 2 = reflexive response, 3 = withdrawal response, 4 = localising response, 5 = response to command. A consistent response at SMART level 5 (on 5 or more consecutive sessions) indicates patients' awareness. SMART was evaluated and a study

showed a significant correlation between SMART and Western Neuro Sensory Stimulation Profile scores ( $r = 0.70$ ), with a very high intra and inter-observer correlation 0.97 and 0.96, respectively (Gill-Thwaites and Munday 2004).

The third scale used in this study, is the WHIM, developed by Shiel, *et al.* (Shiel, Horn et al. 2000). This is based on clinical observations of behaviours occurring spontaneously or in response to stimulation in patients during the recovery from a coma. The portfolio/repertoire of their behaviours had been summarised and categorised into the WHIM scale. The authors identified 62 behaviours occurring during the recovery time, and they are listed in the hierarchical order, some of the behaviours are as simple as “eyes open briefly”, while other are more complex, for instance, “remembers something from earlier in the day”.

The WHIM scale reliability was initially tested on small group of pDOC patients ( $n=25$ ). The mean kappa scores were 0.86 for inter-rater reliability and 0.74 for test-retest reliability. Thus there was an excellent agreement between two raters in regard to the score of behaviours, and substantial consistent between scores for the same subjects but on different occasions (Shiel, Horn et al. 2000).

More recently, Turner-Stokes *et al.* (Turner-Stokes, Bassett et al. 2015) reviewed the use of WHIM in pDOC patients, and correlated the retrospective data with the most advanced behaviours and with the diagnostic validity of the tool. The WHIM was shown to be a valid tool for patients’ stratifications into the diagnostic group (VS versus MCS vs emergence from pDOC).

These three scales, the SMART, WHIM and CRS-R, as discussed above, assess the pDOC patients' behaviours and how they respond to environmental stimuli (Table 3.1)

*Table 3.1 Summary of the behaviours observed on SMART, WHIM and CRS-R*

	Observed behaviours								
	Eye movements	Blink to light and pupils light reaction	Eye contact	Arousal protocols	Following verbal instruction	Tactile response, ie tap shoulder or discrimination two tactile stimuli	Vocalisation	Functional activity ie using a pen or a comb	Response to olfactory stimuli
WHIM	Yes	Yes	Yes	Yes	Yes	No	No	Yes	No
CRS-R	Yes	Yes	Yes	Yes	Yes	No	Yes	Yes	No
SMART	Yes	Yes	Yes	Yes	Yes	Yes	Yes	Yes	Yes

*This table describes various behavioural responses monitored by using the three main scales used for assessment of pDOC patients, modified from Royal College of Physical guidance "The Prolonged disorders of consciousness national clinical guidelines" (RCP 2013)*

Nevertheless, even if the best standardised tools (WHIM, SMART and CRS-R) are used, approximately ten percent of pDOC patients are misdiagnosed, in particular those who are diagnosed as being in Vegetative state. These patients are not able to respond behaviourally to any of these scales. Interestingly, these patients may be able to exhibit strong brain response to a command "imagine you are playing tennis" from a motor

cortex and to a command “imaging walking around your house” from a parahippocampal using the fMRI (Monti, Vanhaudenhuyse et al. 2010).

Other studies showed that also other techniques such as EEG can be used for bedside detection of brain function in pDOC patients (Bruno, Vanhaudenhuyse et al. 2011).

### **3.2 Near Infrared Spectroscopy**

The use of NIRS in medicine and neuroscience has been discussed in Chapter 2. For the purpose of this study, a NIRS laboratory has been established at the Royal Hospital for Neuro-disability, Putney, London.

All NIRS measurements were performed using a NIRScout system (*NIRx Medical Technologies LLC, Berlin, Germany*) (Figure 3.1).

*Figure 3.1 Near Infrared Spectroscopy laboratory*



*This figure presents a Near Infrared Spectroscopy and Electroencephalography systems as a mobile units built for the purpose of this PhD study at the Royal Hospital for Neuro-disability; A) both systems NIRS and EEG; B) NIRS unit*

As discussed in Chapter 2 a DPF was used to account for the NIR light scattering and hence, to allow establish an arbitrary baseline of oxy and deoxy Hb concentration and relative changes in oxy and deoxyHb changes during brain activation.

As showed by Hiroaka, *et al.* (Hiraoka, Firbank et al. 1993) the modified Beer-Lambert law underestimates the concentration change and to correct for this underestimation the DPF should be used. Several studies have shown that the data analysis without implementing of the DPF led to approximately 15% error in estimation of the

concentration changes for an individual subject (Duncan, Meek et al. 1995; Matcher, Elwell et al. 1995).

For this study the corrector factors not only DPF but also epsilon for oxyHb and deoxyHb, as suggested by NIRx were used (Table 3.1). The light emitters emitted two-wavelength NIR namely 730 nm and 850 nm, because of the minimal cross talk between these two wavelengths, as discussed in Chapter 2.

*Table 3.2 Wavelengths, the differential pathlength factor and epsilon of NIRS system*

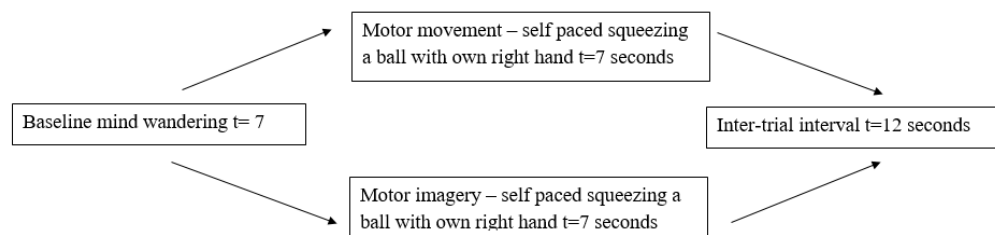
<b>Wavelength</b>	<b>DPF</b>	<b>Epsilon oxyHb</b>	<b>Epsilon deoxyHb</b>
730 nm	7.15	1.4866	3.8437
850 nm	5.98	2.5264	1.7986

*This table presents the wavelengths, the differential pathlength factor (DPF) and an epsilon separate for oxy and deoxyHb respectively. This was a specification of the NIRS system used in this PhD study for estimation of the haemoglobin concentration changes.*

As discussed in detail in Chapter 2, the haemodynamic response to the stimulus consists of two components, the direct, evoked response to the stimuli and a background brain spontaneous activity. The haemodynamic response secondary to the cerebral neuronal activity can be detected using CW NIRS and expressed as a difference between resting state and activation giving the readings of  $\Delta \sim 0.5 \mu\text{M}$  for oxyHb and  $\Delta \sim 0.2 \mu\text{M}$  for deoxyHb respectively (Wolf, Wolf et al. 2002).

The experiment used in this study relied on activation of the motor cortex. This type of paradigm has been called “active”, because it requires a subject’s active participation in the task. The paradigm was a block design with periods of rest intermittent interspersed with the tasks, either a motor imagery or actual motor movement (Figure 3.2), (results please see Chapter 5)

*Figure 3.2 Motor task experiments*



*This figure presents an overview on the motor task experiment, participants were asked to imagine squeezing a ball with own right hand. The controls underwent the both arms of the paradigm; first, the actual movement, followed next by imagery.*

The NIRS system performed dual-wavelength CW near infrared tomographic measurements at a 10.42 Hz sampling rate. The device emits light at 2 distinct wavelengths, 760 and 850 nm, for discrimination of two oxygenation states of tissue. Changes in oxy and deoxyHb concentration were analysed separately, giving in total 32 channels. The inter- optode distance was 2.5 cm. As shown in Chapter 2, Figure 2.4, the NIR light forms a hypothetical “banana” shape when travels through the tissue. The general rule is such that with increase the inter-optodes distance, the depth of NIR light penetration increases, hence, the likelihood of NIR light reaching the cortex increases,

however, there is on balance, also higher noise ratio. It was found that the most recommended inter-optode distance is from 2.5 to 3.5 cm (Strangman, Li et al. 2013).

The optodes were placed using the Waveguard cap (*ANT Neuro, The Netherlands*) and secured by using a dedicated black fabric cap. The raw NIRS data were converted into a readable Matlab format using Nilab2 software (NIRx Medical Technologies LLC). The data were low-pass filtered to remove the high frequency signal ~0.3 Hz breathing and 1 Hz heart rate. Low frequency (less than 0.01 Hz) vascular or metabolic oscillations were removed by using a high frequency cut-off filter of 32 sec (0.03 Hz). Then using the modified Beer-Lambert law as described by Delpy (Scholkmann, Kleiser et al. 2014) changes in both oxy and deoxyHb concentration (expressed in  $\mu\text{Mol/l}$ ) were calculated. The data was mean-corrected so that, at each time-point, the value represents the amplitude minus the average for the entire record for each channel.

### **3.3 Electroencephalography**

As discussed in detail in the Chapter 2, EEG data can add important information about the patients' brain function. The EEG technique has well-established role in research on disorders of consciousness; however, some of the previous studies used complex protocols and data analysis approach.

In this study, the EEG was used to assess brain function in pDOC patients in two experiments. The first EEG experiment assessed the brain responses to a motor task such as “imagine you are squeezing your hand”, which is called an “active” paradigm. The second EEG experiment was an ERP paradigm, where the patients were asked to

listen to the pre-recorded names. This experiment is called a “passive” paradigm, because it did not require an active patient’s participation.

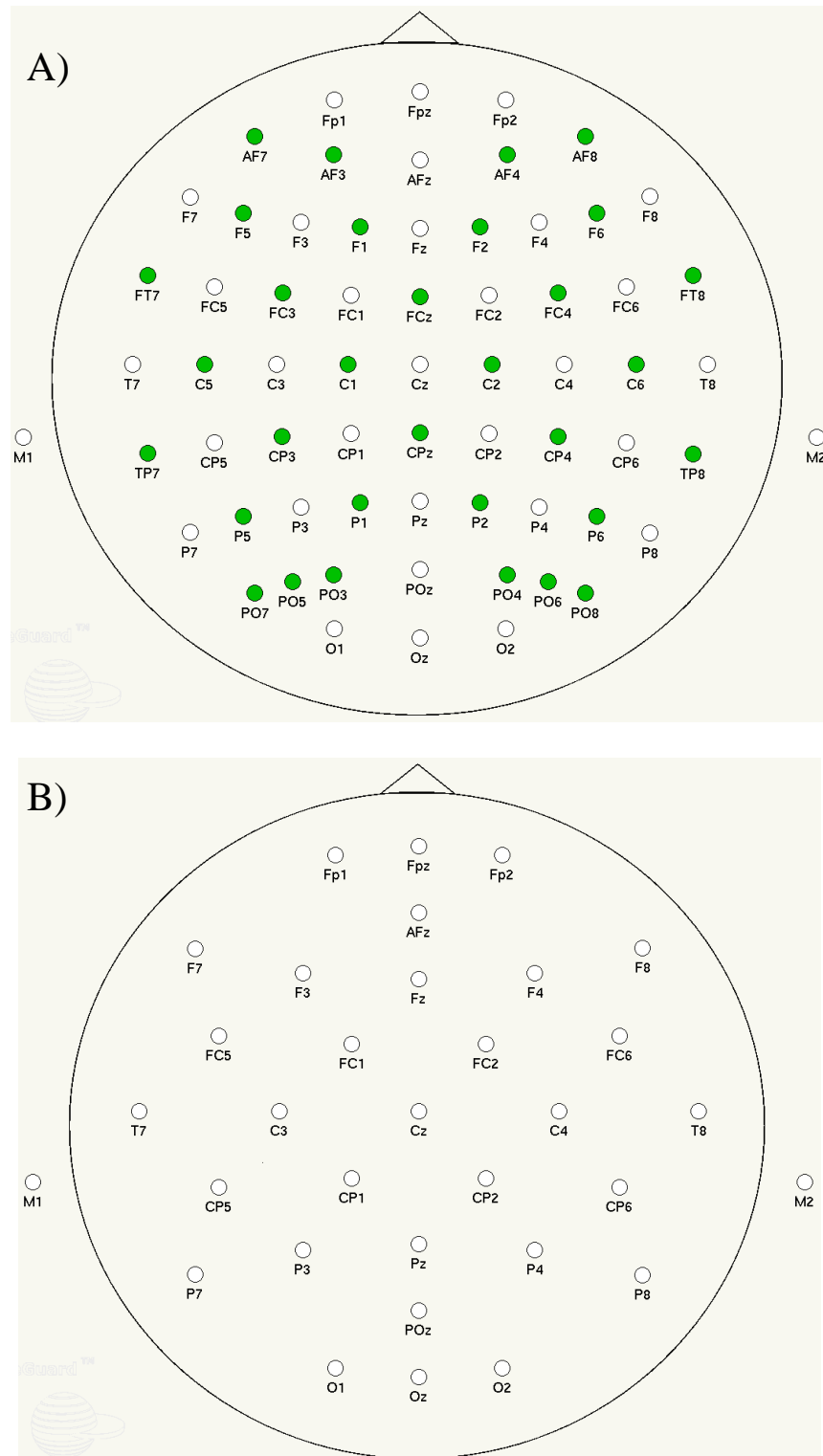
The EEG in this study was acquired using an Asalab system and a Waveguard 64 EEG sensor-cap (*ANT-Neuro, Enscheda, the Netherlands*) (Figure 3.3) and the EEG 32 and 62 sensor position according to the 20-10 and 10-10 systems (Figure 3.4).

Figure 3.3 The 64 electrode EEG cap



*This figure presents the 64 electrode EEG cap used in this PhD study: A frontal view, B top view, C lateral view and D the view on the single EEG electrode*

Figure 3.4 EEG layouts used in the PhD study



This figure EEG layout, A) the 64 EEG sensor layout, I used in this study for the name paradigm, B) the 32 EEG sensor layout, I used in this study for the motor task paradigm (the figures provided by the ANT Neuro).

### ***3.3.1 Motor paradigm***

As mentioned in Chapter 2 of this thesis, during both movement and an imagery of the movement, the EEG produces the ERS or ERD. These phenomena occur during the activation of the motor cortex and either slow down the EEG rhythm (ERD) or increase in frequency of EEG (ERS).

If a patient is not able to behaviourally respond to a command, for instance, “make a fist or squeeze your hand”, but the EEG shows changes such as ERD or ERS, then it can be argued that this patient tried to follow a motor command. This could potentially mean that this patient thought about the movement, was trying to imagine that she /he is squeezing their hands.

The motor imagery paradigm was implemented in both techniques: the EEG and NIRS signal (Figure 3.2), however, for the EEG the number of loops was higher. While in the NIRS paradigm 30 repetitions were used, in the EEG paradigm 120 repetitions of the motor task were needed to evoke the EEG changes.

The same EEG system was used for the name paradigm and for the motor imagery paradigm, however, in the motor paradigm, the EEG was recorded from four sensor positions, F4, F3, C4 and C3 (according to the 10-20 EEG system position placement). The EEG sensors were configured in a bipolar montage. For the purposes of this study, electrode positions C4 and C3 were referenced to F4 and F3 respectively. The online filtering regime was 0.53-40 Hz, without mains suppression; taken at a sampling rate of 1024 Hz. online sensitivity was set to 70  $\mu\text{V}/\text{cm}$ .

ERD was calculated at alpha (7-11 Hz). In order to measure the ERD, pre-processing steps were performed. The EEG was subjected to artefact rejection protocols, where the EEG signal was run through an amplitude window of  $\pm 150 \mu\text{V}$  and potentials in the

EEG, which were in excess of this amplitude was rejected. This ensured that ocular artefacts were excluded from the EEG signal. The EEG was subjected to direct current flow removal, which excluded the slow drifts in the EEG caused by scalp potentials. The EEG was then segmented according to the event marker types in order to define the Epoch type. Three epoch types were defined: i) Motor imagery, ii) Mind wandering and iii) Resting state. The epoch was set at 3 seconds before the event and 5 seconds after the event, thus the total event duration was 8 seconds. The reference baseline, from which the % ERD would be calculated, was defined at -1 second up to time zero. The EEG signal was then subjected to band pass filtering. For the alpha band, a band pass of 7-11 Hz was adopted using an FIR filter at a slope of 24 dB. The final processing step required the calculation of the amplitude envelope. The full power spectra were made available through full wave rectification prior to imposing the Hilbert transform onto the EEG signal.

The ERD was calculated according to the procedure defined by Pfurtscheller and described in detail in Chapter 2 of this thesis (Pfurtscheller and Lopes da Silva 1999).

### ***3.3.2 Own Subject Name Paradigm***

In this study EEG responses to subjects' own name in healthy controls and pDOC patients were evaluated. The theoretical background for the cognitive evoked related potentials was outlined in Chapter 2 of this work. I used three types of the auditory stimuli; the subject's own name, other first names and reversed names. Because both: the subject's own name and the other names are auditory stimuli carrying information, while the reversed names, are the "non-sense" sounds. By contrasting the brain response to own name vs other names and own name vs reversed name, it would be possible to evaluate the different aspects of the brain function.

I aimed to answer two main questions in this study: i) if the EEG response was different towards subject own name vs. reversed and/or from the EEG response to subject own name vs other names, ii) if the responses were different, this could potentially mean that the subject was able to discriminate between own name vs other names

The results of this study are in Chapter 8 of this thesis.

The EEG was acquired using a Waveguard 64 EEG sensor cap (ANT Neuro) (Figure 3.4), whose standard sensor positions were derived from the 10-20 system (Jasper, 1958) and additional positions being determined from the 10-10 electrode placement system. In this study, EEG was recorded from 64 sensor positions. The EEG sensors were configured in a bipolar montage. The online filtering regime was 0.53-40 Hz, without mains suppression, taken at a sampling rate of 512 Hz.

Online sensitivity was set to 70  $\mu\text{V}/\text{cm}$ . Electrode impedances were below 5 kohm. Further data processing was performed using statistical parametric mapping software (SPM, version 8, *the Welcome Trust Centre for Neuroimaging*, UCL, London, UK) and Matlab (version R 2012 a- the MathWorks, Natick, MA, USA) for the sensor –level analysis (Litvak, Mattout et al. 2011).

## Chapter Four

## **CHAPTER 4 PATIENT CHARACTERISTICS**

This chapter describes the pDOC patients included to the study, in particular, in detail, their demographic characteristics, and the results of the behavioural assessments as well as the undertaken neurophysiology assessment. For the behavioural assessment, I used scales such as the WHIM, CRS-R and the SMART; the characteristics of these scales were discussed in Chapter 3.

This Chapter outlines the complexity of the pDOC patients' presentation.

### **4.1 Demographic characteristic**

Sixteen patients with Disorders of Consciousness or prolonged Disorders of Consciousness were included in this study. All patients were inpatients at Royal Hospital for Neuro-disability in London, UK. This 26-bedded unit provides a comprehensive neuro-rehabilitation programme for patients with DOC in the post-acute phase following severe brain injury (GCS<8).

The inclusion criteria were as follows: i) severe brain injury leading to DOC or to pDOC as defined in Chapter 1: ii) conservative management of their brain injury, no neurosurgery was performed at any point of time, iii) at least unilateral intact auditory brainstem evoked potentials. This is because, both paradigms as described in Chapter 3,

relayed on the auditory stimuli or commands, such as being able to hear own name or being able to hear and follow a motor command.

The patients were recruited into the study after consultation with their relatives and treating team. The study was carried out in accordance with the latest version of the Declaration of Helsinki and the study was approved by a National Research Ethics Committee London-Queen Square, Charring Cross Hospital, Fulham Palace Road, London, on the 14.02.2012 with the REC reference number 11/LO/1233 and SSA reference number 11/LO/2052, copy please see the appendix 1. The copy of the Consultee Information Sheet and assent form has been attached in Appendix 2 and 3.

Six patients were female and ten were male, with the mean age of 46 years, SD 11. The patients had following aetiologies of the brain injury leading to disorders of consciousness: intracerebral haemorrhage (n=6), anoxic brain injury (n=5), traumatic brain injury (n=4) and tuberculosis meningitis (n=1). The patients had been in DOC for 17.31 months on average, ranging from 1.8 to 80.9 months (Table 4.1).

The data collection on patients took place from April 2013 to November 2013. During this time patients were included to the study, one patient at a time. All included pDOC patients underwent a comprehensive neuro-rehabilitation and assessment of their needs. Appropriate aids, such as bed or wheelchair positioning guidelines were implemented to ensure that pDOC patients were optimised from physical point of view. Additionally all patients were reviewed from medical point of view to ensure they were medically stable, for instance, infection free. The data collection usually took place in early afternoon, always in the same research office.

*Table 4.1 Study group characteristics*

Number	Patient's diagnosis	Gender	Age in yrs.	Duration of pDOC in mo.	Aetiology
1	MCS	F	18	4.7	Anoxic brain injury post self-hanging
2	MCS	F	61	55.1	Right frontal lobe bleed
3	MCS	M	55	9.1	Large intracerebral bleed
4	VS	M	45	5.4	Anoxic brain injury post cardiac arrest
5	MCS	M	68	4.0	Grade V SAH due to aneurysm left ACM
6	MCS	M	46	4.7	Extensive fronto-temporal left haemorrhage
7	MCS	M	38	9.1	Left fronto-temporo-parietal contusions following assault
8	MCS	F	30	80.9	Petechial haemorrhage following road traffic accident
9	MCS	F	37	1.8	Bilateral intracerebral bleed
10	VS	M	24	6.4	Hydrocephalus following TB meningitis
11	VS	M	20	13.6	Diffuse axonal injury following road traffic accident
12	VS	M	51	40.4	Right temporo-parietal bleed
13	VS	F	62	5.0	Anoxic brain injury post cardiac arrest
14	MCS	M	52	6.4	Left parietal haemorrhage following road traffic accident
15	MCS	F	31	26.0	Anoxic brain injury following cardiac arrest
16	MCS	M	53	4.4	Anoxic brain injury following cardiac arrest

*This table presents the study group characteristics, M-male, F-female, MCS-minimally conscious state, VS vegetative state.*

## **4.2 Assessment of the awareness using bedside tools**

I used in this study the three main tools for bedside assessment, which are standardised and recommended by the RCP. For the detailed description of the WHIM, CRS-R and SMART please see chapter 3 and for the patients' responses (Table 4.2). There is an agreement between scales in regard to the diagnosis, namely a patient received the same diagnosis of either VS or MCS regardless of the used scale. In only case, patient number 1 is there discrepancy between the scales, then the WHIM and CRS-R indicated the diagnosis of MCS, while the SMART alone indicated the diagnosis of VS. The final diagnosis for this patient was MCS, as established by the MDT team based on the results of the informal assessment, the feedback from the nurses, team and family as well as the results of WHIM and CRS-R.

Table 4.2 Patients 'responses to the environmental stimuli measured with WHIM, CRS-R and SMART

No	Patient's diagnosis	WHIM the highest score	CRS-R sum	auditory	visual	motor	Oro-motor	Communication	arousal	SMART-diagnosis
1	MCS	frowns, grimaces to show dislike (26)	11	2	3	3	1	0	2	VS
2	MCS	silent mouthing (25)	14	3	2	3	1	1	3	MCS
3	MCS	maintain eye contact for more than 5s (24)	10	2	3	2	1	0	2	MCS
4	VS	looks at person briefly (5)	4	1	1	0	1	0	1	VS
5	MCS	can attend the task – eating (39)	18	3	4	5	2	1	3	MCS
6	MCS	seeks eye contact (33)	12	2	3	4	1	0	2	MCS
7	MCS	tracks a source of sound (22)	8	2	2	2	1	0	1	MCS
8	MCS	crying (21)	11	3	1	3	1	1	2	MCS
9	MCS	silent mouthing (25)	11	2	3	3	2	0	1	MCS
10	VS	tracks for 3-5s (18)	3	0	0	1	1	0	1	VS
11	VS	tracks for 3-5s (18)	8	1	2	2	1	0	2	VS
12	VS	tracks for 3-5s (18)	10	2	2	2	2	0	2	VS
13	VS	grinding teeth (7)	5	2	0	1	0	0	2	VS
14	MCS	attending task when eats (39)	13	1	4	4	2	0	2	MCS
15	MCS	tracks for 3-5s (18)	7	1	2	2	1	0	1	MCS
16	MCS	smile (43)	16	2	4	4	2	1	3	MCS

This table presents patients' responses to the environmental stimuli measured with three different scales for consciousness assessment, WHIM – Wessex Head Injury matrix, CRS-R Coma Recovery Scale Revised and SMART the Sensory Modality Assessment for Rehabilitation Technique, definitions of the CRS-R score: auditory scale (0)- none, (1)- auditory startle, (2) localisation to sound, (3) reproducible movement to command, visual- (0)-none, (1)-visual startle, (2)-fixation, (3)-visual pursuit, (4)-object localisation, reaching, (5)-object recognition, motor- (0)-none, (1)-abnormal posturing, (2)-flexion withdrawal, (3)-localisation to noxious stimulation, (4)-object manipulation, (5)-automatic motor response, oro-motor-(0)-none, (1)-oral reflexive movement, (2)-vocalisation, communication-(0)-none, (1)-non-functional, arousal – (0)-unarousable, (1)-eye opening with stimulation, (2)-eye opening w/o stimulation, 3-attention

### **4.3 Brainstem Auditory Evoked Potentials**

One of the inclusion criterion to the study was at least unilateral positive brainstem auditory evoked potential (BAEP). A careful bedside assessment using the three mentioned above scales would be sufficient to detect gross sensory deficits. However, because this study relied on understanding of the similar auditory stimuli such as own name and other names commands ability to follow a command “imagine you are squeezing your own right hand”, the BAEP were performed to ensure all subjects have intact the auditory pathways. As shown in the table 4.3 all included patients had a positive BAEP and none was excluded because of this criterion.

A normal BAEP consists of five waves, where the waves I to III are generated by the auditory branch of cranial nerve VIII and lower brainstem and the waves IV and V are generated by the by the upper brainstem. The BAEP values were delayed in 10 out of 16 pDOC subjects with the mean time for inter-peak I to III of 2.55 ms, the reference value for normal subjects is 2.21 ms (Tusa, Stewart et al. 1994). The similar observation was for the interpeak III-V, which in the pDOC patients was 2.1ms, while the reference is 1.93 ms (Tusa, Stewart et al. 1994), the interpeak I to V was only slightly delayed in the study population to 4.44 ms vs. 4.13 ms as a reference value. (Tusa, Stewart et al. 1994).

*Table 4.3 Brainstem Auditory Evoked Potentials in pDOC patients*

Patient's No	Right ear					Left ear				
	I	II	III	IV	V	I	II	III	IV	V
1 MCS	1.5	2.5	3.5	4.8	5.5	1.4	2.7	3.5	4.8	5.6
2 MCS*	1.8	3.0	3.8	4.9	5.5	1.9	3.0	3.9	4.6	5.5
3 MCS	1.8	3.2	4.3	5.5	6.7	absent	absent	absent	absent	absent
4 VS	1.7	2.4	5.0	7.6	8.2	1.6	2.3	3.7	5.9	6.4
5 MCS*	absent	absent	absent	absent	absent	1.9	2.7	3.9	4.9	5.4
6 MCS	1.6	2.6	4.0	5.1	5.6	1.6	3.2	3.7	5.3	6.1
7 MCS	1.5	2.5	4.0	5.7	6.8	absent	absent	absent	absent	absent
8 MCS*	1.4	2.4	3.5	4.6	5.2	1.9	2.7	3.7	4.7	5.3
9 MCS*	1.6	2.8	3.9	5.2	6.0	1.5	2.8	3.8	5.0	5.5
10 VS	1.6	3.7	5.1	6.0	7.9	1.6	2.8	3.6	5.0	5.7
11 VS	2.1	4.2	5.8	7.0	8.2	1.8	absent	3.9	absent	absent
12 VS	absent	absent	absent	absent	absent	1.5	2.7	3.9	6.0	7.1
13 VS*	1.5	2.3	3.9	4.9	5.5	1.5	2.3	3.7	4.9	5.5
14 MCS	1.7	3.3	4.2	5.3	5.7	1.6	3.0	4.0	5.3	6.0
15 MCS*	1.4	2.6	3.5	4.5	5.3	1.6	2.9	3.9	5.0	5.9
16 MCS	1.4	3.0	4.1	5.1	5.8	absent	absent	absent	absent	absent

*This table represents the brainstem auditory evoked potentials (BAEP) responses for right and left side, the wave's latency is expressed in millisecond, inclusion criteria was to have at least unilateral positive BAEP.\* indicates pDOC patients with normal BAEP, defined as at least unilateral interpeak I to III is 2.1 ms and III-V -1.93 ms.*

#### **4.4 Qualitative analysis of Electroencephalography**

The EEG and NIRS laboratory was shown on the figure 3.1 in the chapter 3. The pDOC patients were taken for the data collection individually, one patient per day. The EEG recordings were usually performed in the early afternoon. This was because all the patients had been undergoing a rehabilitation programme at the time of the data collection, and the data collection should not interfere with the physical therapy. Patients were put in the laboratory room, the EEG cap was applied and then the several minutes of the baseline EEG was recorded. The resting state EEG was obtained too see the baseline electrical activity of the brain, however, as discussed in the Chapter 2, the standard EEG is not used to make a diagnosis of VS or MCS. The resting state EEG is presented in the table 4.4.

*Table 4.4 Resting state EEG to obtain the background electrical activity in the study population*

<b>Number</b>	<b>Patient's diagnosis</b>	<b>Resting state EEG</b>
1	MCS	low amplitude and without distinguishable features
2	MCS	polymorphic activity at 2-2.5 Hz
3	MCS	diffuse polymorphic delta activity at 1.5-3 Hz, with low amplitude theta at 5-6 Hz superimposed, small amount of beta activity at 18-20 Hz frontal bilaterally
4	VS	low amplitude and without distinguishable features
5	MCS	diffuse activity at 1.0-1.5 Hz, rhythm at 8.5 Hz superimposed over post central regions
6	MCS	supressed posterior rhythm, frontal derivation 4-6 Hz rhythm
7	MCS	asymmetrical R>L, activity 5-7 Hz
8	MCS	asymmetrical, diffuse activity at 1.5-3 Hz, occasional activity at 6 Hz central
9	MCS	well- formed posterior rhythm 4-6 Hz
10	VS	slow activity at 1-3 Hz, occasionally over right centro- temporal regions 4.0-4.5 Hz
11	VS	diffuse polymorphic activity at 1.5-3 Hz with low amplitude at 5-6 Hz
12	VS	over both hemispheres activity at 5-6 Hz, focal activity at 4-2.5 Hz over the right superior frontal region
13	VS	symmetrical, low voltage activity mainly 3-4 Hz
14	MCS	activity at 5-6 Hz over central
15	MCS	low amplitude activity at 2-4 Hz
16	MCS	occipital rhythm diminished, frontal 7-10 Hz

*This table presents the results of standard clinical resting state EEG, which was performed to obtain the background electrical activity in the study population*

#### 4.5 Quantitative analysis of encephalography

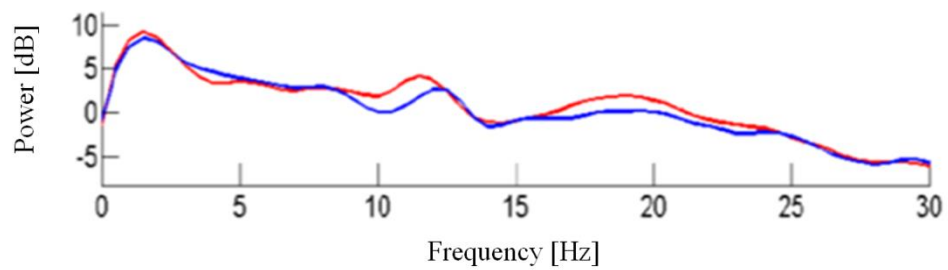
As mentioned above the clinical EEG from the pDOC patients was evaluated using a visual inspection technique, which relays on assessment of EEG traces voltage changes over the time (Pivik, Broughton et al. 1993). As suggested by Pivik *et al.* (Pivik, Broughton et al. 1993) much additional information about the EEG background activity can be retrieved by analysis of its frequency. To do this an EEG will need to be decomposed into frequency domains and the frequency bands are clustered together; hence, this gives an overview of the most dominant background activity in the patient's cohort. For instance as showed on the Figure 4.1 a healthy subject has a peak frequency at 12 Hz and 20 Hz, meaning that majority of the background activity were alpha (12 Hz) and beta frequency bands (20 Hz).

The methodology of this procedure was as follows: the raw EEG signal from a pDOC patient was re-sampled to 512 Hz and band-pass filtered between 1-60 Hz, next the bipolar montages- F3-C3; F4-C4, this step was performed using the Asalab (*ANT Neuro, the Netherlands*). The next step of EEG analysis involved a power spectral analysis using EEGlab. The Fourier transform decomposes time series into a sinusoid component of different frequencies. In other words it produces a spectral graph called the "power spectrum" that shows a distribution of power values as a function of frequency, where power is considered as an average of the signal (University College San Diego. Swartz Center fo Computational Neuroscience 2014).

EEG power spectra were determined for the C3 and C4 positions. In a normal subject there were two peaks on the power spectrum analysis, at the 8- 12 Hz for the alpha band frequency and a peak around 20 Hz for beta band frequencies, since they are dominant electrical features of an EEG from a healthy subjects (Figure 4.1).

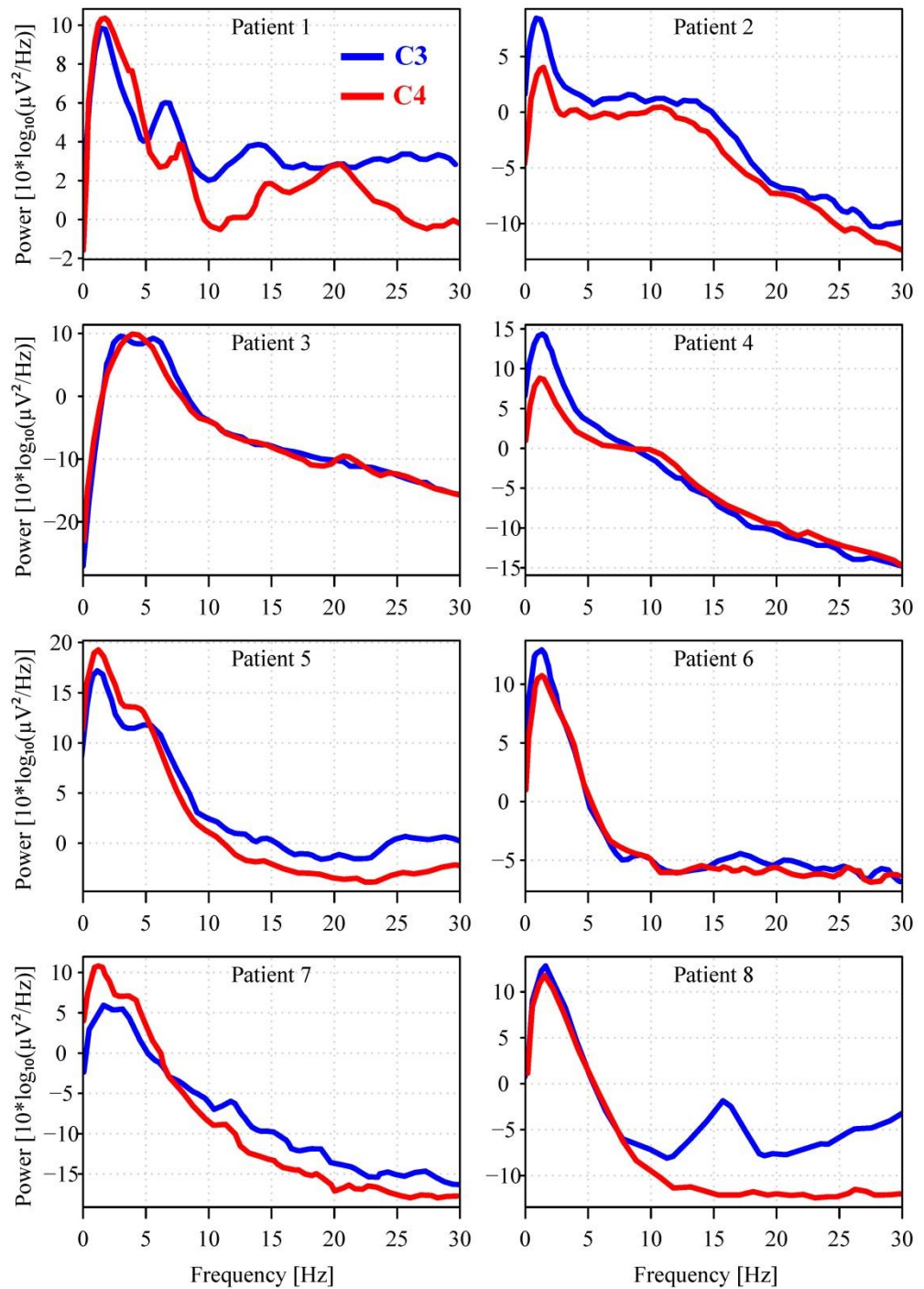
The majority of patients had their peaks on the spectral EEG analysis at delta frequency band in EEG (Figure 4.2), which is compatible with the resting state EEG, where the most frequent and predominant rhythm of the baseline brain activity was the slow delta rhythm.

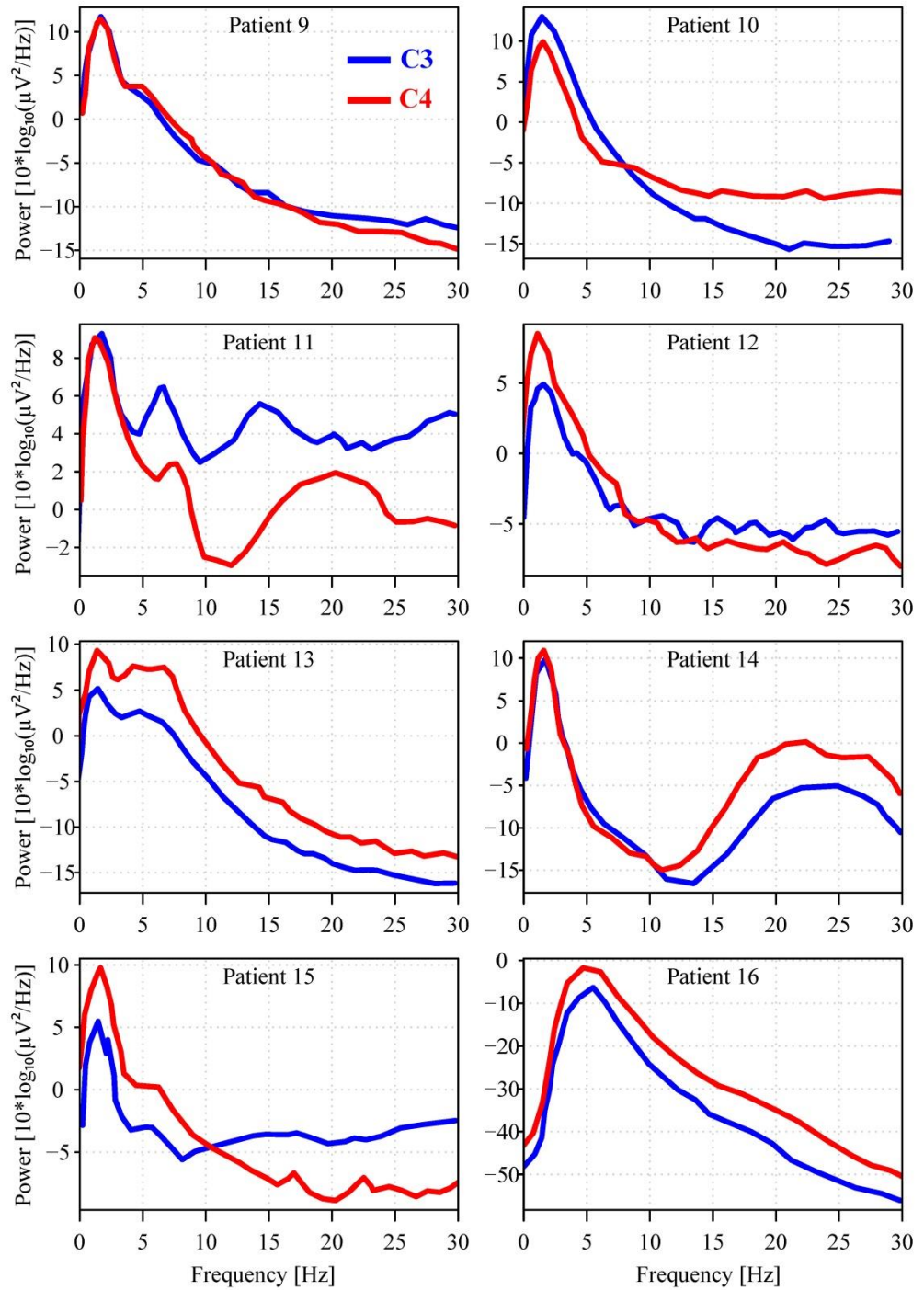
*Figure 4.1 EEG spectral analyses in a healthy subject*



*This figure presents an EEG spectral analysis in a single healthy subject. Power spectra from the left hemisphere (C3) is represented by a blue line, from the right hemisphere (C4) as a red line respectively; there are two peaks at alpha band approx. at 12 Hz and at beta band approx. at 19 Hz; the analysis was performed using EEGLab.*

Figure 4.2 Spectral analyses of EEG signals in positions C3 and C4 in patients with prolonged disorder of consciousness included to the study





*This figure presents an EEG spectral analysis in all pDOC patients included to the study; power spectra from the left hemisphere (C3) is represented by a blue line, from the right hemisphere (C4) as a red line respectively; the analysis was performed using EEGLab.*

As I have shown in this chapter the patients with disorders of consciousness are complex. Their presentation is complex and an assessment of their brain function needs an input from the multi-disciplinary team. The routine EEG usually shows slow background activity usually delta or theta frequency bands, however, this does not tell us if a patient is aware about himself or his environment. Only functional EEG and functional NIRS have potential to answer these questions, because a change in electrical or haemodynamic signals can be observed.

The next chapter introduces the functional Electroencephalography for brain function assessment in DOC patients.

## Chapter Five

## **CHAPTER 5 NEAR INFRARED SPECTROSCOPY FOR BRAIN FUNCTION ASSESSMENT IN PDOC PATIENTS**

This is an experimental chapter, where the practical application of the use of the NIRS in the pDOC patients was described. The pDOC patients performed a motor imagery task. Additionally, a validation study on healthy subjects, who performed both, the real and motor imagery movements was also performed.

### **5.1 Introduction**

Functional NIRS (fNIRS) is a methodology that has potential to improve the assessment of pDOC patients. The term pDOC is an umbrella term encompassing both: the VS and MCS patients. As described in detail in the Chapter 1 of this work, unlike VS, patients in MCS are partially aware of themselves and their environment and are able to follow simple commands, albeit inconsistently (Giacino, Ashwal et al. 2002). The diagnosis process includes the use of the behavioural measures and the use of technology as discussed in the Chapter 3 of this work.

The hypothesis of this study is that a motor task would elicit changes in oxy and/or deoxyHb concentration indicating that a subject followed, without behavioural response, specific verbal commands such as “ imagine you are squeezing your own right hand”.

Two main patterns of the functional NIRS responses during a motor task on healthy subjects have been identified: a typical NIRS signal changes when the concentrations

of the oxyHb increases and the deoxyHb decreases (Leff, Orihuela-Espina et al. 2011) and an inverted response when the concentration of the oxyHb decreases and the deoxyHb increases (Holper, Shalom et al. 2011). Also usually the amplitude of the oxyHb concentration changes is higher than changes in deoxyHb and the response to the task usually starts approximately 2 seconds post stimuli, as discussed in Chapter 2.1 and 3.2.

Therefore, the aim was to explore the functional NIRS responses from pDOC patients during a motor imagery.

## **5.2 Aims**

The aims of this study are:

1. To show that haemoglobin concentration changes during a motor task can be calculated using the NIRS apparatus in pDOC patients
2. To obtain patterns of haemodynamic responses occurring during real and imagery motor movements
3. To identify patterns of haemodynamic changes as a response to imagery motor task in pDOC patients

## **5.3 Methods**

### ***5.3.1 Subjects***

Ten healthy, right – handed volunteers (six female, mean age 39.6 yrs. SD 7.87) performed both the real movement of the right hand (squeezing a rubber ball) and the kinaesthetic motor imagery task. None of them suffered from neurological or psychiatric disorders, substance abuse or brain injury, also none of them was on psychotropic medications (according to self-reports). Handedness of the subjects was measured by a self-report of the side of their hand used in writing and eating. None of them had history of handedness correction. All volunteers were staff working at Royal Hospital for Neuro-disability. All subjects were given informed written consent.

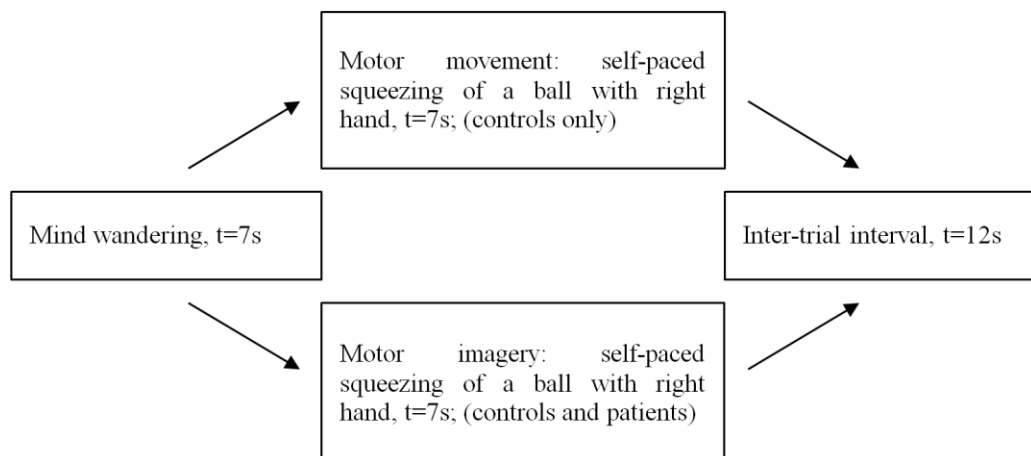
For the study group sixteen pDOC patients were included, the detailed description of the study population please see the Chapter 4 of this thesis.

### ***5.3.2 Tasks***

The controls performed two parts of the experiment: motor movement and motor imagery. The paradigm was divided into 2 blocks: the self-paced squeezing of a ball with own right hand for 6 seconds followed by a 12 seconds resting state. It consisted of 30 trials, but the exact length of the data collected was depending on subject's availability and tolerance of the experiment (Figure 5.1). In the second part of experiment subjects were asked to imagine the same movement with a self-paced rate approximately 1/ second. The patients performed only the imagery of the movement as patients in pDOC are not able to consistently execute physical movement to command.

Twelve seconds of an interval between the motor tasks was chosen, based on a previous studies showing that hemodynamic recovery to a baseline appears approximately 9-10 second after cessation of stimulus (Boden, Obrig et al. 2007). At the beginning of the experiment the participants were familiarized with the experiment design and with the instructions presented during the data acquisition. Each block began with the auditory presentation of the task for the block for instance “when you hear the instruction start squeeze/imagine squeezing a ball with your right hand, “start” and “stop”.

*Figure 5.1 Overview on the motor task experiment*



*The study and the control group were asked to imagine squeezing a ball with the right hand. The controls underwent the both arms of this paradigm, first the actual movement followed by movement imagery. Patients performed only the imagery task. The exact length of the recordings varied and depended on the individual tolerance but the aim was to complete 30 trials of the task.*

During the motor imagery part the subjects were instructed to concentrate on muscle contraction within the own right hand as it would be a real movement, with avoidance of the visualisation of this movement, as it should be first person perspective kinaesthetic movement imagery and also to ensure that motor cortex rather than occipital cortex will be activated (Guillot, Collet et al. 2009).

The control subjects were instructed to look ahead blankly and if possible, to avoid any movements during the data acquisition. They were sitting on a comfortable chair with their hands on their laps in a dim-lighted room. An effort was made to keep as consistent environmental conditions as possible, for instance, the same position in the room, the use of the blinds to minimize NIRS signal contamination due to external factors, such as additional source of light or movements' artefact.

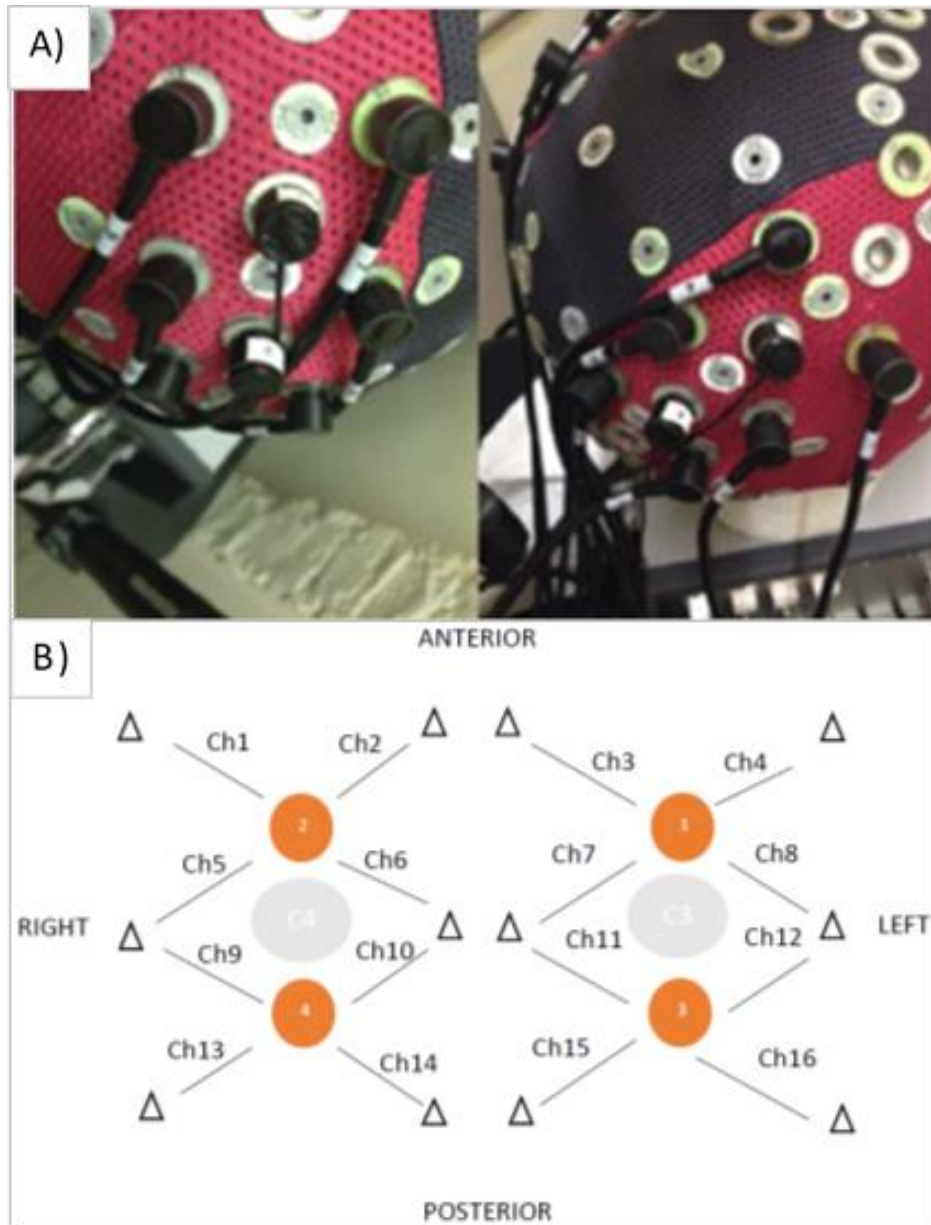
### ***5.3.3 Near Infrared Spectroscopy Instrumentation***

The fNIRS signal was recorded bilaterally over the premotor area and supplementary motor area (EEG corresponding areas FC3, FC1, FCz, FC2 and FC4) and over the primary motor cortex (EEG corresponding areas C4, C2, Cz, C1 and C3), as combinations of these areas were likely to be active in response to both motor paradigms. All fNIRS measurements were performed using a NIRScout system (*NIRx Medical Technologies LLC, Berlin, Germany*) using a 16-channel array of optodes. The system performed dual-wavelength CW near infrared tomographic measurements at a

10.42 Hz sampling rate. For the technical specification such as wavelengths and the NIRS laboratory set up, please see the Chapter 3 of this work.

The four sources and 12 detectors were placed on subject's skull in the usual primary and secondary motor areas, according to the International 10-20 system (Klem, Luders et al. 1999), with each detector receiving light originating in its neighbouring light source and scattered in the adjacent tissue. Each detector and the most closely placed light source built a channel. In total, there were 16 channels containing information about deoxy and oxyHb concentration changes (Figure 5.2). Changes in oxy and deoxyHb concentration were analysed separately, giving in total 32 channels. The inter-optodes distance was 2.5 cm.

Figure 5.2 Waveguard cap and fibre arrangement



This figure presents the Waveguard cap used for the NIRS data collection and fibre arrangement, (A) Waveguard cap with an array of detectors and light sources and (B) fibre arrangement. The orange dots indicate sources position and the triangles indicate position of detectors; each source - detector (triangle).

#### ***5.3.4 Data processing and analysis***

The raw NIRS data was converted into a readable Matlab format using Nilab2 software (NIRx Medical Technologies LLC). The data was low-pass filtered to remove the high frequency signal ~0.3 Hz breathing and 1 Hz heart rate. Low frequency (less than 0.01 Hz) vascular or metabolic oscillations were removed by using a high frequency cut-off filter of 32 sec (0.03 Hz).

The changes in both oxy and deoxyHb concentration expressed in ( $\mu\text{Mol/l}$ ) were calculated using the modified Beer-Lambert law as described by Delpy (Scholkmann, Kleiser et al. 2014). Further to discussion in Chapter 2.1, the modified Beer – Lambert law was applied, since the light attenuation in highly scattering media, such as brain tissue, has two major confounders. The first confounder of the NIR light scattering is an increase in distance that the light is traveling, which can be greater than source-detector separation, second that not all NIR light photons will be reaching detectors (Smith and Elwell 2009). Additionally, all NIRS validation studies have been performed on anatomically intact brain. Brain pathology may significantly change the results, however, in this study all patients were managed conservatively during their injury and at least twice a structural assessment on their brain was performed (during their stay at acute hospitals). I reviewed the CTs or MRIs of the patient cohort and all of them had intact anatomical structures of their brain, which was also an inclusion criterion as mentioned in Chapter 4.

Initially, I intended to perform NIRS data analysis using the General Linear Model (GLM), which is a part of the Nilab software (*NIRx Medical Technologies LLC, Berlin, Germany*). The GLM approach to data analysis is a well-recognised approach in fMRI studies; however, the GLM analysis considers changes only in BOLD, while in the

NIRS model there are at least two variables: Oxy and deoxyHb. Therefore, the GLM methodology needed some adjustments to eliminate the risk of errors: type one (false positive) and type two (false negative) (Uga, Dan et al. 2014).

At the time of this study only one publication was published on the use of the GLM of NIRS signal in two patients with MCS (Molteni, Arrigoni et al. 2013), and because the GLM in NIRS has been still emerging approach, I decided to analyse the NIRS results using a classical approach. The classical approach of NIRS data analysis considers contrasting an average data from the task period against the average data from the rest period using student t-test test or Mann-Whitney test depending on the data distribution. This approach was particularly common in the block design paradigm, which has been used for hypothesis testing in this thesis (Uga, Dan et al. 2014).

Therefore, the analysis included the export from Nilab2/Matlab of raw data, pre-processed as described above. In each channel, the data represent amplitude minus the average for the entire record in each channel. The sampling rate was 10.42 Hz and the time of triggers for tasks (motor imagery or motor action) were stored in a separate file. Further analysis and data visualisation was performed using R-package for windows, version 3.1.1. Furthermore, the concentration changes were considered as “absolute difference” or “relative difference”. The former ( $\Delta_{abs}$ ) refers to the median difference between the signal amplitude before (7s to zero s) and task period (zero s to 7s), while the latter ( $\Delta_{rel}$ ) was calculated as the ratio of the absolute difference ( $\Delta_{abs}$ ) to the 5th to 95th quantile range of the signal amplitude for the entire study. The detailed descriptions of how the data was analysed and presented is as follows:

- 1) Oxy-Hb entire study plots.

Each of the 16 graphs presents Oxy-Hb signal recorded in a single channel. The range of the vertical axis has been adjusted to the signal amplitude while the range of the horizontal axis was adjusted for the total, subject specific, recording time. The grey rectangles, for longer studies visible as vertical lines, cover the task periods. The horizontal, dashed red lines present the 5th and the 95th quantile of signal amplitude distribution.

2) Deoxy-Hb entire study plots.

Each of the 16 graphs presents Deoxy-Hb signal recorded in a single channel. The range of the vertical axis has been adjusted to the signal amplitude while the range of the horizontal axis was adjusted for the total, subject specific, recording time. The grey rectangles, for longer studies visible as vertical lines, cover the task periods. The horizontal, dashed red lines present the 5th and the 95th percentile of signal amplitude distribution.

3) Oxy-Hb signal analysis plot

Each of the 16 graphs present analysis for 7 seconds before task signal (-7s to 0s), task period (0s to 7s) and the post-task period (7s to 14s). The red lines present the 10th, 50th (median) and the 90th percentile of the signal for the entire study, relative to each of the task triggers (second zero for each task). The horizontal black lines present the median value of signal proceeding the task (-7s to 0s) and the median value of signal during the task period (time 0s to 7s).

The absolute difference ( $\Delta_{abs}$ ) refers to the median difference between the signal amplitude before (7s to 0s) and task period (0s to 7s). The relative difference ( $\Delta_{rel}$ ) was

calculated as the ratio of the absolute difference ( $\Delta_{abs}$ ) to the 5th to 95th quantile range of the signal amplitude for the entire study.

The P-values were calculated using two-sided Mann-Whitney U test statistics.

#### 4) Deoxy-Hb signal analysis plot

Each of the 16 graphs present analysis for 7 seconds before task signal (-7s to 0s), task period (0s to 7s) and the post-task period (7s to 14s). The blue lines present the 10th, 50th (median) and the 90th percentile of the signal for the entire study, relative to each of the task triggers (second zero for each task). The horizontal black lines present the median value of signal preceding the task (-7s to 0s) and the median value of signal during the task period (time 0s to 7s).

The absolute difference ( $\Delta_{abs}$ ) refers to the median difference between the signal amplitude before (7s to 0s) and task period (0s to 7s). The relative difference ( $\Delta_{rel}$ ) was calculated as the ratio of the absolute difference ( $\Delta_{abs}$ ) to the 5th to 95th quantile range of the signal amplitude for the entire study. The P-values were calculated using two-sided Mann-Whitney U test statistics.

Then the NIRS signal was averaged over both: the left (8 channels) and right (8 channels) hemispheres was averaged to check for any lateralisation of haemoglobin concentration change, including looking either for ipsilateral negative oxygenation or contralateral positive or negative oxygenation, as these patterns were described elsewhere (Holper, Shalom et al. 2011; McGregor, Sudhyadhom et al. 2015).

Two patients, 1 MCS and 14 MCS (see Table 4.1), were excluded from the analysis. Both of them were in the MCS group and had high amplitude artefacts in all channels,

which were clearly synchronous with involuntary movements. The presence of high amplitude artefacts throughout recording did not allow for data analysis with the Nilab2 software (NIRx Medical Technologies LLC).

Data was entered into appropriate ANOVA model using SPSS (version 22). For the controls, this was a 2\*2 within –subject analysis (task: motor movement and motor imagery; hemisphere (within –subjects’ factor): L/R). For the patients it was a 3\*2 (group (between –subject factor): controls/MCS/VS; hemisphere: L/R).

P-values were set at <0.05 as a criterion for statistical significance for all planned analyses. I first examined interactions, then main effects.

## **5.4 Results**

### ***5.4.1 NIRS results on healthy subjects***

The global changes of oxy and deoxyHb concentrations during the motor tasks showed that nine out of 10 controls elicited stronger haemodynamic response to actual motor movement than to motor imagery. The global changes were expressed as a sum of concentration changes in each channel and expressed as a percentage of the change during the motor task and in relation to the pre-stimulus baseline (Table 5.1).

*Table 5.1 Global relative changes in Oxy and DeoxyHb in controls*

Healthy controls	Global change in the oxyHb concentration—relative change in percentage in relation to the pre-stimulus baseline	Global change in the deoxyHb concentration—relative change in percentage in relation to the pre-stimulus baseline
Control 1 MI	25.9	-20.3
Control 1 MM	-10.2	5.8
Control 2 MI	5.0	-6.3
Control 2 MM	24.2	-7.5
Control 3 MI	21.3	-0.3
Control 3 MM	-22.3	-3.9
Control 4 MI	9.5	-13.1
Control 4 MM	-39.6	-44.8
Control 5 MI	9.3	-13.3
Control 5 MM	-30.0	-3.2
Control 6 MI	-58.4	-4.5
Control 6 MM	-76.2	12.0
Control 7 MI	-12.7	16.5
Control 7 MM	-27.8	14.7
Control 8 MI	1.3	7.6
Control 8 MM	-5.4	-12.5
Control 9 MI	-11.0	5.3
Control 9 MM	-71.2	-52.1
Control 10 MI	15.2	-17.8
Control 10 MM	16.2	24.9

*This table presents the global relative changes in Oxy and DeoxyHb concentration. The changes is expressed as a percentage of increase/ decrease in during the activation in relation to resting state, MI- motor imagery, MM- motor movement.*

After examining the global tendency of the oxy and deoxyHb concentration changes, the NIRS channels were averaged according to the hemisphere: left (8 channels) and right (8 channels) hemispheres to check for the significance of the hemisphere effect. The results for oxy-deoxyHb concentration changes expressed a percentage of change in relation to the pre-stimulus baseline showed for the OxyHb as a dependent measure a main effect for task (imagery or movement against the pre-stimuli baseline) with  $p=0.043$  ( $F=5.521$ ). Changes in deoxyHb did not reach significant level (Table 5.2)

*Table 5.2 Oxy and deoxyHb concentration changes in controls in relation to the hemisphere*

Area	Mean of percentage of change	Std. Deviation	Controls N
Left_hemisphere_oxy/deoxyHb_MI	-0.26/-0.56	10.48/13.16	10
Left_hemisphere_oxy/deoxyHb_MM	-9.89/-4.14	17.85/18.52	10
Right_hemisphere_oxy/deoxyHb_MI	-1.32/-3.17	12.62/11.92	10
Right_hemisphere_oxy/deoxyHb_MM	-13.66/-7.07	18.02/15.98	10

*This table presents the mean of concentration changes expressed as percentage of change in relation to the pre-stimuli baseline in 10 controls during motor imagery (MI) and during the actual hand movement (MM) in both oxy and deoxyHb and in relation to the left vs. right hemisphere.*

### NIRS absolute changes

During the motor movement in controls (n=10) the mean oxyHb concentration change over the left hemisphere was -0.38  $\mu\text{Mol/L}$  (SD=standard deviation, 0.81) and -0.64  $\mu\text{Mol/L}$  (SD 0.82) over the right hemisphere respectively. The changes of deoxyHb concentration were relatively smaller than oxyHb and over the left hemisphere were -0.1202  $\mu\text{Mol/L}$  (SD 0.36) and over the right were -0.0089  $\mu\text{Mol/L}$  (SD 0.39) respectively.

The oxyHb concentration changes in controls during the motor imagery task were 10 times weaker when compared with the actual movement and were 0.03  $\mu\text{Mol/L}$  (SD 0.83) left and -0.08 (SD 0.95) right respectively. The changes in deoxyHb followed the same pattern namely: left hemisphere -0.086  $\mu\text{Mol/L}$  (SD 0.45) and 0.011  $\mu\text{Mol/L}$  (SD 0.29) over the right hemisphere respectively.

In control group, these changes were statistically significant in regard to the lateralization of the response for oxyHb (in  $\mu\text{Mol/L}$ ) as the dependent measure  $F=5.97$ ,  $df=1$  ( $p=0.037$ ) with a difference between left and right hemisphere and a trend for task  $F=3.48$  ( $p=0.095$ ) and this result is similar to the result expressed as percentage of change during motor movement in relation to a pre-stimulus baseline.

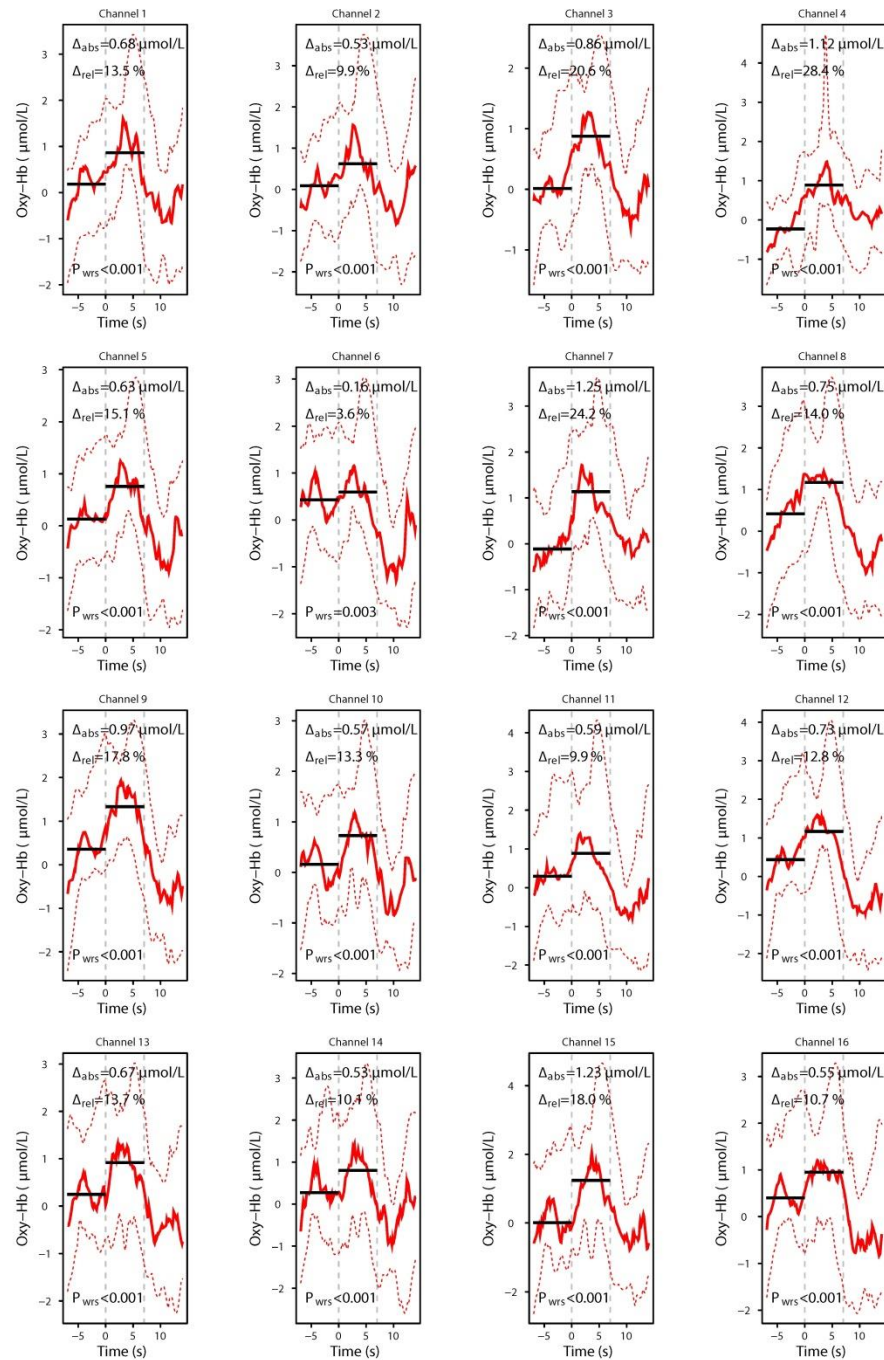
### A single subject NIRS signal plot

The NIRS signal changes over time during the motor imagery clearly showed an increase in oxyHb concentration during the motor imagery when compared to oxyHb

concentration changes during the pre-stimulus resting state. The opposite trend was noticed for deoxyHb, where a decrease of deoxyHb was noted during a motor imagery. Moreover, the corresponding channels showed a direct proportional changes with increase in one of haemoglobin and decrease in other one (Figure 5.3 and Figure 5.4).

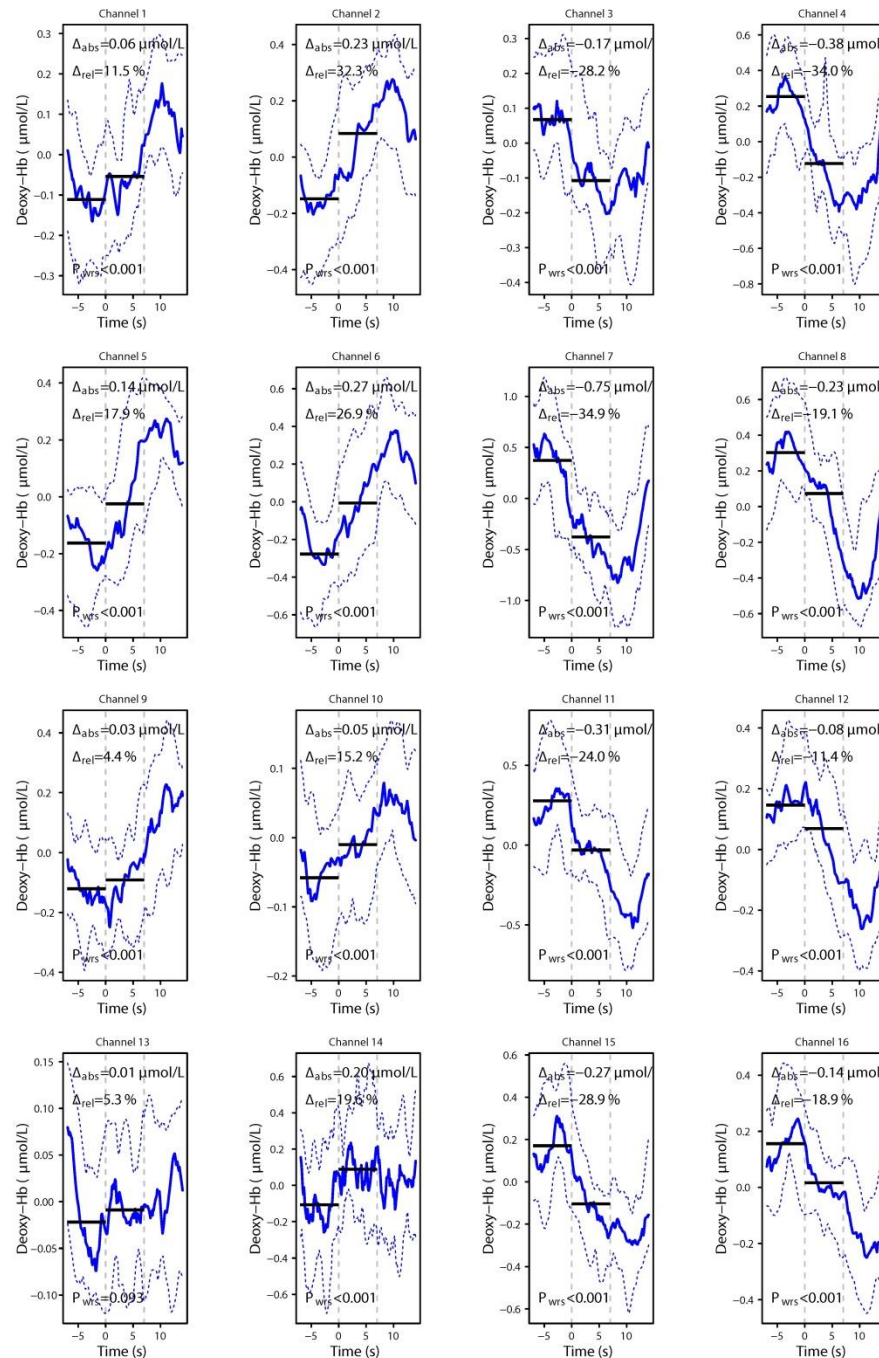
A combined figure, presenting changes in both oxyHb and deoxyHb during motor imagery in healthy subjects, shows the differences in magnitude of these changes (Figure 5.5).

Figure 5.3 Changes in oxygenated haemoglobin in a control subject during the motor imagery task



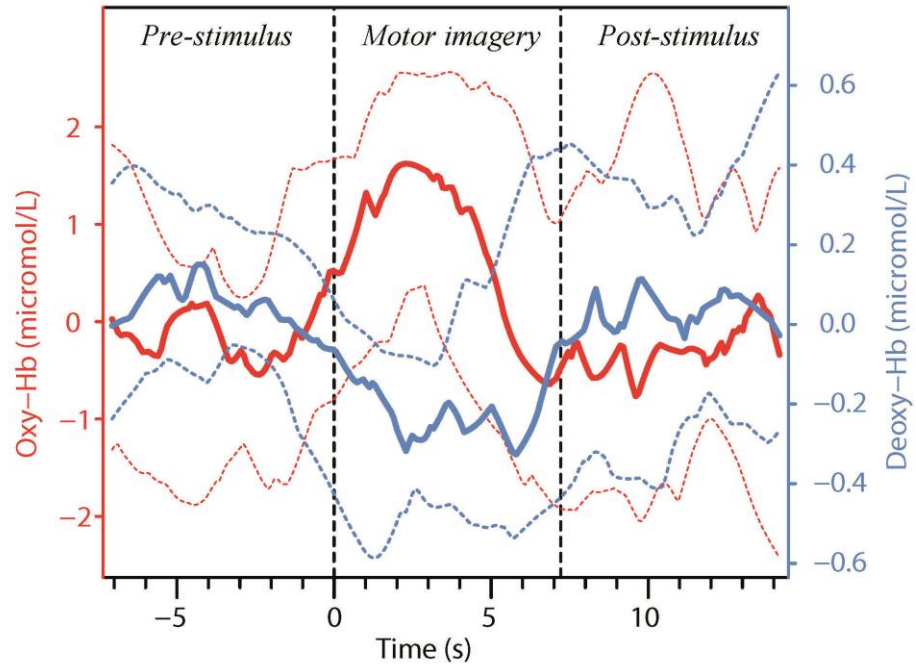
This figure presents the OxyHb changes in a control subject (subject number 10) during the motor imagery task; the dashed vertical lines represent start and stop of the task. The solid black lines present pre and post activation values. Red lines present the 50th quantile (solid red line) and the 10th and 90th quantile (dashed red lines). The relative difference ( $\Delta_{rel}$ ) refers to the median difference between the signal amplitude before (7s+ to 0s) and task period (0s to 7s), and was calculated as the ratio of the absolute difference ( $\Delta_{abs}$ ) to the 5th to 95th quantile range of the signal amplitude for the entire study.

Figure 5.4 Changes in deoxygenated haemoglobin in a control subject during the motor imagery task



This figure presents the DeoxyHb changes in a control subject (subject number 10) during the motor imagery task; the dashed vertical lines represent start and stop of the task. The solid black lines present pre and post activation values. Red lines present the 50th quantile (solid blue line) and the 10th and 90th quantile (dashed blue lines). The relative difference ( $\Delta_{rel}$ ) refers to the median difference between the signal amplitude before (7s+ to 0s) and task period (0s to 7s), and was calculated as the ratio of the absolute difference ( $\Delta_{abs}$ ) to the 5th to 95th quantile range of the signal amplitude for the entire study.

Figure 5.5 Combined changes in oxy and deoxyHb during the motor imagery task in healthy subject



This figure presents oxy and deoxyHb concentration changes during a motor imagery task, highlighting a difference in magnitude of these changes.

#### *5.4.2 NIRS Results on pDOC patients*

##### NIRS global and relative changes

The global haemoglobin concentration changes in pDOC patients showed less variability when compared with the controls (Table 5.3). The range of relative changes in oxyHb concentration ranged from -12.88 percent to 6.0 percent. The similar amplitude of the relative deoxyHb concentration changes was found, namely the deoxyHb changes ranged from -8.7% to 5.2%, whereas the healthy controls elicited stronger responses with the global relative change for oxyHb ranged from -71.2% to 25.9% and for deoxyHb ranged from 44.8 to -52.1% respectively.

*Table 5.3 Global relative and absolute changes in OxyHb and DeoxyHb in patients*

Patients in pDOC	Global change in the oxyHb concentration—relative change in percentage in relation to the pre-stimulus baseline	Global change in the oxyHb concentration—absolute in $\mu\text{Mol/L}$ in relation to the pre-stimulus baseline	Global change in the deoxyHb concentration—relative change in percentage in relation to the pre-stimulus baseline	Global change in the deoxyHb concentration—absolute in $\mu\text{Mol/L}$ in relation to the pre-stimulus baseline
Patient 2 MSC	-6.3	-2.3	1.4	0.4
Patient 3 MCS	-1.2	1.8	2.7	0.4
Patient 4 VS	-1.5	-3.7	1.2	1.71
Patient 5 MCS	6.0	3.7	-1.8	-0.8
Patient 6 MCS	2.1	-0.7	-8.7	-0.4
Patient 7 MSC	5.8	0.4	-4.6	0.4
Patient 8 MCS	-1.3	0.8	-2.3	1.8
Patient 9 MCS	5.6	-1.7	-2.1	0.2
Patient 10 VS	-12.9	0.9	-5.2	-2.7
Patient 11 VS	-3.4	-1.1	-1.7	0.03
Patient 12 VS	1.5	-1.3	-1.2	-2.4
Patient 13 VS	-5.9	15.2	5.3	10.8
Patient 15 MCS	-0.2	-7.52	0.2	5.05
Patient 16 MCS	-0.2	15.1	0.1	-2.06

*This table presents global relative (expressed in %) and absolute ( $\mu\text{Mol/L}$ ) changes in OxyHb and DeoxyHb concentration change during the motor activation in relation to resting state in patients with disorders of consciousness (pDOC) including those with vegetative state (VS) and minimally conscious state (MCS)*

The patient group was divided according to diagnosis into two groups: VS (N=5) and MCS (N=9) and the absolute changes in concentration of oxy and deoxyHb were compared between the groups. There were no significant differences between VS and MCS patients, however, interestingly all patients developed stronger response over the left haemisphere (right hand movement) then over the right hemisphere. This

lateralization of the haemodynamic response was seen in both: oxy and deoxyhaemoglobins (Table 5.4).

*Table 5.3 Concentration changes in oxy and deoxyHb during a motor imagery task in pDOC patients over the left and right hemisphere*

Patients in MCS N=9	Mean Oxy/deoxyHb $\mu\text{Mol/L}$	SD
Left hemisphere	0.16 / 0.035	1.95/ 0.63
Right hemisphere	-0.07 / 0.023	0.39/0.33
Patients in VS N=5	Mean Oxy/deoxyHb $\mu\text{Mol/L}$	SD
Left hemisphere	0.34 /0.18	1.72/ 1.34
Right hemisphere	-0.019 / 0.006	0.89/ 0.08

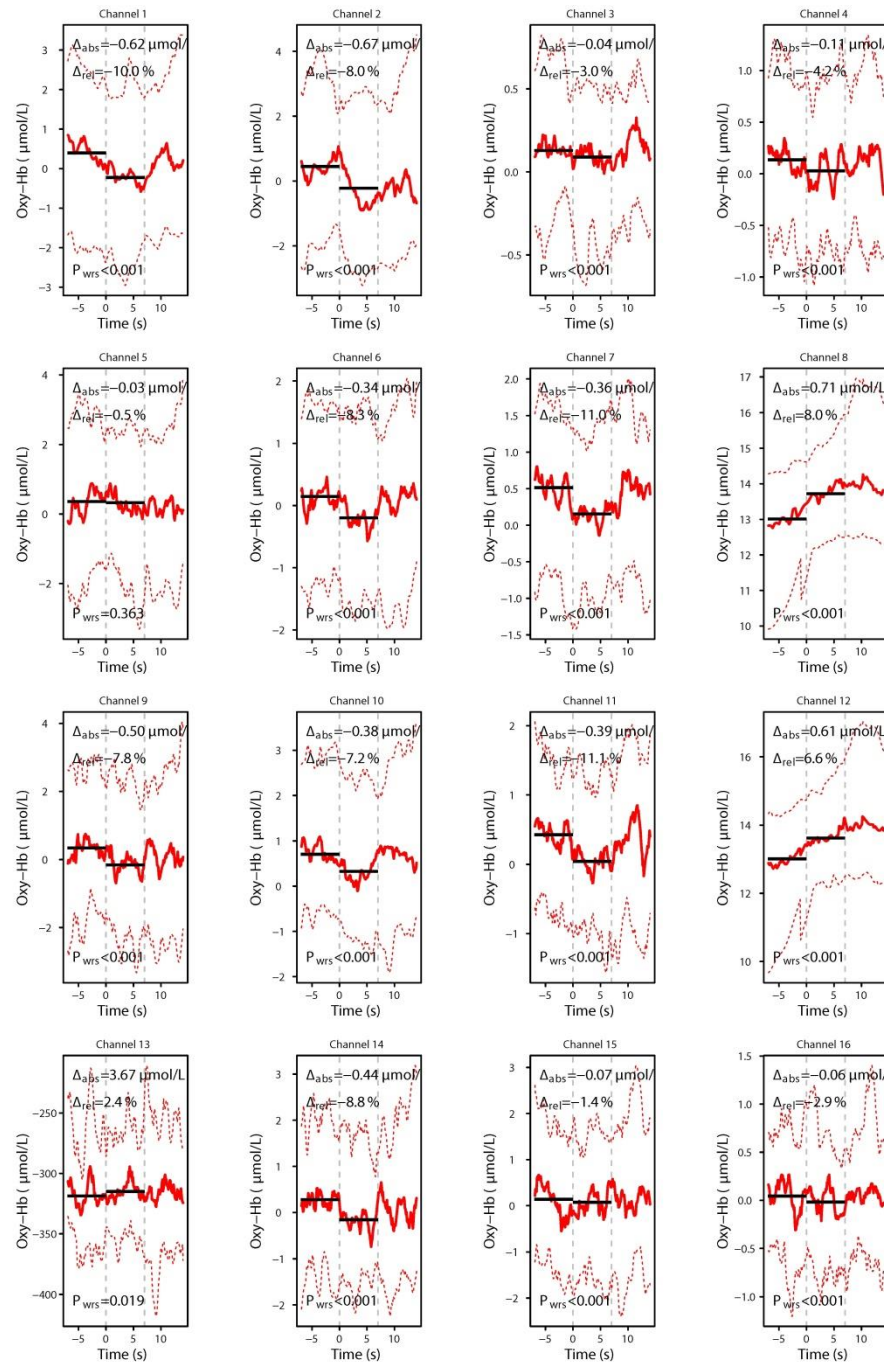
*This table presents concentration changes in oxy and deoxyHb in  $\mu\text{Mol/L}$  during a motor imagery task in pDOC patients over the left and right hemisphere. There is a lateralised response across both groups and both types of haemoglobins.*

Additionally, one patient (VS10), who as behaviourally diagnosed with VS, did demonstrate blood flow changes similar to the healthy group, global oxyHb changes -12.9% vs. mean for controls -11.8% SD30.8 and global deoxyHb change was -5.2% vs. mean for controls -5.6% SD 18.9. These CBF changes may indicate ability to follow commands and that this patient understood the instruction and tried to execute thought of right hand movement.

These fNIRS findings were found in isolation from the behavioural assessment at the time of the investigation; therefore, fNIRS provided additional information about this

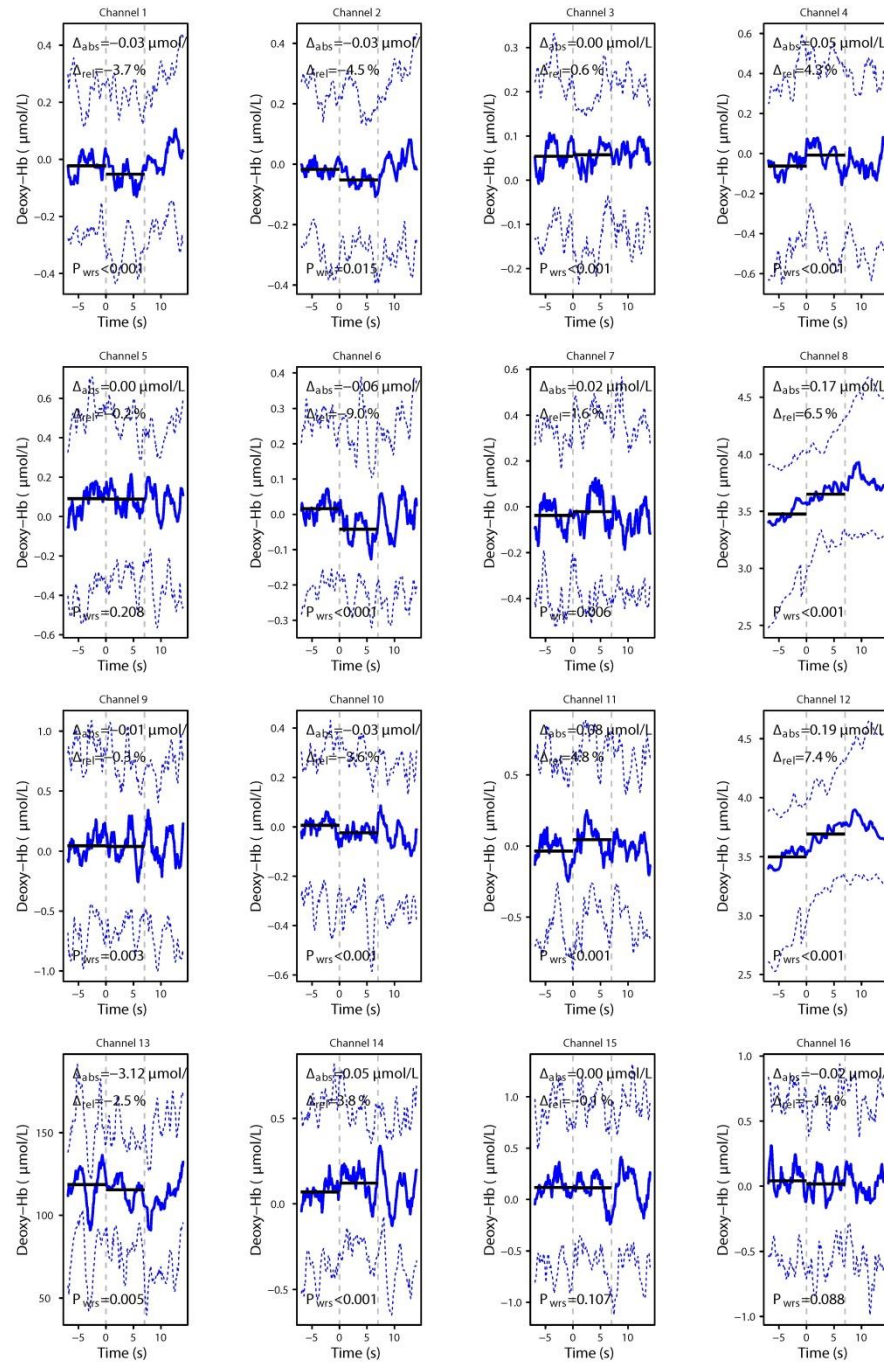
patient's brain function. Interestingly, this patient responded with a decrease of oxyHb concentration during a right hand motor imagery (Figure 5.5 and 5.6).

Figure 5.6 Changes in oxygenated haemoglobin in a vegetative state patient during the motor imagery task



This figure presents the OxyHb changes in a vegetative state patient during the motor imagery task; the dashed vertical lines represent start and stop of the task. The solid black lines present pre and post activation values. Red lines present the 50th quantile (solid red line) and the 10th and 90th quantile (dashed red lines). The relative difference ( $\Delta_{rel}$ ) refers to the median difference between the signal amplitude before (7s+ to 0s) and task period (0s to 7s), and was calculated as the ratio of the absolute difference ( $\Delta_{abs}$ ) to the 5th to 95th quantile range of the signal amplitude for the entire study.

Figure 5.7 Changes in deoxygenated haemoglobin in a vegetative state patient during the motor imagery task



This figure presents the DeoxyHb changes in a patient diagnosed with vegetative state during the motor imagery task; the dashed vertical lines represent start and stop of the task. The solid black lines present pre and post activation values. Red lines present the 50th quantile (solid thick line) and the 10th and 90th quantile (dashed thick lines). The relative difference ( $\Delta_{rel}$ ) refers to the median difference between the signal amplitude before (7s+ to 0 s) and task period (0 s to 7s), and was calculated as the ratio of the absolute difference ( $\Delta_{abs}$ ) to the 5th to 95th quantile range of the signal amplitude for the entire study.

### 5.4.3 Different patterns of the NIRS responses from healthy and study subjects

Based on the individual subject's responses (controls n=10 and the pDOC patients n=14) three different types of fNIRS responses can be identified. The first type can be called a "typical" NIRS response is when the oxyHb is positive and deoxyHb negative during the brain activation. The typical NIRS response was seen in 60 percent (6/10) healthy subjects and 36 percentage (5/14) of the DOC patients. The second type of the NIRS response can be called "inverted", where the oxyHb concentration change was negative in value and deoxyHb was positive, which was seen in two of the 10 healthy subjects and in six of the 14 patients. Finally, the third type of the NIRS response can be called "undefined" where the oxy and deoxyHb are both either negative or positive in values. The undefined response was seen in two of the ten healthy subjects and three of the 14 pDOC patients (Table 5.5).

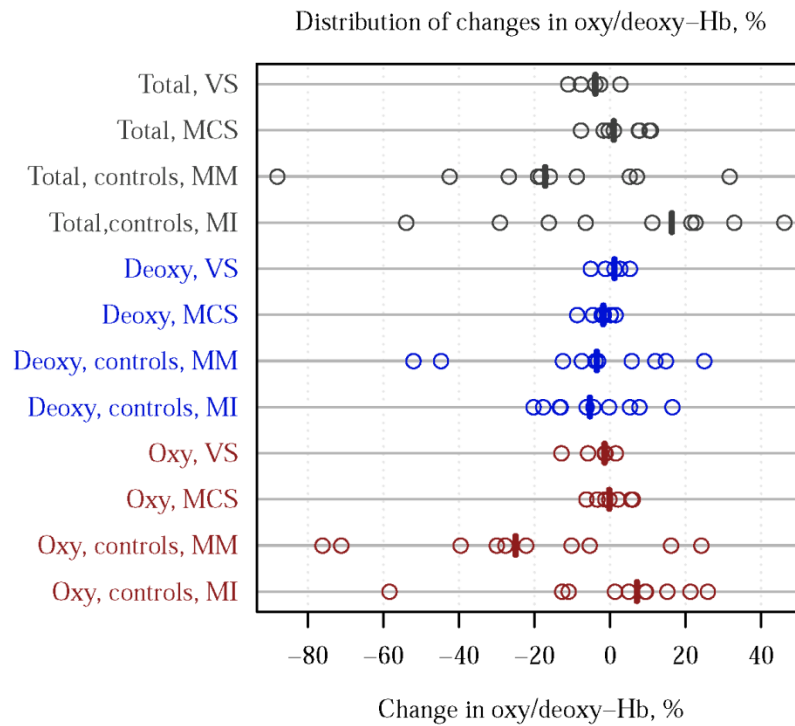
Table 5.4 Identifiable types of fNIRS responses based on the polarity

Type of fNIRS response	Typical response- OxyHb positive and deoxyHb negative	Inverted response- oxyHb negative and deoxyHb positive	Unclassified response oxyHb and deoxyHb positive or oxyHb and deoxyHb negative
Healthy controls, n=10	6	2	2
pDOC patients, n=14	5	6	3

This table presents the identifiable types of fNIRS responses based on the polarity of the global oxy and deoxyHb concentration changes in control group and pDOC patients.

The distribution of haemoglobin concentration changes for all subjects showed the higher amplitude of the concentration changes for the healthy subjects and for the oxyHb and motor movement. The hemodynamic response to motor imagery was weaker than to actual movement. Additionally as expected the change in concentration in deoxyHb was lower than oxyHb. The pDOC patients presented with the less pronounced response than healthy (Figure 5.7).

Figure 5.8 Distribution of concentration changes in total, oxy and deoxyHb across all three study groups



This figure presents the distribution of concentration changes in total, oxy and deoxyHb: vegetative state (VS), minimally conscious state (MCS), controls – motor movement (MM) and controls – motor imagery task (MI). Each dot denotes a subject and bold vertical lines indicate means. The horizontal axis denotes concentration changes expressed as a percentage of change in relation to the pre-stimuli haemoglobin concentration.

## 5.5 Discussion

This is a first report on the use of functional near infrared spectroscopy for brain function assessment in patients in VS and MCS.

This study explores the NIRS responses to motor movement and motor imagery tasks. Further, this study shows the patterns of NIRS responses from healthy controls to both the motor movement and to motor imagery, and then I used these patterns for validation of NIRS response in pDOC patients. This study identifies three types of haemodynamic response patterns present in both the healthy subjects and the patient group.

The controls in this study performed both types of tasks (imagery and motor movement) while the pDOC patients performed only the motor imagery task. The healthy controls elicited stronger NIRS responses during an actual movement when compared to motor imagery. Previous studies on motor tasks showed that NIRS cortical responses should generate a change ( $\Delta$ ) in oxyHb  $\sim 0.5 \mu\text{Mol/L}$  and in deoxyHb ( $\Delta$ )  $\sim 0.2 \mu\text{Mol/L}$  (Hirth, Obrig et al. 1996; Wolf, Wolf et al. 2002) and similar response is reported from this PhD study

Additionally, the responses to the motor imagery task were comparable with others (Iso, Moriuchi et al. 2015) and Wriessnegger *et al.* (Wriessnegger, Kurzmann et al. 2008).

### *5.5.1 Interpretation of fNIRS response*

Majority of healthy subjects and five out of 14 pDOC patients had a “typical” response to a motor task. The “inverted” response was seen in two out of 10 healthy subjects and in majority of pDOC patients. Although, the initial studies suggested that the typical fNIRS response to movement and motor imagery is characterised by an increase in the concentration of oxyHb accompanied by a less pronounced decrease of the deoxyHb level concentration (Sato, Ito et al. 2007), more recent studies report different patterns of fNIRS responses depending on the optical probe localisations and task difficulty (Mihara, Miyai et al. 2012). For example, Morihiro *et al.* (Morihiro, Tsubone et al. 2009) showed that oxyHb response over the left primary motor cortex decreased over time during a repetitive, right-handed tapping task, while the channels covering the supplementary motor cortex recorded an increase. In this PhD study, the NIRS signal was averaged over a broad area covering the premotor area, supplementary motor area (EEG corresponding areas FC3, FC1, FCz, FC2 and FC4) as well as the primary motor cortex (EEG corresponding areas C4, C2, Cz, C1 and C3), which may explain why healthy subjects and the patients tended to have an inverted oxyHb response.

The task is also a factor, Holper *et al.* (Holper, Shalom et al. 2011) found an inversed oxyHb response during motor imagery, which was related to the task difficulty, while the more complex task would produce stronger negativity of the oxyHb response. These factors may explain why my study showed both the typical and inverted haemodynamic responses in the study groups.

There is a very little research on NIRS and types of the haemodynamic responses that can be detected, however, there have been published studies on BOLD both typical and inverted responses. Recently, Sten *et al.* (Sten, Lundengard et al. 2017), showed and explained a physiologically based model for a negative BOLD and discussed a

mechanistic hypothesis for negative BOLD response which is the neural inhibition hypothesis. Authors hypothesised that inhibitory activity on physiological level is related with increased GABA levels which reduces signalling to astrocytes and production of vasoactive substances which leads to reduced (see Chapter 2.1.3) (Sten, Lundengard et al. 2017).

### ***5.5.2 Motor imagery versus motor task***

All three groups: controls, MCS and VS showed lateralised response with the stronger negative values of oxyHb over the right hemisphere during the right hand motor imagery tasks. Motor imagery has been shown in many studies to be associated with a greater bilateral functional imaging signal than actual motor movements, particularly in pre-motor and supplementary motor areas (Binkofski, Amunts et al. 2000; Pfurtscheller, Brunner et al. 2006). Ipsilateral (right-hemisphere) signal changes have been reported in several fMRI studies, that is, BOLD not fNIRS response, in anterior frontal regions (BA 9, 10 and 11) (Sharma, Pomeroy et al. 2006) (Porro, Cettolo et al. 2000), but also in the precentral gyrus (BA 6) during hand movement imagery (Hanakawa, Parikh et al. 2005). Another possible explanation of the inverted oxyHb results in NIRS also derives from the fMRI BOLD studies.

An ipsilateral “negative” BOLD response means an “U” shaped, as opposed to the bell-shaped MR signal changes, during an unimanual task activity was reported by McGregor *et al.*, who also suggested that this phenomenon is related to an active inhibition of cortical areas (McGregor, Sudhyadhom et al. 2015). Another group showed that ipsilateral negative BOLD during a unimanual task reflects normal transcallosal inhibition, while its dissipation impairs motor activity (Lenzi, Conte et al. 2007).

### ***5.5.3 Vegetative State/Unresponsive Wakefulness State vs. Minimally Conscious State Patients***

There were no statistically significant differences in NIRS responses between the two patient groups, which may be because of the study group size or because of heterogeneous aetiology of brain damage of patients included in this study. In this study the typical haemodynamic response was seen in four MCS patients (n=9) and only one VS patient (n=5), while the inverted haemodynamic response was present in two VS patients and four MCS patients. The unclassified response was in two VS and one MCS respectively.

There are reports of subpopulations of VS patients who remain behaviourally unresponsive, but their brain function, as measured using fMRI or EEG techniques, is more in keeping with a diagnosis of MCS (Coleman, Rodd et al. 2007; Schnakers, Vanhaudenhuyse et al. 2009; Monti, Vanhaudenhuyse et al. 2010; Cruse, Chennu et al. 2012). Hence, this may be one of the possible explanations. Another interpretation may be such as presented by Liberati *et al.* (Liberati, Hunefeldt et al. 2014), who reviewed of PET, EEG and fMRI studies and demonstrated that only half of the publications reported statistically significant differences between VS and MCS patients.

### ***5.5.4 Limitation of the NIRS technique***

The NIRS technique has several limitations and they are mostly related to signal contamination. The limitations related to NIR light propagation; scattering and absorption were discussed in Chapter 2.1.2.

Another problem related to the NIRS signal interpretation is how to ensure that the signal originated from cerebral cortex, since, there have been identified, also, non - cortical sources that can affect the NIRS measurements, such as, for instance, heart rate,

respiration, blood pressure and skin perspiration. It is a challenge to control for all of these factors, however, a block-design paradigm (task versus resting state) should at least partially eliminate the background noise related to the physiological factors (Amaro and Barker 2006). That is why, the paradigm used in this PhD study was a block designed.

Nethertheless, the NIRS technique using the traditional source detectors arrays (separation 2.5-3.5 cm), suffers from a low resolution and physiological noise contamination, however, recently these limitations were addressed by the use of high-density diffuse optical tomography (Ferradal, Liao et al. 2016). The high density refers to both, the use of dense optode arrays consisting of 32 sources and 34 detectors, and the source-detector pair measurements at multiple distances; for example, one source has been linked with four detectors at 1.0, 2.2, 3.0, and 3.6 cm, respectively (Ferradal, Liao et al. 2016).

## **5.6 Conclusion**

The assessment of the brain function in people with pDOC is complex and complicated by multiple interacting motor, sensory and cognitive impairments. This study, however, demonstrated that NIRS can be used for detection the task-induced brain activity changes in pDOC patients using a motor imagery task. Given both its relatively low-cost and that it is well tolerated by patients in a clinical ward setting, certainly compared with fMRI, NIRS represents a translatable imaging tool that can be used to gain new insights into brain function in patients with disorders of consciousness.

## Chapter Six

## **CHAPTER 6 EVENT RELATED EEG SYNCHRONIZATIONS AND DESYNCHRONIZATIONS DURING MOTOR IMAGERY IN PDOC PATIENTS**

Similar to Chapter 5, this is also an experimental chapter where the practical aspect of the theory presented Chapter 2 was described.

The data was collected in the EEG laboratory at the Royal Hospital for Neuro-disability, which was established for this study. The main aim of this chapter is to explore the feasibility of the use of ERS and ERD for assessment of brain function.

### **6.1 Introduction**

Both ERS and ERD are EEG phenomena occurring during mental processes or during attention to sensory stimuli. One of the stimuli that can be used to evoke the EEG changes is either motor imagery or actual motor movement task. The motor tasks activate cortical areas such as motor cortex and either can decrease frequency of the EEG rhythm (ERD) or increase in frequency of EEG (ERS) (Klimesch, Doppelmayr et al. 2000) (Krause, Lang et al. 1996). Theoretical background of ERD and ERS was discussed in the Chapters 2 and 3 of this work.

The occurrence of ERD during a simple motor imagery task was first described by Gert Pfurtscheller, *et al.* (Pfurtscheller and Andrew 1999). ERD phenomenon, a decrease in

EEG frequency, can occur during beta (13-21Hz), alpha (7-12Hz) and theta (4-7Hz) EEG frequency rhythm. Pfurtscheller showed that during a motor imagery task the subjects developed significant higher beta band ERS and alpha ERD (Pfurtscheller and Lopes da Silva 1999).

Despite the fact, that the concept of ERD has been known for some time, but there are not many studies assessing brain function in pDOC patients using this approach. There are, however, several studies reporting on feasibility of the use of ERD for assessment of brain function in pDOC patients. For instance, Julia Lechinger, *et al.* (Lechinger, Chwala-Schlegel et al. 2013) examined the occurrence of the ERD in ten VS and seven MCS patients during observation and imagery of holding a cup and drinking out of this cup. Healthy controls showed typical desynchronizations while in MCS there was a synchronisations and only one out of ten VS patients showed ERS response similar to this seen in the MCS group.

## **6.2 Aims**

This study had following aims:

1. To assess the ability to evoke an event related oscillatory change expressed as ERD or ERS during a simple motor task in pDOC patients.
2. To compare results from the healthy subjects with the results from the patients to establish patterns of responses from healthy controls and pDOC patients.
3. To explore the feasibility of the bedside use of the EEG in brain function assessment in pDOC patients.

## **6.3 Methods**

### ***6.3.1 Subjects***

Ten healthy, right – handed volunteers (6 female mean age 39.6 yrs. SD 7.87) were included to the study.

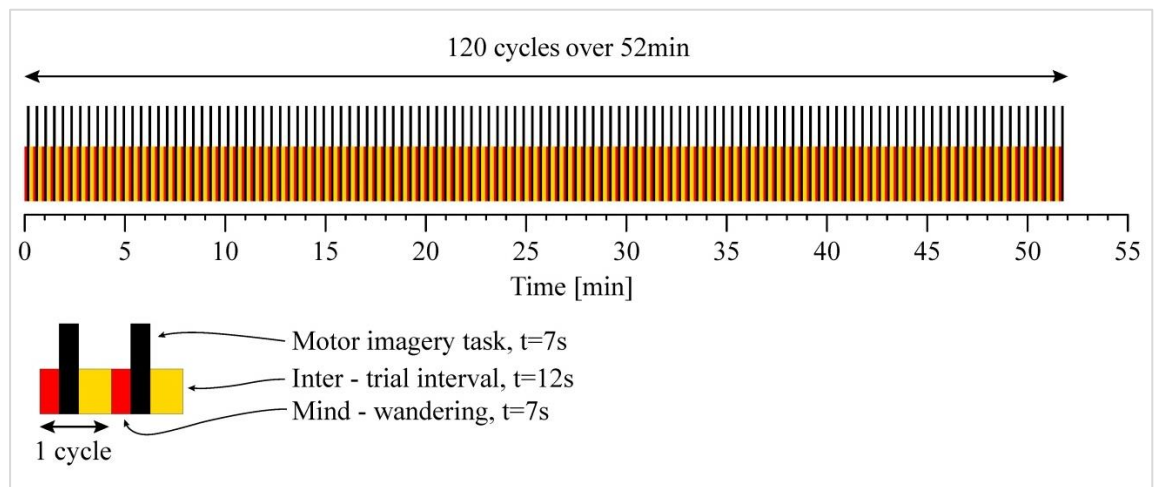
None of the control group suffered from neurological disorder nor was on psychotropic medications (according to self-reports). Handedness of the subjects was measured by a self-report of the side of their hand used in writing and eating. None of them had history of handedness correction. All volunteers were staff from the Royal Hospital for Neuro-disability. All subjects were given informed written consent.

For the patients group sixteen patients were included, the detailed description of the study population please see Chapter 4 of this thesis.

### 6.3.2 Task

The controls and the patients underwent the same paradigm. The paradigm was divided into 3 blocks as follows: mind wandering for seven seconds, then seven seconds of imagery of the right hand movement followed by twelve seconds of resting state. The aim was to repeat this paradigm at least 120 times, but the exact length of the collected data depended on subject's availability and tolerance of the experiment, since that total time spent for the data collection was 52 minutes. The subjects were asked to imagine the movement of their right hand, by imaging the self-paced movement with approximate speed of 1 Hz (Figure 6.1). During the "mind wandering" the subjects were instructed "let your mind wander" and during the resting state the instruction was "now rest".

Figure 6.1 Motor imagery task used to evoke EEG oscillatory changes



This figure presents the paradigm used in this study, there were 3 blocks in one cycle, and the aim was to perform in total of 120 cycles, which should be sufficient to evoke Event Related Desynchronization or Event Related Synchronization.

### ***6.3.3 EEG data acquisition and analysis***

The EEG was acquired using a WaveGuard 64 EEG sensor cap (*ANT-Neuro, Enscheda, the Netherlands*) with a standard sensor positions derived from the 10-20 system (Figure 3.7). For the further analysis four sensor positions, the F4, F3, C4 and C3 were configured in a bipolar montage. For the purposes of this study, electrode positions C4 and C3 were referenced to F4 and F3 respectively.

#### **EEG Pre-processing**

The ERD/ERS were calculated at alpha (7-11 Hz) band frequency. In order to derive the ERD/ERS measure, pre-processing steps were imposed on the EEG signal. The EEG was subjected to artefact rejection protocols, where the EEG was run through an amplitude window of  $\pm 150 \mu\text{V}$ . This ensured that ocular artefacts were excluded from the EEG signal. The EEG was then segmented according to the event marker types in order to define the epoch type. Three epoch types were defined, motor imagery, mind wandering and resting state. The epoch was set at 3 seconds before the event and 5 seconds after the event, thus the total event duration was 8 seconds. The reference baseline from which the %ERD would be calculated was defined at -1 second up to time zero. The EEG signal was then subjected to band pass filtering. For the alpha band, a band pass of 7-11 Hz was adopted using a finite impulse response (FIR) filter at a slope of 24d B (Higashi and Tanaka 2013). The FIR filter is a standard filter used to extract EEG signal to its basic components such as delta wave, theta wave, alpha wave and beta waves.

The data in this PhD study was analysed in a similar way to this used by Lechinger, *et al.* (Lechinger, Chwala-Schlegel *et al.* 2013). However, the motor command was different in my study “imagine you are squeezing a ball with your right hand”, from the used by Lechinger *et al.* “imagine you are holding a cup and drink from it”. The hand

movement task was previously validated for the use to obtain ERD and ERS from healthy subjects (see Chapter 2).

R-package for statistical computing, version 3.2.2 for Windows, was used for statistical analyses and data visualization (R development Core Team 2015). Figures were further adjusted using Adobe Illustrator®, Creative Studio 5; Version 15.0.0.

The ERD/ERS values for the left and right hemisphere were analysed using a T-test, the P-values were set at  $<0.05$  for a two-tailed distribution as a criterion for statistical significance for all analyses.

## **6.4 Results**

### ***6.4.1 ERD motor imagery in healthy subjects***

Eight out of ten controls responded with the ERD to the imagery task, and two healthy controls responded with ERS to the motor imagery task within the alpha rhythm band. The mean response to the ERD (excluded subjects numbered 7 and 10 as developed ERS response) over the left hemisphere was -24.39 % (95% CI -29.45 to -19.31) over the C3 EEG position and over C4 was -14.18% (95% CI -18.40 to- 9.95) respectively, the  $p = 0.0026$  (Table 6.1).

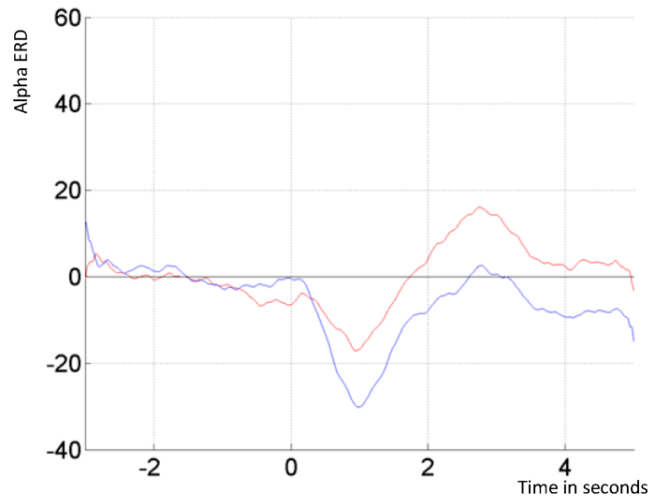
*Table 6.1 EEG event related desynchronizations and synchronizations.*

<b>Healthy controls</b>	<b>C3 7-11 Hz ERD%</b>	<b>C4 7-11 Hz ERD%</b>	<b>C3 time in sec</b>	<b>C4 time in sec</b>
1	-30.14	-16.98	0.98	0.93
2	-22.21	-5.10	0.87	1.22
3	-16.73	-16.56	2.74	2.41
4	-26.10	-9.30	1.69	1.34
5	-34.55	-20.06	1.22	1.28
6	-21.32	-17.62	1.01	1.03
7*	34.19	15.05	0.97	0.83
8	-26.15	-16.30	2.60	2.56
9	-17.90	-11.80	1.86	1.86
10*	14.78	24.01	2.36	2.27

*This table presents EEG event related desynchronization (negative value) and event related synchronizations (positive value) over the C3 (left) and C4 (right) hemisphere calculated for the alpha band in healthy controls during self-paced kinaesthetic motor imagery, \* denotes ERS. The difference between C3 and C4 response was statistically significant ( $p=0.0026$ ).*

The ERD response was lateralised and stronger over the left hemisphere (Figure 6.2).

*Figure 6.2 Example of EEG response to the motor imagery task*



*This figure presents Event Related Desynchronization (ERD) on EEG as response to a motor imagery task (imagine you are squeezing your right hand), alpha rhythm desynchronization, single subject response (control 1) the blue line denotes left, and red line right side respectively; x axis denotes time in second and y axis the ERD expressed as a percentage of change in relation to the pre-stimuli baseline.*

#### ***6.4.2 ERD /ERS motor imagery in pDOC patients***

Sixteen pDOC patients performed the self-paced motor imagery paradigm. Thirty seven percent of patients (6 out of 16) did not elicit any clearly identifiable EEG synchronizations or desynchronizations during the motor task. Among these six patients, who did not show a clear response, three were MCS and three in the VS.

The mean ERD response calculated for 10 out of 16 pDOC subjects, for the alpha rhythm over the C3 (left) was -5.75% (95% CI -11.21 to -0.32) and over the C4 was 2.62% (95% CI -1.48 to 6.71) respectively with statistically significant difference between hemispheres,  $p = 0.04$  (Table 6.2).

The pDOC patients responded with a delay when compared to healthy subjects, with the mean time to peak over C4 1.29 seconds (95%CI 0.68 to 1.89), whereas for controls over C4 it was 1.11 seconds (95% CI 0.39 to 1.83). The mean time to peak for the ERD over the left hemisphere was in controls 1.37 seconds (95% CI 0.61 to 2.14), and for patients the mean time was 1.73 seconds (95% CI 0.12 to 3.36).

*Table 6.2 EEG event related desynchronization and synchronisations for the alpha band.*

<b>Study group</b>	<b>C3 7-11 Hz ERD/ERS in %</b>	<b>C4 7-11 Hz ERD/ERS in %</b>	<b>C3 time in sec</b>	<b>C4 time in sec</b>
Patient 1 MCS	-11.33	10.01	1.99	2.42
Patient 2 MSC	-5.503	4.94	3.33	1.57
Patient 3 MCS	-2.20	5.02	1.11	2.26
Patient 4 VS	-9.34	-8.05	0.45	0.45
Patient 5 MCS	-19.26	10.34	4.05	0.66
Patient 6 MCS	NA	NA	NA	NA
Patient 7 MSC	-5.89	4.54	0.77	1.023
Patient 8 MCS	10.44	1.56	0.70	0.73
Patient 9 MCS	NA	NA	NA	NA
Patient 10 VS	NA	NA	NA	NA
Patient 11VS	NA	NA	NA	NA
Patient 12 VS	-1.63	2.40	1,73	1.95
Patient 13 VS	NA	NA	NA	NA
Patient 14 MCS	-7.31	-1.34	1.86	1.89
Patient 15 MCS	NA	NA	NA	NA
Patient 16 MCS	-5.57	-3.28	2.01	1.96

*This table presents EEG event related desynchronization and synchronisations calculated for the alpha band in pDOC patients during a self-paced kinaesthetic motor imagery; the Event Related Desynchronization (ERD) has a negative value while Event Related Synchronization (ERS) has a positive value; NA- if no ERD/ERS identifiable. VS = Vegetative State; MCS = Minimally Conscious State. There was a statistically significant difference in signal recorded in C3 and C4 (p=0.04).*

## **6.5 Discussion**

In this study the ERD and ERS responses from the pDOC patients were evaluated. Ten out of 16 patients developed lateralised, over the left hemisphere response and this response was statistically significant different from the one over the right hemisphere (on group level). On individual case-by case review only 3 out of 11 patients with MCS developed ERD/ERS with differences more than 10 percentages between the tasks. Only one out of 5 VS patients develops ERS of 9%. Similar observations were published elsewhere (Cruse, Chennu et al. 2011).

### ***6.5.1 Methodological considerations***

The control group showed lateralised ERD response and this result was consistent with Pfurtscheller and Lopes da Silva previous findings (Pfurtscheller and Lopes da Silva 1999).

Eighty percent of the healthy group (8 out of 10) developed a significant contralateral ERD, however two healthy subjects responded to the motor imagery task with the EEG synchronizations, which is an increase in rhythm frequency. This may be because, the ERD is a focal response and spatially occupies only limited space, unlike the ERS, which represents cortical inhibition and is spatially less focal than ERDs (Franzkowiak, Pollok et al. 2010).

The usual pattern of the occurrence of the ERD and ERS derived from the alpha and beta bands was described by van Burik and Pfurtscheller (van Burik and Pfurtscheller 1999) and the pattern is as follows: first occurs the alpha ERD during a movement preparation or an actual movement and this is followed by the beta ERS bursts.

Furthermore, the both phenomena, the alpha and beta band ERD were found to be anatomically and functionally specific, since “a foot movement resulted in post movement beta oscillation within the 19-26 Hz band, whereas finger movement would cause changes within the 16-21 Hz band”. In regard to the anatomy, as van Burik and Pfurtscheller (van Burik and Pfurtscheller 1999) suggested that the oscillations occur according to the homunculus. Hence, the topography of the oscillations was as follows: the beta band oscillation for hand movement was detectable laterally in the sensorimotor strip, while a foot area was located medially within the interhemispheric fissure.

As mentioned above the ERD can be also detected using the beta band frequency. Majority of pDOC patients, however, received medication, which can potentially influence the beta band brain oscillations. Some drugs can cause an increase in beta band oscillation such as, for instance SSRI's and Benzodiazepines (Salinsky, Binder et al. 2002) or a decrease as for instance, Baclofen (beta-(p-chlorophenyl)-gamma-aminobutyric acid). Additionally, Baclofen was shown to increase in slow waves and decrease of fast EEG activity (Badr, Matousek et al. 1983). Therefore, the beta band oscillation-changes could not to be used as a reliable measure in pDOC population.

### ***6.5.2 Reliability and stability of the event related de- or-synchronizations***

The EEG data in this study was analysed according to the classical approach, as suggested by Pfurtscheller and discussed in the Chapters 2 and 3 of this work.

The classical approach to the ERD/ERS encompasses a conventional time-averaged EEG. This type of analysis was shown to be a reliable tool with a high internal consistency (Cronbach's alpha >0.07) (Burgess and Gruzelier 1996).

Burgess and Gruzelier (Burgess and Gruzelier 1993) showed that ERD/ERS can have an idiosyncratic inter- subject difference, however, this difference is stable. Moreover, they showed that spatio-temporal stability of the ERD was good on a single subject level and excellent on the group comparison level.

Others also examined the temporal stability of the ERDs. For instance, Friedrich, *et al.* (Friedrich, Scherer *et al.* 2013) investigated the temporal stability of the ERDs during the period of two weeks and four sessions using several mental tasks such as: mental rotation, word association, auditory imagery, mental subtraction, and spatial navigation, imagery of the familiar faces and the motor imagery. The motor imagery task was almost identical to the one used in the current study, namely: imagination of the repetitive self-paced movements of the own right hand, squeezing a ball. The Cronbach's alpha coefficient was >0.7 for this task.

The ERD data from the pDOC patients can be also analysed using a support vector machine also known as machine Learning analysis. This is an algorithm that analyses data using the classification and regression analysis. Cruse, *et al.* (Cruse, Chennu *et al.* 2012), assessed the presence of ERD/ERS in pDOC patients using this way of analysis. Their study showed that using the support vector machine it was possible to detect the ERD in some of the VS patients. This study indicated patients' ability to follow

commands in three out of 16 VS patients (19%) with the classification accuracy of 61-78%.

### ***6.5.3 Event related synchronization and desynchronizations in pDOC patients***

Four pDOC patients (3 in MCS and 1 in VS) responded to a motor imagery task with either synchronizations or desynchronizations. In this study the frequency of EEG during the task “imagine you are squeezing your right hand” was compared with the pre-stimulus baseline as discussed in Chapter 1.4 and 2.2. Others showed that a VS patient was able not only to perform a motor imagery task but also differentiate between left and right hand, since the commands were “try to move your right hand”. “try to move your left”, and “now rest” (Cruse, Chennu et al. 2012). Also a complex motor imagery such as sport of their choice and navigation around a house, are deemed as feasible for use for brain function in pDOC patients (Horki, Bauernfeind et al. 2014).

## **6.6 Conclusion**

The ERD and ERS have been established, valid and reliable EEG phenomena occurring during various cognitive tasks that can be used for bedside assessment of brain function in pDOC patients. In this study an imagery of right hand movement task was used, since the previous studies confirmed the highest stability and reliability of this type of movement. The ERD/ERS analysis had been incorporated as a part of the commercially available software (*A.S.Alab the Netherlands*) for the EEG data analysis, which makes this approach feasible for the routine and clinical use for assessment of brain function in pDOC patients.

All control subjects in this study responded with the ERD/ERS over the contralateral hemisphere to the motor imagery task, moreover, four out of 16 pDOC patients developed ERD/ERS responses with the significant difference between left and right hemisphere. Furthermore, three MCS patients developed the response similar to healthy population.

## Chapter Seven

## **CHAPTER 7 HAEMODYNAMIC AND ELECTRICAL BRAIN RESPONSES IN PDOC PATIENTS**

The main aim of this chapter is to explore the feasibility of simultaneous recording of EEG and NIRS signals for assessment of brain function in pDOC patients. This chapter summarises the results from Chapters 5 and 6. In previous Chapters both: the NIRS and EEG signals were analysed, albeit separately. This chapter focuses on relationship between the NIRS and EEG signals during a motor imagery task.

### **7.1 Introduction**

As discussed in Chapter 2, both: the NIRS and EEG techniques can be used to assess brain activity during a motor task. These two techniques focus on different aspects of the brain activity, namely on haemodynamic and electrical. The theory is, however, that these processes are coupled together and described as the neuro-vascular coupling theory. Previous studies, for instance, on the brain responses to language, epilepsy and the motor function showed the feasibility of the use of NIRS and EEG as complementary methods for comprehensive brain function assessment (Wallois, Mahmoudzadeh et al. 2012; Peng, Nguyen et al. 2014; Zama and Shimada 2015).

Furthermore, specifically the motor imagery task appeared to produce reliable NIRS and EEG signal changes, and that is why the both of these techniques were proposed to be used for the Brain Computer Interface (BCI) (Kaiser, Bauernfeind et al. 2014). The highest accuracy was found for the “right-hand motor imagery ”(Hwang, Lim et al. 2014).

The tasks involving movements of the right hand were shown to be a reliable and recommended for the use in NIRS/EEG studies.

Zama and Shimada (Zama and Shimada 2015) investigated correlation between readiness potential occurring during a movement preparation and NIRS changes and found out that the readiness potential was positively correlated with the increased in concentration of oxyHb.

## **7.2 Aims**

The aim of this study was to compare changes in EEG, expressed as ERD or ERS with the changes in oxy and deoxyHb concentration during a motor task in patients with pDOC and controls.

## **7.3 Methods**

The controls and the subjects are described previously in Chapters 5 and 6.

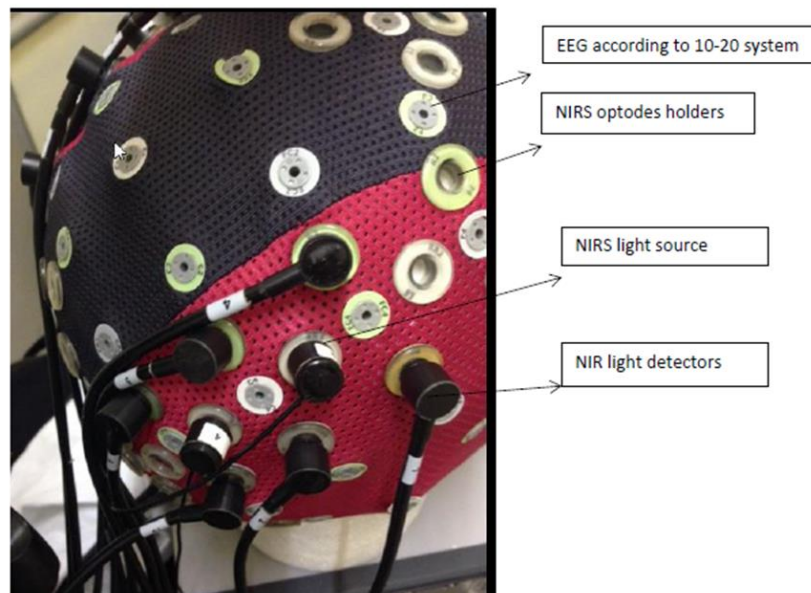
The EEG and NIRS apparatus as well as methods of the data collection were also described in Chapters 5 and 6 this work. The task was a motor imagery, self-paced right hand squeezing for 7 seconds (Figure 6.1).

Nevertheless, because of the different time scales for the NIRS and EEG responses, namely the EEG response taken for analysis in this study ranged from 300 ms to 800

ms, while the NIRS response began at 1000 ms. Although the same paradigm was implemented in the EEG and NIRS study, as presented on the figure 6.1, the NIRS study required some adjustments. Hence, in the NIRS part of the study the resting state and the mind wandering were treated as a pre-stimulus baseline and the epoch was set as described above -7 sec to 0 as a baseline and 0 to 7 sec for the motor task response. This was because the NIRS response needed not only the longer latency before the onset but also required longer time for the haemodynamic response to achieve a pre-stimulus baseline. A study by Miezin, *et al.* (Miezin, Maccotta et al. 2000) showed that the haemodynamic response achieved the pre-stimulus baseline after 10 to 12 seconds post causation of the activation.

An integrated system enabling recording of NIRS (NIRx Medical Technologies LLC, Berlin, Germany) and EEG (ANT-Neuro, Enschede, the Netherlands) signals was used in this PhD study. The head cap had holders for both EEG electrodes and NIRS optodes (Figure 7.1) signals. First the NIRS study was performed and the NIRS data collection lasted approximately 10 min, then the same paradigm was used for the EEG and the data collection lasted approximately 40 min.

*Figure 7.1 NIRS and EEG integrated head cap for data collection*



*This figure presents a head cap used for the data collection in this PhD study. This cap has both EEG (ANT-Neuro, Enschede, the Netherlands) and NIRS (NIRx Medical Technologies LLC, Berlin, Germany) holders.*

The Region of Interest was specified as C3 according to the 10-20 International System and the NIRS channels surrounding the C3 position, namely: Channels 7, 8, 11 and 12 (Figure 5.2). In the analysis only one channel out of four was chosen, where the change was the biggest. This methodology was previously by Zama and Shimada (Zama and Shimada 2015).

## 7.4 Results

### *7.4.1 C3 ERD and NIRS activation in controls*

Eight out of ten controls responded with the ERD at alpha band (7-11 Hz) to the motor imagery task, with the stronger response over the C3 position than C4 (left hemisphere vs right hemisphere, -24.38 SD 6.6 vs. -14.21 SD 5.01,  $p=0.001$ ). The global NIRS response followed the same pattern with greater response over the left hemisphere, for oxy and deoxyHb respectively (Table 7.1).

*Table 7.1 ERD and NIRS responses to a motor task in control subjects*

Healthy controls	C4 ERD	oxyHb relative change right channels	deoxyHb relative change-right channels	C3 ERD	oxyHb relative change left channels	deoxyHb relative change left channels
1	-16.98	24.211	-17.188	<b>-30.14</b>	<b>23.077</b>	<b>-17.455</b>
2	-5.1	-6.608	-25.221	<b>-22.21</b>	<b>14.191</b>	<b>12.552</b>
3	-16.56	27.158	29.432	<b>-16.73</b>	<b>20.358</b>	<b>-29.967</b>
4	-9.3	8.996	-16.525	<b>-26.1</b>	<b>11.385</b>	<b>-16.118</b>
5	-20.06	11.016	-17.238	<b>-34.55</b>	<b>7.848</b>	<b>-21.555</b>
6	-17.62	-38.426	-25.231	<b>-21.32</b>	<b>-44.652</b>	<b>29.997</b>
8	-16.3	-4.845	8.714	<b>-26.15</b>	<b>-4.396</b>	<b>14.753</b>
9	-11.8	-10.865	6.812	<b>-17.9</b>	<b>-7.744</b>	<b>13.219</b>

*This table presents the event related desynchronization (ERD) and oxy and deoxyHb concentration changes in response to a motor task. The NIRS response has been taken from channels surrounding C3 (left) or C4 right positions respectively.*

#### *7.4.2 C3 ERD and NIRS activation in pDOC patients*

Eight out of sixteen patients with pDOC responded with the ERD over the C3 position to the motor imagery task, six of them were in the MCS and two were diagnosed with the VS (for detailed patients' characteristics please see the Chapter 4 of this thesis). Moreover, all of the patients who responded with the ERD also developed a haemodynamic response measurable using the NIRS apparatus.

The ERD response was stronger over the left hemisphere (C3)  $-4.87$  SD  $8.29$  vs. over the C4, where it was  $2.18$  SD  $5.64$  ( $p=0.06$ ), moreover this response was followed by a global haemodynamic response expressed as changes in oxy and deoxyHb over the left hemisphere similar to the pattern that was in the healthy subjects (Table 7.2).

*Table 7.2 ERD and NIRS response to a motor task in pDOC patients*

Patient's No	Right hemisphere			Left hemisphere		
	C4 ERD	oxyHb relative change right channels	deoxyHb relative change- right channels	C3 ERD	oxyHb relative change left channels	deoxyHb relative change left channels
2 MSC	4.94	-9.851	-3.48	-5.503	-10.678	-11.867
3 MCS	5.02	7.318	8.037	-2.2	7.944	4.375
4 VS	-8.05	-2.149	-4.251	-9.34	-3.011	-3.714
5 MCS	10.34	3.672	1.804	-19.26	4.871	2.442
7 MSC	4.54	6.997	1.986	-5.89	7.819	-4.973
8 MCS	1.56	3.45	6.396	10.44	2.309	4.053
12 VS	2.4	3.749	5.444	-1.63	7.774	4.65
16MCS	-3.28	2.238	-2.725	-5.57	7.413	-2.438

*This table presents event related desynchronization (ERD) and oxy and deoxyHb concentration changes in response to a motor task; the NIRS response has been taken from channels surrounding C3 (left) or C4 right positions respectively.*

## 7.5 Discussion

This is the first study that describes relation between electrical and haemodynamic brain responses to the motor imagery task in pDOC patients.

The main aim of this study was to analyse the electrical and haemodynamic responses from the area surrounding C3 (left side) EEG position according to the 10-20 system during the motor imagery activation of the right hand.

This study showed that the eight out of 16 pDOC patients, who underwent an assessment using both the NIRS and EEG, developed similar responses on both modalities. As expected, there was a stronger response from the left hemisphere (C3 EEG position) because the task was to imagine a right hand movement.

### *7.5.1 Motor cortex activation measurement using NIRS and EEG*

In this study, the NIRS channels covered a scalp area of approximately of 11.25 cm<sup>2</sup> where the C3 position was in the hypothetical centre of this area. The motor cortex of the human brain is a complex structure and was subjected many studies. Also the definition of the motor cortex evolved over time, for instance, Fulton (Fulton 1950) published a manuscript, which suggested that the motor cortex was built of a motor area and consisted, only, with a gigantopyramidalis (Area 4 of Brodmann). Later a premotor cortex was described and assigned as an Area 6 of Brodmann. Later, a third component of the motor cortex was included: Areas 9,10,11 and 12 of Brodmann (Halsband, Ito et al. 1993).

A recent fMRI study on motor cortex activation during a motor imagery revealed activation in Areas 3 (primary somatosensory cortex) and 6 (premotor cortex and supplementary motor area) of Brodmann as well as cerebellum and thalamus (Mokienko, Chervyakov et al. 2013).

However, Berman, *et al.* (Berman, Horovitz et al. 2012) showed that during a motor imagery task the participants frequently and involuntarily activated muscle and even a minimal and accidental muscle activation can lead to an increase in BOLD signal over the primary motor cortex area. Hence, the electromyography can potentially help to eliminate any muscle activation attributable to motor imagery.

The limitation of this study is such that electromyography was not used. Another problem is that the pDOC patients can have involuntary muscle spasms. All these factors, therefore, could potentially lead to the haemoglobin concentration changes. That is why it would be recommended to use the ERD/ERS, which would be an additional way of the validation of the signal's origin namely: cortical activity vs not cortical sources. Moreover, as presented in table 7.1 and 7.2, there was a pattern of the signal changes, with the stronger response from the healthy group then from the pDOC patients. Within the pDOC patients there also was a pattern of general stronger response from the MCS then from the VS patients. Additionally the pattern shows lateralised, over the left hemisphere, response on both modalities, the EEG and NIRS.

### ***7.5.2 Correlation between NIRS and EEG response to motor imagery task***

Another problem is how to correlate the EEG and NIRS signal changes occurring during a motor activation over the EEG C3 position region. Recently, Zama and Shimada (Zama and Shimada 2015) found a strong negative correlation between NIRS oxyHb concentration changes and EEG changes expressed as a readiness potential (Pearson's correlation  $r(2)=0.235$ ,  $p=0.03$ ) occurring during a self-paced motor imagery of pressing a button in healthy controls.

The main difference from the Zama's study and this study is such that their study reports on the readiness potential, which is a negative small voltage shift one second prior to the motor task execution. While the current study assesses the ERD/ERS, which is a change in the synchrony of neuronal population expressed as a change in the power frequency bands (Mehnert 2014).

Moreover, Zama and Shimada, used different statistical approach to compare responses from EEG and NIRS, namely they assessed the area under curve on receiver operator curve statistics, from the Z values of the oxyHb concentration changes (Zama and Shimada 2015).

There are advantages of the simultaneous recording of NIRS and EEG. As shown by Fazli, *et al.* (Fazli, Mehnert et al. 2012) simultaneous measurements of NIRS and EEG may lead to improvements the classification accuracy of motor imagery by 5%, reached statistical significance ( $p<0.001$ ). Not only the NIRS and EEG was built within one BCI system, but also another group developed a probe for simultaneous recording of NIRS and EEG signals (Cooper, Everdell et al. 2009). There are also commercially available combined NIRS and EEG systems, for instance, Artinis (*Artinis Medical Systems, The Netherlands*), or from the Brain Products (*Brain Products GmbH, Germany*).

## **7.6 Conclusion**

This work presents the brain responses measurable with the EEG and NIRS techniques during a motor task in patients with pDOC.

The main aim was to establish whether the electrical and hemodynamic changes are temporally and spatially related, hence, whether the measured changes on NIRS and EEG signal were related and occurred in a response to the motor task. The study showed some positive results on coexistence of both electrical and haemodynamic responses, indicating, therefore, a feasibility of the use of NIRS and EEG for assessment of the brain function in pDOC patients. However, the results warrant the need for further research to explore more in detail the relation between neuronal and haemodynamic responses after the brain injury.

## Chapter Eight

## **CHAPTER 8 ABILITY TO DISCRIMINATE BETWEEN OWN NAME AND OTHER NAMES IN PDOC PATIENTS**

This is an experimental chapter exploring the difference in brain reaction to one's own name and to others names in pDOC patients using EEG. The feasibility of the use of a subject's own name has been established previously, this study, however, is novel because of the way of the data analysis (Statistical Parametric Mapping software) and the used stimuli (subject's own name contrasted against other names).

### **8.1 Introduction**

Our first name has been used for assessment of attention since Wood and Cowan (Wood and Cowan 1995) described a "cocktail party phenomenon", which is the ability to detect one's own first name, even if it is said by an unattended speaker in a noisy environment.

The brain responses to a subject's own name have been evaluated using event related potentials (ERP) approach for assessment of a brain electrical activation. The brain response to subject's own name usually occurs within the time window of 250 to 800 ms post stimuli.

The first component of ERP is a positive-going-wave occurring approximately at 250-350 ms post stimuli with the maximum amplitude over fronto-central electrodes and it

is called a P300. The P300 is usually a marker of various cognitive functions such as stimulus recognition, subjective significance and working memory updating (Coles, Gratton et al. 1988), (Polich 1987). The P300 can also be evoked by a rare stimulus presented with a trail of standard stimuli (an oddball paradigm). The P300 component is characterised by its amplitude and latency. Amplitude ( $\mu\text{V}$ ) is defined as the difference between the mean pre-stimulus baseline voltage and the largest positive-going peak of ERP within a time window. Latency is expressed in milliseconds and this is the time from stimulus onset to the point of maximum amplitude within a time window (Polich 2007).

As mentioned above, the P300 component can be elicited by an unpredictable or surprising stimulus occurring during listening to the trail of auditory stimuli. Interestingly, despite many years of studies there is still lack of consensus about the exact meaning of the ERP. The most widely recognised, but also criticized theory is the “context updating” theory proposed by Donchin (Donchin 1981). This theory says that any sensory information initially has been stored in the working memory and compared with the previous one, if the new one is different or unexpected, then P300 is elicited (Polich 2007).

The P300 wave has two distinguishable spatially components: a frontal one - P3a and parietal P3b component. The meaning of these two components was further investigated by Verleger, *et al.* (Verleger, Jaskowski et al. 1994) who hypothesised that the P3b component was observed for targets that were infrequent but in some sense expected, while P3a seems to be elicited by a stimulus truly unexpected. Others authors also have shown that P3b increases with the task relevance and motivation for processing of the information; this may be interpreted as stimulus evaluation and categorization, which is a part of context updating theory (Lenartowicz, Escobedo-Quiroz et al. 2010).

The brain responses to subjects' own name were studied in many different clinical and developmental scenarios, for example on neonates, on normal subjects in sleep, in coma and on people with disorders of consciousness. Parise, *et al.* (Parise, Friederici et al. 2010) investigated brain responses to the subject's own name in four month old infants and showed, that the infants were able to differentiate from an own first name and other names based only on a first phoneme. Moreover, the infants from their study appeared to be more attentive to a person calling their name when compared to other name.

Another component of the ERP brain response to the own name occurs approximately from 400 ms to 800 ms and is called a posterior positive (PP). The studies showed that this occurs during a recollection and retrieval processes (Holeckova, Fischer et al. 2006).

Hence, the use of the responses from around 300 ms and 700 ms post stimuli and contrasting the response to the own name against the response to other names may add to our understanding of brain function in pDOC patients.

## **8.2 Aims**

The main aims of this study were as follows;

1. To obtain a spatial and temporal pattern of the ERP response to subject's own name and other names from the control group
2. To obtain a spatial and temporal pattern of the ERP response to own name and to other names from the pDOC patients
3. To use the SPM software to visualise the EEG responses

## **8.3 Methods**

### **8.3.1 Subjects**

#### Controls

Twelve healthy, right – handed volunteers (5 female mean age 39.09 years, SD 5.26) were included in the study. None of them suffered from neurological or psychiatric disorders, substance abuse or brain injury, also none of them was on psychotropic medications (according to a self-report). Handedness of the subjects was measured by the self-report of the side they used in writing and eating. None of them had history of handedness correction.

Written informed consent was obtained from all the subjects or relatives of the patients prior to the study. The investigation was carried out in accordance with the latest version of the Declaration of Helsinki and the study was approved by the Ethics Committee (please see Appendix 1).

#### Prolonged Disorders of Consciousness Patients

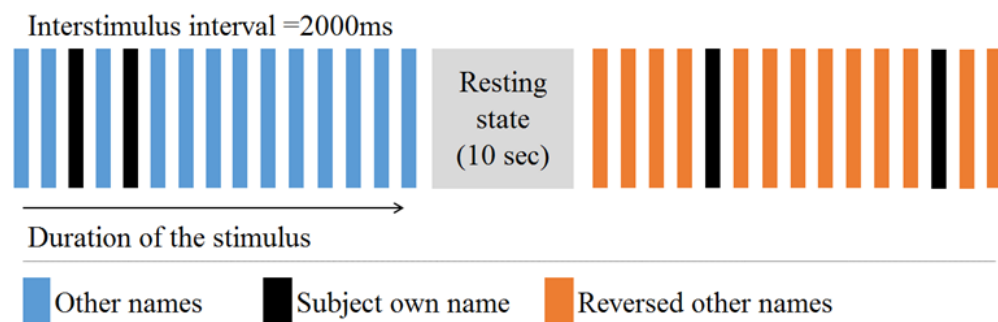
Please see the chapter 4 of this thesis for a detailed description of the patients included in the study.

### **8.3.2 Experiment**

During the experiment three types of auditory stimuli were presented: subject's own name, other names and reversed names. There were three block types: other names, reversed names and rest (no auditory stimuli). The auditory stimuli were presented in

blocks totalling 15 stimuli each. The inter-stimulus interval was fixed at 2000 ms. Each auditory block lasted for 35.5 secs and was followed by a 10 sec long rest block. 22 blocks were presented producing 44 subject's own name trials, 143 other name trials and 143 reversed name trials in total, per subject. The duration of the audio stimuli ranged from 292 ms to 736 ms, average = 500 ms (Figure 8.1).

*Figure 8.1 Auditory paradigm used for event related potential responses to subject's own name paradigm*



*This figure presents an overview on the auditory paradigm used to evoke an Event Related Potentials; each activation block lasted for 35.5 sec, 15 stimuli per block with a random presentation of two 'subject own name' events and 13 other stimuli or reversed names, in total 22 blocks were presented, 11 with the other names and 11 with reversed names.*

The auditory stimuli (names) were recorded by a male native English speaker using a Magix music editor version 2.0 and the audio files were edited using the Praat software. The reversed name stimuli were simply time reversed other names used in this experiment (spectrogram was reflected across the midpoint of the y axis. The stimuli were delivered binaurally through the earphones using evoke software 3.1.5 (ANT Neuro, Enschede, The Netherlands) with , sound levels set to 70 dB.

### ***8.3.3 EEG Data registration and analysis***

EEG was acquired using a Waveguard 64 EEG sensor-cap (*ANT-Neuro, Enscheda, the Netherlands*) whose standard sensor positions were derived from the 10-20 system (Jasper, 1958) and additional positions being determined from the 10-10 electrode placement system. In this study, EEG was recorded from 64 sensor positions (see Chapter 3).

The data was analysed using the SPM. The EEG data were converted from the \*.cnt format to the readable by SPM8 run using Matlab (*Matlab version R2011a, MathWorks, Natick MA*). The converted EEG data was subjected a high-pass filter of 1 Hz to eliminate slow drift correction, then eye artefact correction according to a script written to the SPM8 (Berg eye movement correction) was performed. At this stage two out of 12 healthy subjects' and one out of 16 pDOC data sets were excluded from the further analysis due to excessive artefacts. Subsequently three epochs were created for each of the three conditions: subject's own name, other names and reversed names with the epoch beginning 100 ms before the stimulus onset and ending 1000 ms after this.

The data were, then, low - pass filtered at 30 Hz to eliminate muscle artefact and the EEG gamma frequency band. Subsequently 3D images were created for each trial, which represented changes of the scalp recorded potentials in scalp space (two dimensions, X and Y) over peri-stimulus time (z dimension). These images were generated from root-mean-square values at each location (Litvak, Mattout et al. 2011). Therefore, a single image per trial contained information about the electrical signal in  $\mu\text{vol}$ . For the controls the data was taken into a further step of analysis, a second level of analysis, where one- way-ANOVA with R-levels and F-test was performed. Three contrasts were identified and the contrast between responses to own name versus

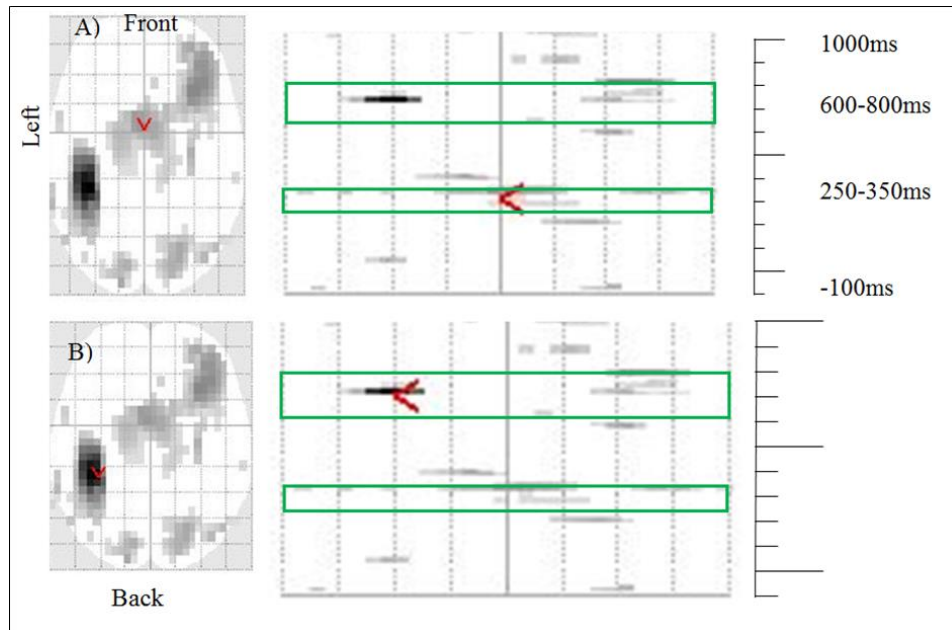
responses to other names was examined for statistical differences, since this contrast was deemed as the most indicative of the self-awareness. The results were assessed with an F test for differences of either polarity. The results were initially thresholded at  $p=0.001$  uncorrected with FWE correction based on random field theory, as described by Litvak and others (Litvak, Mattout et al. 2011). As the epoch lasted 1100 ms and I was not expecting ERP responses throughout this time, I used two time defined volumes of interest at 250-350 ms and 600-800 ms post-stimulus. These masks were applied to the SPM as a small volume correction and only those regions that survived a family wise error correction (FEW) of  $p < .05$  corrected for multiple comparisons are reported (Litvak, Mattout et al. 2011).

## **8.4 Results**

### ***8.4.1 EEG responses to subject's own name in control population***

In ten controls both auditory stimuli carrying information (own name and other names) elicited a large P3 component culminating at the Cz position and occurring between 250 to 350 ms post stimuli. Interestingly, the non-sense stimuli (reversed names) elicited only minimal response. A repeated measures of variances showed significant differences between all three types of stimuli, Bonferroni corrected  $p=0.02$ . The most significant responses within the two time windows from 250 to 350 ms and from 600 to 800 ms post stimuli and the graphical presentation of the sensors \*time\*space are presented in the Figure 8.2 and Table 8.1.

Figure 8.2 Control subjects response to own name at latency of 250-350 ms and at 600-800 ms



This figure presents responses to subject's own name in control subjects ( $n=10$ ) with (A) response at a latency of 250-350 ms and (B) a latency of 600-800 ms. Red arrows indicate the most significant response using the  $F$  test to the contrast own name against other names

*Table 8.1 Early and late EEG responses to subject own name paradigm in in control subjects*

N=10, controls	Peak – level							
	Response time	P FEW corrected	F	Z <sub>i</sub>	P uncorrected	mm	mm	ms
250-350 ms	0.003	25.58	3.77	<0.0001	0	2	307	Superior frontal*
600-800 ms	0.012	49.22	4.67	<0.0001	-34	-36	703	Superior parietal

*This table presents the responses in healthy controls (n=10) showing the difference between responses to subject's own name vs. other names. The result was consider as significant if the correction using familywise error (FEW) and false discovery rate were <.05, the mm x mm shows the spatial position and ms indicates the time since onset for the most significant response. \* positions taken from (Koessler, Maillard et al. 2009).*

As shown in the Table 8.1 and Figure 8.2 a small volume correction analysis detected the most significant responses over the central region for the time range from 250 ms to 350 ms and over the left temporo-parietal cortex for the time from 600 to 800 ms respectively.

The maps were generated for analysis with a minimum threshold of  $p < 0.001$ , uncorrected for multiple comparisons). Then a non-paired t test; differences in responses to own name versus to other names were considered as significant only after correction for multiple comparisons using the FEW and the false discovery rate (FDR) corrections.

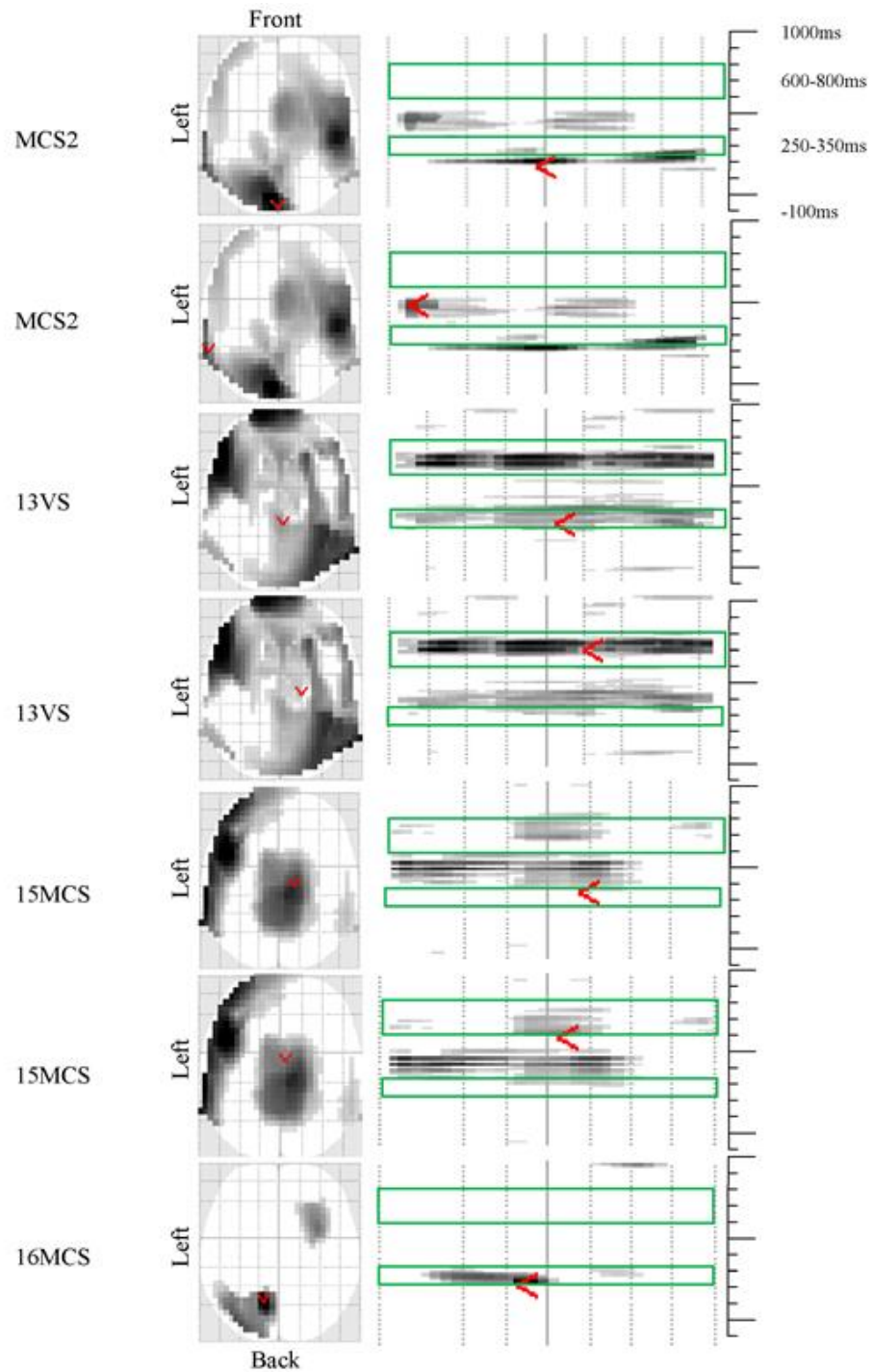
#### ***8.4.2 EEG responses to subject's own name in a study population***

The average response in pDOC patients (n=15) was weaker to the subject's own name, other names and reversed names than the control group. The mean of the EEG responses in  $\mu\text{Vol}$  was at Cz 250-350 ms for own name  $-1.20 \mu\text{vol}$  SD 4.17 vs other names  $-0.42 \mu\text{vol}$  SD 2.59. Interestingly, the non-sense stimuli (reversed names) elicited similar response as to other named response of  $-0.41 \mu\text{vol}$  SD 2.13.

The EEG response with the latency of 600-800 ms to subject's own name was  $0.41 \mu\text{vol}$  SD 3.93 and to other names  $-0.25 \mu\text{vol}$  SD 1.52. The reversed names in pDOC patients produced a mean response of  $0.32 \mu\text{vol}$  SD 1.52.

On group level these responses were not significantly different, however, on the single subject level, I have identified four patients, who developed significantly different responses to own name from the responses to other names (Figure 8.3 and Table 8.2).

Figure 8.3 Patients' responses to own name at latency of 250-350 ms and at 600-800 ms



This figure presents both; early (250-350 ms) response and late (600-800 ms) responses in four patients with disorder of consciousness; Red arrows indicate the most significant response using the  $F$  test to the contrast own name against other names. VS= Vegetative State, MCS= Minimally Conscious State

*Table 8.2 Responses from four pDOC patients showing the ERP different response to subject own name paradigm*

Peak – level								
Subject number	P value; FEW corrected	F	Z	P uncorrected	mm	mm	ms	Cortical projection *
2MCS	<0.001	34.33	5.59	<0.0001	-4	-8	180	cuneus
2MCS	0.013	25.09	4.78	<0.0001	-50	-52	471	Middle temporal
13VS	0.021	20.46	4.30	<0.0001	4	35	265	Pre-central / superior frontal
13VS	0.001	29.14	5.15	<0.0001	26	29	625	Pre-central / superior frontal
15MCS	0.065	16.19	3.80	<0.0001	-47	40	346	Post-central
15MCS	0.016	21.02	4.36	<0.0001	4	-9	617	Post-central
16MCS	0.050	22.14	4.48	<0.0001	-13	-62	268	Middle / inferior temporal left

*This table presents the responses in four patients with disorder of consciousness (pDOC), including vegetative state (VS) and minimally conscious state (MCS) patients; to subjects own name and other names. The result was consider as significant if the correction using familywise error (FEW) and false discovery rate (FDR) were <.05, the mm x mm shows the spatial position and ms indicates the time since onset for the most significant response. \* according to (Koessler, Maillard et al. 2009).*

## 8.5 Discussion

The main aim of this study was to evaluate whether some patients with pDOC can elicit similar EEG patterns to the control subjects to the own name. Furthermore, the difference in the response to subject's own name and response to other names was investigated. This was because significant differences between brain responses to own versus others' names are unlikely to be due to any low-level auditory or even phonemic factors, but more plausibly to higher-level (auditory object) (Snyder, Gregg et al. 2012) detection, or to the personal and emotional salience associated with hearing one's own name. Hence, the positive results I observed in a sub-group of patients (three MCS patients out of 11 and one VS patient out of five) could be an index of a certain level of self-awareness.

### *8.5.1 Endogenous potentials and exogenous potentials*

The BAEP were reported in Chapter 4.

Seven out of 16 pDOC patients had BAEP latencies in normal range. The BAEP technique has been used for detection of ability to hear, but not confirm an ability to understand spoken language, while the late cognitive potentials, at latencies around 300 ms and 800 ms are cortically derived. For instance, Boris Kotchoubey (Kotchoubey 2005) explored the relation between exogenous, also known as the evoked auditory or a short latency potentials with the latencies up to 100 ms and endogenous, known as event related potentials with latency above 200 ms. The former (exogenous) depend mainly on stimulus qualities, while the latter (endogenous) depend on the task and the subjects' state, hence both potentials assess different aspects of the brain function. In other words, the exogenous components correspond with the activation of the ascending

pathways to the primary cortex and the endogenous components correspond with the cortical, subcortical and associative areas activation (Demertzi, Vanhaudenhuyse et al. 2008).

Previously it has been shown that own name stimuli activate subjects cortex and produce responses with latency approximately 300 ms, also called P3 potentials as well as late response around 700 ms. Schnakers and Perrin (Schnakers, Perrin et al. 2008) showed that the response to subject's own name, both in active and passive paradigm can be expected around 650 ms post stimuli, or even with latencies up to 762 ms in VS patients and in MCS patients to 711 ms post subject's own name stimulus respectively (Perrin, Schnakers et al. 2006).

The paradigm in the current study was similar to that used by other researchers in the field (where either others' names or time reversed names have been used (Fischer, Dailler et al. 2008; Fischer, Luaute et al. 2010), or use both others' and reversed names in the same paradigm in healthy controls (Holler, Kronbichler et al. 2011) but not in pDOC patients yet. Also, I embedded the subject's own name stimuli in blocks of either others' names or reversed names to be sure that ERPs are in response to transient changes in the acoustic signal rather than fluctuations in brain state that may confound blocked experimental trials.

#### ***8.5.2 Awareness of self, as an ability to differentiate between the own name and other names***

The aim of this study was to identify brain responses to subject's own name and others' names. I accomplished this by embedding SON stimuli in blocks of either others' names or reversed names to be sure that ERPs were in response to transient changes in the acoustic signal rather than fluctuations in brain state that may confound blocked experimental trials. I chose the contrast SON vs. others' names as these were the most

similar conditions and differed in semantic salience. While the reversed names were part of the experimental paradigm, I did not contrast these trials directly with SON trials because any ERP differences could have been driven by either semantic or phonotactics differences. I did however utilize the SON trials that were embedded in the reversed name blocks. For the 10 control subjects I identified two main positive responses in keeping with previous studies: A) an early polarity positive response around 300ms, which is typically maximal in the frontal or central midline electrodes (Berlad and Pratt 1995); B) a later, also polarity positive, ERP between 600-800ms, also known as a “late slow wave” with left parietal topology (Holeckova, Fischer et al. 2006). The early response is deemed to reflect cognitive functions such as stimulus recognition and working memory updating (Polich 1987) while the late response is believed to occur during recollection and retrieval processes (Holeckova, Fischer et al. 2006). The topology of these two responses in the control subjects was consistent with the earlier studies cited above i.e. central for the early response and left-lateralized (parietal) for the later response.

In the patient group, 4/16 (25%) had statistically significant responses to SON vs others’ names. Two had a very similar topology to controls while two had an opposite polarity in response to others’ names. Two pDOC patients had significant response in both time windows, while one subject only had an early response. The final responder had two peaks occurring a little earlier than the controls.

This PhD study extends, those performed previously studies in this field through focussing on a salient contrast i.e. that between SON and others names. Fisher et al (Fischer, Dailler et al. 2008) assessed comatose rather than pDOC patients and found in 21 out of 51 a positive ERP to subject’s own name at the latency of 602ms, 671ms and 722ms at Fz, Cz and Pz respectively. Others showed that pDOC patients had stronger ERP response to own name uttered by familiar voice (Holeckova, Fischer et al. 2006)

(Del Giudice, Blume et al. 2016). Additionally, it was shown that pDOC patients in active condition such as counting down the SONs evoked stronger response than in unattended (passive) condition (Schnakers, Giacino et al. 2015) (Hauger, Schnakers et al. 2015). Furthermore, a strong response to a SON in pDOC patients was reported if a SON was contrasted against a meaningless sound (Demertzi, Vanhaudenhuyse et al. 2008).

In this study one VS patient (13VS) who demonstrated consistent ERP responses to their own name was diagnosed using the SMART assessment, and was not thought to have any behavioural responses indicating self-awareness, or awareness of the environment. The clinical EEG of this patient was dominated by delta rhythm, yet this patient had normal BAEPs and similar ERPs on the own name paradigm to controls. This finding is in keeping with previous studies, strongly suggesting that some of the VS patients had preserved cognitive function, hence, these patients should be considered as “functionally locked-in patients” (Formisano, D'Ippolito et al. 2013).

Various psychological experiments have shown that hearing one's own name can lead to an increase in attention. For instance, by using shadowing procedures or distractions, Howarth and Ellis (Howarth and Ellis 1961) showed that the auditory threshold for perceiving one's own name was lower than for hearing other names. Others have suggested that there is a connection between one's name, personal identity, memory and attention (Dion 1983). It has been shown that one's own name, when presented as a novel stimuli or 'deviant' in an oddball paradigm can generate responses related to cognitive abilities such as attention orienting, categorization and memory updating (Holeckova, Fischer et al. 2006), in healthy controls (Tateuchi, Itoh et al. 2012) and in pDOC patients (Schnakers, Perrin et al. 2008).

The event related response to one's own name occur during both a passive listening (Perrin, Schnakers et al. 2006) and an active condition when pDOC patients were asked to count the amount of the subject's own name presented (Schnakers, Perrin et al. 2008), (Lechinger, Wielek et al. 2016). Furthermore, a strong response to subject's own name in pDOC patients was reported if the subject's own name was contrasted against a meaningless sound (Demertzi, Vanhaudenhuyse et al. 2008). Additionally, the presence of the cognitive potentials had a positive predictive value in regard to further recovery of consciousness (Vanhaudenhuyse, Laureys et al. 2008).

Only recently has it been proposed that for the assessment of brain function in pDOC patients it would be good to use a person specific and person relevant stimuli. For instance, del Giudice *et al.* (Del Giudice, Blume et al. 2016) showed that one in four patients with VS/MCS responded not only to own name (using an ERD approach), but even stronger to own name uttered by a familiar voice. The approach doesn't have to be auditory, an alternative sensory route is visual, where pictures of one's own face are contrasted with unfamiliar faces (Laureys, Perrin et al. 2007). Even clinical studies suggest that person-relevant stimuli may be best for bedside and behavioural assessment. Cheng *et al.* (Cheng, Gosseries et al. 2013) showed in eighty six VS subjects that using the patient's own name as opposed to a meaningless loud sound, such as ringing a bell, was more effective in evoking a localisation-to-sound response, for instance, turning eyes or head towards the sound source. Others have also suggested using personally meaningful stimuli for brain function assessment in pDOC patients, for instance, by using pre- injury personally relevant stimuli, such as patients' favourite music or similar (Perrin, Castro et al. 2015).

## **8.6 Conclusion**

This study has shown the feasibility of the use of self-relevant stimuli such as subject's own name, for assessment of brain function in pDOC patients, in particular for patients who were deemed to be in the VS. The results of this study can help the treating team to tailor medical and psycho-social management accordingly, for instance, with the careful pain and mood management as well as appropriate leisure activities, for patients, who are considered as being "functionally locked in syndrome".

## Chapter Nine

## **CHAPTER 9 GENERAL DISCUSSION**

### **9.1 Summary of the experiments results performed for this thesis**

This thesis comprise of several experiments performed in order to better understand brain function in pDOC patients. Sixteen pDOC patients and 22 controls were included into this study. Patients included to this study underwent both: clinical and experimental assessments.

Clinically, the patients were assessed using several techniques to confirm the diagnosis of pDOC and to assign them into the VS or MCS group. I used meticulous, bedside behavioural assessment tools; the CRS-R, WHIM and SMART. I also applied neurophysiological assessments such as resting state EEG and BAEP. I performed further analysis of the resting state EEG in order to obtain an EEG spectral analysis.

The results of the bedside, behavioural assessments were corresponding with the neurophysiological results, hence, VS patients, who were diagnosed using the behavioural scales, had more frequently slow, mainly delta rhythm EEG. The MCS patients usually had better formed brain electrical activity with some intermittent theta frequencies. EEG spectral analysis, however, shown that all the patients have predominantly slower brain activity.

Experimental phase of this PhD included using two different techniques: NIRS and EEG and two different activation tasks; namely passive and active tasks.

First, brain responses were evaluated using a motor task, during which the pDOC patients were asked “imagine you are squeezing a ball with your right hand”. This study showed that the NIRS technique can be used for the assessment of responsiveness in pDOC patients. Moreover, this PhD thesis identifies three main types of haemodynamic response patterns during the motor imagery. Furthermore, the analysis of simultaneous recorded NIRS and EEG signals during the motor imagery task showed that eight out of 16 pDOC developed similar responses on both modalities. This is potentially an important contribution of this PhD study, because until now only EEG was used for the bedside brain function assessment, hence, this thesis enriches the possible diagnostic tools for the use for the pDOC patients.

In a passive paradigm I assessed the EEG differences in responses to subjects’ own name and other names in pDOC patients. Both stimuli can be meaningful, hence, the ability to discriminate the own name from the other first names, could indicate self-awareness. In this study, four patients developed a significant response to own name as opposed to the other names. This result contributes to the field, since only recently, it was suggested that the use of a person-important and specific stimuli, for example, autobiographical events or favourite music can promote responsiveness in the pDOC patients. The finding from this thesis could be potentially implemented in the daily clinical practise. For example, by using familiar stimuli such as music or pictures for bedside assessment of brain function in pDOC patients during their rehabilitation process.

Interestingly, this thesis indicated that some of the VS patients were able to wilfully modulate their brain activity; hence, on the group level there was not statistical significant difference between the two groups of patients. One possible explanation would be that this strict approach to make a diagnosis of either VS or MCS should be reviewed. To support this statement, recently, Liberati, *et al.* (Liberati, Hunefeldt et al. 2014) reviewed PET, EEG and fMRI studies, which were performed with the aim to confirm behaviourally established diagnosis of VS or MCS diagnosis and showed that only half of these studies reported statistically significant differences between VS and MCS patients.

However others, for instance, Coleman, *et al.* (Coleman, Menon et al. 2005) and Lehembre, *et al.* (Lehembre, Marie-Aurelie et al. 2012) showed that using EEG and fMRI techniques it was possible to stratify patients into either the VS or MCS group, solely based on the strength of brain signal. It was found that the MCS patients had higher frontal-to-posterior connectivity in theta band or increased BOLD signal as a response to stimuli respectively.

Another group found the relation between EEG alpha and theta oscillations with the higher scores on the CRS-R, however, with no statistical difference between VS and MCS patients (Lechinger, Bothe et al. 2013). Similar results were reported by Kotchoubey, *et al.*, (Kotchoubey, Merz et al. 2013) when authors showed there was no significant difference in response to emotional stimuli in patients with VS and MCS using the fMRI technique, even though the MSC patients (n=6) showed significant higher global connectivity in the brain regions linked to empathy.

Notwithstanding, the functional neuroimaging results suggest possible correlation between the strength of the brain signal and a better prognosis for the pDOC patients in

regard to the future emergence from disorder of consciousness (Coleman, Davis et al. 2009; Monti, Vanhaudenhuyse et al. 2010).

The results of this thesis contributed to the field by providing further evidence that some VS patients have indeed preserved brain function and their brain function enabled them to respond to environmental stimuli, albeit this could be detected only by using technology such as NIRS or EEG.

## **9.2 Further work and future prospects**

The important area, where the findings of this thesis could be potentially implemented is the BCI. Initially, the EEG was the golden standard used for BCI systems, however, recently it has been suggested that the use of concurrent recordings of NIRS and EEG may be beneficial. Recently, NIRS based BCI systems have been implemented on healthy subjects with promising results. More importantly, not only cross-validation accuracies were high for the binary tasks, but also for the three-, four-, and five-class problems, respectively, which has the potential to provide users with more outputs, thereby increasing the rate of communication (Weyand and Chau 2015).

This PhD study shows that some of the pDOC patients could have preserved brain function enabling them to alter the EEG and NIRS signals, hence, these patients were in a state called “functionally locked-in syndrome”. Potentially, this subpopulation of patients would benefit from the use of a NIRS-BCI system.

Another area

## APPENDIX 1

**NHS**  
**Health Research Authority**  
NRES Committee London - Queen Square

Room 4W/12, 4th Floor West  
Charing Cross Hospital  
Fulham Palace Road  
London  
W6 8RF

Telephone: 020 3311 7287  
Facsimile: 020 3311 7280

14 February 2012

Dr Diane Playford  
Director of the Institute  
Royal Hospital for Neuro-disability  
West Hill  
Putney  
London  
SW15 3SW

Dear Dr Playford

**Study title:** Optimising therapy and characterising brain function in low awareness states  
**REC reference:** 11/LO/1233  
**SSA reference:** 11/LO/2052

The REC gave a favourable ethical opinion to this study on 01 November 2011.

Notification(s) have been received from local assessor(s), following site-specific assessment. On behalf of the Committee, I am pleased to confirm the extension of the favourable opinion to the new site(s) and investigator(s) listed below:

Research Site	Principal Investigator / Local Collaborator
Royal Hospital for Neuro-disability	Dr Diane Playford

The favourable opinion is subject to management permission or approval being obtained from the host organisation prior to the start of the study at the site concerned.

### Statement of compliance

*The Committee is constituted in accordance with the Governance Arrangements for Research Ethics Committees and complies fully with the Standard Operating Procedures for Research Ethics Committees in the UK.*

**11/LO/1233**

***Please quote this number on all correspondence***

*Yours sincerely*

  
**Audrey Adams**

## APPENDIX 2

### CONSULTEE INFORMATION SHEET

**Study title “Optimising therapy and characterising brain function in low awareness states”**

**Investigators:**

Dr Diane Playford	Director of the Institute, Royal Hospital for Neuro-disability , West Hill Putney, SW15 3SW <a href="mailto:dplayford@rhn.org.uk">dplayford@rhn.org.uk</a> 0208 780 4500 ext 5115
Dr Ashraff Ali	Senior physician , Royal Hospital for Neuro-disability, West Hill, Putney SW15 3SW <a href="mailto:aali@rhn.org.uk">aali@rhn.org.uk</a> 0208 780 4500 ext 5135
Dr Kudret Yelden	Research Physician Royal Hospital for Neuro-disability , West Hill Putney, SW15 3SW <a href="mailto:kyelden@rhn.org.uk">kyelden@rhn.org.uk</a> 0208 780 4505
Dr Agnieszka Kempny	Research Physician Royal Hospital for Neuro-disability , West Hill Putney, SW15 3SW <a href="mailto:akempny@rhn.org.uk">akempny@rhn.org.uk</a> 0208 780 4505

We are contacting you about a research project that your relative/partner/friend .....  
(patients name) can participate in.

We are seeking your opinion of whether with your knowledge of this person, they would be willing or unwilling to take part. It is important for you to understand why the research is being done and what it will involve. Please read the following information carefully and discuss it with others if you wish. If you have no objection to the patient participating in the study, you are kindly asked to complete and sign the ‘Statement for Relatives and Carers’ sheet attached. Please do not hesitate to contact us if there is anything that is unclear or if you would like more information concerning the study.

More information about being involved in research is provided by the Consumers Association Tel: 0207 730 3469 and ‘INVOLVE’ at <http://www.invo.org.uk>.

#### 1-What is the purpose of the study?

Everybody is aware of the daily cycle which involves changes in alertness (sleep-wake). This is known as the circadian rhythm. It is influenced by the amount of light people are exposed to and when they eat. People in low awareness states have periods when their eyes are shut and periods when their eyes are open. This is described as a sleep wake cycle but may not correspond to sleep and is better described as an eyes open – eyes shut cycle. We want to know in people with low awareness states if

1. having the eyes open-eyes shut corresponds to sleep-wake,
2. people respond more when awake,

- 3 we can make the sleep-wake cycle more normal and  
4 a normal sleep wake cycle is associated with a higher level of awareness.

### **2-Why has the participant been chosen?**

The participant has been chosen because s/he has been admitted to the Royal Hospital for Neuro-disability with a Low Awareness States. Participation is entirely voluntary and we are asking you to sign a statement saying that you have been informed of the participant's involvement. Refusal to sign this form or subsequent withdrawal will not affect the standard of care s/he receives. You are free to withdraw the participant at any time and without giving a reason.

### **3-What will happen to the participant if she/he takes part?**

The research may be considered in three phases. First we will record the person's current sleep wake cycle, and assess their level of awareness clinically. Then we will try to make the sleep wake cycle more normal and repeat the assessments of level of awareness. We will then also undertake some further studies to assess brain function at different parts of the sleep wale cycle. This studies will use

- (a) behavioural assessments, that is assessments of how the participant responds to various stimuli, such as a instruction to do something, or a bright light, or picture.
- (b) brain scans using Magnetic Resonance Imaging (MRI), and technique called near infrared spectroscopy or NIRS
- (c) neurophysiological studies such as EEG –

Each of these three phases and the techniques is described in more detail below.

#### **Phase 1: Establishing a behavioural, physiological and structural baseline and measuring variability in the sleep-wake cycle and circadian rhythm.**

Each participant will undergo a comprehensive behavioural, neurophysiological and imaging assessment to establish the sleep/wake cycle. Not all participants will have all measurements done (e.g. Magnetic Resonance Imaging – MRI may not be possible )

All the assessments except MRI will be carried out at RHN. The MRI will be carried out at University College Hospital London.

#### **Behavioural assessments:**

These include SMART (Sensory Modality Assessment and Rehabilitation Technique), WHIM (The Wessex Head Injury Matrix) and MATLAS (musical assessment tool for low awareness states), Coma Recovery Scale-Revised. These are routinely used for assessment of patients in low awareness states to find out level of awareness, identify the type and quality of patients' behaviours and sensory responses by using various stimuli, depending on the design of the assessment tool. For example, while a SMART

assessor may use a feather to observe the response to tactile stimuli, MATLAS uses music. These assessments are not invasive or unpleasant.

#### **Neurophysiological assessments:**

Electroencephalography (EEG) is the non – invasive measurement of the electrical activity of the brain by electrodes placed on the scalp.

An evoked potential is an electrical potential recorded from the nervous system following presentation of a stimulus such as a flashing light ( a visual evoked potential), or sound (an auditory evoked potential). Analysis of evoked potentials can provide information about the severity and distribution of brain damage. The entire set of evoked potentials will be carried out once on the participant and should last about one hour.

Polysomnography measures physiological changes and the brains electrical activity and so measures the sleep wake cycle. We will monitor the brain activity continuously for a minimum of 2 days and a maximum of 5 day period.

#### **Measuring salivary melatonin.**

The sleep/wake cycle will be measured by sampling melatonin using a swab to take the saliva from mouth every 4 hours for 48 hours

#### **Brain scans:**

These assessments are not routinely performed on people with low awareness states as part of their rehabilitation programme. For the study we need to know the extent of brain damage that the patients have and we need these measures to be carried out in a consistent manner in research participants to enable comparison. These assessments will be conducted using the scanners at University College Hospital London. The transport and escort for the patients will be similar to any routine transport and escort to an external hospital appointment. Structural assessments include;

Magnetic Resonance Imaging (MRI) scanning will be used to identify areas of the brain affected by the injury. MRI scanners use a magnetic field to create pictures of brain and are routinely used in hospitals, where a detailed examination of the participant and their medical notes has confirmed beyond any doubt that they are safe to enter the scanner. Where there is any doubt we will not scan the participant. The scans are painless and last for about 20 - 30 minutes. The scanner makes loud clicks.

At the same time, Diffusion Tensor Imaging (DTI-MRI) a special type of MRI scanning will help us to assess the potential microscopic damages to the brain tissue. Arterial spin labelling (ASL) will be done to assess resting brain blood flow. It is a completely non-invasive test and therefore very suitable for VS and MCS patients. It does not require the use of a radioactive tracers or dyes.

None of the investigations above expose patients to risk of radiation.

**Phase 2: Intervening to optimize patients' sleep-wake cycle and circadian rhythm.**

On hospital wards there are often lights on during the night and level of light during the day are relatively low. Simple procedures to increase light during the day and decrease light at night will be introduced.

Currently many patients are fed via PEG tubes during the night as this is easier to manage. Where possible feeds will be given during the day.

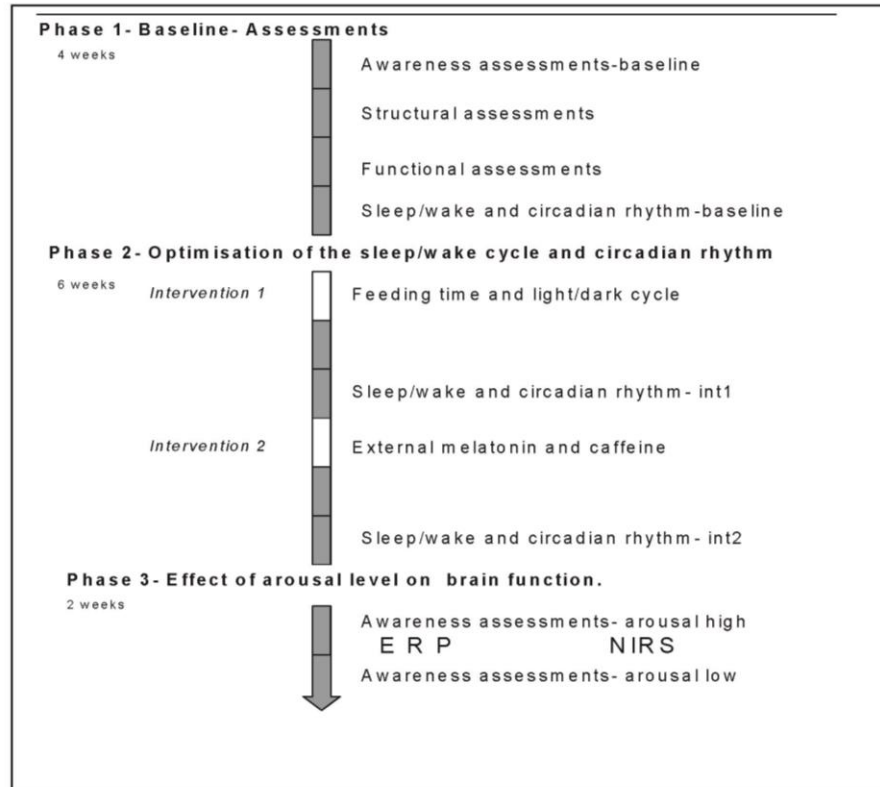
If the measures optimising the light-dark cycle and feeding regime do not result in a normal sleep-wake cycle patients will be given a dose of caffeine equivalent of one cup of coffee in the morning and melatonin a hormone which helps you sleep at night.

After these measures have been put in place we will repeat the behavioural assessments, polysomnography and measures of salivary melatonin.

**Phase 3: Measuring the effect of arousal level on brain function and assessments.**

Event related potentials (ERP) are a non-invasive measurement of brain's electrical activity caused by the "higher" processes, that might involve memory, expectation, attention, or changes in the mental state, among others and recorded by a machine very similar to the EEG machine.

Near Infrared Spectroscopy (NIRS) is also non-invasive method using non visible near infrared light (650-1000nm). NIRS can be used for assessment of brain function through the intact skull in human subjects by detecting changes in take up of oxygen in brain



**4-What do the participant has to do?**

There are no additional requirements for taking part in the study

**5-What are the possible disadvantages and risks of taking part?**

Potential participants will be risk assessed for the participation in this study. The risk assessment team comprises a dietician, a speech and language therapist, the ward manager and the investigators.

Agitated patients and patients with hypersensitivity around the mouth will be excluded.

Nevertheless there are some potential risks:

-There is a risk of not adjusting to the new feeding regime, 2 weeks will be allowed adjust to the new routine. If after one week the patient is unable to be fed adequately the original feeding pattern will be re-introduced. The patient will not be withdrawn from the project but this stage will be skipped.

-For some patients continuous EEG may be difficult to tolerate. If at any time the participant is showing sign of discomfort due to the EEG we will discontinue the monitoring, we may either resume it later at another time or if we have enough recording to measure the sleep-wake cycle we will stop.

#### **6-What are the possible benefits of taking part?**

This study may help participants improve their sleep and provide them with better awareness episodes. This study will provide us with a better understanding of the biological clock of people in low awareness states. It will enable us to utilize this cycle in every day care and schedule therapeutic treatments more appropriately.

This study will also inform us about the way to optimize therapies and rehabilitation for low awareness states.

#### **7-What happens when the research study stops?**

If the routine that was introduced during the study (feeding time, bright days and dark nights) was beneficial to the participant then it will continue after the end of the study.

#### **8-What if something goes wrong?**

The Royal Hospital for Neuro-disability has a complaint policy in place. If you wish to make a complaint about the way you or the patients are treated by staff and/or researchers please see the ward manager who will go through the procedure with you.

If despite all our efforts to minimise risk and discomfort to the patient any undesirable event happen as a result of participating in this study, inform us as soon as possible and contact the ward manager who will follow the incident report policy.

#### **9-Confidentiality- who will have access to the data?**

All information which is collected about the participant during the course of the research will be kept strictly confidential. Any information about the participant that leaves the Hospital will have their name removed so that s/he cannot be recognised from it. For this study we will need your permission to allow restricted access to the medical records

of the participant by authorised person for the research (investigators) and for audit and monitoring purposes (Research Department). All data collected will be kept securely for eight years.

#### **10-What will happen to the results of the research study?**

Outcomes of this study will be published in peer-reviewed scientific journal(s), and communicated at conferences as appropriate. You will be informed of the results of the study by correspondence presenting a layman description of the outcomes and highlighting the impact of the study.

The results of this study will be presented to the Hospital staff. This enables staff to give their comments on how the study may impact on the care/therapy of the patients.

We will also be reporting the results to the Research Advisory Committee of the Royal Hospital for Neuro-disability. A copy of this report can be obtained on request to the Research Department at the Royal Hospital for Neuro-disability. Outcomes of this study will be available on the RHN website [www.rhn.org.uk/](http://www.rhn.org.uk/)

#### **11-Who is organising and funding the research?**

The sponsor is the Royal Hospital for Neuro-disability. This study is funded by the Neuro-disability Research Trust. No persons carrying out the study are receiving any greater remuneration than what they are currently earning, for doing this work. Similarly there is no remuneration for participants.

#### **12-Who has reviewed this study?**

The proposal (a detailed document of the study) was first sent to two independent reviewers for their expert opinion. It was then reviewed by the Hospitals' Research Advisory Committee, before being sent to the National Research Ethics Service Committee London – Queen Square for external ethical review.

#### **13-Contact for further information**

If you have any questions, concerns or comments please feel free to contact:

Dr Sophie Duport	Head of Research, Research Department, The Royal Hospital for Neuro-disability, Putney SW15 3SW. 0208 780 4531 -- <a href="mailto:sduport@rhn.org.uk">sduport@rhn.org.uk</a>
Dr Kudret Yelden	Research Physician Royal Hospital for Neuro-disability , West Hill Putney, SW15 3SW <a href="mailto:kyelden@rhn.org.uk">kyelden@rhn.org.uk</a> 0208 780 4505
Dr Agnieszka Kempny	Research Physician Royal Hospital for Neuro-disability , West Hill Putney, SW15 3SW <a href="mailto:akempny@rhn.org.uk">akempny@rhn.org.uk</a> 0208 780 4505

**Thank you for reading this information sheet.** If you have no objection to the patient taking part in this study, please sign the attached 'Consultee declaration sheet' form and return it to the investigators either directly or by using the envelope provided.

### APPENDIX 3

#### STATEMENT FOR RELATIVES/CARERS

**Title of Study: Optimising therapy and characterising brain function in low awareness states**

**Investigators:**

Dr Diane Playford	Director of the Institute, Royal Hospital for Neuro-disability , West Hill Putney, SW15 3SW <a href="mailto:dplayford@rh.n.org.uk">dplayford@rh.n.org.uk</a> 0208 780 4500 ext 5115
Dr Ashraff Ali	Senior physician , Royal Hospital for Neuro-disability, West Hill, Putney SW15 3SW <a href="mailto:aali@rh.n.org.uk">aali@rh.n.org.uk</a> 0208 780 4500 ext 5135
Dr Kudret Yelden	Research Physician Royal Hospital for Neuro-disability , West Hill Putney, SW15 3SW <a href="mailto:kyelden@rh.n.org.uk">kyelden@rh.n.org.uk</a> 0208 780 4505
Dr Agnieszka Kempny	Research Physician Royal Hospital for Neuro-disability , West Hill Putney, SW15 3SW <a href="mailto:akempny@rh.n.org.uk">akempny@rh.n.org.uk</a> 0208 780 4505

**Patient's Name:.....**

I have been fully informed of what the study involves for my relative/partner/friend who is named above. This has been explained to me by:

.....  
.....

*(Insert name, designation, telephone number and e-mail address)*

I have received, read and understand the Consultee Information Sheet and any questions I had relating to the study have been answered to my satisfaction.

I have discussed the possible benefits and risk from participation. I understand that my relative's/partner's/friend's participation is voluntary and that she/he is free to withdraw at any time, without reason and without prejudice to her/his further treatment. I am not aware that the above patient would be unwilling to participate in such a study.

I am informed that the Senior Physician/Consultant/GP is usually advised of a patient's participation in a study.

I understand that personal information about my relative/partner/friend will be treated as strictly confidential, but that their medical records may be consulted by authorised persons and that the findings of the study may be presented anonymously for publication in medical journals and at clinical/scientific meetings. Also, that the Local Ethics Committee or Department of Health Assessors may review this form as part of a monitoring process.

Name of relative/partner/friend (block letters):

Signature of relative/partner/friend:

Relationship to patient:

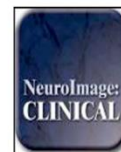
Date:

I confirm that I have explained to the patient's relative/carer/friend the nature of this project.

Signed .....  
(Member of the research team)

Date .....

**COPY OF PUBLICATIONS ARISING DIRECTLY FROM THIS WORK**



## Functional near infrared spectroscopy as a probe of brain function in people with prolonged disorders of consciousness

Agnieszka M. Kempny<sup>a,b,\*</sup>, Leon James<sup>a</sup>, Kudret Yelden<sup>a,b</sup>, Sophie Dupont<sup>a</sup>, Simon Farmer<sup>d</sup>, E. Diane Playford<sup>a,b</sup>, Alexander P. Leff<sup>b,c</sup>

<sup>a</sup>The Institute of Neuro-palliative Rehabilitation, Royal Hospital for Neuro-disability, SW15 3SW London, UK

<sup>b</sup>Department of Brain Repair and Rehabilitation, Institute of Neurology, University College London, Queen Square, WC1N 3BG London, UK

<sup>c</sup>Institute of Cognitive Neuroscience, University College London, Queen Square, WC1N 3AR London, UK

<sup>d</sup>The National Hospital for Neurology & Neurosurgery, Queen Square, London WC1N 3BG, UK

### ARTICLE INFO

#### Article history:

Received 28 January 2016

Received in revised form 27 June 2016

Accepted 27 July 2016

Available online 27 July 2016

#### Keywords:

(Prolonged) disorders of consciousness  
Functional near infrared spectroscopy  
Brain function assessment in disorders of consciousness

### ABSTRACT

Near infrared spectroscopy (NIRS) is a non-invasive technique which measures changes in brain tissue oxygenation. NIRS has been used for continuous monitoring of brain oxygenation during medical procedures carrying high risk of iatrogenic brain ischemia and also has been adopted by cognitive neuroscience for studies on executive and cognitive functions. Until now, NIRS has not been used to detect residual cognitive functions in patients with prolonged disorders of consciousness (pDOC). In this study we aimed to evaluate the brain function of patients with pDOC by using a motor imagery task while recording NIRS. We also collected data from a group of age and gender matched healthy controls while they carried out both real and imagined motor movements to command. We studied 16 pDOC patients in total, split into two groups: five had a diagnosis of Vegetative state/Unresponsive Wakefulness State, and eleven had a diagnosis of Minimally Conscious State. In the control subjects we found a greater oxy-haemoglobin (oxyHb) response during real movement compared with imagined movement. For the between group comparison, we found a main effect of hemisphere, with greater depression of oxyHb signal in the right > left hemisphere compared with rest period for all three groups. A post-hoc analysis including only the two pDOC patient groups was also significant suggesting that this effect was not just being driven by the control subjects. This study demonstrates for the first time the feasibility of using NIRS for the assessment of brain function in pDOC patients using a motor imagery task.

Crown Copyright © 2016 Published by Elsevier Inc. This is an open access article under the CC BY-NC-ND license (<http://creativecommons.org/licenses/by-nc-nd/4.0/>).

### 1. Introduction

Near infrared spectroscopy (NIRS) was described by Frans Jobsis, who noticed a good transparency of biological tissues for a near infrared light and suggested its use for monitoring of tissue oxygenation (Jobsis, 1977). NIRS systems are commercially available for monitoring cerebral oxygenation of frontal lobes, for example, during a surgery carrying risk of iatrogenic brain ischemia (Murkin and Arango, 2009). NIRS has also been used on neonatal intensive care with currently ongoing phase II randomized clinical trial (SafeBoosC) evaluating cerebral hypoxia treatment controlled with NIRS responses (Pellicer et al., 2013).

Functional NIRS (fNIRS) is a methodology that has the potential to improve the assessment of patients with prolonged disorders of

consciousness (pDOC). The clinical assessment of awareness as well as assessment of any response to therapy is challenging in this group of patients. The term DOC is an umbrella term encompassing two diagnoses: Vegetative State (VS), known also as Unresponsive Wakefulness State (UWS), and Minimally Conscious State (MCS). Patients in VS/UWS are awake but lack awareness of themselves and their environment. They are able to breathe spontaneously and have a stable circulation (Jennett and Plum, 1972; Laureys et al., 2010). Unlike VS/UWS, patients in MCS are partially aware of themselves and their environment and are able to follow simple commands, albeit inconsistently. At present the description of MCS patients includes: ability to visually track a person, item or to follow a self-reflection in a mirror, ability to intentionally communicate “yes” and “no” responses, although the patients remain unable to interact functionally with their environment (Giacino et al., 2002; Vanhaudenhuyse et al., 2008; Bruno et al., 2011).

In the clinical setting distinguishing these two entities is challenging, time consuming and may lack objectivity (Andrews et al., 1996). Therefore, in addition to meticulous clinical assessment several adjunct methods are used. Responses to environmental stimuli using behavioural scales are used for assessment of consciousness (Majerus et al., 2005), although this measurement method often remains subjective.

*Abbreviations:* pDOC, prolonged disorders of consciousness; VS, vegetative state; UWS, unresponsive wakefulness state; MCS, minimally conscious state; fNIRS, functional near infrared spectroscopy; MI, motor imagery; MM, motor movement; M1, primary motor cortex; SMA, supplementary motor area; SMART, Sensory Modality Assessment for Rehabilitation Technique.

\* Corresponding author at: Institute of Neuro-palliative Rehabilitation, Royal Hospital for Neuro-disability, SW15 3SW, Putney, London, UK

E-mail address: [agnieszka.kempny@gmail.com](mailto:agnieszka.kempny@gmail.com) (A.M. Kempny).

<http://dx.doi.org/10.1016/j.nicl.2016.07.013>

2213-1582/Crown Copyright © 2016 Published by Elsevier Inc. This is an open access article under the CC BY-NC-ND license (<http://creativecommons.org/licenses/by-nc-nd/4.0/>).

Therefore, several techniques have been employed to measure brain responses to stimuli. These included Positron Emission Tomography (PET), Transcranial magnetic stimulation (TMS) and functional Magnetic Resonance Imaging (fMRI), although none of these techniques are used routinely in clinical practice for a variety of reasons including: extra costs; expert analysis of the data and availability of the methods (Di Perri et al., 2014). In this study we wished to explore the feasibility of detecting brain-based haemodynamic changes during motor tasks using bed-side apparatus, NIRS in patients with DOC.

We hypothesized that a motor task would elicit changes in oxy and/or deoxyHb concentration indicating that a subject is able to follow specific commands, and, hence, be a useful biomarker for awareness. Two main patterns of the functional NIRS responses during a motor task have been identified: a typical NIRS signal changes when the concentrations of the oxyHb increases and of the deoxyHb decreases (Leff et al., 2011) and an inverted response when the concentration of the oxyHb decreases and the deoxyHb increases (Holper et al., 2011). Therefore, we aimed to explore the fNIRS responses from the healthy controls during both motor movement and motor imagery. Furthermore, we wanted to look for differences in the fNIRS responses from the supplementary motor area (SMA) and primary motor cortex (M1). A final aim was to investigate any differences in haemodynamic response to a motor task between patients with a diagnosis of VS/UWS and those with MCS.

## 2. Methodology

### 2.1. Subjects

We included patients from Royal Hospital for Neuro-disability in London, UK. This 26-bedded unit provides a comprehensive neuro-rehabilitation programme for patients with DOC in the post-acute phase following severe brain injury (GCS < 8).

The inclusion criteria were as follows: 1) severe acquired brain injury leading to prolonged DOC (longer than 4 weeks since brain injury) or permanent DOC. The permanent DOC was defined according to the Royal College of Physician Guidance (RCP, 2013) for traumatic aetiology if lasted longer than 12 months or anoxic aetiology if longer than 6 months; 2) conservative management of brain injury (no neurosurgery); 3) at least unilateral intact auditory brainstem evoked potentials.

Awareness of the environment was measured using a Sensory Modality Assessment for Rehabilitation Technique (SMART) (Gill-Thwaites and Munday, 2004). The SMART is a validated tool for assessment of awareness in pDOC. The assessment comprises of ten one to one (patient-assessor) sessions lasting approximately 60 min each and is composed of eight modalities as follows: sensory modality (visual, auditory, tactile, gustatory, and olfactory), motor function, communication and arousal/wakefulness.

The control group consisted of 10 healthy, right-handed volunteers (6 females, mean age 40 years SD 8). Written informed consent was obtained from all the control subjects. The patients were recruited into the study after consultation with their relatives and the treating team. The study was carried out in accordance with the latest version of the Declaration of Helsinki and the study was approved by a National Research Ethics Committee (NRES Committee London-Queen Square).

### 2.2. The tasks

The control subjects performed both a motor movement (MM) of the right hand (squeezing a ball) and a kinaesthetic motor imagery (MI) task (the same movement but imagined) both to command. A hand movement task has been extensively used in the fNIRS studies, for instance, this task was found as reliable in healthy and also in subjects after traumatic brain injury (Bhambhani et al., 2006), and for mapping of the motor cortex (Wilson et al., 2014; Sato et al., 2007). The experiment consisted of 20 blocks of executions of MM followed by 20

blocks of MI, separated by a 10 min long break. Patients with pDOC performed only the motor imagery task, which consisted of 20 blocks of MI.

During MI the subjects were instructed to concentrate on the muscle contraction of their right hand as if it were a real movement rather than visualisation of the movement; thus the subjects were asked to perform first person perspective kinaesthetic motor imagery (Guillot et al., 2009). The paradigm was divided into 2 blocks: 7 s of real right hand movement or imagery of ball squeezing followed by 12 s of resting state. At the beginning of the experiment the participants were familiarized with the experiment design and with the instructions. Each block began with the auditory presentation of the task for the block for instance: “start” and “stop”. The twelve second interval between the imagery task was chosen, based on previous studies showing that haemodynamic recovery to baseline occurs 9 to 10 s after cessation of stimulus (Boden et al., 2007). In the pDOC group, the MI algorithm was used, the recorded instruction was as follows “imagine you are squeezing a ball with your own right hand” “start” and “stop”.

### 2.3. Near infrared spectroscopy instrumentation

The fNIRS signal was recorded bilaterally over the premotor area and supplementary motor area (EEG corresponding areas FC3, FC1, FCz, FC2 and FC4) and over the primary motor cortex (EEG corresponding areas C4, C2, Cz, C1 and C3), as combinations of these areas were likely to be active in response to both motor paradigms. All NIRS measurements were performed using a NIRScount system (NIRx Medical Technologies LLC, Berlin, Germany) using a 16-channel array of optodes. The system performed dual-wavelength continuous-wave (CW) near infrared tomographic measurements at a 10.42 Hz sampling rate. The device emits light at 2 distinct wavelengths, 760 and 850 nm, for discrimination of two oxygenation states of tissue. The 4 sources and 12 detectors were placed on subject's skull in the usual primary and secondary motor areas, according to the International 10–20 system (Klem et al., 1999), with each detector receiving light originating in its neighbouring light source and scattered in the adjacent tissue. Each detector and the most closely placed light source built a channel. In total there were 16 channels containing information about deoxy and oxyHb concentration changes (Fig. 1). Changes in oxy and deoxyHb concentration were analysed separately, giving in total 32 channels. The inter-optodes distance was 2.5 cm. For the analysis of the haemoglobin concentration changes within the supplementary motor area (SMA) and primary motor cortex (M1) we used following spatial localisations: SMA: right channels :1,2,5,6 and the left channels: 3,4,7,8, respectively. For the M1 right channels: 9,10,13,14 and the left channels: 11,12,15,16 respectively. Since the NIRS channels were placed around the C3 and C4 EEG 10–20 positions, the presumption was that the SMA will occupy the anterior aspect of this area while the M1 posterior aspect of this area (Grafton, 1994; Rizzolatti and Luppino, 2001; Chouinard and Paus, 2006). The optodes were placed using the Waveguard cap (ANT Neuro, The Netherlands) and secured by using a dedicated black fabric cap (Fig. 1).

### 2.4. Data processing and analysis

The raw NIRS data were converted into a readable Matlab format using Nilab2 software (NIRx Medical Technologies LLC). The data were low-pass filtered to remove the high frequency signal ~0.3 Hz breathing and 1 Hz heart rate. Low frequency (<0.01 Hz) vascular or metabolic oscillations were removed by using a high frequency cut-off filter of 32 s (0.03 Hz). We then calculated changes in both oxy and deoxyHb concentration (expressed in  $\mu\text{mol/L}$ ) using the modified Beer-Lambert law as described by Delpy (Scholkmann et al., 2014). The data was mean corrected so that, at each time-point, the value represents the amplitude minus the average for the entire record for each channel.

Using a custom-written script in R language (Rx 64 1.1) we calculated relative differences in haemoglobin concentration changes during

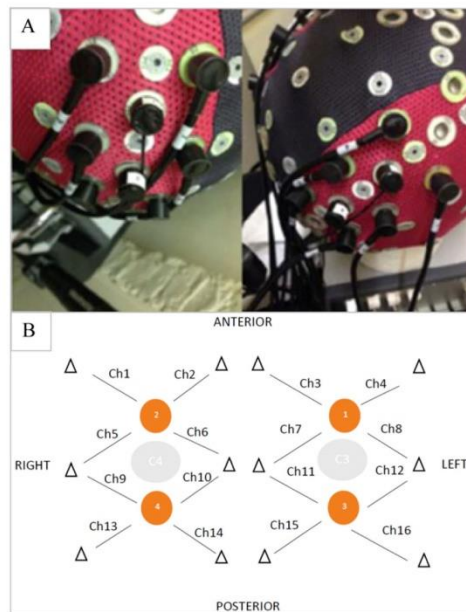


**Fig. 1.** Waveguard cap and fibre arrangement. Caption: (A) Waveguard cap with an array of detectors and light sources and (B) fibre arrangement. The orange dots indicate sources position and the triangles indicate position of detectors. Each source – detector (triangle) pair forms a hypothetical channel (Ch). (For interpretation of the references to colour in this figure legend, the reader is referred to the web version of this article.)

the resting state and during the two motor tasks. The relative difference ( $\Delta_{rel}$ ) refers to the median difference between the signal amplitude before (7 s + to 0 s) and during the task period (0 s to 7 s), and was calculated as the ratio of the absolute difference ( $\Delta_{abs}$ ) to the 5th to 95th quantile range of the signal amplitude for the entire study. These values were calculated for both oxy and deoxyHb, our two main dependent measures, at each channel. After examining the global tendency of the concentration changes, we averaged over both the left (8 channels) and right (8 channels) hemispheres to check for any lateralisation of haemoglobin concentration change, including looking either for ipsilateral negative oxygenation or contralateral positive or negative oxygenation, as these patterns were described elsewhere (Holper et al., 2011;

McGregor et al., 2015). Two patients, numbered 1 and 14 from the Table 1, were excluded from our analysis. Both of them were in the MCS group and had high amplitude artefacts in all channels which were clearly synchronous with involuntary movements. The presence of high amplitude artefacts throughout recording did not allow for data analysis with the Nilab2 software (NIRx Medical Technologies LLC). In response to a reviewer's suggestion, we tried to localise responses to M1 and SMA by averaging over a smaller number of channels: SMA = channels 1,2,5,6 (right), and 3,4,7,8, (left); primary motor cortex (M1) = channels 9,10,13,14 (right) and 11,12,5,16 (left).

Data were entered into ANOVAS using SPSS (version 22). For the controls this was a  $2 \times 2$  within-subject analysis (task: MM/MI; hemisphere (within-subjects' factor): L/R). For the patients it was a  $3 \times 2$  (group (between-subject factor): controls/MCS/VS-UWS; hemisphere: L/R). p-Values were set at  $<0.05$  as a criterion for statistical significance for all planned analyses. We first examined interactions, then main effects.

### 3. Results

Sixteen patients with pDOC were included in the study (six female, mean age was 46 years, SD 11), with the following aetiologies: intracerebral haemorrhage (n = 6), anoxic brain injury (n = 5), traumatic brain injury (n = 4) and tuberculosis meningitis (n = 1). The patients had been in pDOC for 17.31 months on average (Table 1).

#### 3.1. Data averaged over each hemisphere:

The controls elicited significant different haemodynamic responses in regard to the right v. left hemisphere. During an actual right hand movement the oxyHb concentration changes were  $-0.63$  (SD 1.20)  $\mu\text{mol/L}$  over the right hemisphere and were  $-0.38$  (SD 1.32)  $\mu\text{mol/L}$  over the left hemisphere ( $p = 0.05$ ). Similar results were shown for the deoxyHb concentration. The changes were  $-0.01$  (SD 0.35)  $\mu\text{mol/L}$  over the right hemisphere and of  $-0.12$  (SD 0.35)  $\mu\text{mol/L}$  over the left hemisphere ( $p = 0.02$ ). The response to a motor imagery in controls was as follows: oxyHb  $-0.08$  (SD 0.99)  $\mu\text{mol/L}$  and deoxyHb  $-0.004$  (SD 0.26)  $\mu\text{mol/L}$  over the right hemisphere and oxyHb 0.03 (SD 1.08)  $\mu\text{mol/L}$  and deoxyHb  $-0.08$  (SD 0.39)  $\mu\text{mol/L}$  over the left hemisphere respectively. The pDOC patients showed a similar pattern of responses to the controls during MI. (Supplemental table).

The time course of changes in oxy and deoxyHb during the motor imagery task in each channel for a representative control subject is shown on the Fig. 2.

Across the three groups and the two tasks, we found greater variability in the oxyHb than the deoxyHb fNIRS measurement (Fig. 3, data averaged across all sensors).

**Table 1**

Demographic data of the study population. VS/UWS-vegetative state/Unresponsive Wakefulness State, MCS-minimally conscious state, pDOC prolonged disorders of consciousness.

Number	Patient's diagnosis, on SMART assessment	Gender	Age in years	Duration of pDOC in months	Aetiology
1	MCS	F	18	4.7	Anoxic brain injury post self-hanging
2	MCS	F	61	55.1	Right frontal lobe bleed
3	MCS	M	55	9.1	Large intracerebral bleed
4	VS/UWS	M	45	5.4	Anoxic brain injury post cardiac arrest
5	MCS	M	68	4.0	Grade V SAH due to aneurysm left ACM
6	MCS	M	46	4.7	Extensive fronto-temporal left haemorrhage
7	MCS	M	38	9.1	Left fronto-temporo-parietal contusions following assault
8	MCS	F	30	80.9	Petechial haemorrhage following road traffic accident
9	MCS	F	37	1.8	Bilateral intracerebral bleed
10	VS/UWS	M	24	6.4	Hydrocephalus following TB meningitis
11	VS/UWS	M	20	13.6	Diffuse axonal injury following road traffic accident
12	VS/UWS	M	51	40.4	Right temporo-parietal bleed
13	VS/UWS	F	62	5.0	Anoxic brain injury post cardiac arrest
14	MCS	M	52	6.4	Left parietal haemorrhage following road traffic accident
15	MCS	F	31	26.0	Anoxic brain injury following cardiac arrest
16	MCS	M	53	4.4	Anoxic brain injury following cardiac arrest

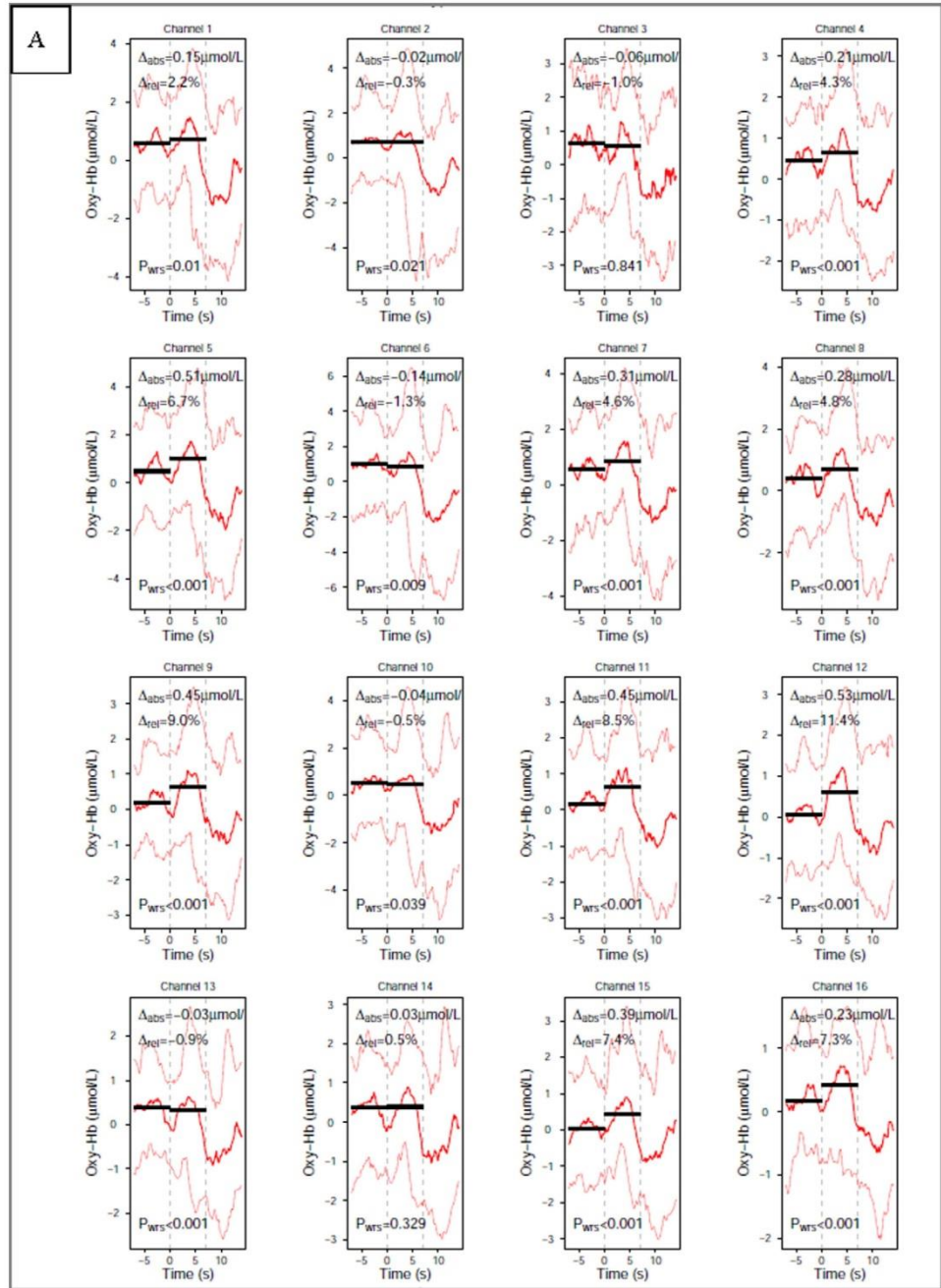


**Fig. 2.** Time course of changes in oxyHb (A) and deoxyHb (B) during the motor imagery task in each channel, single subject (subject number 4). Caption: (A) oxyHb and (B) deoxyHb on activation in a single subject to motor imagery task, dashed vertical lines represent start and stop of the task. Solid black lines present the pre and post-stimulus activation median values, red (A) and blue (B) lines present the 50th quantile (solid thick line) and the 10th and 90th quantile (dashed thin lines). (For interpretation of the references to colour in this figure legend, the reader is referred to the web version of this article.)

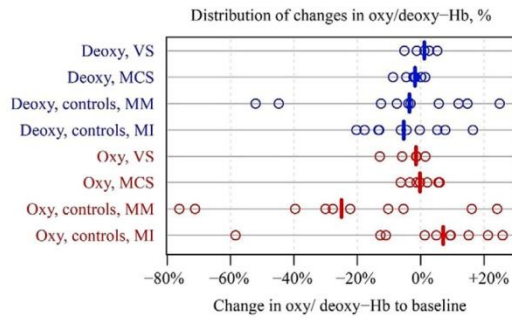


**Fig. 3.** Distribution of concentration changes in oxy and deoxy-haemoglobin. Caption: Distribution of concentration changes in oxy and deoxy-haemoglobin across four categories: vegetative state (VS), minimally conscious state (MCS), controls – motor movement (MM) and controls – motor imagery task (MI). Each dot denotes a subject and bold vertical lines indicate means. The horizontal axis denotes concentration changes expressed as a percentage of change in relation to the pre-stimuli haemoglobin concentration.

Based on the individual subject’s responses (controls  $n = 10$  and the pDOC patients  $n = 14$ ) we identified three different types of fNIRS responses to a motor imagery task in regard to the polarity of global oxy and deoxyHb changes. The typical fNIRS response (oxyHb positive and deoxyHb negative) was seen in 60% (6/10) healthy subjects and 36 percentage (5/14) of the pDOC patients. Another response was an “inverted fNIRS response”, where the oxyHb concentration change was negative in value and deoxyHb was positive, was seen in two of the 10 healthy subjects and in six of the 14 patients. Two of the ten healthy subjects and three of the 14 pDOC patients, could not be clearly classified into either of the two main response types (Table 2).

The ten controls elicited greater haemodynamic response during MM then during the MI task (Fig. 4). With oxyHb as the dependent measure we did not find a task \* hemisphere interaction  $p = 0.229$ . We did however find a main effect of task  $F(1, 9) = 5.52, p = 0.043$ , with  $MM > MI$  (greater depression of oxyHb signal compared with rest period), but not of hemisphere  $p = 0.186$  (Table 3).

With deoxyHb as the dependent measure there was no significant interaction or main effects ( $p > 0.3$ , data not shown).

For the patients there was only one task (MI). In this group we looked for a group (healthy controls vs. VS/UWS group vs. MCS patients) \* hemisphere interaction. With oxyHb as the dependent measure we found no significant interaction ( $p = 0.40$ ). We did however find a main effect of hemisphere  $F(1, 21) = 4.89, p = 0.038$ , with greater depression of oxyHb signal in the right > left hemisphere, compared with rest period (Fig. 4). A post-hoc analysis including only the two patient groups was also significant  $F(1, 12) = 9.14, p = 0.011$  suggesting that this effect was not just being driven by the control subjects.

With deoxyHb as the dependent measure there was no significant interaction or main effect of group or hemisphere ( $p > 0.4$ , data not shown).

**Table 2**

The identifiable types of fNIRS responses to a motor imagery task based on the polarity of the global oxy and deoxyHb concentration changes.

Type of fNIRS response	Typical response-OxyHb positive and deoxyHb negative	Inverted response-oxyHb negative and deoxyHb positive	Unclassified response oxyHb and deoxyHb positive or oxyHb and deoxyHb negative
Healthy controls, $n = 10$	6	2	2
pDOC patients, $n = 14$	5	6	3

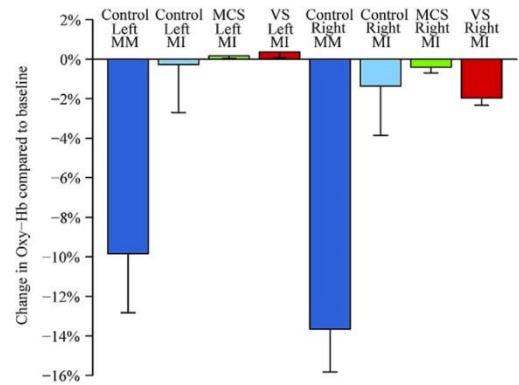


**Fig. 4.** Relative changes of oxy-haemoglobin concentration. Caption: relative changes of oxy-haemoglobin concentration in healthy subjects, minimally conscious state (MCS) and vegetative state (VS) patients over the right and left hemisphere on motor imagery (MI, all three groups) and motor movement (MM, controls only) task. The bars denote mean change and whiskers are for standard error of the mean.

3.2. Sub-analysis of M1 and SMA data

3.2.1. Main effect of task (controls only)

The control subjects showed greater responses during the motor movement compared with motor imagery in both SMA and M1. In right SMA oxyHb concentration mean changes were greater during MM  $-0.59$  SD (0.93)  $\mu\text{mol/L}$  then during MI  $-0.13$ SD (0.97)  $\mu\text{mol/L}$  ( $p = 0.03$ ). The same pattern was seen in the left SMA, where the oxyHb concentration changes were greater during MM  $-0.36$  SD (1.35) then during MI  $-0.20$  SD (1.23) ( $p = 0.05$ ).

In right M1 oxyHb concentration changes during MM were greater  $-0.66$ SD (1.42) then during MI  $-0.05$  SD (0.99)  $\mu\text{mol/L}$  respectively ( $p = 0.04$ ). In left M1 we identified the same pattern but the difference was not statistically significant: changes of oxyHb during MM =  $-0.40$  SD (0.89) and MI =  $-0.15$  SD (0.90) ( $p = 0.2$ ).

The changes of the deoxyHb in supplementary motor areas and primary motor cortex in relation to the task (MM vs. MI) did not reach statistical significance.

3.2.2. Main effect of hemisphere

In the motor movement task controls had significantly greater NIRS responses in right > left hemispheres (Table 4).

The control group showed significant differences between the SMA right vs. SMA left during MM for both oxyHb ( $-0.59$   $\mu\text{mol/L}$  SD (0.93) vs.  $-0.36$   $\mu\text{mol/L}$  SD 1.35oxyHb ( $p = 0.03$ )) and deoxyHb ( $-0.05$   $\mu\text{mol/L}$  SD (0.25) vs.  $-0.19$   $\mu\text{mol/L}$ SD (0.56) ( $p = 0.02$ )). During motor imagery only changes in deoxyHb (right SMA vs. left SMA))

**Table 3**

The mean ( $n = 10$ ) of oxyHb concentration changes expressed as percentage of change in relation to the pre-stimuli baseline in 10 controls during motor imagery (MI) and motor movement (MM).

	Mean (within-subject SEM) expressed as percentage of change	Mean (within-subject SEM) expressed as a change in $\mu\text{mol/L}$
Left_hemisphere_oxy(MI)	-0.3(2.4)	0.029 (0.83)
Right_hemisphere_oxy(MI)	-1.3(2.5)	-0.089(0.81)
Left_hemisphere_oxy(MM)	-9.9(0.3)	-0.38(0.81)
Right_hemisphere_oxy(MM)	-13.7(2.2)	-0.64 (0.82)

**Table 4**

The oxy and deoxyHb concentration changes in  $\mu\text{mol/L}$  in the supplementary motor cortex (SMA), channels 1,2,5,6 (right), and 3,4,7,8, (left), and primary motor cortex (M1) channels 9,10,13,14 (right) and 11,12,5,16 (left) during the motor movement and motor imagery in healthy controls and a motor imagery in pDOC patients, SD - Standard Deviation, oxyHb - oxyhaemoglobin, deoxyHb - deoxyhaemoglobin, VS/UWS Vegetative/Unresponsive Wakefulness State, MCS - Minimally Conscious State, bold front indicates significant task effects and asterisk (\*) indicates significant hemisphere effects.

Spatial localisation	Healthy subjects (n = 10)		pDOC patients	
	Motor movement	Motor imagery	MCS (n = 9)	VS/UWS (n = 5)
SMA right	<b>-0.59 (SD = 0.93)oxyHb*</b> <b>-0.05 (SD = 0.25)deoxyHb*</b>	0.13 (SD = 0.97)oxyHb 0.02 (SD 0.23)deoxyHb	-0.05 (SD = 0.2)oxyHb -0.01 (SD = 0.04)deoxyHb	-0.08 (SD = 0.20)oxyHb -0.08 (SD = 0.03)deoxyHb
SMA left	<b>-0.36 (SD = 1.35)oxyHb* (p = 0.03)</b> <b>-0.19 (SD = 0.56)deoxyHb* (p = 0.02)</b>	-0.20 (SD = 1.23)oxyHb <b>-0.13 (SD = 0.52)deoxyHb*</b>	0.38 (SD = 2.43)oxyHb 0.05 (SD = 0.9)deoxyHb	0.19 (SD = 1.40)oxyHb 0.37 (SD = 0.88)deoxyHb
M1 right	-0.66 (SD = 1.42)oxyHb 0.02 (SD = 0.43)deoxyHb	-0.05 (SD = 0.99)oxyHb 0.09 (SD = 0.30)deoxyHb	-0.07 (SD = 0.83)oxyHb 0.03 (SD = 0.75)deoxyHb	-0.08 (SD = 0.82)oxyHb -0.21 (SD = 0.68)deoxyHb
M1 left	-0.40 (SD = 0.89)oxyHb -0.05 (SD = 0.19)deoxyHb	-0.15 (SD = 0.90)oxyHb <b>-0.04 (SD = 0.49)deoxyHb* (p = 0.02)</b>	0.001 (SD = 1.10)oxyHb 0.06 (SD = 0.74)deoxyHb	0.41 (SD = 1.21)oxyHb 0.21 (SD = 0.86)deoxyHb

were statistically significant (0.02  $\mu\text{mol/L}$  SD 0.23 vs -0.13 SD 0.52  $\mu\text{mol/L}$  p = 0.05).

None of these analyses, using this subset of NIRS channels were significant in the pDOC patients.

#### 4. Discussion

This study is the first report of the use of functional near infrared spectroscopy for brain function assessment in people in Vegetative State/Unresponsive Wakefulness syndrome and Minimally Conscious State. We determined patterns of fNIRS responses from healthy controls to both the motor movement and to motor imagery, and then we used these patterns for validation of fNIRS response in pDOC patients. We identified two main types of haemodynamic response patterns present in both the healthy subjects and the patient group.

##### 4.1. Methodological considerations

The controls in this study performed both types of tasks (imagery and motor movement) while the pDOC patients performed only the motor imagery task. The healthy controls elicited stronger fNIRS responses during actual movement when compared to motor imagery. Previous studies on motor tasks showed that NIRS cortical responses should generate a change ( $\Delta$ ) in oxyHb  $\sim 0.5\mu\text{mol/L}$  and in deoxyHb ( $\Delta$ )  $\sim 0.2\mu\text{mol/L}$  (Hirth et al., 1996; Wolf et al., 2002). Our control subjects had similar sized responses during the MM task. With regard to the MI task, our results are comparable with others, for instance Iso et al. (Iso et al., 2015) and Wriessnegger et al. (Wriessnegger et al., 2008) showed similar level of haemodynamic response to a imagery motor task from SMA and M1 respectively.

Both the controls and the patients elicited different type of haemodynamic responses in regard to the polarity of haemoglobin concentration changes during the unilateral motor movement.

Although the initial studies suggested that the typical fNIRS response to movement and motor imagery is characterised by an increase in the concentration of oxyHb accompanied by a less pronounced decrease in deoxyHb level concentration (Sato et al., 2007), more recent studies report different patterns of fNIRS responses depending on the optical probe localisations and task difficulty (Mihara et al., 2012). For example, Morihiro et al. (Morihiro et al., 2009) showed that oxyHb response over the left primary motor cortex decreased over time during a repetitive, right-handed tapping task, while the channels covering the supplementary motor cortex recorded an increase. We averaged fNIRS signal over a broad area covering the premotor area, supplementary motor area (EEG corresponding areas FC3, FC1, FCz, FC2 and FC4) as well as the primary motor cortex (EEG corresponding areas C4, C2, Cz, C1 and C3), which may explain why healthy subjects and the patients tended to have an inverted oxyHb response. Task is also a factor, Holper et al. (Holper et al., 2011) found an inverse oxyHb response during motor imagery, which was related to the task difficulty, while the more complex task

would produce stronger negativity of the oxyHb response. These factors may explain why we found both the typical and inverted haemodynamic responses in our study groups.

##### 4.2. Interpretation of fNIRS response

Our main finding was that of a hemispheric difference in oxyHb depression in the right hemisphere across all three groups for the motor imagery task. This effect was not driven solely by the control subjects as a sub-analysis demonstrated that this effect was present in the VS/UWS and MCS patient groups alone. Motor imagery has been shown in many studies to be associated with a greater bilateral functional imaging signal than actual motor movements, particularly in pre-motor and supplementary motor areas (Binkofski et al., 2000; Pfurtscheller et al., 2006). Ipsilateral (right-hemisphere) signal changes have been reported in several fMRI studies, that is, BOLD not fNIRS response, in anterior frontal regions (BA 9, 10 and 11) (Sharma et al., 2006; Porro et al., 2000), but also in the precentral gyrus (BA 6) during hand movement imagery (Hanakawa et al., 2005). Another possible explanation of the inverted oxyHb results in fNIRS also derives from the fMRI BOLD studies. An ipsilateral "negative" BOLD response means an "U" shaped, as opposed to the bell-shaped MR signal changes, during an unimanual task activity was reported by McGregor et al., who suggested that this phenomenon is related to an active inhibition of cortical areas (McGregor et al., 2015). Another group showed that ipsilateral negative BOLD during a unimanual task reflects normal transcallosal inhibition, while its dissipation impairs motor activity (Lenzi et al., 2007).

##### 4.3. Supplementary motor area versus primary motor cortex during an imagery and actual movement motor task

Traditionally, the human motor cortex is classified into a primary motor area activated during a motor movement and the secondary or higher order motor systems activated in learning, planning or initiation of the voluntary movements, and these include the SMA (Drenkhahn, Koch et al., 2015). Previous studies have shown that a simple motor movement elicits a maximal response over the primary motor cortex (Leff et al., 2011), and our results in healthy subjects are consistent with this finding. Additionally, the self-paced motor task is known to elicit stronger activity in the SMA (Wilson et al., 2014), which may explain why in our study group in both SMA and M1 showed activation during motor imagery and motor movement, however, for motor movement we observed M1 > SMA and during for motor imagery (SMA > M1).

We have carried out more detailed analyses of these effects using a Dynamic Casual Modelling for fNIRS and confirmed that motor imagery negatively modulates connections from SMA to M1, resulting in the suppressive influence of SMA on M1 (Tak et al., 2015).

#### 4.4. Vegetative state/unresponsive wakefulness state vs. minimally conscious state patients

We did not find statistically significant differences in fNIRS responses between the two patient groups, which may be because we only studied a small number with heterogeneous aetiology and pathophysiology of brain damage. Another possibility is dissociation between the clinical diagnosis and actual brain function. In our study the typical haemodynamic response was seen in four MCS patients ( $n = 9$ ) and only one VS/UWS patient ( $n = 5$ ), while the inverted haemodynamic response was present in two VS/UWS patients and four MCS patients. The unclassified response was in two VS/UWS and one MCS respectively. There are reports of subpopulations of VS/UWS patients who remain behaviourally unresponsive, but their brain function, as measured using fMRI or EEG techniques, is more in keeping with a diagnosis of MCS (Coleman et al., 2007; Schnakers et al., 2009; Monti et al., 2010; Cruse et al., 2012). This interpretation is supported by a recent review of PET, EEG and fMRI studies by Liberati et al. who demonstrated that only half of the publications reported statistically significant differences between VS/UWS and MCS patients (Liberati et al., 2014).

The assessment of the brain function in people with pDOC is complex and complicated by multiple interacting motor, sensory and cognitive impairments. Also cognitive and emotional processes are known to affect peripheral physiology including heart rate, respiration, blood pressure and skin perspiration which can affect NIRS measurements (Minati et al., 2011). It is not possible to fully control for these factors, however, a block-design paradigm (task versus resting state) should at least partially eliminate the background noise related to the physiological factors (Amaro and Barker, 2006). Nevertheless, taking these factors into account, we have demonstrated that fNIRS can be used to detect task-induced brain activity changes in pDOC patients using a motor imagery task. Our study showed that the MCS patients have more often the "typical" fNIRS response, and their haemodynamic response is similar to the fNIRS response from the controls. Given both its relatively low-cost and that it is well tolerated by patients in a clinical ward setting, certainly compared with fMRI, fNIRS represents a translatable imaging tool that can be used to gain new insights into brain function in patients with disorders of consciousness.

Supplementary data to this article can be found online at <http://dx.doi.org/10.1016/j.nicl.2016.07.013>.

#### Declaration of conflicting interests

The authors declared no potential conflicts of interest with respect to the research, authorship, and/or publication of this article.

#### Acknowledgements

The authors thank to the staff of the Royal Hospital for Neuro-disability for their availability and volunteering in the study. The authors also wanted to thank the relatives and the patients for their assistance in participating in this study. AMK and KY are funded by a Neuro-disability Research Trust (RHN 11/2). SFF and APL acknowledge support from the UCLH Biomedical Research Centre.

#### References

- Amaro Jr., E., Barker, G.J., 2006. Study design in fMRI: basic principles. *Brain Cogn.* 60 (3), 220–232.
- Andrews, K., Murphy, L., et al., 1996. Misdiagnosis of the vegetative state: retrospective study in a rehabilitation unit. *BMJ* 313 (7048), 13–16.
- Bhambhani, Y., Maikala, R., et al., 2006. Reliability of near-infrared spectroscopy measures of cerebral oxygenation and blood volume during handgrip exercise in nondisabled and traumatic brain-injured subjects. *J. Rehabil. Res. Dev.* 43 (7), 845–856.
- Binkofski, F., Amunts, K., et al., 2000. Broca's region subserves imagery of motion: a combined cytoarchitectonic and fMRI study. *Hum. Brain Mapp.* 11 (4), 273–285.
- Boden, S., Obrig, H., et al., 2007. The oxygenation response to functional stimulation: is there a physiological meaning to the lag between parameters? *NeuroImage* 36 (1), 100–107.
- Bruno, M.A., Vanhaudenhuyse, A., et al., 2011. From unresponsive wakefulness to minimally conscious PLUS and functional locked-in syndromes: recent advances in our understanding of disorders of consciousness. *J. Neurol.* 258 (7), 1373–1384.
- Chouinard, P.A., Paus, T., 2006. The primary motor and premotor areas of the human cerebral cortex. *Neuroscientist* 12 (2), 143–152.
- Coleman, M.R., Rodd, J.M., et al., 2007. Do vegetative patients retain aspects of language comprehension? Evidence from fMRI. *Brain* 130 (Pt 10), 2494–2507.
- Cruse, D., Chennu, S., et al., 2012. Detecting awareness in the vegetative state: electroencephalographic evidence for attempted movements to command. *PLoS One* 7 (11), e49933.
- Di Perri, C., Heine, L., et al., 2014. Technology-based assessment in patients with disorders of consciousness. *Ann. Ist. Super. Sanita.* 50 (3), 209–220.
- Drenckhahn, C., Koch, S.P., et al., 2015. A validation study of the use of near-infrared spectroscopy imaging in primary and secondary motor areas of the human brain. *Epilepsy Behav.* 49, 118–125.
- Giaccio, J.T., Ashwal, S., et al., 2002. The minimally conscious state: definition and diagnostic criteria. *Neurology* 58 (3), 349–353.
- Gill-Thwaites, H., Munday, R., 2004. The Sensory Modality Assessment and Rehabilitation Technique (SMART): a valid and reliable assessment for vegetative state and minimally conscious state patients. *Brain Inj.* 18 (12), 1255–1269.
- Grafton, S.T., 1994. Cortical control of movement. *Ann. Neurol.* 36 (1), 3–4.
- Guillot, A., Collet, C., et al., 2009. Brain activity during visual versus kinesthetic imagery: an fMRI study. *Hum. Brain Mapp.* 30 (7), 2157–2172.
- Hanakawa, T., Parikh, S., et al., 2005. Finger and face representations in the ipsilateral precentral motor areas in humans. *J. Neurophysiol.* 93 (5), 2950–2958.
- Hirth, C., Obrig, H., et al., 1996. Non-invasive functional mapping of the human motor cortex using near-infrared spectroscopy. *Neuroreport* 7 (12), 1977–1981.
- Holper, L., Shalom, D.E., et al., 2011. Understanding inverse oxygenation responses during motor imagery: a functional near-infrared spectroscopy study. *Eur. J. Neurosci.* 33 (12), 2318–2328.
- Iso, N., Moriuchi, T., et al., 2015. Monitoring local regional hemodynamic signal changes during motor execution and motor imagery using near-infrared spectroscopy. *Front. Physiol.* 6, 416.
- Jennett, B., Plum, F., 1972. Persistent vegetative state after brain damage. A syndrome in search of a name. *Lancet* 1 (7753), 734–737.
- Jobsis, F.F., 1977. Noninvasive, infrared monitoring of cerebral and myocardial oxygen sufficiency and circulatory parameters. *Science* 198 (4323), 1264–1267.
- Klem, G.H., Luders, H.O., et al., 1999. The ten-twenty electrode system of the international federation. The International Federation of Clinical Neurophysiology. *Electroencephalogr. Clin. Neurophysiol. Suppl.* 52, 3–6.
- Laureys, S., Celesia, G.G., et al., 2010. Unresponsive wakefulness syndrome: a new name for the vegetative state or apallic syndrome. *BMC Med.* 8, 68.
- Leff, D.R., Orihuela-Espina, F., et al., 2011. Assessment of the cerebral cortex during motor task behaviours in adults: a systematic review of functional near infrared spectroscopy (fNIRS) studies. *NeuroImage* 54 (4), 2922–2936.
- Lenzi, D., Conte, A., et al., 2007. Effect of corpus callosum damage on ipsilateral motor activation in patients with multiple sclerosis: a functional and anatomical study. *Hum. Brain Mapp.* 28 (7), 636–644.
- Liberati, G., Hunefeldt, T., et al., 2014. Questioning the dichotomy between vegetative state and minimally conscious state: a review of the statistical evidence. *Front. Hum. Neurosci.* 8, 865.
- Majerus, S., Gill-Thwaites, H., et al., 2005. Behavioral evaluation of consciousness in severe brain damage. *Prog. Brain Res.* 150, 397–413.
- McGregor, K.M., Sudhyadhom, A., et al., 2015. Reliability of negative BOLD in ipsilateral sensorimotor areas during unimanual task activity. *Brain Imaging Behav.* 9 (2), 245–254.
- Mihara, M., Miyai, I., et al., 2012. Neurofeedback using real-time near-infrared spectroscopy enhances motor imagery related cortical activation. *PLoS One* 7 (3), e32234.
- Minati, L., Kress, I.U., et al., 2011. Intra- and extra-cranial effects of transient blood pressure changes on brain near-infrared spectroscopy (NIRS) measurements. *J. Neurosci. Methods* 197 (2), 283–288.
- Monti, M.M., Vanhaudenhuyse, A., et al., 2010. Willful modulation of brain activity in disorders of consciousness. *N. Engl. J. Med.* 362 (7), 579–589.
- Morihiro, M., Tsubone, T., et al., 2009. Relation between NIRS signal and motor capability. *Conf. Proc. IEEE Eng. Med. Biol. Soc.* 2009, 3991–3994.
- Murkin, J.M., Arango, M., 2009. Near-infrared spectroscopy as an index of brain and tissue oxygenation. *Br. J. Anaesth.* 103 (Suppl. 1), i3–i13.
- Pellier, A., Greisen, G., et al., 2013. The SafeBoosC phase II randomised clinical trial: a treatment guideline for targeted near-infrared-derived cerebral tissue oxygenation versus standard treatment in extremely preterm infants. *Neonatology* 104 (3), 171–178.
- Pfurtscheller, G., Brunner, C., et al., 2006. Mu rhythm (de)synchronization and EEG single-trial classification of different motor imagery tasks. *NeuroImage* 31 (1), 153–159.
- Porro, C.A., Cattolo, V., et al., 2000. Ipsilateral involvement of primary motor cortex during motor imagery. *Eur. J. Neurosci.* 12 (8), 3059–3063.
- RCP, 2013. Prolonged Disorders of Consciousness National Clinical Guidelines.
- Rizzolatti, G., Luppino, G., 2001. The cortical motor system. *Neuron* 31 (6), 889–901.
- Sato, T., Ito, M., et al., 2007. Time courses of brain activation and their implications for function: a multichannel near-infrared spectroscopy study during finger tapping. *Neurosci. Res.* 58 (3), 297–304.
- Schnakers, C., Vanhaudenhuyse, A., et al., 2009. Diagnostic accuracy of the vegetative and minimally conscious state: clinical consensus versus standardized neurobehavioral assessment. *BMC Neurol.* 9, 35.

- Scholkmann, F., Kleiser, S., et al., 2014. A review on continuous wave functional near-infrared spectroscopy and imaging instrumentation and methodology. *NeuroImage* 85 (Pt 1), 6–27.
- Sharma, N., Pomeroy, V.M., et al., 2006. Motor imagery: a backdoor to the motor system after stroke? *Stroke* 37 (7), 1941–1952.
- Tak, S., Kempny, A.M., et al., 2015. Dynamic causal modelling for functional near-infrared spectroscopy. *NeuroImage* 111, 338–349.
- Vanhaudenhuyse, A., Schnakers, C., et al., 2008. Assessment of visual pursuit in post-comatose states: use a mirror. *J. Neurol. Neurosurg. Psychiatry* 79 (2), 223.
- Wilson, T.W., Kurz, M.J., et al., 2014. Functional specialization within the supplementary motor area: a fNIRS study of bimanual coordination. *NeuroImage* 85 (Pt 1), 445–450.
- Wolf, M., Wolf, U., et al., 2002. Different time evolution of oxyhemoglobin and deoxyhemoglobin concentration changes in the visual and motor cortices during functional stimulation: a near-infrared spectroscopy study. *NeuroImage* 16 (3 Pt 1), 704–712.
- Wriessnegger, S.C., Kurzmann, J., et al., 2008. Spatio-temporal differences in brain oxygenation between movement execution and imagery: a multichannel near-infrared spectroscopy study. *Int. J. Psychophysiol.* 67 (1), 54–63.



## Dynamic causal modelling for functional near-infrared spectroscopy



S. Tak<sup>a,\*</sup>, A.M. Kempny<sup>b</sup>, K.J. Friston<sup>a</sup>, A.P. Leff<sup>a,c</sup>, W.D. Penny<sup>a,\*</sup>

<sup>a</sup> Wellcome Trust Centre for Neuroimaging, University College London, 12 Queen Square, London WC1N 3BG, UK

<sup>b</sup> Royal Hospital for Neuro-disability, West Hill, London SW15 3SW, UK

<sup>c</sup> Institute of Cognitive Neuroscience, University College London, 17 Queen Square, London WC1N 3AR, UK

### ARTICLE INFO

#### Article history:

Accepted 16 February 2015

Available online 25 February 2015

#### Keywords:

Dynamic causal modelling  
Functional near-infrared spectroscopy  
Effective connectivity

### ABSTRACT

Functional near-infrared spectroscopy (fNIRS) is an emerging technique for measuring changes in cerebral hemoglobin concentration via optical absorption changes. Although there is great interest in using fNIRS to study brain connectivity, current methods are unable to infer the directionality of neuronal connections. In this paper, we apply Dynamic Causal Modelling (DCM) to fNIRS data. Specifically, we present a generative model of how observed fNIRS data are caused by interactions among hidden neuronal states. Inversion of this generative model, using an established Bayesian framework (variational Laplace), then enables inference about changes in directed connectivity at the neuronal level. Using experimental data acquired during motor imagery and motor execution tasks, we show that directed (i.e., effective) connectivity from the supplementary motor area to the primary motor cortex is negatively modulated by motor imagery, and this suppressive influence causes reduced activity in the primary motor cortex during motor imagery. These results are consistent with findings of previous functional magnetic resonance imaging (fMRI) studies, suggesting that the proposed method enables one to infer directed interactions in the brain mediated by neuronal dynamics from measurements of optical density changes.

© 2015 The Authors. Published by Elsevier Inc. This is an open access article under the CC BY license (<http://creativecommons.org/licenses/by/4.0/>).

### Introduction

Functional near-infrared spectroscopy (fNIRS) is a noninvasive method for monitoring hemodynamic changes in the brain (Jobsis, 1977; Villringer et al., 1993; Hoshi, 2007; Ferrari and Quaresima, 2012; Scholkman et al., 2014). fNIRS works by shining near-infrared light in the spectral range between 650 and 950 nm from fiber-optic emitters placed on the scalp. Because the absorption of chromophores in tissue is relatively low within this spectral range, near-infrared light can propagate several centimeters through tissue. Changes in light photon density reaching the detectors correspond to changes in the optical properties of the tissue, reflecting changes in oxygenated and deoxygenated hemoglobin (HbO and HbR). The loss of light levels can then be used to calculate the changes in hemoglobin concentrations in underlying brain regions (Delpy et al., 1988). As neuronal processes require extra delivery of oxygen, this provides a marker of underlying neuronal activity.

fNIRS has many advantages that make it highly useful in cognitive and clinical neuroscience studies. Compared to other imaging modalities, such as functional magnetic resonance imaging (fMRI), fNIRS is mobile and compact, and the data acquisition is quiet. Furthermore, as compared to fMRI, fNIRS provides a more direct measure of changes in HbO, HbR, and total hemoglobin (HbT), and the time series

are sampled at high temporal resolution. It has therefore proved to be an effective tool for studying physiological mechanisms in the healthy brain and in cerebrovascular disease (Highton et al., 2010; Wolf et al., 2012; Obrig, 2014). It is also finding unique applications in clinical areas, including bedside monitoring of infants, and studies of auditory and language systems (Lloyd-Fox et al., 2010; Eggebrecht et al., 2014).

There is currently a surge of interest in characterizing brain connectivity using fNIRS. Recent fNIRS studies have assessed the coupling between brain regions in terms of a measure of functional connectivity (Homae et al., 2010; Sasai et al., 2011) and effective connectivity (Im et al., 2010; Yuan, 2013). Specifically, Homae et al. (2010) explored developmental changes of brain networks in early infancy, using functional connectivity defined as temporal correlation between pairs of fNIRS measurements. Sasai et al. (2011) investigated the frequency-specific characteristics of functional connectivity based on spontaneous oscillation in the low-frequency range in HbO and HbR signals. However, functional connectivity does not provide any insight into the directed causal interactions among brain regions underlying cognitive processing. To address this shortcoming, Im et al. (2010) and Yuan (2013) applied Granger causality analysis to fNIRS data, which provides estimation of the directed functional connectivity between brain regions. The analyses of both functional connectivity and effective (via Granger causality) connectivity are usually performed at the level of measured hemodynamic signals, such as HbO, HbR, and HbT responses (White et al., 2009; Im et al., 2010; Homae et al., 2010; Sasai et al., 2011; Yuan, 2013). However, connectivity estimates at the level of

\* Corresponding authors. Fax: +44 20 7813 1420.

E-mail addresses: [s.tak@ucl.ac.uk](mailto:s.tak@ucl.ac.uk) (S. Tak), [w.penny@ucl.ac.uk](mailto:w.penny@ucl.ac.uk) (W.D. Penny).

hemodynamic measurements are not direct measures of connectivity changes at the neuronal level, because the hemodynamic response to neuronal activation depends on the balance of the changes in cerebral blood flow and oxidative metabolism, and also on the changes in cerebral blood volume (Fox and Raichle, 1986; Buxton, 2012). This complex interplay between processes can cause functional connectivity to differ with the type of hemoglobin changes (e.g., HbO and HbR), while underlying interactions between neuronal populations do not vary (Lu et al., 2010). This highlights the importance of estimating causal influences among neuronal populations, referring to a biophysical model of how neuronal activity is transformed into fNIRS measurements.

Several fNIRS studies have used biophysical models relating blood inflow to HbO and HbR changes, or neuronal activity to HbO and HbR changes during brain activation. Specifically, Cui et al. (2010) generated synthetic HbO and HbR responses induced by blood inflow using the Balloon model in a study that investigated the effect of head motion on the fNIRS signal. Dubeau et al. (2012) recovered neuronal inputs from hemodynamic measurements by deconvolving the extended Balloon model (Friston et al., 2000), and showed significant correlation between estimated neural inputs and measurements of local field potentials and multiunit activity. However, to our knowledge, there have been no studies focusing on model-based estimation of neuronal interaction among multiple regions from the optical density changes using fNIRS.

In this paper, we apply Dynamic Causal Modelling (DCM) to fNIRS data, to estimate effective connectivity at the neuronal level from the measurement of optical density changes. Effective connectivity is defined as the (model-based) influence of one (neuronal) system on another. DCM is a framework for fitting differential equation or state space models of neuronal activity to brain imaging data using Bayesian inference (Friston et al., 2003). There is now a library of DCMs and variants differ according to their level of biological realism and the data features which they explain. The DCM approach can be applied to fMRI (Friston et al., 2003, 2014), electroencephalographic (EEG), and Magnetoencephalographic (MEG) data (Moran et al., 2007; Penny et al., 2009; Daunizeau et al., 2009b).

This paper extends the DCM approach to fNIRS. Because the variational Bayesian estimation algorithm is the same as that used for DCMs for other imaging modalities, this paper focuses on development of a generative model of how observed fNIRS data are caused by the interactions among hidden neuronal states. In particular, we extend the neurodynamic and hemodynamic models used for DCM-fMRI analysis (Friston et al., 2003) to additionally include the total hemoglobin state (Cui et al., 2010), and optics model that describes the detected optical density changes as a linear combination of light absorption changes due to HbO and HbR (Delpy et al., 1988; Arridge, 1999). The model is further augmented by including spatially extended hemodynamic sources (Shmuel et al., 2007) and pial vein contamination effects (Gagnon et al., 2012). In short, the proposed method allows fNIRS to be used for making inference about changes in directed connectivity at the neuronal level.

This paper is structured as follows: In the Methods section we first describe a generative model of fNIRS data, and then describe the model optimization procedure for estimating the connectivity parameters from this data. In the Results section we provide an illustrative analysis using fNIRS data acquired during the motor imagery and motor execution tasks. In the Discussion section we discuss future extensions of the proposed method.

## Methods

The generative model for fNIRS data comprises three components: (i) neurodynamics describing neural activity in terms of inter-regional interactions and its experimentally induced modulation (Friston et al., 2003), (ii) hemodynamics linking neural activity with the changes in total hemoglobin, and deoxy-hemoglobin based on the Balloon model

(Friston et al., 2000; Buxton et al., 2004; Cui et al., 2010), and (iii) optics relating the hemodynamic sources to optical density changes (Delpy et al., 1988; Arridge, 1999). A schematic of the generative model is summarized in Fig. 1. The following subsections describe each of these components. These are followed by sections on computing the optical sensitivity matrix and confounding effects that underlie the optical model, and a section on model estimation.

### Neurodynamics

The neurodynamics are described by the following multivariate differential equation

$$\begin{aligned} \dot{z}_t &= \mathcal{J}z_t + Cu_t \\ \mathcal{J} &= A + \sum_{i=1}^M u_t(i)B^i, \end{aligned} \quad (1)$$

where  $t$  indexes continuous time and the dot notation denotes a time derivative. The entries in  $z$  correspond to neuronal activity in  $j = 1, \dots, L$  cortical source regions, and  $u(i)$  is the  $i$ th of  $M$  experimental inputs. An  $[L \times L]$  matrix,  $\mathcal{J}$ , denotes the effective connectivity between

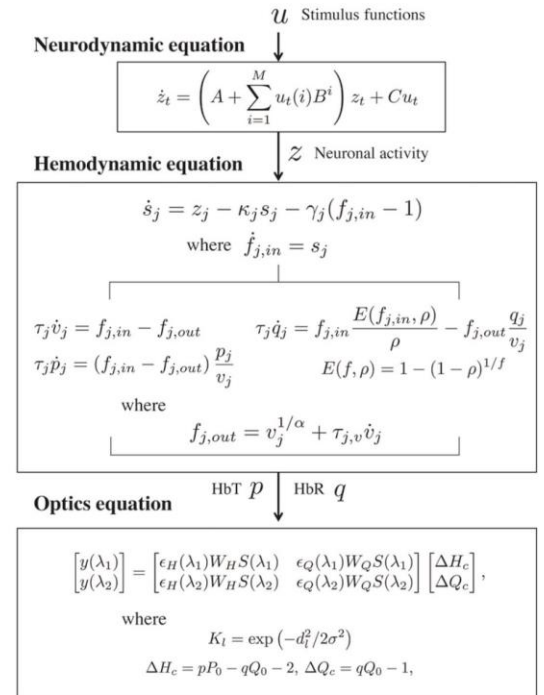


**Fig. 1.** Schematic of the generative model of fNIRS data. The neurodynamic equation uses linear differential equations and a single state variable per region describing neural activity. Coupling parameter matrices  $A$ ,  $B^i$ , and  $C$  represent the average connectivity among regions, the modulation of effective connectivity by experimental manipulation, and the influence of inputs on regions, respectively. The hemodynamic equation uses the Balloon model and its extensions to describe how neural activity causes a change in a flow inducing signal which in turn causes an increase in blood flow with concomitant changes in relative blood volume and deoxy-hemoglobin. The optics equation uses a sensitivity matrix,  $S$ , describing how changes in hemodynamic sources cause changes in optical measurements. Potential pial vein contamination of the fNIRS measurements is corrected using matrices  $W_H$  and  $W_Q$ . Spatially distributed hemodynamic source is generated using Gaussian spatial smoothing kernel  $K$ .

and within regions, and an  $[L \times M]$  matrix,  $C$ , defines a set of experimental input connections that specify which inputs are connected to which regions.

The effective connectivity  $\mathcal{J}$  is characterized by an  $[L \times L]$  connectivity matrix,  $A$ , that specifies which regions are connected in the absence of exogenous or experimental input and whether these connections are unidirectional or bidirectional. We also define an  $[L \times L]$  modulatory matrix,  $B^i$ , that specifies which intrinsic connections can be changed as a result of input  $i$ . Usually, the  $B^i$  parameters are of greatest interest – as these describe how connections among brain regions respond to experimental manipulations. For example, in the application in this paper we show how connections among regions in the motor system are modulated by motor imagery.

The overall specification of input, intrinsic and modulatory connectivity comprises our assumptions about model structure. This in turn represents a scientific hypothesis about the structure of the large-scale neuronal network mediating the underlying function.

The above neurodynamical model is bilinear, and deterministic, and has a single-state variable per region. However, as we can build on developments made in DCM for fMRI, these models are readily extended to the nonlinear and stochastic cases (Stephan et al., 2008; Daunizeau et al., 2009a). In future publications we will also explore the use of richer dynamical models, employing for example two-state variables per region (Marreiros et al., 2008).

To enforce constraints on the parameters being estimated, we make use of latent variables. For example, the use of latent variables,  $\tilde{A}_{ij}$  and  $\tilde{B}_{ij}$ , ensures that self connections,  $\mathcal{J}_{ii}$ , are negative with a typical value of 0.5:  $\mathcal{J}_{ii} = -0.5 \exp(\tilde{A}_{ii} + \sum_k U_r(k) \tilde{B}_{ii}^k)$ . Thus, although  $\tilde{A}_{ii}$  and  $\tilde{B}_{ii}$  have Gaussian priors (see the Priors, estimation, and model selection section) and can be positive or negative,  $\mathcal{J}_{ii}$  will be strictly negative. For the off-diagonal terms, we have no such constraints, i.e.  $A_{ij} = \tilde{A}_{ij}$ ,  $B_{ij} = \tilde{B}_{ij}$ . Overall, the neuronal parameters are  $\theta_n = \{\tilde{A}, \tilde{B}, C\}$ .

#### Hemodynamics

The hemodynamic model involves a set of hemodynamic state variables, state equations and hemodynamic parameters,  $\theta_h$ . Neuronal activity in source region  $j$ ,  $z_j$ , causes an increase in vasodilatory signal  $s_j$  that is subject to autoregulatory feedback, and inflow  $f_{j,in}$  responds in proportion to this (Friston et al., 2000)

$$\begin{aligned} \dot{s}_j &= z_j - \kappa_j s_j - \gamma_j (f_{j,in} - 1) \\ \dot{f}_{j,in} &= s_j, \end{aligned} \quad (2)$$

where  $\kappa_j$  is the rate of signal decay, and  $\gamma_j$  is the rate of autoregulatory feedback by blood flow.

The rate of blood volume  $v_j$  (Buxton et al., 1998) and total hemoglobin concentration  $p_j$  (Cui et al., 2010) changes as

$$\begin{aligned} \tau_j \dot{v}_j &= f_{j,in} - f_{j,out} \\ \tau_j \dot{p}_j &= (f_{j,in} - f_{j,out}) \frac{p_j}{v_j}, \end{aligned} \quad (3)$$

where the first equation describes the filling of the venous ‘Balloon’ until inflow equals outflow,  $f_{j,out}$ , which happens with the transit time  $\tau_j$ .

The rate of deoxy-hemoglobin  $q_j$  changes is modeled as the delivery of deoxy-hemoglobin into the venous compartment minus that expelled (Buxton et al., 1998)

$$\begin{aligned} \tau_j \dot{q}_j &= f_{j,in} \frac{E(f_{j,in}, \rho)}{\rho} - f_{j,out} \frac{q_j}{v_j} \\ E(f, \rho) &= 1 - (1 - \rho)^{1/f} \end{aligned} \quad (4)$$

where  $E(f, \rho)$  is the proportion of oxygen extracted from the blood and  $\rho$  is the resting oxygen extraction fraction.

In the steady-state the outflow is modeled as a power of blood volume (Grubb et al., 1974). However, in the transient state the blood volume changes often lag behind the blood flow changes. To address this dynamic relationship, the outflow model is further augmented by including viscoelastic time parameter  $\tau_{j,v}$  (Buxton et al., 2004):

$$f_{j,out} = v_j^{1/\alpha} + \tau_{j,v} \dot{v}_j, \quad (5)$$

where  $\alpha$  is Grubb's exponent (Grubb et al., 1974), and  $\tau_{j,v}$  describes an additional resistance of venous blood vessels to rapid blood volume changes.

Four of the hemodynamic parameters are estimated from each source activity:  $\theta_h = \{\tilde{\kappa}_j, \tilde{\gamma}_j, \tilde{\tau}_j, \tilde{\tau}_{j,v}\}$ . The use of latent variables ensures that estimated hemodynamic parameters are within a physiologically realistic range:

$$\begin{aligned} \kappa_j &= 0.64 \exp(\tilde{\kappa}_j) \\ \gamma_j &= 0.32 \exp(\tilde{\gamma}_j) \\ \tau_j &= 2 \exp(\tilde{\tau}_j) \\ \tau_{j,v} &= 2 \exp(\tilde{\tau}_{j,v}). \end{aligned} \quad (6)$$

The other parameters are fixed to  $\alpha = \rho = 0.32$  in accordance with previous work (Stephan et al., 2007).

The viscoelastic time constant  $\tau_{j,v}$  ranges from 0 to 30 s (Buxton et al., 2004). However, it is known from high field fMRI studies (Yacoub et al., 2005; Jin and Kim, 2008) that  $\tau_{j,v}$  can decrease as one moves from deep to more superficial cortical layers. fNIRS measures signal mainly from the superficial cortical layers, potentially reflecting tissue properties from deeper layers through draining veins. We therefore used, a broad prior over  $\tau_{j,v}$  having a mean of 2 with prior standard deviation of latent variable  $\tilde{\tau}_{j,v} = 1$  in Eq. (6), so that three standard deviations (i.e.,  $2 \exp(3) = 40.17$ ) can cover the physiological ranges.

#### Optics

A fNIRS optode array comprises  $N_s$  optical sources (emitters) and  $N_d$  optical detectors which are paired up to form  $i = 1, \dots, N$  channels. In principle, all optical channels are sensitive to all neuronal sources. In practice, the sensitivity of channels to sources is governed by the sensitivity matrix (see below). It provides  $N$  channel measurements of optical density changes at time  $t$  and wavelength  $\lambda_1$ , and  $N$  at  $\lambda_2$ . These are written as the  $[N \times 1]$  vectors  $y(\lambda_1)$  and  $y(\lambda_2)$ . These channel measurements are then related to the  $[L \times 1]$  vectors of HbO and HbR,  $\Delta H_c$  and  $\Delta Q_c$ , in the  $L$  cortical source regions of interest as

$$\begin{bmatrix} y(\lambda_1) \\ y(\lambda_2) \end{bmatrix} = \begin{bmatrix} \epsilon_H(\lambda_1) W_H S(\lambda_1) & \epsilon_Q(\lambda_1) W_Q S(\lambda_1) \\ \epsilon_H(\lambda_2) W_H S(\lambda_2) & \epsilon_Q(\lambda_2) W_Q S(\lambda_2) \end{bmatrix} \begin{bmatrix} \Delta H_c \\ \Delta Q_c \end{bmatrix}, \quad (7)$$

with

$$\begin{aligned} \Delta H_c &= \Delta P_c - \Delta Q_c \\ \Delta P_c &= P_0 \cdot p - 1 \\ \Delta Q_c &= Q_0 \cdot q - 1, \end{aligned}$$

where  $\epsilon_H$  and  $\epsilon_Q$  are the extinction coefficients for HbO and HbR;  $S$  is the  $[N \times L]$  sensitivity matrix;  $p$  and  $q$  are HbT and HbR normalized to their baseline concentrations  $P_0$  and  $Q_0 = P_0(1 - SO_2)$  where  $SO_2$  is the

baseline oxygenation saturation; and  $W_H$  and  $W_Q$  are  $[N \times N]$  matrices for correcting pial vein contamination of fNIRS measurements:

$$W_H = \text{diag} \left[ \frac{1}{\omega_{1,H}}, \dots, \frac{1}{\omega_{N,H}} \right],$$

$$W_Q = \text{diag} \left[ \frac{1}{\omega_{1,Q}}, \dots, \frac{1}{\omega_{N,Q}} \right], \quad (8)$$

where  $\omega$  is the ratio of cortical tissue signal over the total activated signal originating from cortical tissue and pial vein:  $\omega = \frac{\text{cortical}}{\text{cortical} + \text{pial}}$  (Gagnon et al., 2012).

Two of the optics parameters are estimated from the data for each channel location:  $\theta_p = \{\tilde{\omega}_{i,H}, \tilde{\omega}_{i,Q}\}$ . The other parameters in Eq. (7) are fixed to  $P_0 = 71 \mu\text{M}$  (Yücel et al., 2012), and  $SO_2 = 0.65$  (Boas et al., 2003). The use of latent variables ensures that the estimated cortical fraction of fNIRS measurements is within a physiologically realistic range:

$$\omega_{i,H} = 0.5 \exp(\tilde{\omega}_{i,H})$$

$$\omega_{i,Q} = 0.5 \exp(\tilde{\omega}_{i,Q}). \quad (9)$$

The optical density measurement,  $y$ , is affected by the signals arising from both cerebral and extracerebral (e.g., pial vasculature and skin) regions, since the fNIRS signal is integrated through the different superficial layers of the head (Liebert et al., 2004; Dehaes et al., 2011; Gagnon et al., 2012; Kirilina et al., 2012). Specifically, Gagnon et al. (2012) showed that evoked oxygenation changes in the cortex can propagate through the pial veins at the surface of the cortex, which leads to different cortical weighting factors for HbO and HbR ( $\omega_H \approx 0.76$ ,  $\omega_Q \approx 0.19$ ). We set prior means of  $\omega_{i,H}$  and  $\omega_{i,Q}$  to 0.5 (Eq. (9)), and then estimated these values from data.

The  $i, j$ th element of the sensitivity matrix,  $S_{ij}$  at wavelength  $\lambda$  in Eq. (7) is given by

$$S_{i,j}(\lambda) = \frac{G(r_{i,s}, r_{j,h})G(r_{j,h}, r_{i,d})}{G(r_{i,s}, r_{i,d})} \quad (10)$$

where  $r_{i,s}$  and  $r_{i,d}$  are the optical source and optical detector positions for the  $i$ th of  $N$  channel measurements, and  $r_{j,h}$  is the hemodynamic source position in the  $j$ th brain region of interest. The quantity  $G(r_1, r_2)$  is Green's function of the photon fluence at position  $r_2$  from a source at  $r_1$ .  $S_{ij}$  is the ratio of light received indirectly (by detector  $d_i$  from source  $s_j$ ) via scattering from hemodynamic source  $h_j$  versus that received directly, which corresponds to the effective pathlength of detected photons for the  $i$ th channel measurement in the  $j$ th hemodynamic source. In practice, the sensitivity matrix can be estimated by simulating photon migration through the head and brain based on a Monte Carlo method (Wang et al., 1995; Boas et al., 2002; Fang, 2010) or finite element methods (Dehghani et al., 2009). These computations require a structural Magnetic Resonance Image (sMRI) of the subject's head and brain. However, when the subject-specific sMRI is not available, it is also possible to use a canonical sMRI (see Cooper et al., 2012; Ferradal et al., 2014 for a comparison). In addition, given a set of standard optode positions and a canonical cortical surface, Green's functions can be pre-computed. This is analogous to the pre-computation of a standard lead field model for M/EEG source reconstruction (or DCM for M/EEG). Thus, users of DCM for fNIRS can use these standard forward models, thus saving a large amount of computation time.

#### Computing the sensitivity matrix

In this study, we used the mesh-based Monte Carlo simulation software (MMC, Fang (2010)) to estimate Green's function of the photon

fluence, and then calculate a matrix of the sensitivity to the absorption coefficient changes  $S$  in Eq. (10). Specifically, given a 3D finite-element mesh generated from a canonical sMRI (Holmes et al., 1998; Fang and Boas, 2009), we launch  $10^8$  photons from the optical source position of each channel  $r_s$  to estimate Green's functions,  $G(r_s, r_h)$  and  $G(r_s, r_d)$ , from the position of optical source  $r_s$  into the positions of the hemodynamic sources  $r_h$  and the position of optical detector  $r_d$ , respectively. We also launch  $10^8$  photons from the optical detector position of each channel  $r_d$  to estimate Green's function  $G(r_d, r_h)$ , which, according to the reciprocity theorem (Arridge, 1999), is equivalent to  $G(r_h, r_d)$ . Since tissue-type specific labeling of optical properties provides a more accurate light model than assuming homogeneous optical properties (Heiskala et al., 2009), each tetrahedral volume element is labeled by tissue type, and assigned optical properties as summarized in Table 1. Optical properties for the scalp/skull, cerebrospinal fluid (CSF), gray matter, and white matter are identical to those used in the literature (Fang, 2010; Eggebrecht et al., 2012).

#### Distributed sources

In Eq. (7), we have modeled each hemodynamic signal as a point source which produces a hemodynamic response at a single specified anatomical location. However, it is also possible to consider hemodynamic responses as being spatially extended. Assuming that the spatial point spread functions of hemodynamic responses are approximately Gaussian (Shmuel et al., 2007), the spatially distributed hemodynamic source can be specified by convolving the temporal response with a Gaussian spatial kernel whose width can be estimated during model inversion. Hemodynamic activity at source location  $r_i$  is then given by

$$\Delta H_c(r_i, r_j) = K(r_i, r_j) \Delta H_c(r_j)$$

$$\Delta Q_c(r_i, r_j) = K(r_i, r_j) \Delta Q_c(r_j) \quad (11)$$

$$K(r_i, r_j) = \exp\left(\frac{-|r_i - r_j|^2}{2\sigma^2(r_j)}\right),$$

where  $r_j$  is the center of the hemodynamic kernel,  $r_i$  is the position in the Montreal Neurological Institute (MNI) space,  $K(r_i, r_j)$  is the Gaussian spatial smoothing kernel at position  $r_i$  from position  $r_j$ , distance between the  $i$ th distributed source and  $j$ th point source,  $|r_i - r_j| \leq d_{j,\text{max}}$ , and bandwidth of kernel,  $\sigma(r_j) = d_{j,\text{max}}/2\sqrt{2\ln 2}$ . Here, the maximum distance between point and distributed sources,  $d_{j,\text{max}}$ , is estimated, and the use of a latent variable,  $\tilde{d}_{j,\text{max}}$ , allows the estimate of  $d_{j,\text{max}}$  to vary about 4 mm as

$$d_{j,\text{max}} = 4 \exp(\tilde{d}_{j,\text{max}}). \quad (12)$$

when using distributed sources, we have three optics parameters to estimate:  $\theta_p = \{\tilde{\omega}_{i,H}, \tilde{\omega}_{i,Q}, \tilde{d}_{j,\text{max}}\}$ .

#### Confounds

One of the challenges for fNIRS-based connectivity studies is that the fNIRS signal can be significantly contaminated with systemic physiological interference. Such systemic physiological noise, induced by heart beat, respiration, and blood pressure variations, may interfere with the estimation of fNIRS-based connectivity (Boas et al., 2004; Kirilina et al., 2012). However, recent fNIRS studies have shown that this physiological interference can be effectively removed by regressing out the global signal (Mesquita et al., 2010), physiological noises generated from different frequency bands of fNIRS data (Tong et al., 2011), or a signal derived from superficial scalp measurements using a short

**Table 1**

Optical properties of scalp & skull, cerebrospinal fluid (CSF), gray matter, and white matter for Monte Carlo simulation. Absorption coefficients  $\mu_a$  and scattering coefficients  $\mu_s$  for various brain tissue types are based on those used in Eggebrecht et al. (2012). Anisotropy factor  $g$  and refraction index  $n$  are based on those used in Fang (2010). The units of  $\mu_a$  and  $\mu_s$  are  $\text{mm}^{-1}$ .

	760 nm		850 nm		Anisotropy factor	Refraction index
	$\mu_a$	$\mu_s$	$\mu_a$	$\mu_s$	$g$	$n$
Scalp & skull	0.0143	7.6364	0.0164	6.7273	0.89	1.37
CSF	0.0040	2.7273	0.0040	2.7273	0.89	1.37
Gray matter	0.0180	7.5991	0.0192	6.1145	0.89	1.37
White matter	0.0167	10.8255	0.0208	9.1882	0.84	1.37

source–detector separation channel (White et al., 2009; Saager et al., 2011; Gagnon et al., 2011; Gagnon et al., 2014; Goodwin et al., 2014).

In our approach, very low-frequency confounds (c.f., drift terms in fMRI convolution models) were removed from the fNIRS channel measurements, by using a high-pass filter with a cutoff frequency of 0.008 Hz. Physiological noises, including respiration and cardiac pulsation, were then removed by using a band-stop filter with cutoff frequencies of [0.12 0.35] and [0.7 1.5] Hz, respectively. In addition, the forward model in Eq. (13) produced by integrating the neuronal and hemodynamic state equations can be extended by adding the confounding effects  $X$  (see below). We therefore used a discrete cosine transform set with cutoff periods of [8 12] seconds and a constant term in  $X$ , to model Mayer waves (Obrig et al., 2000) and baseline shift. Confounding effects on the observed signal were then estimated and removed during model inversion. Note that additional measurements of systemic confounds e.g., changes in blood pressure (Minati et al., 2011; Tachtsidis et al., 2009; Takahashi et al., 2011) and arterial partial pressure of  $\text{CO}_2$  (Scholkmann et al., 2013) can also be used in the proposed method, which may enhance the efficiency of effective connectivity estimates.

#### Priors, estimation, and model selection

The neurodynamic, hemodynamic, and optics parameters can be concatenated in a vector of free parameters,  $\theta = \{\theta_n, \theta_h, \theta_p\}$ . The DCM parameters are then estimated from the data,  $y$ , using Bayesian inference, where competing hypotheses or models are compared using their evidence (Penny, 2012).

For any given parameters  $\theta$ , model predictions,  $g(\theta)$  can be generated by integrating the forward equations as described in Friston et al. (2003). The observed data  $y$  is then modeled as

$$y = g(\theta, m) + X\beta + e, \quad (13)$$

where  $X$  contains confounding effects,  $\beta$  is the associated parameter vector, and  $e$  is the zero mean additive Gaussian noise with covariance

**Table 2**

Prior mean and standard deviation (SD) on neurodynamic and hemodynamic parameters.  $i$  and  $j$  index source regions,  $k$  indexes an experimental input,  $l$  indexes sensor region, and  $\bar{X}$  denotes the latent variables from which  $X$  is derived.

Parameter	Description	Prior mean	Prior SD
$\bar{A}_{ij}$	Extrinsic connection in the absence of input	0.0078	0.25
$\bar{A}_{ii}$	Intrinsic connection in the absence of input	0	0.25
$\bar{B}_{ij}^k$	Extrinsic connection modulated by input	0	1
$\bar{B}_{ii}^k$	Intrinsic connection modulated by input	0	1
$C_{ij}$	Influence of input on regional activity	0	1
$\bar{\tau}_{ij}$	Signal decay rate	0	0.05
$\bar{\gamma}_j$	Rate of autoregulatory feedback	0	0.05
$\bar{\tau}_j$	Transit time	0	0.05
$\bar{\tau}_{jv}$	Viscoelastic time	0	1
$\bar{d}_{j,\text{max}}$	Spatial kernel width	0	0.05
$\bar{\omega}_{i,H}$	Cortical fraction of HbO	0	0.22
$\bar{\omega}_{i,Q}$	Cortical fraction of HbR	0	0.22

$C_y$ . The error covariances are assumed to decompose into terms of the form  $C_y^{-1} = \sum_i \exp(\lambda_i) Q_i$ ; where  $Q_i$  are the known precision basis functions. The likelihood of the data is therefore

$$p(y|\theta, \lambda, m) = N(y; g(\theta, m), C_y). \quad (14)$$

The priors,  $p(\theta|m)$ , assume to be Gaussian. The priors used in this paper correspond to those implemented in SPM12 software, and their mean and variance are summarized in Table 2. We also use a normal prior  $p(\lambda|m)$  over the log error precision,  $\lambda$ .

The posterior distribution is then estimated using a variational Laplace (VL) method (Friston et al., 2007). Specifically, the VL algorithm assumes an approximate posterior density of the following factorized form

$$q(\theta, \lambda|y, m) = q(\theta|y, m)q(\lambda|y, m), \quad (15)$$

where  $q(\theta|y, m) = N(\theta; m_\theta, S_\theta)$ , and  $q(\lambda|y, m) = N(\lambda; m_\lambda, S_\lambda)$ . The DCM parameters  $\theta$  and hyperparameters  $\lambda$  of these approximate posteriors are then iteratively updated so as to minimize the Kullback–Leibler (KL)-divergence between the true and approximate posteriors. This is a standard approach in Bayesian statistics and machine learning (Bishop, 2006).

The structure of a DCM is defined by the connectivity matrices  $A$ ,  $B$ , and  $C$ . Different models can be compared using the evidence for each model. This can be thought of as a second-level of Bayesian inference. The model evidence is given by

$$p(y|m) = \iint p(y|\theta, \lambda, m)p(\theta|m)p(\lambda|m)d\theta d\lambda. \quad (16)$$

While the model evidence is not straightforward to compute, it is possible to place a lower bound on the log model evidence of the following form

$$\log p(y|m) = F(m) + KL[q(\theta, \lambda|m)||p(\theta, \lambda|y, m)], \quad (17)$$

where  $F(m)$  is known as the negative variational free energy and the last term is the Kullback–Leibler (KL) distance between the true posterior density,  $p(\theta, \lambda|y, m)$ , and an approximate posterior  $q(\theta, \lambda|m)$ . Free energy is estimated as above using the Laplace approximation (Friston et al., 2007). Once the evidence has been computed, Bayesian inference at the model level can then be implemented using the Bayes rule:

$$p(m|y) = \frac{p(y|m)p(m)}{\sum_{m=1}^M p(y|m)p(m)}, \quad (18)$$

where  $M$  is the total number of models to be tested, and  $p(m) = 1/M$  under uniform model priors.

Inference about a characteristic of interest, such as (i) which regions receive driving input? and (ii) which connections are modulated by other experimental factors?, and so on can be calculated by family level inference (Penny et al., 2010). That is inference at the level of model families, rather than at the level of the individual models. To implement family level inference, one specifies which models belong

to which families. The posterior distribution over families is then given by summing up the relevant posterior model probabilities

$$p(f_k|y) = \sum_{m \in f_k} p(m|y), \quad (19)$$

where the subset  $f_k$  contains all models belonging to family  $k$ .

#### Motor execution and imagery data

In this section, we applied DCM for fNIRS to experimental data from a single subject recorded during the motor execution and motor imagery tasks. Specifically, in the first run, the subject was instructed to squeeze and release a ball with her right hand during task blocks. In the second run, the subject was seated on a comfortable chair with her hands on her laps in a dim-lighted room, and was instructed to look ahead blankly and perform kinesthetic imagery of the same hand movement, but without moving the hand. That is, the auditory cue prompted motor imagery rather actual movement. For both runs, there were 5 second blocks of tasks where the cue was presented with an auditory beep, interspersed with 25 second rest blocks.

The optical density changes during motor execution and imagery were acquired using a continuous wave fNIRS instrument (NIRScout, NIRx, Medizintechnik, GmbH, Germany). The fNIRS system had 16 channels for bilateral placements, consisting of 2 optical sources with wavelengths of 760 nm and 850 nm, and 6 optical detectors. The supplementary motor area (SMA) and primary motor cortex (M1) of both hemispheres were covered within the optical holder cap. However, only fNIRS data from the left hemisphere was used in this study, as our goal was to study the contralateral activation of brain regions during right hand movement. The sampling frequency was 10.4 Hz. The distance between the optical source and the detector was 2.5 cm. The geometry of optical probes on the left hemisphere is shown in Fig. 2.

A previous study found consistent activation in the SMA and premotor cortex during motor execution and imagery, and reduced activation in M1 during motor imagery (Hanakawa et al., 2003). Moreover, a recent study has revealed, using DCM for fMRI (Kasess et al., 2008), that coupling between SMA and M1 may serve to attenuate the activation of M1 during motor imagery. In this paper, we test 9 models depicted in Fig. 3, in order to investigate (i) how the motor imagery condition affects the directed connections between SMA and M1, and (ii) how these interactions are associated with the regional activity in M1 and SMA during motor execution and imagery. All models comprise two regions including SMA and M1, and assume reciprocal connections between SMA and M1 for the  $A$  matrix; this connectivity is supported by anatomical studies in monkeys (Muakkassa and Strick, 1979; Luppino

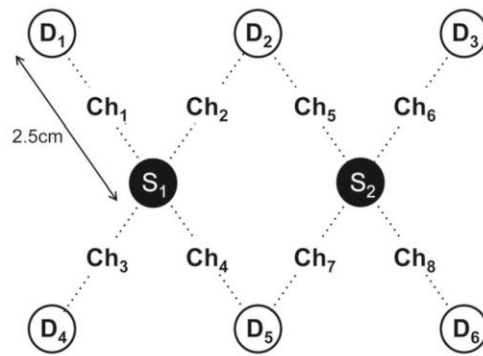


Fig. 2. Geometry of the optical probes. S, D, and Ch denote optical source, optical detector, and channel, respectively. The distance between the source and the detector is 2.5 cm.

et al., 1993). The models then differ in regions receiving task input: M1, SMA, and both M1 and SMA. The models also differ in which connections are modulated by motor imagery: modulation of intrinsic (within-region) connectivity, modulation of extrinsic (between-region) connectivity, and modulation of both intrinsic and extrinsic connectivities. Additionally, for each of these 9 configurations, we fit two models; one with hemodynamic response modeled as point source and one with a spatially distributed source. Overall, these 18 models allow us to address 3 experimental questions (i) which regions receive task input?, (ii) which type of connections is modulated by imagery?, and (iii) are distributed sources better than point source models?

## Results

### SPM analysis

Prior to DCM analysis, brain regions whose dynamics are driven by experimental conditions were identified using Statistical Parametric Mapping (SPM) analysis (Friston et al., 1995; Ye et al., 2009). Specifically, the HbO response was calculated from fNIRS data using the modified Beer–Lambert law (Delpy et al., 1988), and was subject to SPM analysis with the canonical hemodynamic response function plus its temporal and dispersion derivatives. Statistical significance was assessed using  $F$ -tests and the resulting statistical maps were thresholded at a voxel level of  $p < 0.000001$ , corrected using random field theory in the usual way. We found that SMA was significantly activated during both motor execution and motor imagery, whereas M1 was only activated during motor execution, as shown in Fig. 4. The most significantly activated voxels within SMA and M1 were then selected as the source positions for DCM analysis: The MNI coordinates are: SMA,  $[-51, -4, 55]$ ; and M1,  $[-44, -16, 65]$ .

### DCM analysis

DCM was then fitted to the optical density signal averaged across trials. Bayesian model selection compared DCM models which differed in spatial extent of hemodynamic source, regions receiving task input, and connections modulated by motor imagery (Fig. 5). Family level inference indicated that the models with spatially distributed hemodynamic source outperformed the models with point source. Moreover, together with Bayesian inference at the model level, the best model structure was model 9 in which task input could affect regional activity in both SMA and M1, and motor imagery modulated both extrinsic and intrinsic connections.

The posterior mean DCM parameters for the best model are

$$A = \begin{bmatrix} -0.16 & -0.49 \\ -0.02 & -0.33 \end{bmatrix}, B^k = \begin{bmatrix} -0.02 & -0.77 \\ 0.33 & -1.31 \end{bmatrix}, C = \begin{bmatrix} 0.08 & 0 \\ 0.06 & 0 \end{bmatrix}$$

$$\begin{bmatrix} \kappa_1 & \gamma_1 & \tau_1 & \tau_{1,v} & d_{1,max} & \bar{\omega}_H \\ \kappa_2 & \gamma_2 & \tau_2 & \tau_{2,v} & d_{2,max} & \bar{\omega}_Q \end{bmatrix} = \begin{bmatrix} 0.69 & 0.28 & 2.11 & 4.12 & 4.26 & 0.72 \\ 0.63 & 0.34 & 1.97 & 0.92 & 3.88 & 0.59 \end{bmatrix},$$

where  $A_{ij}$  represents the connectivity from region  $j$  to region  $i$  in the absence of experimental input;  $B^k_{ij}$  represents the change in connectivity from region  $j$  to region  $i$  induced by  $k$ th input; and  $C_{ik}$  represents the influence of input on region  $i$ . The units of connections are the rates (Hz) of neural population changes. In other words, in models based upon differential equations, effective connectivity plays the role of a rate constant; where a strong influence implies a fast response. The posterior mean of estimated hemodynamic and optics parameters is within the range of values reported from the literature (Buxton et al., 2004; Huppert et al., 2009; Gagnon et al., 2012). Among estimated parameters, cortical fraction of HbO averaged across the channels ( $\bar{\omega}_H = 0.72$ ) was higher than that of HbR ( $\bar{\omega}_Q = 0.59$ ). This result suggests that the remaining 28% and 41% of the signal for HbO and HbR arise from extracerebral regions, including pial vasculature and skin, where oxygenation changes occur following brain activation. While  $\bar{\omega}_Q$  was

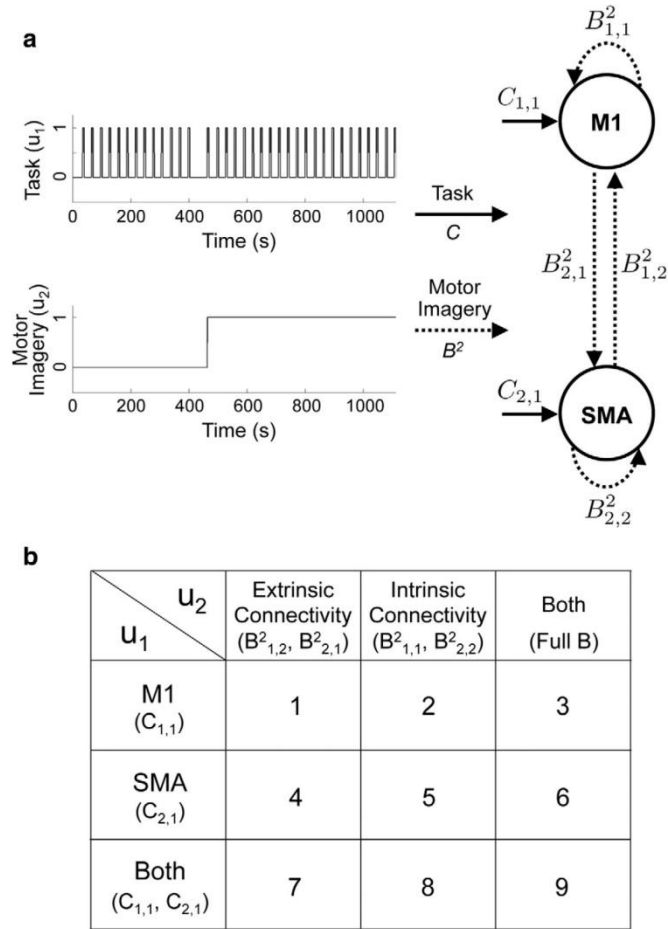


**Fig. 3.** The model structure for the DCM analysis of motor execution and imagery data. (a) The model comprises two regions including supplementary motor area (SMA) and primary motor cortex (M1), and two inputs according to the experimental paradigm. The first input variable (i.e., task) encodes the occurrence of motor execution and motor imagery tasks. Activation of the second input variable (i.e., motor imagery) indicates that the task is motor imagery. (b) 9 models are tested in this study. The models differ in regions receiving task input, and connections modulated by motor imagery.

slightly higher than the values estimated in Gagnon et al. (2012), this discrepancy may be caused by differences in anatomical vasculature, channel position, or experimental protocol.

We selected M1 and SMA for source region 1 and source region 2, task for the first input, and motor imagery for the second input. So, as an example of analysis results,  $B_{1,2}^2$  indicates that connectivity strength

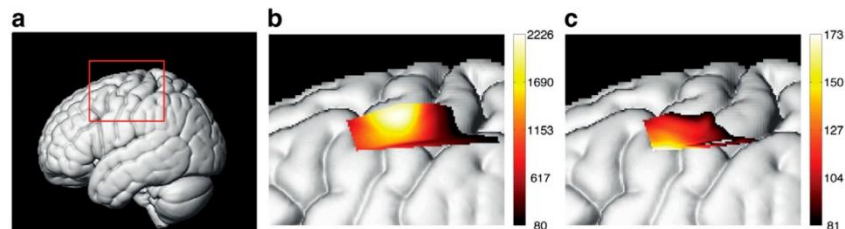


**Fig. 4.** Cortical activation during motor tasks detected using oxy-hemoglobin (HbO) responses. (a) Left lateral view of volume rendered brain with bounding box showing region displayed on other two panels. (b) Main effects of motor execution task, and (c) main effects of motor imagery task. A conventional SPM analysis was applied to fNIRS data, and the resultant  $F$ -statistic maps were thresholded at a voxel level of  $p < 0.000001$  (corrected). Results show that SMA is significantly activated during both motor execution and imagery tasks, whereas M1 was only activated during motor execution. Two regions of interest for the DCM analysis were selected using the local maxima of the  $F$ -statistics closest to M1 and lateral SMA.

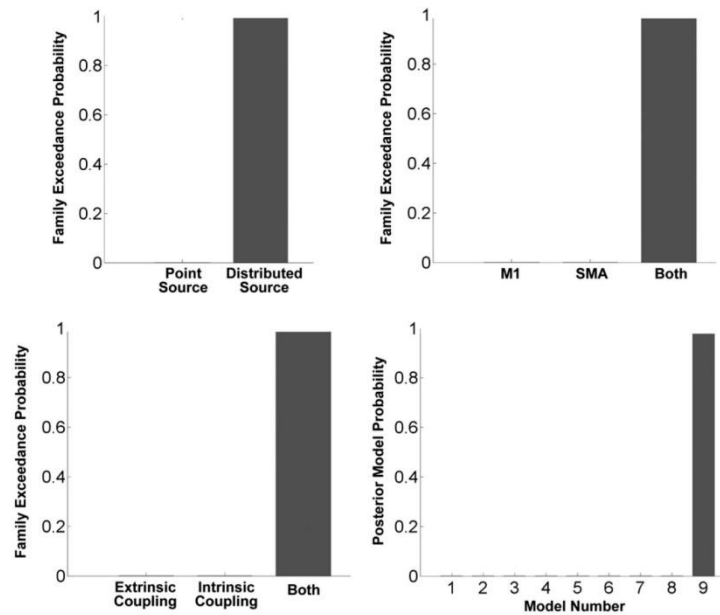


**Fig. 5.** Results of Bayesian model comparison. Family level inference indicated that models with spatially distributed hemodynamic source outperformed models with point sources. Moreover, together with Bayesian inference at the model level, the best model structure was model 9 in which task input could affect regional activity in both supplementary motor area (SMA) and primary motor cortex (M1), and motor imagery could modulate both the extrinsic and intrinsic connections.

from SMA to M1 was reduced by motor imagery ( $-0.77$ ). This is entirely consistent with previous fMRI activation studies of this paradigm – and the notion that imagined movement calls on the same sensorimotor schemata here as executed movements – but gated at the level of the motor cortex. More details about the estimate of DCM parameters, including posterior variance, are shown in Fig. 6.

Fig. 7 shows the parameter estimates as a network model. The results indicate that while all motor stimuli positively affect the regional activity in M1, motor imagery negatively modulates the connection from SMA to M1, resulting in the suppressive influence of SMA on M1. Quantitatively, the strength of connectivity from SMA to M1,  $-0.49$  is significantly reduced by motor imagery,  $-0.77$ . This suppressive influence causes reduced activity in M1 during motor imagery. Interestingly, we also found that motor imagery positively modulates the connection from M1 to SMA.

As an example of the accuracy of DCM model fits, Fig. 8 shows the predicted and measured optical density signals. Note that our DCM models comprise two neuronal sources, including M1 and SMA,

whose activities each generate optical density changes in all eight channels using the forward model in Eq. (13). To compare model fit to the channel measurements, we selected channels 2, 5, and channels 3, 4, whose sensitivities to M1 and SMA are highest among eight channels, respectively. DCM produces similar traces to the actual fNIRS data at both wavelengths 760 nm and 850 nm.

Estimated neural responses shown in Fig. 9 show that during motor imagery, neural activity in M1 is significantly reduced, while neural activity in SMA is relatively consistent, compared with activity during motor execution. These results correspond to the findings of previous fMRI studies which have shown that M1 is more active during motor execution, while lateral SMA is more involved in motor imagery (Kasess et al., 2008; Gerardin et al., 2000).

## Discussion

In this paper, we have introduced DCM for fNIRS. The generative model of fNIRS data is created by linking the fNIRS optics equation to

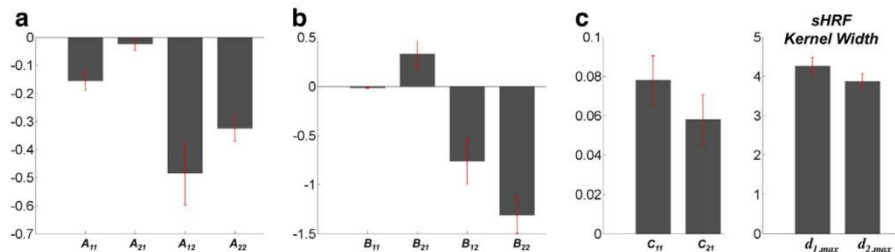


**Fig. 6.** Estimates of DCM parameters, including neurodynamic and hemodynamic effects. Magnitude of bar graph indicates posterior mean of each parameter, and the red error bar indicates the standard deviation (square root of posterior variance) for model 9.

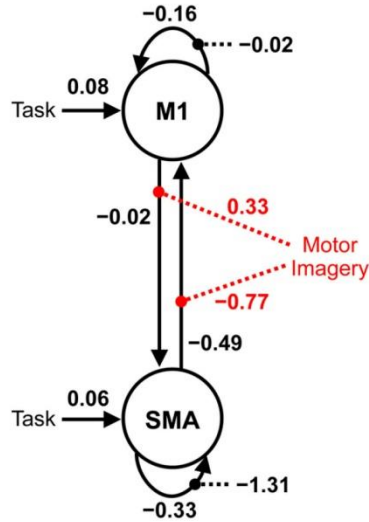


**Fig. 7.** Model with estimated parameters of effective connectivity. The units of connections are the rates (Hz) of neural population changes. Black and red dotted lines indicate intrinsic and extrinsic connections modulated by motor imagery, respectively. The results indicate that while all motor stimuli positively affect the regional activity in primary motor cortex (M1), motor imagery negatively modulates connection from supplementary motor area (SMA) to M1, resulting in the suppressive influence of SMA on M1. These results are consistent with the findings of previous fMRI studies (Kasess et al., 2008; Gerardin et al., 2000).

the hemodynamic and neurodynamic equations. DCM parameters are estimated using the same Bayesian scheme which is used for dynamic causal modelling of other imaging modalities. Bayesian inference at

the family and model levels then allows one to test specific hypotheses about functional brain architectures and select a model structure which explains the fNIRS data best.

Using fNIRS data whose protocol was similar to that of recent fMRI studies, we have demonstrated the validity of estimates of effective connectivity in this context. Specifically, by applying DCM to experimental data acquired during motor imagery and motor execution, we showed that the best-performing model comprised regions of SMA and M1 driven by task input, and both extrinsic and intrinsic connections are modulated by motor imagery. The corresponding estimates of DCM parameters indicated that reduced activity in M1 during motor imagery can be explained by the suppression of M1 sensitivity to extrinsic projections from SMA. These results suggest that the proposed method enables one to infer directed interactions in the brain mediated by neuronal dynamics from optical density changes.

In the following, we discuss potential extensions to the current DCM for fNIRS. One extension would be to parameterize the sensitivity matrix so that the optimal locations of hemodynamic sources are estimated from the data. Currently, we have used a fixed hemodynamic source location as identified using a prior general linear model analysis. However, because the spatial location of neuronal activation may be slightly different from hemoglobin changes, it may be appropriate to specify the location of neuronal sources as free parameters with informed priors. Motivated by the lead field parameterization in DCM for EEG and MEG (Kiebel et al., 2006), we can make the sensitivity matrix a function of three location parameters,  $S(\theta)$  where  $\theta = (x^{\text{pos}}, y^{\text{pos}}, z^{\text{pos}})$ . The expectation of the location prior can be given by an activated voxel location at the cortical level. Then, hemodynamic source locations can be estimated simultaneously with other DCM parameters using Bayesian inversion. Furthermore, we can test the hypothesis that neuronal and hemodynamic responses are spatially dislocated by comparing models with and without free location parameters.

A further area of research concerns the development of the hemodynamic equation. In the proposed scheme, the hemodynamic component is based on the extended Balloon model (Buxton et al., 2004). This

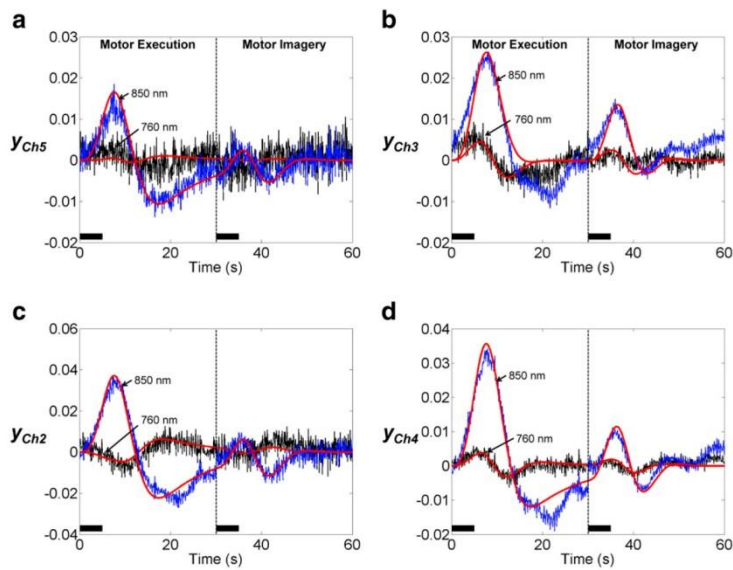


**Fig. 8.** DCM fit to optical signal measured during motor execution and motor imagery. Black and blue plots indicate average optical density changes measured at wavelengths 760 nm and 850 nm, respectively. Red plots indicate the corresponding estimates from DCM model 9. To compare model fit to the measurements, we selected channels 2, 5, and channels 3, 4, whose sensitivities to M1 and SMA were highest among eight channels, respectively. DCM produces similar traces to the fNIRS data at both wavelengths. The solid black line indicates the empirical task periods (5 s), including motor execution and motor imagery.

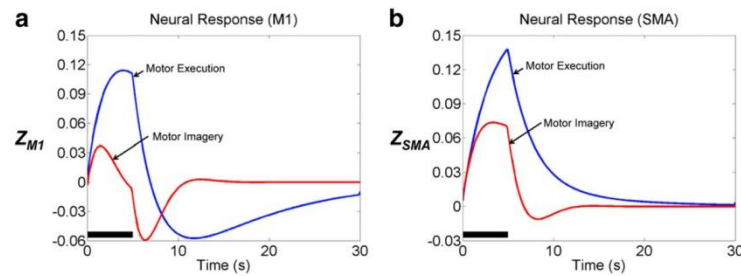


**Fig. 9.** Estimated neural responses ( $z$ ). During motor imagery, neural activity in primary motor cortex (M1) is significantly reduced, while neural activity in supplementary motor area (SMA) is relatively consistent, compared with activity during motor execution. The solid black line indicates the task period (5 s).

model can describe transient characteristics of blood flow and blood volume, particularly in the return-to-baseline stages of the response, using viscoelastic time constant  $\tau_{jv}$ . As shown in Fig. 8, an undershoot of optical responses was observed during post-stimulus. In the M1 source, significantly suppressed neuronal activity and longer viscoelastic time constants were estimated. These estimates lead to decreased blood flow and delayed blood volume recovery, which increases HbR, and then leads to an undershoot of optical responses in the corresponding channels, 2, 4, and 5. This result is supported by simultaneous fMRI and electrophysiological recording studies, demonstrating the correlation between negative fMRI response and decreased neuronal activity (Shmuel et al., 2006). However, our model did not fit the post-stimulus undershoot of optical response in channel 3 (Fig. 8(b)). Note that sensitivity of channel 3 to the SMA source was approximately 9 times higher than the sensitivity to the M1 source:  $S_{3,SMA}/(S_{3,M1} + S_{3,SMA}) = 0.89$ . Therefore, less suppression of neuronal activity during motor execution or shorter viscoelastic time constants in SMA would cause less undershoot of estimated optical response in channel 3. More sophisticated neurodynamic (Marreiros et al., 2008; Kumar and Penny, 2014), vascular (Kong et al., 2004; Boas et al., 2008), and hemodynamic (Zheng et al., 2002; Havlicek et al., 2014) models may allow the transient hemodynamic response, such as post-stimulus undershoot, to be better fitted from fNIRS data, and to be explained by either neuronal or hemodynamic effects or both.

In this paper we have modeled each hemodynamic source as either a point process or a spatially distributed process at a specified anatomical location. In the latter case, the spatial point spread function is modeled as a Gaussian kernel whose width is estimated from data. However, this implies that the hemodynamic response is a simple low-pass spatial filter of neuronal activity. Instead, intrinsic spatiotemporal hemodynamics could be specified using differential equations specifying such spatio-temporal dynamics as a function of position on the cortical surface (Aquino et al., 2012, 2014).

Finally, we will extend the neurodynamic model to include both excitatory and inhibitory states in each region. Current DCM for fNIRS is based on a model which describes the neurodynamics with one state in each region (see Eq. (1)). By adopting a two-state neurodynamic model (Marreiros et al., 2008), we can not only model both intrinsic and excitatory activities within intrinsic coupling, but also relax the priors used to ensure stability in the one-state model. The high temporal resolution of fNIRS should in principle allow fNIRS data to support these much richer dynamical models.

A current limitation of DCM for fNIRS is that model fitting is computationally demanding, compared with functional connectivity and Granger causality analyses. For the analysis of our fNIRS data, parameter estimation in the fully connected network model comprising two regions took approximately 6 min (for point hemodynamic sources), and 18 min (for spatially distributed hemodynamic sources) on a desktop PC running Windows 7 (64 bit) with an Intel Xeon W3570 (3.2 GHz) and 12 GB RAM. The VL optimization procedure required 20 iterations and 49 iterations until it converged, respectively.

In this study, we focused on the development and description of a novel method to estimate effective connectivity from fNIRS data. We therefore showed an illustrative analysis using fNIRS data from a single subject. In a subsequent paper, we will focus on analysis of fNIRS data from a group of subjects (including random effects model comparison Stephan et al., 2009), and show clinical applications of DCM-fNIRS in patients in low awareness states.

The proposed methods are implemented in Matlab code and will be available freely in the next beta version of SPM software (<http://fil.ion.ucl.ac.uk/spm>).

#### Acknowledgments

This work is supported by a Newton International Fellowship to ST. AMK is supported by a grant from the Neuro-disability Research Trust (RHN11/02). KJF is funded by a Wellcome Trust Principal Research Fellowship (Ref: 088130/Z/09/Z). WDP is supported by a core grant from the Wellcome Trust (Ref: 091593/Z/10/Z).

#### References

- Aquino, K.M., Schira, M.M., Robinson, P.A., Drysdale, P.M., Breakspear, M., 2012. Hemodynamic traveling waves in human visual cortex. *PLoS Comput. Biol.* 8 (3), e1002435.
- Aquino, K.M., Robinson, P.A., Drysdale, P.M., 2014. Spatiotemporal hemodynamic response functions derived from physiology. *J. Theor. Biol.* 347, 118–136.
- Arridge, S.R., 1999. Optical tomography in medical imaging. *Inverse Prob.* 15, R41–R93.
- Bishop, C.M., 2006. *Pattern Recognition and Machine Learning* vol. 1. Springer, New York.
- Boas, D.A., Culver, J.P., Stott, J.J., Dunn, A.K., 2002. Three dimensional Monte Carlo code for photon migration through complex heterogeneous media including the adult human head. *Opt. Express* 10, 159–170.
- Boas, D.A., Strangman, G., Culver, J.P., Hoge, R.D., Jaszewski, G., Poldrack, R.A., Rosen, B.R., Mandeville, J.B., 2003. Can the cerebral metabolic rate of oxygen be estimated with near-infrared spectroscopy? *Phys. Med. Biol.* 48 (15), 2405–2418.
- Boas, D.A., Dale, A.M., Franceschini, M.A., 2004. Diffuse optical imaging of brain activation: approaches to optimizing image sensitivity, resolution, and accuracy. *NeuroImage* 23, S275–S288.
- Boas, D.A., Jones, S.R., Devor, A., Huppert, T.J., Dale, A.M., 2008. A vascular anatomical network model of the spatio-temporal response to brain activation. *NeuroImage* 40 (3), 1116–1129.
- Buxton, R.B., 2012. Dynamic models of BOLD contrast. *NeuroImage* 62 (2), 953–961.
- Buxton, R., Wong, E., Frank, L., 1998. Dynamics of blood flow and oxygenation changes during brain activation: the balloon model. *Magn. Reson. Med.* 39, 855–864.
- Buxton, R.B., Uludag, K., Dubowitz, D.J., Liu, T.T., 2004. Modeling the hemodynamic response to brain activation. *NeuroImage* 23, 220–233.
- Cooper, R.J., Caffini, M., Dubb, J., Fang, Q., Custo, A., Tsuzuki, D., Fischl, B., Wells III, W., Dan, I., Boas, D.A., 2012. Validating atlas-guided DOT: a comparison of diffuse optical tomography informed by atlas and subject-specific anatomies. *NeuroImage* 62, 1999–2006.
- Cui, X., Bray, S., Reiss, A.L., 2010. Functional near infrared spectroscopy (fNIRS) signal improvement based on negative correlation between oxygenated and deoxygenated hemoglobin dynamics. *NeuroImage* 49, 3039–3046.
- Daunizeau, J., Friston, K.J., Kiebel, S.J., 2009a. Variational Bayesian identification and prediction of stochastic nonlinear dynamic causal models. *Physica D* 238 (21), 2089–2118.
- Daunizeau, J., Kiebel, S.J., Friston, K.J., 2009b. Dynamic causal modelling of distributed electromagnetic responses. *NeuroImage* 47 (2), 590–601.
- Dehaes, M., Gagnon, L., Lesage, F., Péligrini-Issac, M., Vignaud, A., Valabregue, R., Grebe, R., Wallois, F., Benali, H., 2011. Quantitative investigation of the effect of the

- extra-cerebral vasculature in diffuse optical imaging: a simulation study. *Biomed. Opt. Express* 2 (3), 680–695.
- Dehghani, H., Eames, M.E., Yalavarthy, P.K., Davis, S.C., Srinivasan, S., Carpenter, C.M., Pogue, B.W., Paulsen, K.D., 2009. Near infrared optical tomography using NIRFAST: algorithm for numerical model and image reconstruction. *Commun. Numer. Methods Eng.* 25, 711–732.
- Delpy, D.T., Cope, M., Van der Zee, P., Arridge, S., Wray, S., Wyatt, J., 1988. Estimation of optical pathlength through tissue from direct time of flight measurement. *Phys. Med. Biol.* 33 (12), 1433–1442.
- Dubeau, S., Havlicek, M., Beaumont, E., Ferland, G., Lesage, F., Pouliot, P., 2012. Neurovascular deconvolution of optical signals as a proxy for the true neuronal inputs. *J. Neurosci. Methods* 210 (2), 247–258.
- Eggebrecht, A.T., White, B.R., Ferradal, S.L., Chen, C., Zhan, Y., Snyder, A.Z., Dehghani, H., Culver, J.P., 2012. A quantitative spatial comparison of high-density diffuse optical tomography and fMRI cortical mapping. *NeuroImage* 61, 1120–1128.
- Eggebrecht, A.T., Ferradal, S.L., Robichaux-Viehoever, A., Hassanpour, M.S., Dehghani, H., Snyder, A.Z., Hershey, T., Culver, J.P., 2014. Mapping distributed brain function and networks with diffuse optical tomography. *Nat. Photonics* 8, 448–454.
- Fang, Q., 2010. Mesh-based Monte Carlo method using fast ray-tracing in Plücker coordinates. *Biomed. Opt. Express* 1, 165–175.
- Fang, Q., Boas, D.A., 2009. Tetrahedral mesh generation from volumetric binary and grayscale images. *IEEE International Symposium on Biomedical Imaging* 2009. *IEEE*, pp. 1142–1145.
- Ferradal, S.L., Eggebrecht, A.T., Hassanpour, M., Snyder, A.Z., Culver, J.P., 2014. Atlas-based head modeling and spatial normalization for high-density diffuse optical tomography: in vivo validation against fMRI. *NeuroImage* 12 (4), 466–477.
- Ferrari, M., Quaresima, V., 2012. A brief review on the history of human functional near-infrared spectroscopy (fNIRS) development and fields of application. *NeuroImage* 63 (2), 921–935.
- Fox, P.T., Raichle, M.E., 1986. Focal physiological uncoupling of cerebral blood flow and oxidative metabolism during somatosensory stimulation in human subjects. *Proc. Natl. Acad. Sci. U. S. A.* 83 (4), 1140–1144.
- Friston, K.J., Holmes, A.P., Worsley, K.J., Poline, J.-B., Frith, C.D., Frackowiak, R.S.J., 1995. Statistical parametric maps in functional imaging: a general linear approach. *Hum. Brain Mapp.* 2, 189–210.
- Friston, K.J., Mechelli, A., Turner, R., Price, C.J., 2000. Nonlinear responses in fMRI: the Balloon model, Volterra kernels, and other hemodynamics. *NeuroImage* 12 (4), 466–477.
- Friston, K.J., Harrison, L.M., Penny, W.D., 2003. Dynamic causal modelling. *NeuroImage* 19 (4), 1273–1302.
- Friston, K.J., Mattout, J., Trujillo-Barreto, N., Ashburner, J., Penny, W.D., 2007. Variational free energy and the Laplace approximation. *NeuroImage* 34 (1), 220–234.
- Friston, K.J., Kahan, J., Biswal, B., Razi, A., 2014. A DCM for resting state fMRI. *NeuroImage* 94, 396–407.
- Gagnon, L., Perdue, K., Greve, D.N., Goldenholz, D., Kashedikar, G., Boas, D.A., 2011. Improved recovery of the hemodynamic response in diffuse optical imaging using short optode separations and state-space modeling. *NeuroImage* 56 (3), 1362–1371.
- Gagnon, L., Yücel, M.A., Dehaes, M., Cooper, R.J., Perdue, K.L., Selb, J., Huppert, T.J., Hoge, R.D., Boas, D.A., 2012. Quantification of the cortical contribution to the NIRS signal over the motor cortex using concurrent NIRS-fMRI measurements. *NeuroImage* 59 (4), 3933–3940.
- Gagnon, L., Yücel, M.A., Boas, D.A., Cooper, R.J., 2014. Further improvement in reducing superficial contamination in NIRS using double short separation measurements. *NeuroImage* 85, 127–135.
- Gerardin, E., Sirigu, A., Lehericy, S., Poline, J.-B., Gaymard, B., Marsault, C., Agid, Y., Le Bihan, D., 2000. Partially overlapping neural networks for real and imagined hand movements. *Cereb. Cortex* 10, 1093–1104.
- Goodwin, J.R., Gaudet, C.R., Berger, A.J., 2014. Short-channel functional near-infrared spectroscopy regressions improve when source-detector separation is reduced. *Neurophotonics* 1 (1), 015002.
- Grubb, R.L., Raichle, M.E., Eichling, J.O., Ter-Pogossian, M.M., 1974. The effects of changes in PaCO<sub>2</sub> on cerebral blood volume, blood flow, and vascular mean transit time. *Stroke* 5 (5), 630–639.
- Hanakawa, T., Immisch, I., Toma, K., Dimyan, M.A., Van Gelderen, P., Hallett, M., 2003. Functional properties of brain areas associated with motor execution and imagery. *J. Neurophysiol.* 89, 989–1002.
- Havlicek, M., Roebroek, A., Friston, K., Gardumi, A., Uludag, K., 2014. New physiological framework for dynamic causal modelling of fMRI data. *OHBM Annual Meeting, Hamburg*. Poster 1839.
- Heiskala, J., Pollari, M., Metsäranta, M., Grant, P.E., Nissilä, I., 2009. Probabilistic atlas can improve reconstruction from optical imaging of the neonatal brain. *Opt. Express* 17, 14977–14992.
- Highton, D., Elwell, C., Smith, M., 2010. Noninvasive cerebral oximetry: is there light at the end of the tunnel? *Curr. Opin. Anaesthesiol.* 23 (5), 576–581.
- Holmes, C.J., Hoge, R., Collins, L., Woods, R., Toga, A.W., Evans, A.C., 1998. Enhancement of MR images using registration for signal averaging. *J. Comput. Assist. Tomogr.* 22, 324–333.
- Homae, F., Watanabe, H., Otobe, T., Nakano, T., Go, T., Konishi, Y., Taga, G., 2010. Development of global cortical networks in early infancy. *J. Neurosci.* 30 (14), 4877–4882.
- Hoshi, Y., 2007. Functional near-infrared spectroscopy: current status and future prospects. *J. Biomed. Opt.* 12 (6), 062106.
- Huppert, T.J., Allen, M.S., Diamond, S.G., Boas, D.A., 2009. Estimating cerebral oxygen metabolism from fMRI with a dynamic multicompartment Windkessel model. *Hum. Brain Mapp.* 30 (5), 1548–1567.
- Im, C.-H., Jung, Y.-J., Lee, S., Koh, D., Kim, D.-W., Kim, B.-M., 2010. Estimation of directional coupling between cortical areas using Near-Infrared Spectroscopy (NIRS). *Opt. Express* 18, 5730–5739.
- Jin, T., Kim, S.-G., 2008. Cortical layer-dependent dynamic blood oxygenation, cerebral blood flow and cerebral blood volume responses during visual stimulation. *NeuroImage* 43 (1), 1–9.
- Jobsis, F.F., 1977. Noninvasive, infrared monitoring of cerebral and myocardial oxygen sufficiency and circulatory parameters. *Science* 198 (4323), 1264–1267.
- Kasesh, C.H., Windischberger, C., Cunnington, R., Lanzenberger, R., Pezawas, L., Moser, E., 2008. The suppressive influence of SMA on M1 in motor imagery revealed by fMRI and dynamic causal modeling. *NeuroImage* 40, 828–837.
- Kiebel, S.J., David, O., Friston, K.J., 2006. Dynamic causal modelling of evoked responses in EEG/MEG with lead field parameterization. *NeuroImage* 30 (4), 1273–1284.
- Kirilina, E., Jelzow, A., Heine, A., Niessing, M., Wabnitz, H., Brühl, R., Itermann, B., Jacobs, A.M., Tachtsidis, I., 2012. The physiological origin of task-evoked systemic artefacts in functional near infrared spectroscopy. *NeuroImage* 61 (1), 70–81.
- Kong, Y., Zheng, Y., Johnston, D., Martindale, J., Jones, M., Billings, S., Mayhew, J., 2004. A model of the dynamic relationship between blood flow and volume changes during brain activation. *J. Cereb. Blood Flow Metab.* 24 (12), 1382–1392.
- Kumar, S., Penny, W., 2014. Estimating neural response functions from fMRI. *Front. Neuroinform.* 8, 48.
- Liebert, A., Wabnitz, H., Steinbrink, J., Obrig, H., Möller, M., Macdonald, R., Villringer, A., Rinneberg, H., 2004. Time-resolved multidistance near-infrared spectroscopy of the adult head: intracerebral and extracerebral absorption changes from moments of distribution of times of flight of photons. *Appl. Opt.* 43 (15), 3037–3047.
- Lloyd-Fox, S., Blasi, A., Elwell, C., 2010. Illuminating the developing brain: the past, present and future of functional near infrared spectroscopy. *Neurosci. Biobehav. Rev.* 34 (3), 269–284.
- Lu, C.-M., Zhang, Y.-J., Biswal, B.B., Zang, Y.-F., Peng, D.-L., Zhu, C.-Z., 2010. Use of fNIRS to assess resting state functional connectivity. *J. Neurosci. Methods* 186 (2), 242–249.
- Luppino, G., Matelli, M., Camarda, R., Rizzolatti, G., 1993. Corticocortical connections of area F3 (SMA-proper) and area F6 (pre-SMA) in the macaque monkey. *J. Comp. Neurol.* 338 (1), 114–140.
- Marreiros, A.C., Kiebel, S.J., Friston, K.J., 2008. Dynamic causal modelling for fMRI: a two-state model. *NeuroImage* 39 (1), 269–278.
- Mesquita, R.C., Franceschini, M.A., Boas, D.A., 2010. Resting state functional connectivity of the whole head with near-infrared spectroscopy. *Biomed. Opt. Express* 1, 324–336.
- Minati, L., Kress, I.U., Visani, E., Medford, N., Critchley, H.D., 2011. Intra- and extra-cranial effects of transient blood pressure changes on brain near-infrared spectroscopy (NIRS) measurements. *J. Neurosci. Methods* 197 (2), 283–288.
- Moran, R.J., Kiebel, S.J., Stephan, K.E., Reilly, R.B., Daunizeau, J., Friston, K.J., Sep 2007. A neural mass model of spectral responses in electrophysiology. *NeuroImage* 37 (3), 706–720.
- Muakassa, K.F., Strick, P.L., 1979. Frontal lobe inputs to primate motor cortex: evidence for four somatotopically organized 'premotor' areas. *Brain Res.* 177 (1), 176–182.
- Obrig, H., 2014. NIRS in clinical neurology – a 'promising' tool? *NeuroImage* 85, 535–546.
- Obrig, H., Neufang, M., Wenzel, R., Kohl, M., Steinbrink, J., Einhäupl, K., Villringer, A., 2000. Spontaneous low frequency oscillations of cerebral hemodynamics and metabolism in human adults. *NeuroImage* 12 (6), 623–639.
- Penny, W.D., 2012. Comparing dynamic causal models using AIC, BIC and free energy. *NeuroImage* 59, 319–330.
- Penny, W., Litvak, V., Fuentemilla, L., Duzel, E., Friston, K., 2009. Dynamic Causal Models for phase coupling. *J. Neurosci. Methods* 183 (1), 19–30.
- Penny, W.D., Stephan, K.E., Daunizeau, J., Rosa, M.J., Friston, K.J., Schofield, T.M., Leff, A.P., 2010. Comparing families of dynamic causal models. *PLoS Comput. Biol.* 6 (3), e1000709.
- Saager, R.B., Telleri, N.L., Berger, A.J., 2011. Two-detector Corrected Near Infrared Spectroscopy (C-NIRS) detects hemodynamic activation responses more robustly than single-detector NIRS. *NeuroImage* 55 (4), 1679–1685.
- Sasai, S., Homae, F., Watanabe, H., Taga, G., 2011. Frequency-specific functional connectivity in the brain during resting state revealed by NIRS. *NeuroImage* 56 (1), 252–257.
- Scholkmann, F., Gerber, U., Wolf, M., Wolf, U., 2013. End-tidal CO<sub>2</sub>: an important parameter for a correct interpretation in functional brain studies using speech tasks. *NeuroImage* 66, 71–79.
- Scholkmann, F., Kleiser, S., Metz, A.J., Zimmermann, R., Mata Pavia, J., Wolf, U., Wolf, M., 2014. A review on continuous wave functional near-infrared spectroscopy and imaging instrumentation and methodology. *NeuroImage* 85, 6–27.
- Shmuel, A., Augath, M., Oeltermann, A., Logothetis, N.K., 2006. Negative functional MRI response correlates with decreases in neuronal activity in monkey visual area V1. *Nat. Neurosci.* 9 (4), 569–577.
- Shmuel, A., Yacoub, E., Chaimow, D., Logothetis, N.K., Ugurbil, K., 2007. Spatio-temporal point-spread function of fMRI signal in human gray matter at 7 Tesla. *NeuroImage* 35 (2), 539–552.
- Stephan, K., Weiskopf, N., Drysdale, P., Robinson, P., Friston, K., 2007. Comparing hemodynamic models with DCM. *NeuroImage* 38 (3), 387–401.
- Stephan, K.E., Kasper, L., Harrison, L.M., Daunizeau, J., den Ouden, H.E., Breakspear, M., Friston, K.J., 2008. Nonlinear dynamic causal models for fMRI. *NeuroImage* 42, 649–662.
- Stephan, K.E., Penny, W.D., Daunizeau, J., Moran, R.J., Friston, K.J., 2009. Bayesian model selection for group studies. *NeuroImage* 46 (4), 1004–1017.
- Tachtsidis, I., Leung, T.S., Chopra, A., Koh, P.H., Reid, C.B., Elwell, C.E., 2009. False positives in functional nearinfrared topography. *Oxygen Transport to Tissue XXX*. Springer, pp. 307–314.
- Takahashi, T., Takikawa, Y., Kawagoe, R., Shibuya, S., Iwano, T., Kitazawa, S., 2011. Influence of skin blood flow on near-infrared spectroscopy signals measured on the forehead during a verbal fluency task. *NeuroImage* 57, 991–1002.
- Tong, Y., Lindsey, K.P., deB Frederick, B., 2011. Partitioning of physiological noise signals in the brain with concurrent near-infrared spectroscopy and fMRI. *J. Cereb. Blood Flow Metab.* 31 (12), 2352–2362.

- Villringer, A., Planck, J., Hock, C., Schleinkofer, L., Dirnagl, U., 1993. Near infrared spectroscopy (NIRS): a new tool to study hemodynamic changes during activation of brain function in human adults. *Neurosci. Lett.* 154 (1), 101–104.
- Wang, L., Jacques, S.L., Zheng, L., 1995. MCML – Monte Carlo modeling of light transport in multi-layered tissues. *Comput. Meth. Programs Biomed.* 47, 131–146.
- White, B.R., Snyder, A.Z., Cohen, A.L., Petersen, S.E., Raichle, M.E., Schlaggar, B.L., Culver, J.P., 2009. Resting-state functional connectivity in the human brain revealed with diffuse optical tomography. *NeuroImage* 47 (1), 148–156.
- Wolf, M., Naulaers, G., van Bel, F., Kleiser, S., Griesen, G., 2012. Review: a review of near infrared spectroscopy for term and preterm newborns. *J. Near Infrared Spectrosc.* 20 (1), 43–55.
- Yacoub, E., Ugurbil, K., Harel, N., 2005. The spatial dependence of the poststimulus undershoot as revealed by high-resolution BOLD- and CBV-weighted fMRI. *J. Cereb. Blood Flow Metab.* 26 (5), 634–644.
- Ye, J.C., Tak, S., Jang, K.E., Jung, J., Jang, J., 2009. NIRS-SPM: statistical parametric mapping for near-infrared spectroscopy. *NeuroImage* 44, 428–447.
- Yuan, Z., 2013. Combining independent component analysis and Granger causality to investigate brain network dynamics with fNIRS measurements. *Biomed. Opt. Express* 4, 2629–2643.
- Yücel, M.A., Huppert, T.J., Boas, D.A., Gagnon, L., 2012. Calibrating the BOLD signal during a motor task using an extended fusion model incorporating DOT, BOLD and ASL data. *NeuroImage* 61 (4), 1268–1276.
- Zheng, Y., Martindale, J., Johnston, D., Jones, M., Berwick, J., Mayhew, J., 2002. A model of the hemodynamic response and oxygen delivery to brain. *NeuroImage* 16 (3), 617–637.

## REFERENCES

- Adams, J. H., D. Doyle, et al. (1989). "Diffuse axonal injury in head injury: definition, diagnosis and grading." Histopathology **15**(1): 49-59.
- Adams, J. H., D. Doyle, et al. (1984). "Diffuse axonal injury in head injuries caused by a fall." Lancet **2**(8417-8418): 1420-1422.
- Amaro, E., Jr. and G. J. Barker (2006). "Study design in fMRI: basic principles." Brain Cogn **60**(3): 220-232.
- Andrews, K., L. Murphy, et al. (1996). "Misdiagnosis of the vegetative state: retrospective study in a rehabilitation unit." BMJ **313**(7048): 13-16.
- Badr, G. G., M. Matousek, et al. (1983). "A quantitative EEG analysis of the effects of baclofen on man." Neuropsychobiology **10**(1): 13-18.
- Bagnato, S., C. Boccagni, et al. (2010). "Prognostic value of standard EEG in traumatic and non-traumatic disorders of consciousness following coma." Clin Neurophysiol **121**(3): 274-280.
- Baker, W. B., A. B. Parthasarathy, et al. (2014). "Modified Beer-Lambert law for blood flow." Biomed Opt Express **5**(11): 4053-4075.
- Bakker, A., B. Smith, et al. (2012). Applied Aspects of Ultrasonography in Humans, Chapter 3: Near-Infrared Spectroscopy, Intech.
- Balestreri, M., M. Czosnyka, et al. (2004). "Predictive value of Glasgow Coma Scale after brain trauma: change in trend over the past ten years." J Neurol Neurosurg Psychiatry **75**(1): 161-162.
- Beaumont, J. G. and P. M. Kenealy (2005). "Incidence and prevalence of the vegetative and minimally conscious states." Neuropsychol Rehabil **15**(3-4): 184-189.
- Beljaars, D. E., W. J. Valckx, et al. (2015). "Prevalence differences of patients in vegetative state in The Netherlands and Vienna, Austria: a comparison of values and ethics." J Head Trauma Rehabil **30**(3): E57-60.
- Benarroch, E. E., A. M. Schmeichel, et al. (2015). "Histaminergic tuberomammillary neuron loss in multiple system atrophy and dementia with Lewy bodies." Mov Disord **30**(8): 1133-1139.
- Berek, K., P. Lechleitner, et al. (1995). "Early determination of neurological outcome after prehospital cardiopulmonary resuscitation." Stroke **26**(4): 543-549.
- Berlad, I. and H. Pratt (1995). "P300 in response to the subject's own name." Electroencephalogr Clin Neurophysiol **96**(5): 472-474.

- Berman, B. D., S. G. Horovitz, et al. (2012). "Self-modulation of primary motor cortex activity with motor and motor imagery tasks using real-time fMRI-based neurofeedback." Neuroimage **59**(2): 917-925.
- Bernat, J. L. (2006). "Chronic disorders of consciousness." Lancet **367**(9517): 1181-1192.
- Bernat, J. L. (2010). "Current controversies in states of chronic unconsciousness." Neurology **75**(18 Suppl 1): S33-38.
- Binkofski, F., K. Amunts, et al. (2000). "Broca's region subserves imagery of motion: a combined cytoarchitectonic and fMRI study." Hum Brain Mapp **11**(4): 273-285.
- Blumergs, P. C., N. R. Jones, et al. (1989). "Diffuse axonal injury in head trauma." J Neurol Neurosurg Psychiatry **52**(7): 838-841.
- Boden, S., H. Obrig, et al. (2007). "The oxygenation response to functional stimulation: is there a physiological meaning to the lag between parameters?" Neuroimage **36**(1): 100-107.
- Boly, M., M. R. Coleman, et al. (2007). "When thoughts become action: an fMRI paradigm to study volitional brain activity in non-communicative brain injured patients." Neuroimage **36**(3): 979-992.
- Boly, M., M. Massimini, et al. (2012). "Brain connectivity in disorders of consciousness." Brain Connect **2**(1): 1-10.
- Boly, M., L. Tshibanda, et al. (2009). "Functional connectivity in the default network during resting state is preserved in a vegetative but not in a brain dead patient." Hum Brain Mapp **30**(8): 2393-2400.
- Bratton, S. L., R. M. Chestnut, et al. (2007). "Guidelines for the management of severe traumatic brain injury. XV. Steroids." J Neurotrauma **24 Suppl 1**: S91-95.
- Bruno, M. A., A. Vanhaudenhuyse, et al. (2011). "From unresponsive wakefulness to minimally conscious PLUS and functional locked-in syndromes: recent advances in our understanding of disorders of consciousness." J Neurol **258**(7): 1373-1384.
- Burgess, A. and J. Gruzelier (1993). "Individual reliability of amplitude distribution in topographical mapping of EEG." Electroencephalogr Clin Neurophysiol **86**(4): 219-223.
- Burgess, A. P. and J. H. Gruzelier (1996). "The reliability of event-related desynchronisation: a generalisability study analysis." Int J Psychophysiol **23**(3): 163-169.
- Carter, B. G. and W. Butt (2001). "Review of the use of somatosensory evoked potentials in the prediction of outcome after severe brain injury." Crit Care Med **29**(1): 178-186.

- Cheng, L., O. Gosseries, et al. (2013). "Assessment of localisation to auditory stimulation in post-comatose states: use the patient's own name." BMC Neurol **13**: 27.
- Chennu, S., J. Annen, et al. (2017). "Brain networks predict metabolism, diagnosis and prognosis at the bedside in disorders of consciousness." Brain **140**(8): 2120-2132.
- Choi, S. P., H. K. Park, et al. (2008). "The density ratio of grey to white matter on computed tomography as an early predictor of vegetative state or death after cardiac arrest." Emerg Med J **25**(10): 666-669.
- Clemmensen, P., S. Strandgaard, et al. (1987). "Cerebrospinal fluid creatine kinase isoenzyme BB levels do not predict the clinical outcome in patients unconscious following cardiac resuscitation." Clin Cardiol **10**(4): 235-236.
- Coleman, M. R., M. H. Davis, et al. (2009). "Towards the routine use of brain imaging to aid the clinical diagnosis of disorders of consciousness." Brain **132**(Pt 9): 2541-2552.
- Coleman, M. R., D. K. Menon, et al. (2005). "Neurometabolic coupling in the vegetative and minimally conscious states: preliminary findings." J Neurol Neurosurg Psychiatry **76**(3): 432-434.
- Coleman, M. R., J. M. Rodd, et al. (2007). "Do vegetative patients retain aspects of language comprehension? Evidence from fMRI." Brain **130**(Pt 10): 2494-2507.
- Coles, M. G., G. Gratton, et al. (1988). "Detecting early communication: using measures of movement-related potentials to illuminate human information processing." Biol Psychol **26**(1-3): 69-89.
- Cooper, R. J., N. L. Everdell, et al. (2009). "Design and evaluation of a probe for simultaneous EEG and near-infrared imaging of cortical activation." Phys Med Biol **54**(7): 2093-2102.
- Crone, J. S., M. Schurz, et al. (2015). "Impaired consciousness is linked to changes in effective connectivity of the posterior cingulate cortex within the default mode network." Neuroimage **110**: 101-109.
- Cruse, D., S. Chennu, et al. (2011). "Bedside detection of awareness in the vegetative state: a cohort study." Lancet **378**(9809): 2088-2094.
- Cruse, D., S. Chennu, et al. (2012). "Detecting awareness in the vegetative state: electroencephalographic evidence for attempted movements to command." PLoS One **7**(11): e49933.
- Cui, X., S. Bray, et al. (2011). "A quantitative comparison of NIRS and fMRI across multiple cognitive tasks." Neuroimage **54**(4): 2808-2821.
- Deepika, A., Prabhuraj, A. R., Saikia, A., Shukla, D (2015). "Comparison of predictability of marshall and rotterdam CT scan scoring system in determining early mortality after traumatic brain injury." Acta Neurochirurgica **157**(11): 2033-2038.

- Del Giudice, R., C. Blume, et al. (2016). "Can self-relevant stimuli help assessing patients with disorders of consciousness?" Conscious Cogn **44**: 51-60.
- Delpy, D. T., M. Cope, et al. (1988). "Estimation of optical pathlength through tissue from direct time of flight measurement." Phys Med Biol **33**(12): 1433-1442.
- Demertzi, A., A. Vanhaudenhuyse, et al. (2008). "Is there anybody in there? Detecting awareness in disorders of consciousness." Expert Rev Neurother **8**(11): 1719-1730.
- Di Saverio, S., G. Gambale, et al. (2014). "Changes in the outcomes of severe trauma patients from 15-year experience in a Western European trauma ICU of Emilia Romagna region (1996-2010). A population cross-sectional survey study." Langenbecks Arch Surg **399**(1): 109-126.
- Dion, K. L. (1983). "Names, Identity, and Self." A Journal of Onomastics **31:4**, : 245-257,.
- Donchin, E. (1981). "Presidential address, 1980. Surprise!...Surprise?" Psychophysiology **18**(5): 493-513.
- Donis, J. and B. Kraftner (2011). "The prevalence of patients in a vegetative state and minimally conscious state in nursing homes in Austria." Brain Inj **25**(11): 1101-1107.
- Dormanns, K., R. G. Brown, et al. (2015). "Neurovascular coupling: a parallel implementation." Front Comput Neurosci **9**: 109.
- Dougherty, J. H., Jr., D. G. Rawlinson, et al. (1981). "Hypoxic-ischemic brain injury and the vegetative state: clinical and neuropathologic correlation." Neurology **31**(8): 991-997.
- Duncan, A., J. H. Meek, et al. (1995). "Optical pathlength measurements on adult head, calf and forearm and the head of the newborn infant using phase resolved optical spectroscopy." Phys Med Biol **40**(2): 295-304.
- Dunn, J. F., N. Nathoo, et al. (2014). "A tale of two methods: combining near-infrared spectroscopy with MRI for studies of brain oxygenation and metabolism." Adv Exp Med Biol **812**: 65-71.
- Duvernoy, H., S. Delon, et al. (1983). "The vascularization of the human cerebellar cortex." Brain Res Bull **11**(4): 419-480.
- Duvernoy, H. M., S. Delon, et al. (1981). "Cortical blood vessels of the human brain." Brain Res Bull **7**(5): 519-579.
- Elwell, C. E. and J. Hebden. "Near- infrared spectroscopy." Retrieved 12.12.2011, from [http://www.medphys.ucl.ac.uk/research/borg/research/NIR\\_topics/nirs.htm](http://www.medphys.ucl.ac.uk/research/borg/research/NIR_topics/nirs.htm).
- Engberg, A. W. and T. W. Teasdale (2004). "A population-based study of survival and discharge status for survivors after head injury." Acta Neurol Scand **110**(5): 281-290.

- Fazli, S., J. Mehnert, et al. (2012). "Enhanced performance by a hybrid NIRS-EEG brain computer interface." Neuroimage **59**(1): 519-529.
- Fernandez-Espejo, D., S. Rossit, et al. (2015). "A Thalamocortical Mechanism for the Absence of Overt Motor Behavior in Covertly Aware Patients." JAMA Neurol **72**(12): 1442-1450.
- Ferradal, S. L., S. M. Liao, et al. (2016). "Functional Imaging of the Developing Brain at the Bedside Using Diffuse Optical Tomography." Cerebral Cortex **26**(4): 1558-1568.
- Fingelkurts, A. A., S. Bagnato, et al. (2011). "Life or death: prognostic value of a resting EEG with regards to survival in patients in vegetative and minimally conscious States." PLoS One **6**(10): e25967.
- Fischer, C., F. Dailier, et al. (2008). "Novelty P3 elicited by the subject's own name in comatose patients." Clin Neurophysiol **119**(10): 2224-2230.
- Fischer, C., J. Luaute, et al. (2010). "Event-related potentials (MMN and novelty P3) in permanent vegetative or minimally conscious states." Clin Neurophysiol **121**(7): 1032-1042.
- Formisano, R., M. D'Ippolito, et al. (2013). "Functional locked-in syndrome as recovery phase of vegetative state." Brain Inj **27**(11): 1332.
- Franzkowiak, S., B. Pollok, et al. (2010). "Altered pattern of motor cortical activation-inhibition during voluntary movements in Tourette syndrome." Mov Disord **25**(12): 1960-1966.
- Friedrich, E. V., R. Scherer, et al. (2013). "Stability of event-related (de-)synchronization during brain-computer interface-relevant mental tasks." Clin Neurophysiol **124**(1): 61-69.
- Fulton, J. F. (1950). "The cerebellum and precentral motor cortex." J Nerv Ment Dis **111**(1): 67-71.
- Gagnon, L., M. A. Yucel, et al. (2012). "Quantification of the cortical contribution to the NIRS signal over the motor cortex using concurrent NIRS-fMRI measurements." Neuroimage **59**(4): 3933-3940.
- Gendo, A., L. Kramer, et al. (2001). "Time-dependency of sensory evoked potentials in comatose cardiac arrest survivors." Intensive Care Med **27**(8): 1305-1311.
- Gennarelli, T. A. (1993). "Mechanisms of brain injury." J Emerg Med **11 Suppl 1**: 5-11.
- Gentleman, S. M., M. J. Nash, et al. (1993). "Beta-amyloid precursor protein (beta APP) as a marker for axonal injury after head injury." Neurosci Lett **160**(2): 139-144.
- Ghosh, A., C. Elwell, et al. (2012). "Review article: cerebral near-infrared spectroscopy in adults: a work in progress." Anesth Analg **115**(6): 1373-1383.

- Giacino, J. T., S. Ashwal, et al. (2002). "The minimally conscious state: definition and diagnostic criteria." Neurology **58**(3): 349-353.
- Giacino, J. T., K. Kalmar, et al. (2004). "The JFK Coma Recovery Scale-Revised: measurement characteristics and diagnostic utility." Arch Phys Med Rehabil **85**(12): 2020-2029.
- Gill-Thwaites, H. and R. Munday (2004). "The Sensory Modality Assessment and Rehabilitation Technique (SMART): a valid and reliable assessment for vegetative state and minimally conscious state patients." Brain Inj **18**(12): 1255-1269.
- Glickstein, M. (2007). "What does the cerebellum really do?" Curr Biol **17**(19): R824-827.
- Gosseries, O., M. A. Bruno, et al. (2011). "Disorders of consciousness: what's in a name?" NeuroRehabilitation **28**(1): 3-14.
- Guillot, A., C. Collet, et al. (2009). "Brain activity during visual versus kinesthetic imagery: an fMRI study." Hum Brain Mapp **30**(7): 2157-2172.
- Halsband, U., N. Ito, et al. (1993). "The role of premotor cortex and the supplementary motor area in the temporal control of movement in man." Brain **116** ( Pt 1): 243-266.
- Hanakawa, T., S. Parikh, et al. (2005). "Finger and face representations in the ipsilateral precentral motor areas in humans." J Neurophysiol **93**(5): 2950-2958.
- Hauger, S. L., C. Schnakers, et al. (2015). "Neurophysiological Indicators of Residual Cognitive Capacity in the Minimally Conscious State." Behav Neurol **2015**: 145913.
- Higashi, H. and T. Tanaka (2013). "Simultaneous design of FIR filter banks and spatial patterns for EEG signal classification." IEEE Trans Biomed Eng **60**(4): 1100-1110.
- Hillman, E. M. (2014). "Coupling mechanism and significance of the BOLD signal: a status report." Annu Rev Neurosci **37**: 161-181.
- Hinchey, P. R., J. B. Myers, et al. (2010). "Improved out-of-hospital cardiac arrest survival after the sequential implementation of 2005 AHA guidelines for compressions, ventilations, and induced hypothermia: the Wake County experience." Ann Emerg Med **56**(4): 348-357.
- Hiraoka, M., M. Firbank, et al. (1993). "A Monte Carlo investigation of optical pathlength in inhomogeneous tissue and its application to near-infrared spectroscopy." Phys Med Biol **38**(12): 1859-1876.
- Hirth, C., H. Obrig, et al. (1996). "Non-invasive functional mapping of the human motor cortex using near-infrared spectroscopy." Neuroreport **7**(12): 1977-1981.
- Holeckova, I., C. Fischer, et al. (2006). "Brain responses to a subject's own name uttered by a familiar voice." Brain Res **1082**(1): 142-152.

- Holler, Y., M. Kronbichler, et al. (2011). "EEG frequency analysis of responses to the own-name stimulus." Clin Neurophysiol **122**(1): 99-106.
- Holper, L., D. E. Shalom, et al. (2011). "Understanding inverse oxygenation responses during motor imagery: a functional near-infrared spectroscopy study." Eur J Neurosci **33**(12): 2318-2328.
- Horki, P., G. Bauernfeind, et al. (2014). "Detection of mental imagery and attempted movements in patients with disorders of consciousness using EEG." Front Hum Neurosci **8**: 1009.
- Howarth, C. I. and K. Ellis (1961). "The relative intelligibility threshold for one's own name compared with other names." Quarterly journal of experimental psychology **13**(4): 236-239.
- Huppert, T. J., R. D. Hoge, et al. (2006). "A temporal comparison of BOLD, ASL, and NIRS hemodynamic responses to motor stimuli in adult humans." Neuroimage **29**(2): 368-382.
- Huston, J. P., U. Wagner, et al. (1997). "The tuberomammillary nucleus projections in the control of learning, memory and reinforcement processes: evidence for an inhibitory role." Behav Brain Res **83**(1-2): 97-105.
- Hutchinson, P. J., A. G. Kolas, et al. (2016). "Trial of Decompressive Craniectomy for Traumatic Intracranial Hypertension." N Engl J Med **375**(12): 1119-1130.
- Hwang, H. J., J. H. Lim, et al. (2014). "Evaluation of various mental task combinations for near-infrared spectroscopy-based brain-computer interfaces." J Biomed Opt **19**(7): 77005.
- Iso, N., T. Moriuchi, et al. (2015). "Monitoring Local Regional Hemodynamic Signal Changes during Motor Execution and Motor Imagery Using Near-Infrared Spectroscopy." Front Physiol **6**: 416.
- Jennett, B. (2002). The vegetative state : medical facts, ethical and legal dilemmas. Cambridge ; New York, Cambridge University Press.
- Jennett, B. and F. Plum (1972). "Persistent vegetative state after brain damage." RN **35**(10): ICU1-4.
- Jobsis, F. F. (1977). "Noninvasive, infrared monitoring of cerebral and myocardial oxygen sufficiency and circulatory parameters." Science **198**(4323): 1264-1267.
- Kaiser, V., G. Bauernfeind, et al. (2014). "Cortical effects of user training in a motor imagery based brain-computer interface measured by fNIRS and EEG." Neuroimage **85 Pt 1**: 432-444.
- Kamran, M. A., M. M. Mannan, et al. (2016). "Cortical Signal Analysis and Advances in Functional Near-Infrared Spectroscopy Signal: A Review." Front Hum Neurosci **10**: 261.

- Kim, S. G. and S. Ogawa (2012). "Biophysical and physiological origins of blood oxygenation level-dependent fMRI signals." J Cereb Blood Flow Metab **32**(7): 1188-1206.
- Kinney, H. C. and M. A. Samuels (1994). "Neuropathology of the persistent vegetative state. A review." J Neuropathol Exp Neurol **53**(6): 548-558.
- Klem, G. H., H. O. Luders, et al. (1999). "The ten-twenty electrode system of the International Federation. The International Federation of Clinical Neurophysiology." Electroencephalogr Clin Neurophysiol Suppl **52**: 3-6.
- Klimesch, W., M. Doppelmayr, et al. (2000). "Simultaneous desynchronization and synchronization of different alpha responses in the human electroencephalograph: a neglected paradox?" Neurosci Lett **284**(1-2): 97-100.
- Kobylarz, E. J. and N. D. Schiff (2005). "Neurophysiological correlates of persistent vegetative and minimally conscious states." Neuropsychol Rehabil **15**(3-4): 323-332.
- Koessler, L., L. Maillard, et al. (2009). "Automated cortical projection of EEG sensors: anatomical correlation via the international 10-10 system." Neuroimage **46**(1): 64-72.
- Kotchoubey, B. (2005). "Event-related potential measures of consciousness: two equations with three unknowns." Prog Brain Res **150**: 427-444.
- Kotchoubey, B., S. Merz, et al. (2013). "Global functional connectivity reveals highly significant differences between the vegetative and the minimally conscious state." J Neurol **260**(4): 975-983.
- Krause, C. M., A. H. Lang, et al. (1996). "Event-related EEG desynchronization and synchronization during an auditory memory task." Electroencephalogr Clin Neurophysiol **98**(4): 319-326.
- Lant, N. D., L. E. Gonzalez-Lara, et al. (2016). "Relationship between the anterior forebrain mesocircuit and the default mode network in the structural bases of disorders of consciousness." NeuroImage : Clinical **10**: 27-35.
- Laureys, S. and M. Boly (2008). "The changing spectrum of coma." Nat Clin Pract Neurol **4**(10): 544-546.
- Laureys, S., G. G. Celesia, et al. (2010). "Unresponsive wakefulness syndrome: a new name for the vegetative state or apallic syndrome." BMC Med **8**: 68.
- Laureys, S., S. Goldman, et al. (1999). "Impaired effective cortical connectivity in vegetative state: preliminary investigation using PET." Neuroimage **9**(4): 377-382.
- Laureys, S., F. Perrin, et al. (2007). "Self-consciousness in non-communicative patients." Conscious Cogn **16**(3): 722-741; discussion 742-725.

- Laureys, S. and G. Tononi (2009). The neurology of consciousness : cognitive neuroscience and neuropathology. Amsterdam ; Boston, Elsevier/Academic Press.
- Lavrijsen, J. C., J. S. van den Bosch, et al. (2005). "Prevalence and characteristics of patients in a vegetative state in Dutch nursing homes." J Neurol Neurosurg Psychiatry **76**(10): 1420-1424.
- Lechinger, J., K. Bothe, et al. (2013). "CRS-R score in disorders of consciousness is strongly related to spectral EEG at rest." J Neurol **260**(9): 2348-2356.
- Lechinger, J., N. Chwala-Schlegel, et al. (2013). "Mirroring of a simple motor behavior in disorders of consciousness." Clin Neurophysiol **124**(1): 27-34.
- Lechinger, J., T. Wielek, et al. (2016). "Event-related EEG power modulations and phase connectivity indicate the focus of attention in an auditory own name paradigm." J Neurol **263**(8): 1530-1543.
- Leff, D. R., F. Orihuela-Espina, et al. (2011). "Assessment of the cerebral cortex during motor task behaviours in adults: a systematic review of functional near infrared spectroscopy (fNIRS) studies." Neuroimage **54**(4): 2922-2936.
- Lehembre, R., B. Marie-Aurelie, et al. (2012). "Resting-state EEG study of comatose patients: a connectivity and frequency analysis to find differences between vegetative and minimally conscious states." Funct Neurol **27**(1): 41-47.
- Lenartowicz, A., R. Escobedo-Quiroz, et al. (2010). "Updating of context in working memory: an event-related potential study." Cogn Affect Behav Neurosci **10**(2): 298-315.
- Lenzi, D., A. Conte, et al. (2007). "Effect of corpus callosum damage on ipsilateral motor activation in patients with multiple sclerosis: a functional and anatomical study." Hum Brain Mapp **28**(7): 636-644.
- Levy, D. E., J. J. Caronna, et al. (1985). "Predicting outcome from hypoxic-ischemic coma." JAMA **253**(10): 1420-1426.
- Lew, H. L., S. Dikmen, et al. (2003). "Use of somatosensory-evoked potentials and cognitive event-related potentials in predicting outcomes of patients with severe traumatic brain injury." Am J Phys Med Rehabil **82**(1): 53-61; quiz 62-54, 80.
- Liberati, G., T. Hunefeldt, et al. (2014). "Questioning the dichotomy between vegetative state and minimally conscious state: a review of the statistical evidence." Front Hum Neurosci **8**: 865.
- Litvak, V., J. Mattout, et al. (2011). "EEG and MEG data analysis in SPM8." Comput Intell Neurosci **2011**: 852961.
- Lloyd-Fox, S., A. Blasi, et al. (2010). "Illuminating the developing brain: the past, present and future of functional near infrared spectroscopy." Neurosci Biobehav Rev **34**(3): 269-284.

- Luaute, J., D. Maucort-Boulch, et al. (2010). "Long-term outcomes of chronic minimally conscious and vegetative states." Neurology **75**(3): 246-252.
- Luck, S. J. (2005). An introduction to the event-related potential technique. Cambridge, Mass., MIT Press.
- Lutkenhoff, E. S., J. Chiang, et al. (2015). "Thalamic and extrathalamic mechanisms of consciousness after severe brain injury." Ann Neurol **78**(1): 68-76.
- Maas, A. I., C. W. Hukkelhoven, et al. (2005). "Prediction of outcome in traumatic brain injury with computed tomographic characteristics: a comparison between the computed tomographic classification and combinations of computed tomographic predictors." Neurosurgery **57**(6): 1173-1182; discussion 1173-1182.
- Maquet, P., C. Degueldre, et al. (1997). "Functional neuroanatomy of human slow wave sleep." J Neurosci **17**(8): 2807-2812.
- Marshall, L. F. (2000). "Head injury: recent past, present, and future." Neurosurgery **47**(3): 546-561.
- Matcher, S. J., C. E. Elwell, et al. (1995). "Performance comparison of several published tissue near-infrared spectroscopy algorithms." Anal Biochem **227**(1): 54-68.
- McCallum, W. C., S. F. Farmer, et al. (1984). "The effects of physical and semantic incongruities on auditory event-related potentials." Electroencephalogr Clin Neurophysiol **59**(6): 477-488.
- McGregor, K. M., A. Sudhyadhom, et al. (2015). "Reliability of negative BOLD in ipsilateral sensorimotor areas during unimanual task activity." Brain Imaging Behav **9**(2): 245-254.
- McHugh, M. L. (2012). "Interrater reliability: the kappa statistic." Biochem Med (Zagreb) **22**(3): 276-282.
- Mehnert, J. (2014). "Hybrid brain computer interfaces." <https://www.cbs.mpg.de/434727/14-hybridbci.pdf>.
- Miezin, F. M., L. Maccotta, et al. (2000). "Characterizing the hemodynamic response: effects of presentation rate, sampling procedure, and the possibility of ordering brain activity based on relative timing." Neuroimage **11**(6 Pt 1): 735-759.
- Mihara, M., N. Hattori, et al. (2013). "Near-infrared spectroscopy-mediated neurofeedback enhances efficacy of motor imagery-based training in poststroke victims: a pilot study." Stroke **44**(4): 1091-1098.
- Mihara, M., I. Miyai, et al. (2012). "Neurofeedback using real-time near-infrared spectroscopy enhances motor imagery related cortical activation." PLoS One **7**(3): e32234.

- Minati, L., I. U. Kress, et al. (2011). "Intra- and extra-cranial effects of transient blood pressure changes on brain near-infrared spectroscopy (NIRS) measurements." J Neurosci Methods **197**(2): 283-288.
- Mokienko, O. A., A. V. Chervyakov, et al. (2013). "Increased motor cortex excitability during motor imagery in brain-computer interface trained subjects." Front Comput Neurosci **7**: 168.
- Molteni, E., F. Arrigoni, et al. (2013). "Bedside assessment of residual functional activation in minimally conscious state using NIRS and general linear models." Conf Proc IEEE Eng Med Biol Soc **2013**: 3551-3554.
- Monrad, P., K. Sannagowdara, et al. (2015). "Haemodynamic response associated with both ictal and interictal epileptiform activity using simultaneous video electroencephalography/near infrared spectroscopy in a within-subject study." J Near Infrared Spectrosc **23**(4): 209-218.
- Monti, M. M., A. Vanhaudenhuyse, et al. (2010). "Willful modulation of brain activity in disorders of consciousness." N Engl J Med **362**(7): 579-589.
- Morihiro, M., T. Tsubone, et al. (2009). "Relation between NIRS signal and motor capability." Conf Proc IEEE Eng Med Biol Soc **2009**: 3991-3994.
- Multi-Society Task Force on PVS (1994). "Medical aspects of the persistent vegetative state (2). The Multi-Society Task Force on PVS." N Engl J Med **330**(22): 1572-1579.
- Murkin, J. M. and M. Arango (2009). "Near-infrared spectroscopy as an index of brain and tissue oxygenation." Br J Anaesth **103** *Suppl 1*: i3-13.
- Neuper, C., M. Wortz, et al. (2006). "ERD/ERS patterns reflecting sensorimotor activation and deactivation." Prog Brain Res **159**: 211-222.
- Obrig, H. (2014). "NIRS in clinical neurology - a 'promising' tool?" Neuroimage **85 Pt 1**: 535-546.
- Ogawa, S. and T. M. Lee (1990). "Magnetic resonance imaging of blood vessels at high fields: in vivo and in vitro measurements and image simulation." Magn Reson Med **16**(1): 9-18.
- Ostby, I., L. Oyehaug, et al. (2009). "Astrocytic mechanisms explaining neural-activity-induced shrinkage of extraneuronal space." PLoS Comput Biol **5**(1): e1000272.
- Owen, A. M., M. R. Coleman, et al. (2007). "Using functional magnetic resonance imaging to detect covert awareness in the vegetative state." Arch Neurol **64**(8): 1098-1102.
- Parise, E., A. D. Friederici, et al. (2010). ""Did you call me?" 5-month-old infants own name guides their attention." PLoS One **5**(12): e14208.
- Parvizi, J. and A. Damasio (2001). "Consciousness and the brainstem." Cognition **79**(1-2): 135-160.

- Pellicer, A. and C. Bravo Mdel (2011). "Near-infrared spectroscopy: a methodology-focused review." Semin Fetal Neonatal Med **16**(1): 42-49.
- Peng, K., D. K. Nguyen, et al. (2014). "fNIRS-EEG study of focal interictal epileptiform discharges." Epilepsy Res **108**(3): 491-505.
- Perrin, F., M. Castro, et al. (2015). "Promoting the use of personally relevant stimuli for investigating patients with disorders of consciousness." Front Psychol **6**: 1102.
- Perrin, F., C. Schnakers, et al. (2006). "Brain response to one's own name in vegetative state, minimally conscious state, and locked-in syndrome." Arch Neurol **63**(4): 562-569.
- Pfeifer, R., A. Borner, et al. (2005). "Outcome after cardiac arrest: predictive values and limitations of the neuroproteins neuron-specific enolase and protein S-100 and the Glasgow Coma Scale." Resuscitation **65**(1): 49-55.
- Pfurtscheller, G. and C. Andrew (1999). "Event-Related changes of band power and coherence: methodology and interpretation." J Clin Neurophysiol **16**(6): 512-519.
- Pfurtscheller, G., C. Brunner, et al. (2006). "Mu rhythm (de)synchronization and EEG single-trial classification of different motor imagery tasks." Neuroimage **31**(1): 153-159.
- Pfurtscheller, G. and F. H. Lopes da Silva (1999). "Event-related EEG/MEG synchronization and desynchronization: basic principles." Clin Neurophysiol **110**(11): 1842-1857.
- Pichler, G., P. Y. Cheung, et al. (2014). "How to monitor the brain during immediate neonatal transition and resuscitation? A systematic qualitative review of the literature." Neonatology **105**(3): 205-210.
- Pierce, J. E., D. H. Smith, et al. (1998). "Enduring cognitive, neurobehavioral and histopathological changes persist for up to one year following severe experimental brain injury in rats." Neuroscience **87**(2): 359-369.
- Pivik, R. T., R. J. Broughton, et al. (1993). "Guidelines for the recording and quantitative analysis of electroencephalographic activity in research contexts." Psychophysiology **30**(6): 547-558.
- Polich, J. (1987). "Comparison of P300 from a passive tone sequence paradigm and an active discrimination task." Psychophysiology **24**(1): 41-46.
- Polich, J. (1987). "Task difficulty, probability, and inter-stimulus interval as determinants of P300 from auditory stimuli." Electroencephalogr Clin Neurophysiol **68**(4): 311-320.
- Polich, J. (2007). "Updating P300: an integrative theory of P3a and P3b." Clin Neurophysiol **118**(10): 2128-2148.
- Porro, C. A., V. Cettolo, et al. (2000). "Ipsilateral involvement of primary motor cortex during motor imagery." Eur J Neurosci **12**(8): 3059-3063.

- R development Core Team (2015). R: A language and environment for statistical computing. Vienna, Austria: R Foundation for Statistical Computing. Retrieved from <http://www.R-project.org>.
- RCP (2013) "Royal College of Physicians. Prolonged disorders of consciousness. National clinical guidelines. Report of a working party 2013."
- Rossi, D. J. (2006). "Another BOLD role for astrocytes: coupling blood flow to neural activity." *Nat Neurosci* **9**(2): 159-161.
- Royal College of Physicians (2013) "Prolonged disorders of consciousness. National clinical guidelines. Report of a working party 2013."
- Ryvlin, P. and S. Rheims (2008). "Epilepsy surgery: eligibility criteria and presurgical evaluation." *Dialogues Clin Neurosci* **10**(1): 91-103.
- Salinsky, M. C., L. M. Binder, et al. (2002). "Effects of gabapentin and carbamazepine on the EEG and cognition in healthy volunteers." *Epilepsia* **43**(5): 482-490.
- Sato, T., M. Ito, et al. (2007). "Time courses of brain activation and their implications for function: a multichannel near-infrared spectroscopy study during finger tapping." *Neurosci Res* **58**(3): 297-304.
- Sato, Y., T. Uzuka, et al. (2012). "Near-infrared spectroscopic study and the Wada test for presurgical evaluation of expressive and receptive language functions in glioma patients: with a case report of dissociated language functions." *Neurosci Lett* **510**(2): 104-109.
- Schiff, N. D. (2008). "Central thalamic contributions to arousal regulation and neurological disorders of consciousness." *Ann N Y Acad Sci* **1129**: 105-118.
- Schnakers, C., J. Giacino, et al. (2007). "Does the Glasgow Coma Scale correctly diagnose the vegetative and minimally conscious states?" *Critical Care* **11**(Suppl 2): P488-P488.
- Schnakers, C., J. T. Giacino, et al. (2015). "Preserved covert cognition in noncommunicative patients with severe brain injury?" *Neurorehabil Neural Repair* **29**(4): 308-317.
- Schnakers, C., F. Perrin, et al. (2008). "Voluntary brain processing in disorders of consciousness." *Neurology* **71**(20): 1614-1620.
- Schnakers, C., A. Vanhaudenhuyse, et al. (2009). "Diagnostic accuracy of the vegetative and minimally conscious state: clinical consensus versus standardized neurobehavioral assessment." *BMC Neurol* **9**: 35.
- Scholkmann, F., S. Kleiser, et al. (2014). "A review on continuous wave functional near-infrared spectroscopy and imaging instrumentation and methodology." *Neuroimage* **85 Pt 1**: 6-27.
- Schwartz, J. R. and T. Roth (2008). "Neurophysiology of sleep and wakefulness: basic science and clinical implications." *Curr Neuropharmacol* **6**(4): 367-378.

- Seel, R. T., M. Sherer, et al. (2010). "Assessment scales for disorders of consciousness: evidence-based recommendations for clinical practice and research." Arch Phys Med Rehabil **91**(12): 1795-1813.
- Servadei, F., G. D. Murray, et al. (2000). "The value of the "worst" computed tomographic scan in clinical studies of moderate and severe head injury. European Brain Injury Consortium." Neurosurgery **46**(1): 70-75; discussion 75-77.
- Sharma, N., V. M. Pomeroy, et al. (2006). "Motor imagery: a backdoor to the motor system after stroke?" Stroke **37**(7): 1941-1952.
- Sharon, H., Y. Pasternak, et al. (2013). "Emotional processing of personally familiar faces in the vegetative state." PLoS One **8**(9): e74711.
- Sherman, S. M. and R. W. Guillery (1998). "On the actions that one nerve cell can have on another: distinguishing "drivers" from "modulators"." Proc Natl Acad Sci U S A **95**(12): 7121-7126.
- Sherman, S. M. and R. W. Guillery (2001). Exploring the thalamus. San Diego, Academic Press.
- Sherman, S. M. and R. W. Guillery (2002). "The role of the thalamus in the flow of information to the cortex." Philos Trans R Soc Lond B Biol Sci **357**(1428): 1695-1708.
- Shiel, A., S. A. Horn, et al. (2000). "The Wessex Head Injury Matrix (WHIM) main scale: a preliminary report on a scale to assess and monitor patient recovery after severe head injury." Clin Rehabil **14**(4): 408-416.
- Sitaram, R., R. Veit, et al. (2012). "Acquired control of ventral premotor cortex activity by feedback training: an exploratory real-time fMRI and TMS study." Neurorehabil Neural Repair **26**(3): 256-265.
- Smith, D. H., D. F. Meaney, et al. (2003). "Diffuse axonal injury in head trauma." J Head Trauma Rehabil **18**(4): 307-316.
- Smith, D. H., J. A. Wolf, et al. (1999). "High tolerance and delayed elastic response of cultured axons to dynamic stretch injury." J Neurosci **19**(11): 4263-4269.
- Smith, M. (2008). "Monitoring intracranial pressure in traumatic brain injury." Anesth Analg **106**(1): 240-248.
- Smith, M. (2015). "Cerebral perfusion pressure." Br J Anaesth **115**(4): 488-490.
- Smith, M. and C. Elwell (2009). "Near-infrared spectroscopy: shedding light on the injured brain." Anesth Analg **108**(4): 1055-1057.
- Snyder, J. S., M. K. Gregg, et al. (2012). "Attention, awareness, and the perception of auditory scenes." Front Psychol **3**: 15.
- Steinbrink, J., A. Villringer, et al. (2006). "Illuminating the BOLD signal: combined fMRI-fNIRS studies." Magn Reson Imaging **24**(4): 495-505.

- Sten, S., K. Lundengard, et al. (2017). "Neural inhibition can explain negative BOLD responses: A mechanistic modelling and fMRI study." Neuroimage **158**: 219-231.
- Steppacher, I., M. Kaps, et al. (2014). "Will time heal? A long-term follow-up of severe disorders of consciousness." Ann Clin Transl Neurol **1**(6): 401-408.
- Strangman, G., J. P. Culver, et al. (2002). "A quantitative comparison of simultaneous BOLD fMRI and NIRS recordings during functional brain activation." Neuroimage **17**(2): 719-731.
- Strangman, G. E., Z. Li, et al. (2013). "Depth sensitivity and source-detector separations for near infrared spectroscopy based on the Colin27 brain template." PLoS One **8**(8): e66319.
- Strauss, D. J., R. M. Shavelle, et al. (1999). "Life expectancy and median survival time in the permanent vegetative state." Pediatr Neurol **21**(3): 626-631.
- Sur, S. and V. K. Sinha (2009). "Event-related potential: An overview." Ind Psychiatry J **18**(1): 70-73.
- Synek, V. M. (1988). "Prognostically important EEG coma patterns in diffuse anoxic and traumatic encephalopathies in adults." J Clin Neurophysiol **5**(2): 161-174.
- Takano, T., G. F. Tian, et al. (2006). "Astrocyte-mediated control of cerebral blood flow." Nat Neurosci **9**(2): 260-267.
- Tateuchi, T., K. Itoh, et al. (2012). "Neural mechanisms underlying the orienting response to subject's own name: an event-related potential study." Psychophysiology **49**(6): 786-791.
- The Multi-Society Task Force on PVS (1994). "Medical Aspects of the Persistent Vegetative State." New England Journal of Medicine **330**(21): 1499-1508.
- Tononi, G. and C. Koch (2008). "The neural correlates of consciousness: an update." Ann N Y Acad Sci **1124**: 239-261.
- Tresch, D. D., F. H. Sims, et al. (1991). "Clinical characteristics of patients in the persistent vegetative state." Arch Intern Med **151**(5): 930-932.
- Turner-Stokes, L., P. Bassett, et al. (2015). "Serial measurement of Wessex Head Injury Matrix in the diagnosis of patients in vegetative and minimally conscious states: a cohort analysis." BMJ Open **5**(4): e006051.
- Tusa, R. J., W. F. Stewart, et al. (1994). "Longitudinal study of brainstem auditory evoked responses in 87 normal human subjects." Neurology **44**(3 Pt 1): 528-532.
- Uga, M., I. Dan, et al. (2014). "Optimizing the general linear model for functional near-infrared spectroscopy: an adaptive hemodynamic response function approach." Neurophotonics **1**(1): 015004.

- University College San Diego. Swartz Center fo Computational Neuroscience. (2014). "EEGLAB guide. Chapter 11: Time/Frequency decomposition." Retrieved 01/07/2014, 2014, from [https://www.google.co.uk/search?q=eeg+lab+Fourier+transform,+&ie=utf-8&oe=utf-8&gws\\_rd=cr&ei=K3K8Vt\\_1MoavU\\_2uk\\_gG](https://www.google.co.uk/search?q=eeg+lab+Fourier+transform,+&ie=utf-8&oe=utf-8&gws_rd=cr&ei=K3K8Vt_1MoavU_2uk_gG).
- van Burik, M. and G. Pfurtscheller (1999). "Functional imaging of postmovement beta event-related synchronization." *J Clin Neurophysiol* **16**(4): 383-390.
- Van Opstal, F., N. Van Laeken, et al. (2014). "Correlation between individual differences in striatal dopamine and in visual consciousness." *Curr Biol* **24**(7): R265-266.
- Van Petten, C. and M. Kutas (1991). "Influences of semantic and syntactic context on open- and closed-class words." *Mem Cognit* **19**(1): 95-112.
- Vanhaudenhuyse, A., S. Laureys, et al. (2008). "Cognitive event-related potentials in comatose and post-comatose states." *Neurocrit Care* **8**(2): 262-270.
- Vanhaudenhuyse, A., Q. Noirhomme, et al. (2010). "Default network connectivity reflects the level of consciousness in non-communicative brain-damaged patients." *Brain* **133**(Pt 1): 161-171.
- Verleger, R., P. Jaskowski, et al. (1994). "Suspense and surprise: on the relationship between expectancies and P3." *Psychophysiology* **31**(4): 359-369.
- Wallois, F., M. Mahmoudzadeh, et al. (2012). "Usefulness of simultaneous EEG-NIRS recording in language studies." *Brain Lang* **121**(2): 110-123.
- Weyand, S. and T. Chau (2015). "Correlates of Near-Infrared Spectroscopy Brain-Computer Interface Accuracy in a Multi-Class Personalization Framework." *Front Hum Neurosci* **9**: 536.
- Whyte, J. and R. Nakase-Richardson (2013). "Disorders of consciousness: outcomes, comorbidities, and care needs." *Arch Phys Med Rehabil* **94**(10): 1851-1854.
- Wijdicks, E. F., A. Hijdra, et al. (2006). "Practice parameter: prediction of outcome in comatose survivors after cardiopulmonary resuscitation (an evidence-based review): report of the Quality Standards Subcommittee of the American Academy of Neurology." *Neurology* **67**(2): 203-210.
- Wilcox, N. E. and E. S. Stauffer (1972). "Follow-up of 423 consecutive patients admitted to the spinal cord centre, Rancho Los Amigos hospital, 1 January to 31 December 1967." *Paraplegia* **10**(2): 115-122.
- Wolf, J. A., P. K. Stys, et al. (2001). "Traumatic axonal injury induces calcium influx modulated by tetrodotoxin-sensitive sodium channels." *J Neurosci* **21**(6): 1923-1930.
- Wolf, M., U. Wolf, et al. (2002). "Different time evolution of oxyhemoglobin and deoxyhemoglobin concentration changes in the visual and motor cortices during functional stimulation: a near-infrared spectroscopy study." *Neuroimage* **16**(3 Pt 1): 704-712.

- Wood, N. and N. Cowan (1995). "The cocktail party phenomenon revisited: how frequent are attention shifts to one's name in an irrelevant auditory channel?" J Exp Psychol Learn Mem Cogn **21**(1): 255-260.
- Wray, S., M. Cope, et al. (1988). "Characterization of the near infrared absorption spectra of cytochrome aa3 and haemoglobin for the non-invasive monitoring of cerebral oxygenation." Biochim Biophys Acta **933**(1): 184-192.
- Wriessnegger, S. C., J. Kurzmann, et al. (2008). "Spatio-temporal differences in brain oxygenation between movement execution and imagery: a multichannel near-infrared spectroscopy study." Int J Psychophysiol **67**(1): 54-63.
- Yamashita, Y., A. Maki, et al. (2001). "Wavelength dependence of the precision of noninvasive optical measurement of oxy-, deoxy-, and total-hemoglobin concentration." Med Phys **28**(6): 1108-1114.
- Young, G. B. (2000). "The EEG in coma." J Clin Neurophysiol **17**(5): 473-485.
- Young, G. B. (2009). "Clinical practice. Neurologic prognosis after cardiac arrest." N Engl J Med **361**(6): 605-611.
- Young, G. B. and G. S. Doig (2005). "Continuous EEG monitoring in comatose intensive care patients: epileptiform activity in etiologically distinct groups." Neurocrit Care **2**(1): 5-10.
- Young, G. B., J. H. Kreeft, et al. (1999). "EEG and clinical associations with mortality in comatose patients in a general intensive care unit." J Clin Neurophysiol **16**(4): 354-360.
- Zama, T. and S. Shimada (2015). "Simultaneous measurement of electroencephalography and near-infrared spectroscopy during voluntary motor preparation." Sci Rep **5**: 16438.
- Zandbergen, E. G., A. Hijdra, et al. (2006). "Prediction of poor outcome within the first 3 days of postanoxic coma." Neurology **66**(1): 62-68.
- Zeman, A. (2001). "Consciousness." Brain **124**(Pt 7): 1263-1289.
- Zingler, V. C., B. Krumm, et al. (2003). "Early prediction of neurological outcome after cardiopulmonary resuscitation: a multimodal approach combining neurobiochemical and electrophysiological investigations may provide high prognostic certainty in patients after cardiac arrest." Eur Neurol **49**(2): 79-84.